INTERACTIONS OF FLEXIBLE POLYMERS AND GLOBULAR COLLOIDS: UNDERSTANDING PROTEIN PARTITIONING IN TWO-PHASE AQUEOUS POLYMER SYSTEMS

by

Nicholas L. Abbott

B. Eng (Chem.), Univ. of Adelaide, Australia, 1986

Submitted to the
Department of Chemical Engineering
in partial fulfillment of the requirement for the degree of

Doctor of Philosophy

at the

Massachusetts Institute of Technology

November, 1991

Signature of Author _____
Department of Chemical Engineering
October 28, 1991

Certified by _____
Professor Daniel Blankschtein
Thesis Advisor

and _____
Professor T. Alan Hatton
Thesis Advisor

Accepted by _____
Professor William M. Deen
Chairman, Departmental Committee on Graduate Students

ABSTRACT

Molecular-level mechanisms guiding the partitioning of globular proteins in two-phase aqueous polymer systems were elucidated using the theoretical tools of polymer-scaling concepts, statistical-thermodynamics, and liquid-state theory, as well as the complementary experimental techniques of equilibrium partitioning and small-angle neutron scattering.

A new theory of protein partitioning in two-phase aqueous polymer systems was advanced with the proposition that certain experimentally observed protein partitioning behaviors arise from a transition in the underlying structure of the polymer solution phases. Specifically, the two-phase aqueous poly(ethylene oxide) (PEO)-dextran system was investigated. With increasing PEO molecular weight, *scaling* predictions and the interpretation of *small angle neutron scattering* (SANS) measurements reveal a crossover in the underlying structure of the PEO solution phases from individually dispersed PEO coils to an extensively entangled PEO mesh. Within this mesh the identities of the individual polymer coils are lost. Novel *molecular-level pictures* for the interactions between globular proteins and polymers in solution were proposed for a variety of scenarios differing in (i) the polymer solution regime, (ii) the relative size of the protein and the polymer coil/mesh, (iii) the nature of the energetic interaction between the flexible polymer chains and the globular protein molecules.

The *essential physics* associated with each scenario was explored through *scaling-thermodynamic* descriptions of the protein-polymer interactions, and the associated protein partitioning behaviors were predicted. Comparison of the theoretical predictions to *experimental protein partitioning measurements* (using two-phase aqueous PEO-dextran systems and a diffusion cell) suggested that although the physical exclusion of the proteins by the polymers contributes to the observed partitioning behavior, other interactions also play a significant role. In particular, the influence of the PEO molecular weight on the partitioning behavior of a series of hydrophilic proteins was observed to be consistent with the presence of a weak attractive interaction between the protein molecules and the polymer coils.

A combined *equation of state/Monte-Carlo approach* was developed to evaluate the free energy of mixing globular colloids and flexible linear polymer coils. The important influence of the penetrability and deformability of the polymer to the protein in determining the thermodynamic properties of the fluid was revealed. Application of the approach to the protein partitioning problem corroborates the important role of non-steric interactions between the proteins and PEO. Comparison with experimental partitioning measurements suggests the presence of a weak attractive interaction energy which increases with protein size, R_p, where $17\text{Å} < R_p < 51\text{Å}$, from order 0.01kT to 0.1kT (per EO segment at the protein surface). However, the net interactions of the proteins and the PEO coils are strongly repulsive.

The measurement and interpretation of the intensity of *neutrons scattered at small angles (SANS)* from bovine serum albumin (BSA, R_p=35Å) in aqueous (D_2O) solutions containing singly dispersed PEO coils were found to be consistent with the existence of a weak attractive interaction (0.05kT) between BSA and PEO (in addition to repulsive steric interactions). The attractive interaction reduced the second virial coefficient for the BSA-PEO interaction to 80% of the value predicted for purely excluded-volume interaction.

From a common molecular-level description, *structural* features and *thermodynamic* properties of aqueous polymer solutions containing globular proteins were elucidated.

Thesis Advisor(s): Prof. Daniel Blankschtein
Prof. Alan Hatton

ACKNOWLEDGEMENTS

I would like to express my sincere gratitude and thanks to my two thesis advisors, Professors Daniel Blankschtein and Alan Hatton. Their stimulating, insightful and guiding comments were always greatly appreciated. From our many discussions I have gained a new perspective of Chemical Engineering and the applied sciences. This new perspective is the most valuable asset of my graduate study. I hope we have sown the seeds for the continuing exchange of ideas in the future. I also wish to thank Professors Bill Deen and Ed Merrill for their kind patience and suggestions at my occasional, yet lengthy, thesis committee meetings.

One of the strengths of MIT is the students it attracts from many regions of the world. Early in my graduate studies I benefited greatly from the advice of Richard Wilson. I have also enjoyed the commentaries of Minos Leodidis and Andy Bommarius who opened my eyes to many interesting topics in physical chemistry. As time progressed, my experience became more Greek. The quality of recent graduate school life has been greatly enhanced by the company, enthusiasm and philosophies of Paschalis Alexandridis and Costakis Patrickios. They are both ideal laboratory partners. I thank Paschalis for his patience and conversation over the recent months during which I have occupied, almost exclusively, our "shared" computer. I also thank Costakis for giving me reason to look up from the computer screen and watch his experiments.

I wish to express my appreciation to the students and postdoc members of Professor Daniel Blankschtein's research group for their friendly manner and interesting discussions on a variety of topic. The sense of community and solidarity within this research group provides an environment which is conducive to creative thinking. In particular, I wish to thank Teresa Carale, Leo Lue, Chia-Li Liu, Yvonne Nikas, Sudhakar Puvvada and Claudia Samoria, - "May all their dreams come true" (Blankschtein, 1986-1991).

I also thank Professors Daniel Blankschtein and Alan Hatton for their financial support during my graduate study. At no stage was I confronted with the daunting issue of funding and I thank them for providing me with a financially solvent research environment. In addition, I thank the George Murray Scholarship Fund of the University of Adelaide, Australia, the Fulbright Exchange Program, the Bioprocess Engineering Center of MIT, and the Whitaker Foundation for financial support during my graduate study.

I express my gratitude to my wife, Rachel. Her patience and encouragement have been greatly appreciated. From Rachel, I hope to learn the art of combining scholarly acheivement, modesty and civility.

I thank my squash coach, Brian Kelly - your patience and good humor on the squash court were always enjoyed. Finally, I thank Carol Phillips for her kind and generous help, and for reminding me that I was in Boston, U.S.A.

TABLE OF CONTENTS

LIST OF FIGURES

LIST OF TABLES

INTRODUCTION

The interactions of *globular colloidal particles* and *flexible chain macromolecules* control phenomena such as the formation of complexes between polymers and micelles (Tokiwa and Tsujii, 1973; Shirahama, 1974; Shirahama and Ide, 1976; Cabane, 1977; Cabane and Duplessix, 1982 and 1987; Goddard, 1986a and 1986b), as well as the polymeric stabilization and flocculation of gold sols (Heller and Pugh, 1956), ceramic particles (Woodhead, 1986), and other colloidal dispersions (Napper, 1983). The macroscopic consequences of these interactions play a central role in the technologies of photographic developing, food processing, emulsion/microemulsion polymerization, and enhanced oil recovery. Central to developing an understanding of the relationship between the molecular-level structure and the macroscopic properties of these complex fluids has been the synthesis of experimental and theoretical techniques from the fields of colloid science, physical chemistry and polymer physics. In contrast, fluids of a biological origin, which bear similar features to these complex fluids, have been less explored using similar philosophies and combinations of theoretical and experimental investigative techniques. One such example, which is explored in this thesis, is aqueous solutions of globular proteins and flexible (synthetic and biological) polymer molecules.

Aqueous solutions of flexible polymers and globular proteins are particularly interesting under conditions where the polymer solution has undergone phase separation (Albertsson, 1986; Walter et al., 1985). In the resulting *two-phase aqueous polymer system*, proteins usually distribute unevenly between the two coexisting polymer solution phases. Investigations of the partitioning of proteins and other biomolecules in two-phase aqueous polymer systems has been stimulated by the potential of these polymer solutions to provide immiscible, yet protein compatible, liquid phases for the purification of proteins by liquid-liquid extraction (Albertsson, 1985; Walter et al., 1985; Kula et al., 1982; Abbott et al., 1988). Furthermore, the presence of polymers in a protein purification process may provide other advantages related to (i) polymer-enhanced protein refolding (Cleland, 1991), and (ii) protein stabilization in the final product formulations. However, at the molecular-level, the understanding of the interactions of globular

proteins and flexible synthetic polymers which are responsible for the potentially useful properties of these solutions, is primitive (Brooks et al, 1985; Baskir et al, 1989a; Abbott et al, 1990).

The absence of a fundamental understanding of protein-polymer interactions, combined with the potential utility of aqueous solutions of proteins and polymers, has motivated and guided the direction of the investigation reported in this thesis. Specifically, three broad questions have been addressed:

(i) What factors constitute a *physical basis* for an understanding of protein partitioning? Specifically, how important are *geometry* and *energetics* in determining protein-polymer interactions?

(ii) Can we usefully apply *scaling concepts* from polymer physics (de Gennes, 1988) to rationalize the macroscopic consequences, such as protein partitioning behaviors, associated with different protein-polymer interaction mechanisms?

(iii) Can we reach a unified *theoretical description* of both the *molecular-level structure* and the *thermodynamic properties* of protein-polymer solutions, and verify both aspects using *experimental* methods?

In order to address these questions we have combined a variety of complementary experimental and theoretical techniques. At the outset, in an effort to understand the essential physics and develop a *physical basis* for understanding protein partitioning in two-phase aqueous polymer systems, polymer *scaling concepts* proved to be a powerful theoretical tool (de Gennes, 1988). For a variety of proposed physical scenarios, *statistical-thermodynamic descriptions* of protein partitioning were developed, and the associated protein partitioning behaviors were predicted. When used in conjunction with *equilibrium partitioning experiments*, these theoretical predictions proved to be a useful approach in discerning the differences among a number of potential partitioning mechanisms. Subsequent and more detailed treatments of possible partitioning mechanisms exploited an *equation of state/Monte-Carlo* approach to predict both

experimental trends in the (equilibrium) protein partitioning behavior, as well as the *scattering of neutrons at small angles* (SANS) from solutions of proteins and polymers.

Finally, it is pertinent to stress how the philosophy behind the theoretical formulation reported in this thesis differs from earlier investigations of protein partitioning in two-phase aqueous polymer systems. First, in this investigation we have stressed the physical nature of aqueous solutions of globular proteins and flexible polymers. Indeed, earlier theoretical investigations appear to have approximated their physical description of the system in favor of theoretically convenient models. For example, the globular protein molecules have been described as random coiling polymer coils with Gaussian statistics (Albertsson et al, 1987; Diamond and Hsu, 1989), or the underlying structure of the polymer solution at the length scale of the proteins has been neglected (Baskir et al, 1987; Baskir et al, 1989b; Forciniti and Hall, 1990). In this thesis, a theory of protein partitioning is advanced which proposes that it is precisely the underlying polymer solution structure that is responsible for a number of observed partitioning behaviors (Abbott et al, 1991a). Finally, it is relevant to mention that for the first time, using the same physical description of the protein-polymer interactions, we have predicted the thermodynamic and structural properties of aqueous solutions of proteins and polymers, and confirmed them using partitioning measurements and small angle neutron scattering techniques (Abbott et al., 1991a-d).

Chapter 1.

An Introduction to the Separation of Biological Molecules using Liquid-Liquid Extraction Techniques

1.1 On the Need for Novel Protein Purification Processes

Biotechnology has received a major boost over the past decade from the rapid advances made in genetic engineering, particularly in the areas of recombinant DNA technology and mammalian cell culture. These advances hint at numerous possibilities for the unprecedented production of a variety of proteins important to the research, pharmaceutical and industrial communities. In many cases, however, the impressive gains made in the technology for cloning genes for these proteins have not been matched by similar advances in the technology for purification of the expressed gene product.

The problems traditionally faced by the chemical engineer in conventional chemical engineering separation operations pale in comparison to the requirements often placed on the separation of bioproducts. To provide conditions that maintain cell viability and a high target protein yield, extremely stringent constraints are placed on the production medium which may hamper the separation process. The proteins of interest are produced in a complex mixture of contaminating proteins (many of which have properties very similar to those of the desired product), cell wall material and nucleic acids. Separation from these complex mixtures is frequently complicated by the lability of the desired products, and by the stringent final product purity specifications. As a result, in recent years there has been an increased interest in the development of efficient methods for the separation, concentration and purification of proteins and other biological products from fermentation and cell culture media. The traditional bench-scale

separation approaches, such as electrophoresis or column liquid chromatography, are difficult to scale-up to production levels and can become prohibitively expensive unless high-valued products are being produced. Other approaches are needed.

Liquid-liquid extraction as a technology has served the chemical, petrochemical and hydrometallurgical industries well in the past, and has been used extensively in the antibiotics industry for about fifty years. It is only recently, however, that liquid extraction has been recognised to be a potentially useful primary purification step in the overall protein recovery train, since it is readily scalable and can, if necessary, be operated on a continuous basis. It is a reasonably high capacity process and can offer moderate to good selectivity for the desired products. However, the sensitivity of the large labile molecules to their solvent environment restricts the range of solvents available for use in such a separation process.

Two classes of solvents that appear to offer many advantages for protein recovery operations are aqueous polymer systems and reversed micellar solutions. In both cases, reliance is placed on the differential partitioning of proteins between the immiscible feed and solvent phases to effect the extraction of the desired protein from the complex production mixture. However, the principles of solubilization differ greatly. For the aqueous polymer extraction processes the partitioning of the protein occurs between two immiscible aqueous phases with each phase being rich in one of two distinct polymer species. Some major advantages of the aqueous polymer systems include high protein capacity, non-denaturing solvent environment, small interfacial resistance to protein transfer and high selectivity. Reversed micellar solvent extraction, on the other hand, relies on the unique solubilising properties of many surfactants which often aggregate in organic solvents to form reversed or inverted micelles. These aggregates consist of a polar core of water and solubilised species stabilised by a surfactant shell layer. For protein extraction two bulk equilibrium phases are used, one being the aqueous feed solution, the other the reversed micellar phase which serves as the extractant. These systems also appear to have many of the advantages cited for the two phase polymer systems. For an overview on the solubilization of proteins in reversed micelles the reader is referred to Luisi et al. (1986, 1988), Martinek et al. (1986), Leser

et al. (1986), Dekker et al. (1986), Goklen and Hatton (1985, 1987) and Khmelnitski (1989).

The aim of Chapter 1 is to outline the principles, process applications, merits and limitations of the method of liquid-liquid extraction for process scale protein recovery using two-phase aqueous polymer systems. The emphasis of Chapter 1 is on practical and technical considerations which are relevant to the practitioner; Chapter 2 provides an overview of the more fundamental considerations and the current understanding of the molecular-level mechanisms which drive the partitioning of proteins between the two coexisiting polymer solution phases of a two-phase aqueous polymer system.

1.2 Aqueous Two-Phase Systems: A Brief Introduction

As first recorded by the Dutch microbiologist Beijernick (1896), who tried unsuccessfully to mix aqueous solutions of starch, gelatin and agar, many hydrophilic polymers are incompatible with other polymers or salts in aqueous solution. This often results in a phase separation, with the formation of two immiscible aqueous phases, each containing primarily only one of the two phase-forming polymers or salts. The observation by Albertsson (1985a,b) in the early fifties that proteins often distribute unevenly between these phases has been the impetus for much research in this area leading to its exploitation by Kula and co-workers (1981, 1982a,b) in large-scale protein recovery operations.

A phase diagram for a typical two-phase aqueous polymer system is shown in Figure 1.1 for the poly(ethylene oxide) (PEO) - dextran system. Both polymers are separately miscible with water in all proportions, and, at low polymer concentrations, with each other. However, as the polymer concentrations increase phase separation occurs, with the formation of a PEO-rich upper phase and a dextran-rich lower phase, each of which consists of greater than 80 percent water. The curve separating the two-phase and homogeneous mixture regions is known as the binodal. Within the two-phase region, any mixture of the three components must split into two phases, the compositions

of these two phases being dictated by the intersections of the tie-line passing through the mixture point with the binodal. For instance, in Figure 1 a system comprised of 95% water, 2.5% dextran and 2.5% PEO (point A) lies above the binodal, and is a stable homogeneous phase. On the other hand, a system of 85% water, 10% dextran and 5% PEO (point B), which falls below the binodal, will separate into two phases, one of which is 90% water and 10% PEO (point C), the other being approximately 80% water, 19% dextran and 1% PEO (point D). The relative volumes of the two phases will be given by the inverse lever arm rule, which states that

$$\frac{V_d}{V_c} = \frac{CB}{BD} \tag{1.1}$$

V_c and V_d are the volumes of the phases at composition points C and D on the phase diagram, and CB and BD are the lengths of the line segments connecting points C with B and B with D, respectively.

The phase behaviour of the polymers is also dependent on the type of salt present, and its concentration, owing to the competition between the salt ions and polymer for water of hydration. In many cases a sufficiently high concentration of salt in a single polymer solution can induce phase separation to form one predominantly salt phase, the other phase containing most of the polymer. The phosphate/PEO/water system, in particular, has attracted much attention because of its favourable properties for protein extraction processes. Examples of other phase forming polymers and salts are presented in Table 1.1.

As noted before, this immiscibility of two predominantly aqueous phases can be exploited in the recovery of proteins from solution using liquid-liquid extraction techniques, since often proteins distribute unevenly between the two phases, depending on specific protein characteristics and phase composition. Such systems have the advantage that since both phases are comprised predominantly of water, they offer a benign environment for the proteins and minimise the possibility of damage to the labile bioproducts. Moreover, the extremely low interfacial tensions characteristic of these

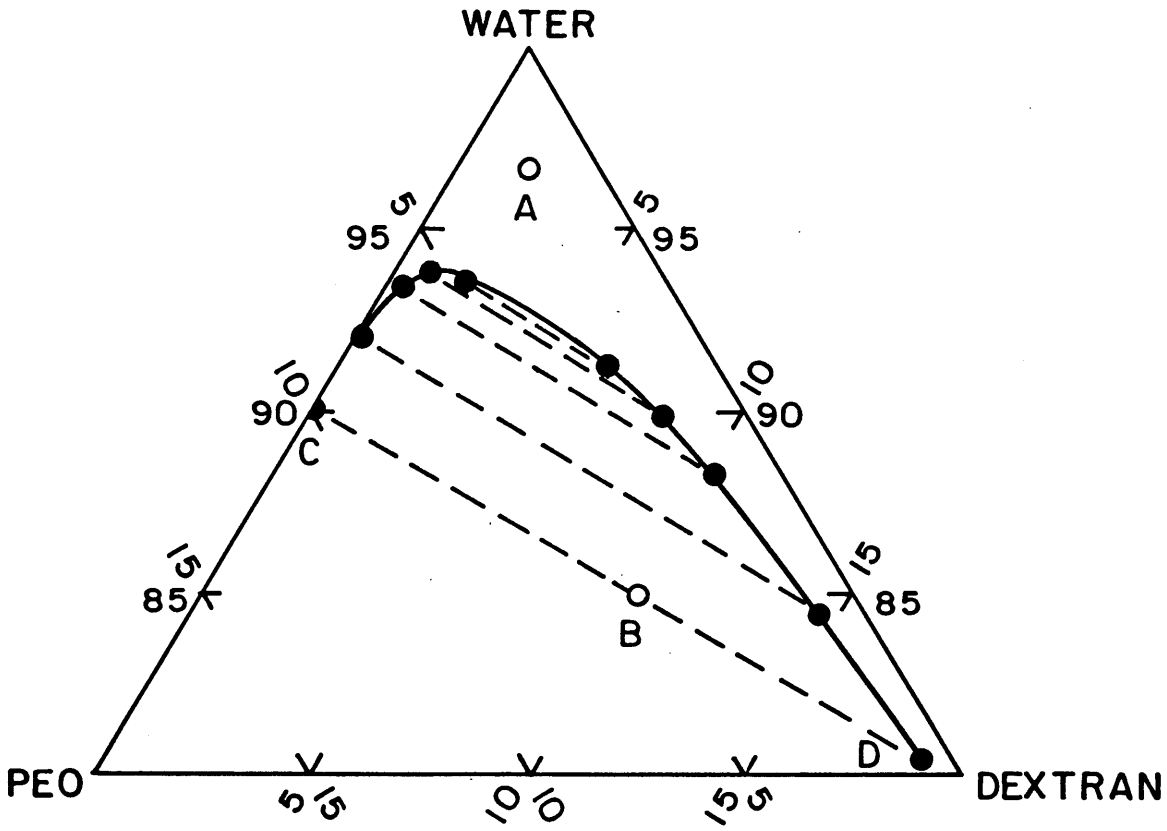

Figure 1.1 Phase diagram for the dextran 68/PEO 6000/water system at 20°C (Albertsson, 1985a).

systems ensure that the proteins are not subjected to undue stress as they cross the interface between the two phases. However, if these phase systems are to be acceptable as separating agents, there must be some level of discrimination between differentproteins. This specificity is evident in the large number of studies reported in the literature over the past three decades, which are detailed in Chapter 2 and very briefly outlined below.

Many factors contribute to the distribution of a protein between the two phases (Albertsson, 1985a; Walter et al., 1985; Walter and Johansson, 1986; Carlson, 1988; Baskir et al., 1989; Abbott et al., 1990; Walter et al., 1991). This distribution is normally characterized in terms of the partition coefficient

$$K_p = \frac{c_t}{c_b} \tag{2.2}$$

where c_t and c_b are the protein concentrations in the top and bottom phases respectively. To a first approximation these factors can be treated as independent so the partition coefficient can be written as

$$\ln K_p = \ln K_o + \ln K_{elect} + \ln K_{biospec} + \ln K_{hydroph} + \ln K_{conf} \tag{3.3}$$

where the subscripts *elect, biospec, hydrophob,* and *conf* represent the electrical, biospecific, hydrophobic and conformational contributions to the partition coefficient. K_o contains factors not specifically accounted for in the other coefficients, including polymer properties, molecular weight and concentration, and protein structural aspects such as size, charge and hydrophobic characteristics.

1.3 Process Considerations

Among the advantages of using two phase liquid extraction for the recovery of proteins are the ease of scale-up and the exploitation of existing knowledge and strategies for production scale implementation in process development. There are,

Poly(ethylene oxide)	**Poly(vinyl alcohol)** **Dextran** **Ficoll** **Potassium Phosphate**
Poly(propylene glycol)	**Methoxypoly(ethylene oxide)** **Hydroxypropyldextran** **Polyvinylpyrrolidone** **Dextran**
Methylcellulose	**Hydroxypropyldextran** **Dextran**

Table 1.1 Selected two-phase systems formed by incompatible neutral polymers and salts.

however, a number of differences that exist between the physical properties of low molecular weight solvent phases and the higher molecular weight aqueous polymer phases, and these must be accounted for in the transfer of technology. For instance, three important parameters in any liquid-liquid extraction process are the phase viscosities, the interfacial tension and the density difference between the solvent phases, since these determine the ease of phase dispersion for mass transfer and the difficulty of the subseqent phase separation step. Compared to most traditional processes the interfacial tension between the two phases is extremely low at approximately 0.1 dyne/cm for PEO/salt and 0.0001 dyne/cm for PEO/dextran systems (Ryden and Albertsson, 1971; Schurch et al., 1981; Bamberger et al., 1984; Forciniti et al, 1990). The primary reason for the low interfacial tension is the high volume fraction of water in each of the phases, typically around 80 - 90% w/w (Albertsson, 1985a). The viscosities are higher than for the low molecular weight solvents with the magnitude depending both on the molecular weight of the phase polymers and the presence of contaminating particles in the system. The viscosity can vary between 10-15 cp up to 3000 cp for the higher molecular weight dextran phases (Johansson, 1978). The presence of cellular matter in protein extraction from cell homogenates results in a further increase in the viscosity of the phases. The small density difference between the phases, typically 5 g/l for PEO and salt, can be enhanced by the partition of cell debris to one of the phases (Ryden and Albertsson, 1971; Albertsson, 1985a).

Phase equilibration in two phase polymer salt systems in agitated vessels is generally rapid, and only low stirrer speeds are required to provide sufficient interfacial area for efficient protein transfer. This is in spite of the very high viscosities exhibited by the polymer phases in the presence of cell debris. The reason for this is that very small droplets are formed with low power inputs because of the low interfacial tensions characteristic of these systems. Indeed, Fauquex and coworkers (1985) suggest that the rate-limiting step in the phase equilibration is the formation of the phases themselves as controlled by the dissolution of the phase polymers and salts, which are normally added as concentrated solutions or solids. It has been suggested that in these systems the usual criteria for scale-up of mixing processes, based on equal power-input

per unit mass, be applied.

Kula et al. (1982a, 1982b) have discussed the technical aspects of the phase separation process. In the absence of any applied force fields the separation rate of the two phases is slow, taking typically 60-90 minutes for good separation to occur in PEO/salt systems, due in part to the small density differences between the phases. To enhance the rate of phase separation disk stack centrifugal separators have been used effectively. The well known formula describing the throughput is

$$Q = \frac{D_{lim}^2 \Delta\rho\omega^2 r\Omega}{18\eta} \qquad \textbf{(1.4)}$$

where Q is the volumetric throughput, D_{lim} is a diameter characteristic of the smallest droplet captured, $\Delta\rho$ is the density difference between the phases, η is the dynamic vicosity, r is the radius of rotation and Ω is a machine parameter characteristic of the cross sectional area available for separation. It is readily apparent that the high viscosity, particularly in the presence of cell homogenates, and the low density difference do not favor high throughputs. The purity of the separated phases depends on the correct positioning of the interface between the phases which is determined both by the discharge radii for each of the phases and by the density difference between the phases. The interface position may be further adjusted by regulation of the discharge phase flowrates from the separator.

A variation on this centrifugal separation of the dispersed phases is the use of nozzle separators (Kula et al., 1982b). This adaptation is particularly useful when one of the phases is very viscous, for example when loaded with cell debris. Rather than discharging the denser phase from the top of the separator the heavy phase is ejected directly from the periphery of the bowl via a set of nozzles. The size of the nozzles is crucial to the effectiveness of the process. Kula et al. (1982b) have demonstrated that the large scale separation of formate dehydrogenase from candida boidinii can be readily accomplished using an Alfa-Laval separator model Gyrotester B with a PEO/salt system. Typical operating conditions with a feed dispersed phase volume ratio of 2.84 and a

process flow rate of 1.5 l/min resulted in formate dehydrogenase yields of 96.5% in the top phase, with 99.5% purity.

An added advantage of using these processes is the small temperature rise, typically about 1.5 K, that occurs during the processing steps. This, coupled with the short process times, obviates the need for the additional cooling of the process streams usually required in traditional separation schemes.

Two-phase polymer systems offer other advantages over conventional separation processes in that cell debris can be efficiently removed simultaneously during the enzyme extraction. The limiting particle size in the design of the centrifuge is the size of the dispersed phase droplet rather than that of the individual cell particles, which are considerably smaller. The result is a more efficient removal of the cell debris from the target enzymes. The advantages gained in capital expenditure and operating cost, however, must be weighed against the cost of the phase polymers and of their recycle.

The individual operations of sequential dispersion, equilibration and phase separation may be replaced by using multistage contacting devices such as extraction columns (Kula et al., 1981). However, the low interfacial tensions and density differences characteristic of two-phase polymer systems require that low stirrer speeds be used to prevent the formation of too fine a dispersion of the one phase in the other, which can lead to poor phase separation, entrainment and flooding of the column. On the other hand, a high interfacial area is required for the rapid equilibration of the protein distribution between the phases. These two conflicting demands place rather severe constraints on the range of agitation speeds that can be used in traditional column-type contactors, and limit their usefulness in this category of separations.

Many of the problems associated with column-type contactors can be avoided using hollow-fibre membrane extractors. In these systems, the membrane acts simply as a support for the interface between the phases, and does not itself perform any specific separation function. The two phases to be contacted flow on either side of the membrane, and, since the phases are never interdispersed, phase disengagement is not a concern. Consequently, there are no severe restrictions on the flow rate ratio. The intimate contact required for efficient mass transfer is obtained by providing a large

membrane surface area, which more than compensates for the diffusional mass transfer resistance offered by the membrane pores, such that overall mass transfer rates can in fact be much greater than those attainable in conventional dispersed phase systems. Dahuron and Cussler (1988) have demonstrateed the effectiveness of these systems for use in two-phase aqueous polymer protein extractions. Overall mass transfer coefficients were well-correlated over a wide range of operating conditions, and for a number of different proteins, using standard correlations for the lumen and shell-side boundary layer resistances. These extractors will best be used with the polymer-salt two-phase systems subsequent to the cell debris removal steps because of the lower phase viscosities associated with these systems.

One of the important issues that needs to be addressed in the large scale implementation of two-phase polymer systems for enzyme recovery is the economic requirement that the phase-forming polymers and salts be recycled to the extent possible. An example of one process that has been reported is provided in the flowsheet shown in Figure 1.2 for the recovery of fumarase from bakers yeast cell homogenates in a PEO/salt system (Hustedt et al., 1984). The enzyme partitioned to the top PEO phase in the primary extraction from the cell homogenate, while the cell debris was collected in the bottom, salt phase which was subsequently discarded. In a second extraction step, the enzyme was recovered from the loaded PEO phase by reporting to the second phase formed when excess phosphate salt was added to the system. The PEO phase polymer was then recycled to be used again in the primary extraction step. Although not shown on the flowsheet, the enzyme could be concentrated by ultrafiltration, and the salt permeate returned with the PEO phase polymer to the primary extraction step. This flowsheet reduces the chemical requirements for the process, but the recycling of the phase forming components can lead to an unacceptable build-up of proteases and other contaminants in the process, which can in principle be controlled by the use of a purge stream, and by further treatment of the recycled streams.

Other methods of phase polymer recovery have also been suggested. These include diafiltration of the protein and polymer following dilution of the phases, washing by repeated centrifugations, enzyme precipitation with organic solvents, salts and

acids, and adsorption of the enzyme onto an ion exchange resin or other suitable adsorbent (Kula et al, 1982a). Also, the PEO polymer may be recovered by organic solvent extraction. The recovery of salts can be accomplished by electrodialysis, which can also be used for the desalting of PEO phases. Which method, if any, is used for chemical recycling will of course depend on the costs of recycling relative to the raw chemical costs.

A novel phase polymer system reported recently uses a random copolymer of amphoteric acrylic acid derivatives (Hughs and Lowe, 1988; Patrickios et al., 1991). In addition to being inexpensive and readily available, the polymers possess the novel property that they can be quantitatively precipitated by adjustment of the solution pH to conditions such that the phase polymers bear no net charge. The apparent ease of recovery of the polymers for recycle combined with their availability suggest that these systems warrant further investigation to assess their potential for liquid-liquid extraction of proteins.

1.4 Economic Considerations

In a few cases, the economics of two phase aqueous polymer extraction have been compared to the cost of protein recovery using other recovery techniques. Kula et al (1982b), for instance, compared the costs of liquid-liquid extraction recovery of formate dehydrogenase with a conventional extraction process using centrifugation, precipitation and column chromatography steps. A summary of the comparison is presented in Table 1.2. A major cost saving for the liquid-liquid extraction process was the reduction in process time compared to the convential process. This permitted the extraction to be carried out at ambient conditions, thereby avoiding the cooling required in conventional processes to limit degradation of the product during the separation; this resulted in significant savings in capital and operating costs. The process cost for the 4 stage liquid-liquid extraction process using a PEO/dextran system was dominated by the cost of the phase polymers, in particular of the dextran, which can contribute up to 90% of the two phase system materials cost. This is particularly significant for processes

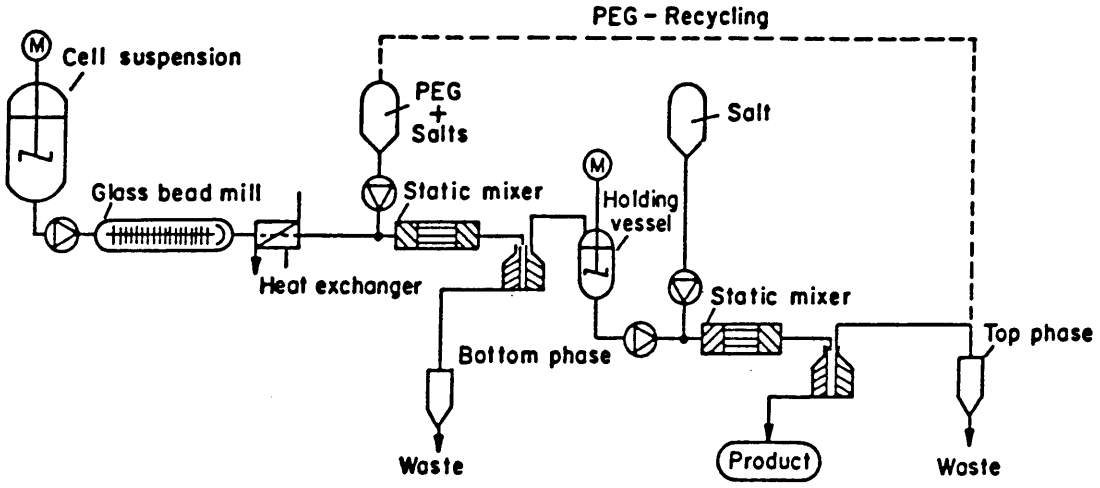

Figure 1.2 Flow diagram of extractive enzyme recovery with recycling of PEO phase polymer (Hustedt et al., 1984)

involving enzyme purification from cell homogenates as the dextran usually has to be discarded along with the cell debris. The cost of the PEO polymer is more tolerable, as is that of the salts in a PEO/salt system.

The dominating cost of the dextran has resulted in a considerable effort targetted at finding inexpensive phase polymers and methods for their recovery and recycle. One potential solution is the use of crude dextran or hydrolysed crude dextran rather than the fairly monodisperse and more expensive fractions used in the early work (Kroner et al., 1984). While these crude fractions seem to have little effect on the protein partitioning behaviour, their rheological properties are less favourable. However, the use of higher molecular weight polymers has the advantage that lower quantities of the polymer are required to form the two-phase polymer system. In many instances, the cell debris assists in the phase separation process, again reducing the polymer concentration required for the formation of the two phases. Indeed, while the cost of the crude dextran on a mass basis is still significantly higher than the other component costs, the lowered mass requirements brings the total cost into line with that of the other polymers used in these systems.

The use of crude phase polymers can influence the separation efficiency of the dispersed phase in an open disc stack centrifugal separator because it permits higher optimal flow rates to be used than with the refined dextran phase system. This can have a significant effect on the cost of cell debris removal, which was found to be 30 to 40 percent lower than the cost associated with the conventional, intermittent operation of high speed centrifuges used for this purpose. The difference was attributed primarily to the batch operation of the high speed centrifuge; no comparison was made to the costs related to the continuous operation of a solids discharging centrifuge.

More recently Tjerneld et al. (1986) and Birkenmeier et al. (1987) have reported on the use of a new low cost phase polymer, a hydroxypropyl derivative of starch. The lower molecular weight hydroxypropyl starch (M_n = 30 000) required higher concentrations of the phase polymers for phase separation when compared with the dextran system (M_n = 200 000). In both cases the other phase forming polymer was PEO-8000. The physical properties of the polymer are attractive as it has a low viscosity

	Partition	Conventional
Total Cell Mass	**50**	**5**
Initial Units	**460 x 10^3**	**31 x 10^3**
Purity (U/mg)	**2.2**	**2.2**
Yield (%)	**70**	**51**
Net Time (hr)	**18**	**121**
Performance Factor (U/kg.hr)	**356**	**26**
Cost Index (DM/unit)	**7 x 10^{-3}**	**374 x 10^{-3}**

Table 1.2 Comparison of technical and economic performance for purification of enzyme formate dehydrogenase by aqueous partition method or conventional extraction precipitation-chromatographic method (Kula et al., 1982a).

and high protein capacity. Further, even with the higher polymer phase concentration the cost of the hydroxypropyl starch phase was estimated at US$ 3-3.5 per litre compared to the refined dextran phase at US$ 22-23 per litre. The cost of the hydroxypropyl starch phase is similar to that of the hydrolysed crude dextran phase, however.

1.5 Conclusions

The liquid-liquid extraction of proteins directly from fermentation media or cell homogenates is an attractive primary purification process, and can be used both to remove cell debris and to provide some initial purification and concentration of the desired products. Suitable solvents for this extraction process are the two phase polymer systems which offer moderate to high selectivities and capacities for the proteins to be recovered. Protein partitioning to the extractants can be controlled in a number of ways, including the changing of pH conditions, varying the ionic strength and salt type, and changing polymer or surfactant concentrations. Affinity partitioning has also been found to be effective in enhancing the selectivity of the extraction for specific proteins

Some of the advantages associated with liquid extraction techniques for protein recovery include easy and reliable scale up from small scale laboratory experiments, and the possibility of continuous operation for the direct, in-situ recovery of products during the fermentation process. Moreover, since the separation is usually rapid, protein stability problems do not arise, and the separation may be carried out at room temperature; in more conventional separation systems, the long processing times require cooling of the process streams to prevent product degradation. Further, the enzymes are often stabilised by the phase-forming polymers.

The effectiveness of liquid-liquid extraction for bioproducts, has led to its commercial applications in a number of processes, and many more plants are currently being planned or implemented. Liquid-liquid extraction is likely to play an increasingly significant role in the further development of the new biotechnology.

1.6 Literature Cited

Abbott, N.L.; Blankschtein, D.; Hatton, T.A., *Bioseparation*, **1990**, 1, 191.

Albertsson, P.-A., *Partition of Cell Particles and Macromolecules*, Wiley and Sons, N.Y., **1985a**.

Albertsson, P.-A., in Partitioning in Aqueous Two Phase Systems, Walter, H.; Brooks, D.E.; Fisher, D., Eds, Academic Press, N.Y., **1985b**.

Baskir, J.N.; Hatton, T.A.; Suter, U.W., *Biotechnol. Bioeng.*, **1989**, 34, 541.

Bamberger, S.; Seaman, G.V.F.; Sharp, K.A.; Brooks, D.E., *J. Colloid Interface Sci.*, **1984**, 99, 194.

Beijerinck, M. W., Zentr. Bl-Bakt., **1896**, 2, 698.

Birkenmeier, G.; Kopperschlager, G.; Albertsson, P.A.; Johansson, G.; Tjerneld, F.; Akerlund, H.E.; Berner, S.; Wickstroem, H., *J. Biotechnology*, **1987**, 5, 115.

Carlson, A., *Separation Science and Technology*, **1988**, 23, 785.

Dahuron, L.; Cussler, E.L., *AIChE Journal*, **1988**, 34, 130.

Dekker, M.; Van'T Riet, K.; Weijers, S.R.; Baltussen, W.J.A.; Laane, C.; Bijsterbosch, B.H., *Chem. Eng. J.*, **1986**, 33, B27.

Fauquex, P.F.; Hustedt, H.; Kula, M.R., *J. Chem. Tech. Biotechnol.*, **1985**, 35B, 51.

Forciniti, D.; Hall, C.K.; Kula, M.R., *J. Biotechnology*, **1990**, 16, 279.

Goklen, K.E.; Hatton, T.A., *Biotech. Prog.*, **1985**, 1, 1985.

Goklen, K.E.; Hatton, T.A., *Sep. Sci. Tech.*, **1987**, 22.

Hughes P.; Lowe, C.R., *Enzyme Microb. Technol.*, **1988**, 10, 115.

Hustedt, H.; Kroner, K.H.; Kula, M.R., *Proc. Eur. Congr. Biotechnol.*, **1984**, 1, 597.

Johansson, G., *J. Chromatogr.*, **1978**, 150, 63.

Kula, M.-R.; Kroner, K.H.; Hustedt, H.; Schutte, H., *Ann. N. Y. Acad. Sci.*, **1981**, 341.

Kula, M.-R.; Kroner, K.H.; Hustedt, H., *Advances in Biochem. Eng.*, **1982a**, 24, 73.

Kula, M.-R.; Kroner, K.H.; Hustedt, H., *Enzyme Engineering*, **1982b**, 6, 69.

Kroner, K. H.; Hustedt, H.; Kula, M.R., Biotech. Bioeng., **1982**, 24, 1015.

Leser, M.E.; Wei, G.; Luisi, P.L.; Maestro, M., *Biochem. Biophys. Res. Commun.*, **1986**, 135, 629.

Luisi, P.L.; Magid, L.J., *CRC Crit. Rev. Biochem.*, **1986**, 20, 409.

Luisi, P.L.; Giomini, M.; Pileni, M.P.; Robinson, B.H., *Biochim. Biophys. Acta*, **1988**, 947, 209.

Martinek, K.; Levashov, A.V.; Klyachko, N.; Khmelnitski, Y.L.; Berezin, I.V., *Eur. J. Biochem.*, **1986**, 155, 453.

Patrickios, C.; Abbott, N.L.; Foss, R.P., Hatton, T.A., *Biosep. Technol.*, **1991**, in press.

Ryden, J.; Albertsson. P.A., *J. Colloid Interf. Sci.*, **1971**, 37, 219.

Schurch, S.; Gerson, D.F.; McIver, D.J.L., *Biochim. Biophys. Acta*, **1981**, 640, 557.

Tjerneld, F., Berner, S.; Cajarville, A.; Johansson, G., *Enzyme Microb.Technol.*, **1986**, 8, 417.

Walter, H.; Brooks, D.E.; Fisher, D., *Partitioning in Aqueous Two Phase Systems*, Academic Press, N.Y., **1985**.

Walter, H.; Johansson, G. *Analytical Biochemistry*, **1986**, 155, 215.

Walter, H.; Johansson, G.; Brooks, D.E., *Analytical Biochemistry*, **1991**, (in press).

Chapter 2.

Mechanisms of Protein Partitioning in Aqueous Two-Phase Polymer Systems.

2.1 Introduction

The partitioning of proteins between two immiscible aqueous polymer solution phases has been known for over 30 years (Albertsson, 1958). Many of the studies in this area have either focussed on developing and assessing the technical merits and limitations of two-phase aqueous polymer systems for the purification of proteins from synthesis media, or on elucidating the physical nature of these systems and the factors influencing protein partitioning (Albertsson, 1985). In general, the former types of investigations, as outlined in Chapter 1, have been concerned with the extraction of proteins from the fermentation broths in which they were synthesized (Kula et al., 1982). Such systems are extremely complex as they contain a myriad of components including residual salts and sugars left over from the fermentation, cells and cell-wall material, and intracellular organelles and macromolecules including DNA. In contrast, the latter types of investigations have been performed in relatively well-defined systems, comprising, at least, two different polymer types to form the two-phase system, water as the solvent, salts to control ionic strength and pH, and at least one type of protein. Even the simplest description of the observed partitioning behavior, treating only the pairwise interactions between the various components which cause the protein partitioning, and thus neglecting possible synergistic effects due to three-body and higher-order interactions, constitutes a formidable task. Indeed, as our current understanding of the individual components is often quite primitive, e.g., the proteins may possess very complex structures, elucidating the essential factors influencing protein partitioning is a challenging

undertaking. In spite of the complexity, a number of well-defined experiments performed with a judicious choice of experimental conditions, and complementary theoretical developments have been successful in shedding light on the nature of the underlying interactions in these systems (Albertsson, 1985; Brooks et al., 1985; Baskir et al., 1989c; Forciniti and Hall, 1990; Abbott et al., 1991).

Protein partition coefficients are observed experimentally to depend on the chemical nature of the phase-forming polymers (Albertsson, 1985), their molecular weight (Hustedt et al., 1978, Albertsson et al., 1987, Forciniti et al., 1991a,b) and concentration (Albertsson, 1985; King et al.; 1988, Baskir et al., 1989a, Forciniti et al., 1991b), and the presence of any functionalities bound to the polymers which may interact with specific sites on the proteins (see Section 2.3.6). The addition of salts also affects the distribution of proteins between the two coexisting polymer solution phases, with the effect dependent on both the type and concentration of the salt (see Section 2.3.5). Variation in solution pH impacts on the interphase distribution of the proteins in a way dependent on the specific salt type present (see Section 2.3.5). As might be anticipated, the size, conformation and chemical nature of the proteins all appear to be important factors in determining their partitioning behavior (see Sections 2.3.1 and 2.3.2).

In general, modelling attempts have been aimed at providing suitable methodologies and design equations for the development and control of separation processes using two-phase aqueous polymer systems, as well as at providing insight into the physical nature of the interplay between the various components present in these systems and their influence on the observed partitioning behavior of proteins. To date, the models can be broadly divided into three classes: (1) lattice models, which are based on a lattice representation of the polymer solutions within each of the two coexisting phases, and (2) virial models, which use a virial-type expansion in the concentration of the components of the system to describe thermodynamic properties.

The central aims of Chapter 2 are to review both experimental and modelling approaches directed at elucidating the nature of the interactions between the components of two-phase aqueous polymer systems and their influence on the observed partitioning of proteins, as well as to review recent modelling approaches for the design

of separation systems using two-phase aqueous polymer systems. In particular, the various modelling approaches will be compared and contrasted with each other, and the merits and limitations of each approach will be emphasized. The remainder of Chapter 2 is organized as follows. In Section 2.2, the nature of the phase separation which gives rise to the formation of two-phase aqueous polymer systems is discussed. Section 2.3 overviews experimental investigations of the factors influencing the partitioning of proteins in two-phase aqueous polymer systems. Section 2.4 reviews models of protein partitioning. Finally, in Section 2.5 we conclude with some comments on the inadequacies of our current understanding of protein partitioning, some of which, are the subject of investigation in this thesis.

2.2 Phase Separation in Aqueous Polymer Solutions

In most cases, experiments and theories aimed at investigating the molecular-level nature of partitioning phenomena in two-phase aqueous polymer systems have been performed in the limit of very low protein concentrations ($<0.1\%$w/w), where the protein presence has been shown to have negligible effect on the two-phase equilibrium associated with the phase forming polymers, water and salts (Baskir, 1988). This important observation is useful, as it suggests that the protein partitioning can be considered to reflect solely the differences in the interactions of the proteins with each of the phases formed in the absence of the proteins, thus avoiding the need to consider the effect of the partitioning of the protein on the equilibrium distribution of the polymers, water and salt between each of the phases. Therefore, it is relevant to review briefly the experimental factors that influence the formation and composition of the two coexisting polymer solution phases in the absence of proteins. Note that at higher protein concentrations, which may indeed be encountered in practical separation processes, the previous assumption need not be valid, and the proteins should be counted as "phase-forming" components (Albertsson, 1985).

Frequently, the mixing of two different polymer types in a common solvent results in the formation of two coexisting polymer solution phases in equilibrium

with each other, with each phase containing predominantly solvent and only one of the polymer types (Dobry and Boyer-Kawenoki, 1947; Kern and Slocombe 1955; Kern, 1956). More specifically, most hydrophilic polymer pairs are incompatible in aqueous solutions at low polymer volume fractions, yielding two-phase systems having high volume fractions of water in each of the two phases (Albertsson, 1985). The resulting biocompatibility of these systems, and hence the suitability of two-phase aqueous polymer systems for the liquid-liquid extraction of proteins and other biomolecules, is a direct result of this remarkable phase behavior. Note that the association of unlike polymer species into a polymer-rich phase coexisting with a polymer-poor phase, referred to as coacervation, can also occur, but these systems will not be discussed here (Perrau et al., 1989). As in any immiscible system of small molecules, e.g., low molecular weight hydrocarbons and water, the driving force for the demixing process in polymer-polymer-solvent systems is the enthalpy associated with the interactions of the components, which is opposed by the loss in entropy associated with the segregation of the components during phase separation (Flory, 1953). The role of the solvent is particularly complex when it is a polar one such as water (Kjellander and Florin, 1981; Goldstein, 1984; Karlstrom, 1985; Sanchez and Balazs, 1989) due to the presence of orientation-specific interactions, for example, hydrogen bonding, between the polar solvent and polymers. In the systems under consideration here, the phase separation occurs at very low polymer volume fractions (typically 5% w/w polymer) owing to the large size of the polymer molecules and hence the corresponding small loss in entropy upon demixing. In addition, the enthalpy associated with the interactions of the polymer coils can be very large because it reflects the sum of the interactions between all the monomers in each polymer (typically a very large number) with the surrounding solution.

A phase diagram for a typical two-phase aqueous polymer system, polyethylene oxide (PEO)-dextran-water, is shown in Figure 1.1 (in Chapter 1). The reader is referred to the accompanying text in Section 1.2 for a discussion of the features of the phase diagram.

The molecular weights of the polymers in polymer-polymer-solvent systems usually influence the phase separation such that higher molecular weight

polymers will phase separate at lower polymer concentrations (Flory, 1953). Furthermore, as the difference in molecular weight between the two polymers increases, the binodal becomes more asymmetric. The increased propensity of high molecular weight polymers to phase separate follows from the smaller entropy loss *per unit mass of polymer* in the system upon demixing, or a larger enthalpy of interaction *per polymer coil* prior to demixing, relative to that experienced by a system containing smaller polymer molecules. Albertsson (1985) reported that a broad molecular-weight distribution in a polymer sample results in a larger region of immiscibility than that observed in a monodisperse polymer system having the same number-average molecular weight. This observation is supported by the results of UNIQUAC calculations, which predict that the two-phase region becomes larger for a broader polymer molecular-weight distribution (Kang and Sandler, 1988a,b). Furthermore, polymer fractionation occurs upon phase separation, with the larger polymer molecules (belonging to the high-molecular weight tail of the distribution) distributing more unequally between the two phases than the smaller polymer molecules (belonging to the low-molecular weight tail of the distribution). The fractionation of polymers between the phases may also be understood in terms of the interplay between enthalpy and entropy which drives phase separation, as discussed above.

The phase behavior of aqueous solutions of polymers can be affected by the addition of salts, the effect depending on both their type and concentration. In many cases, a sufficiently high concentration of salt in a single polymer-solvent system can induce phase separation to form a salt-rich, polymer-poor solution phase , which coexists with a salt-poor, polymer-rich solution phase (Boucher and Hines, 1976, 1978; Ataman and Boucher, 1982; Florin et al., 1984; Ananthapadmanabhan and Goddard, 1986; Ataman, 1987). The decreasing order of anion effectiveness in promoting phase separation of aqueous PEO solutions has been reported as $PO_4^{3-} > HPO_4^{2-} > SO_4^{2-} = CO_3^{2-} > S_2O_3^{2-} > H_2PO_4^- > F^- > HCOO^- > CH_3COO^- > Cl^- > NO_3^- > Br^- > I^-$, while for the cations it has been observed as $Rb^+ = K^+ = Na^+ > Cs^+ > Sr^+ > Ca^{2+} = Ba^{2+} > NH_4^+ > Li^+$. In general, while salts affect the phase separation of aqueous PEO solutions through a combined cation and anion effect, the anion effect

seems to be the dominant one. The mechanisms through which salts influence the phase separation of aqueous polymer solutions are still poorly understood. The difficulty in elucidating the origin of the salt effects in nonionic polymer systems appears to result from the important role of water structure (resulting from the polar nature of water molecules) in these systems. Indeed, these systems are rather different from the relatively well understood aqueous solutions in which fully-charged components interact through charge-charge (Coulomb) interactions. In systems which contain fully charged components, the strength of the charge-charge interactions is greater than that of the charge-dipole or dipole-dipole interactions involving water molecules. Consequently, one can make the remarkably successful approximation that the local structure of water may be neglected, and therefore water may be treated as a continuum characterized by either a constant or a spatially dependent dielectric permittivity (Booth, 1951, 1955). On the other hand, for systems such as PEO-water-salt, electrostatic interactions occur between the salt charges, dipoles or partial charges on the PEO, and the dipoles associated with water, and are similar in strength to the interactions occurring between water molecules. Thus, in contrast to electrostatic models, in which water is approximated as a continuum, salt effects are intimately associated with the structure of water about the ions and PEO, and therefore the continuum approximation appears less reasonable. To date, no quantitative models for salt effects in aqueous nonionic polymer systems exist. Qualitative explanations relate the observed behavior to the water-structure breaking attributes of the ions (Boucher and Hines, 1976; Ataman 1987), the binding of salts to PEO (Boucher and Hines, 1978), the competition between polymer and salt for water of hydration (Ananthapadmanabhan and Goddard, 1986; Ataman, 1987), and the presence of zones about the polymers which are depleted of salt due to the asymmetric hydration of ions near the polymer (Florin et al., 1984). For systems of the type polymer 1-polymer 2-water-salt, Zaslavsky et al. (1986, 1987 and 1988) reported that the aqueous system of PEO and dextran showed an increased tendency to phase separate with increasing salt concentration for the salts KBr, KCl, KNO_3, KI, KSCN, KF and K_2SO_4. In contrast, the aqueous ficoll-dextran polymer system displayed an initial decreased tendency to phase separate with the addition of salt (with the exception of KF and

K_2SO_4), followed by an increased tendency to phase separate at higher salt concentrations. An unambiguous interpretation of the mechanisms causing the observed behavior is not currently possible, and the relative roles of polymer-polymer, polymer-salt, polymer-water and salt-water interactions are unclear. Tentatively, the salt effects were attributed to two competing effects. The first is the influence of salts on polymer-water interactions (dipole-dipole), and the second is the effect of the salts on water-water interactions in the vicinity of the polymers. Zaslavsky et al. (1986) also suggest that direct ion-polymer binding affects the PEO-dextran system, but not other aqueous polymer systems.

The experimental observations of Sjoberg and Karlstrom (1989) indicate that moderate temperature changes (below 90°C) have only a small effect on the resulting ternary phase diagram for the PEO-dextran-water system. The extent of the two-phase region is almost unaffected by temperature changes, while the slopes of the tie-lines are changed, that is, an increase in temperature increases the concentration of PEO in the PEO-rich phase and decreases the concentration of dextran in the dextran-rich phase. Above 90°C, the two-phase region grows in size. Sjoberg and Karlstrom (1989) suggested that the temperature-dependent conformations of the polymers are the origin of these temperature effects, arguing that PEO (in water) can adopt a large number of conformations with differing polarities which interact with water with differing energies. The more polar conformations interact with water more favorably. At low temperatures, low-energy polar conformations dominate, whereas at high temperatures the polymer samples both low- and high- energy conformations resulting in the polymer becoming less hydrophilic, ultimately leading to phase separation at high temperatures. Similarly, the interactions of PEO and dextran, and dextran and water are assigned analogous temperature dependences to explain the observed ternary phase diagrams. In this model, the phase separation at low temperatures is suggested to be a consequence of the PEO-dextran interactions, whereas at high temperatures the role of PEO-water interactions becomes increasingly more important.

Chemical modifications to the phase forming polymers, to enhance protein partitioning to one phase or the other, include the covalent binding of charged groups

(Johansson, 1970b; Johansson et al., 1973), hydrophobic groups (Shanbhag and Johansson, 1974; Shanbhag and Axelsson, 1975; Johansson, 1976; Axelsson, 1978; Shanbhag and Johansson, 1979; Johansson and Shanbhag, 1984) and other ligands (for example, Flanagan and Barondes, 1975; Kopperschlager and Johansson, 1982; Cordes et al., 1987; Suh and Arnold, 1990) having specific affinity for particular proteins. These modifications of the phase forming polymers, particularly the introduction of charge groups covalently bound to the polymer, can alter their phase behavior.

2.3 Experimental Investigations of Protein Partitioning Mechanisms

As outlined in Chapter 1, it is instructive to express the partition coefficient as a sum of terms, each reflecting a characteristic physical factor contributing to its observed value (Albertsson, 1985), that is, to write the partition coefficient as

$$\ln K_p = lnK_p^{protein} + lnK_p^{polymer} + lnK_p^{salt} + lnK_p^{affinity} \qquad (2.1)$$

where $\ln K_p^{protein}$ and $\ln K_p^{polymer}$ reflect the contributions of the protein and polymer properties to the partition coefficient, $\ln K_p^{salt}$ reflects the contribution of the added salts to the partition coefficient, and $\ln K_p^{affinity}$ reflects the contributions of specific interactions between the polymer functionalities and sites on the protein. These factors are elaborated upon further in the discussions that follow. Note that the natural logarithm of the protein partition coefficient, $\ln K_p$, is used in Eq.(2.1), as this term is closely related to the free-energy change that characterizes the partitioning of the protein between the two coexisting aqueous polymer solution phases (see Section 2.4.5).

2.3.1 Protein Size

It is generally observed that as the size of the proteins and peptides increases, they tend to distribute more unevenly between the two phases (Sasakawa and Walter, 1972). For example, the partition coefficients of a number of dinitrophenylated

amino acids measured in the aqueous PEO-dextran (Sasakawa and Walter, 1974) and aqueous ficoll-dextran systems (Zaslavsky et al., 1980), and of dipeptides in the aqueous PEO-dextran system (Sasakawa and Walter, 1974; Diamond and Hsu, 1989) indicated a relatively even distribution of these small molecules between the two phases. For larger polypeptides such as proteins, however, the partitioning was generally less even, with large proteins partitioning more unevenly than small ones. The protein partition coefficients reported in Figure 2.1 (Sasakawa and Walter, 1972) were obtained in buffered systems at the isoelectric pH's of the respective proteins. At solution conditions away from the isoelectric pH, the correlation between protein size and partition coefficient is lost, for reasons that will be detailed below. Although the size of the protein appears to be an important factor, it is not clear whether the most appropriate measure of size is the volume or the surface area of the proteins. The data in Figure 2.1 for the partition coefficient are too scattered to resolve between an M (proportional to the volume of a globular protein) or an $M^{2/3}$ (proportional to the surface area of a globular protein) dependency, where M is the protein molecular weight. Although the correlation between the partition coefficient and the molecular weight of the protein, as shown in Figure 2.1, is evident, exceptions to this behavior have also been reported. For example, Sasakawa and Walter (1972) have reported that 16 different hemoproteins partition in two-phase aqueous polymer systems in a manner that appears to be independent of the protein molecular weight. Furthermore, specific exceptions to the general relation for non-hemoproteins, for example, papain, also exist (Sasakawa and Walter, 1972; Kuboi et al., 1990). Therefore, although the size of the protein is important in affecting their distribution between the two coexisting phases, properties other than the size, e.g., surface properties, are important, and, in some instances, these can be the dominant factors.

In general, when two-phase aqueous polymer systems are used for the extraction of proteins from fermentation broths, cell debris or entire cells are present in the system. It is therefore interesting to note that cells and cell fragments generally partition either almost entirely to one phase, to the interface between the two phases or, as is most often the case, to both the interface and one of the bulk phases (Albertsson,

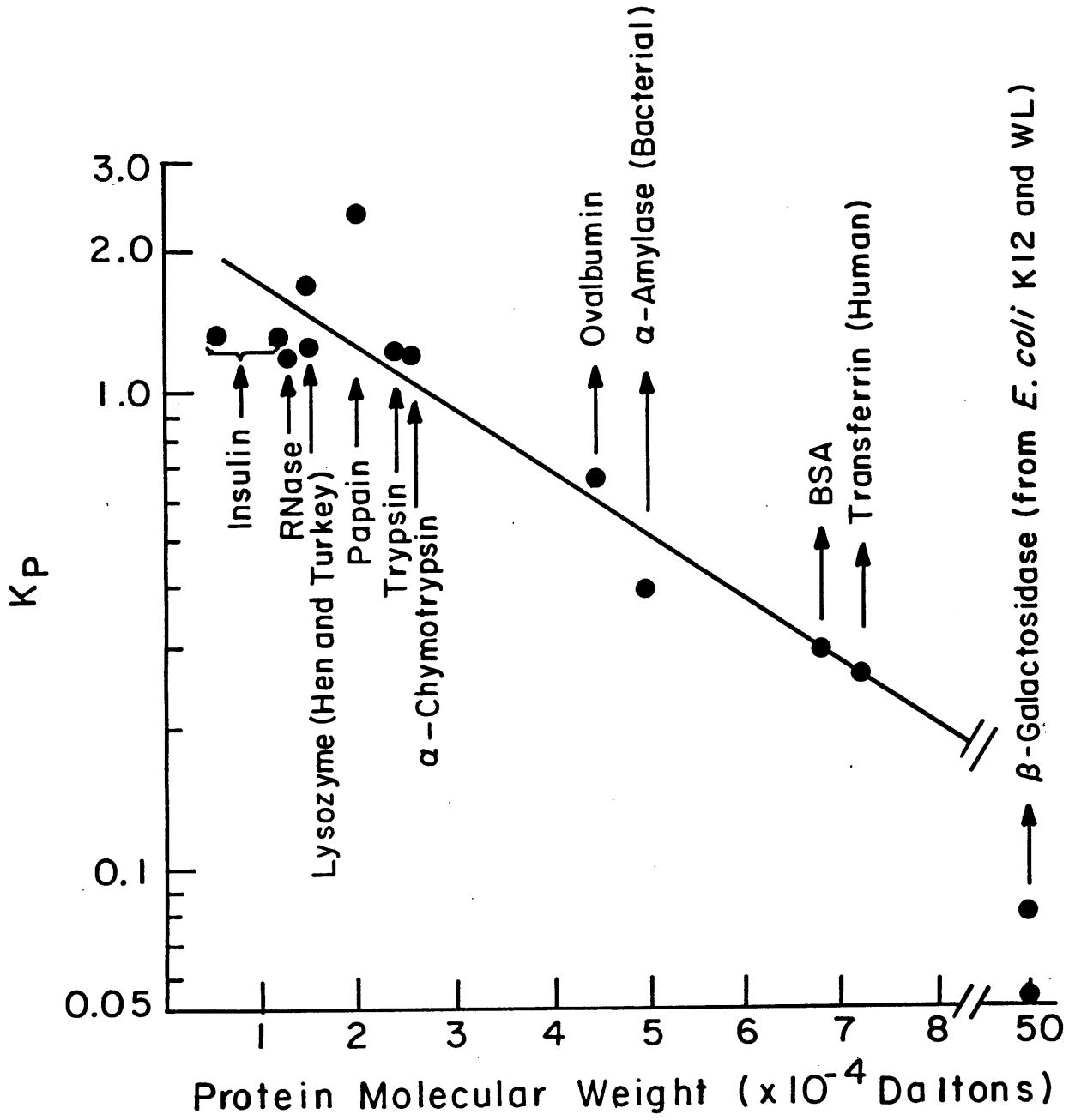

Figure 2.1 Relationship between protein partition coefficient, K_p, and protein molecular weight for the two-phase system 4.4% w/w PEO (8,000 Daltons), 7% w/w dextran (500,000 Daltons), 0.1 M NaCl or 0.05 M Na_2SO_4, 10 mM phosphate or glycine buffer at 20°C (Sasakawa and Walter, 1972).

1985). Thus, it is often possible to partition the soluble proteins away from the cells and cell debris and reduce the total number of unit operations required in the downstream-processing sequence.

2.3.2 Protein Surface Properties

The interactions between the proteins and the two polymer solution phases determine the manner in which the proteins distribute between these phases. These interactions may be, in part, of the excluded-volume type, as suggested by the importance of the protein size in determining the protein partition coefficients (Sasakawa and Walter, 1972), although polymer coils in the vicinity of the protein may also interact through longer-range forces, such as van der Waals attractions. As chemical and physical properties can vary significantly from protein to protein, the contributions of the longer-range forces to the total protein-polymer interactions may also be expected to vary with the type of protein. For instance, those proteins associated with the membrane functions of cells tend, on average, to be more hydrophobic in nature than the blood plasma proteins, in spite of the fact that all proteins expose hydrophobic and hydrophilic amino acid residues at their surfaces. This latter fact is evident in Figure 2.2, where the covalent bonding of an aliphatic ligand to PEO increases the partition coefficient of a variety of proteins towards the PEO-rich phase (Shanbhag and Johansson, 1974; Shanbhag and Axelsson, 1975; Johansson, 1976; Axelsson, 1978; Shanbhag and Johansson, 1979; Johansson and Shanbhag, 1984). The partition coefficient of human serum albumin increases by almost two orders of magnitude, whereas the partition coefficient of cytochrome-c increases only slightly. This can be understood by noting that the aliphatic ligands interact strongly with hydrophobic pockets present on the surface of the proteins which are, for example, more prevalent on serum albumin than cytochrome-c (Note that although cytochrome-c is a membrane-associated protein, this property is a consequence of an asymmetric distribution of surface charges, rather than the prevalence of hydrophobic pockets on the protein surface.) As the aliphatic ligands interact with small areas of the proteins surface, local variations in the surface properties

of the proteins can be important in determining the partitioning behavior of the proteins. In this respect, a change in protein conformation can give rise to the exposure of new amino acid groups to the protein surface, thus affecting protein partitioning behavior (Albertsson, 1985).

The protein surface contains a large variety of amino acid types, some of which possess charges which can vary in their magnitude and sign depending on solution pH (Cohn and Edsall, 1943). Consequently, as the solution pH is varied, a protein may possess a net charge, z_p, which is either positive, negative, or zero. Furthermore, it is observed experimentally that the solution pH can have a profound effect on protein partitioning. In this respect, it has been established that the relationship between the protein partition coefficient and solution pH depends on the type of salt present, (see Figure 2.3(a)) (Albertsson and Nyns, 1961; Albertsson et al., 1970; Johansson, 1971; Walter et al., 1972; Sasakawa and Walter, 1972, 1974; Gelsema and De Ligny, 1982; Johansson, 1985), but that it does not depend strongly on the salt concentration. A common intersection of the curves is observed at a pH which corresponds closely to the isoelectric pH of the protein (Albertsson et al., 1970). Determination of the net protein charge, z_p, from titration experiments has revealed (see Figure 2.3(b)) an approximately linear relationship between $\log K_p$ and z_p, with the slope dependent on the specific salt type (Johansson, 1974). In general, the dependence of the protein partition coefficient on solution pH has been interpreted in terms of an apparent electrical potential difference between the two coexisting phases (Johansson, 1974; Brooks et al., 1984), under the influence of which charged proteins partition. Although this viewpoint suggests a useful correlation for experimental data, some authors refute the appropriateness of the concept of a bulk electrical potential difference between the phases and prefer to discuss the dependence of K_p on pH in terms of the intermolecular forces operating between the salts, proteins, water and polymers (Zaslavsky et al., 1978, 1979, 1981, 1982 and 1983). Indeed, these two viewpoints are not inconsistent, as the intermolecular forces are the origin of the interphase potential, although the latter viewpoint appears a potentially more fruitful framework with which to elucidate the molecular-level mechanisms causing the observed salt effects.

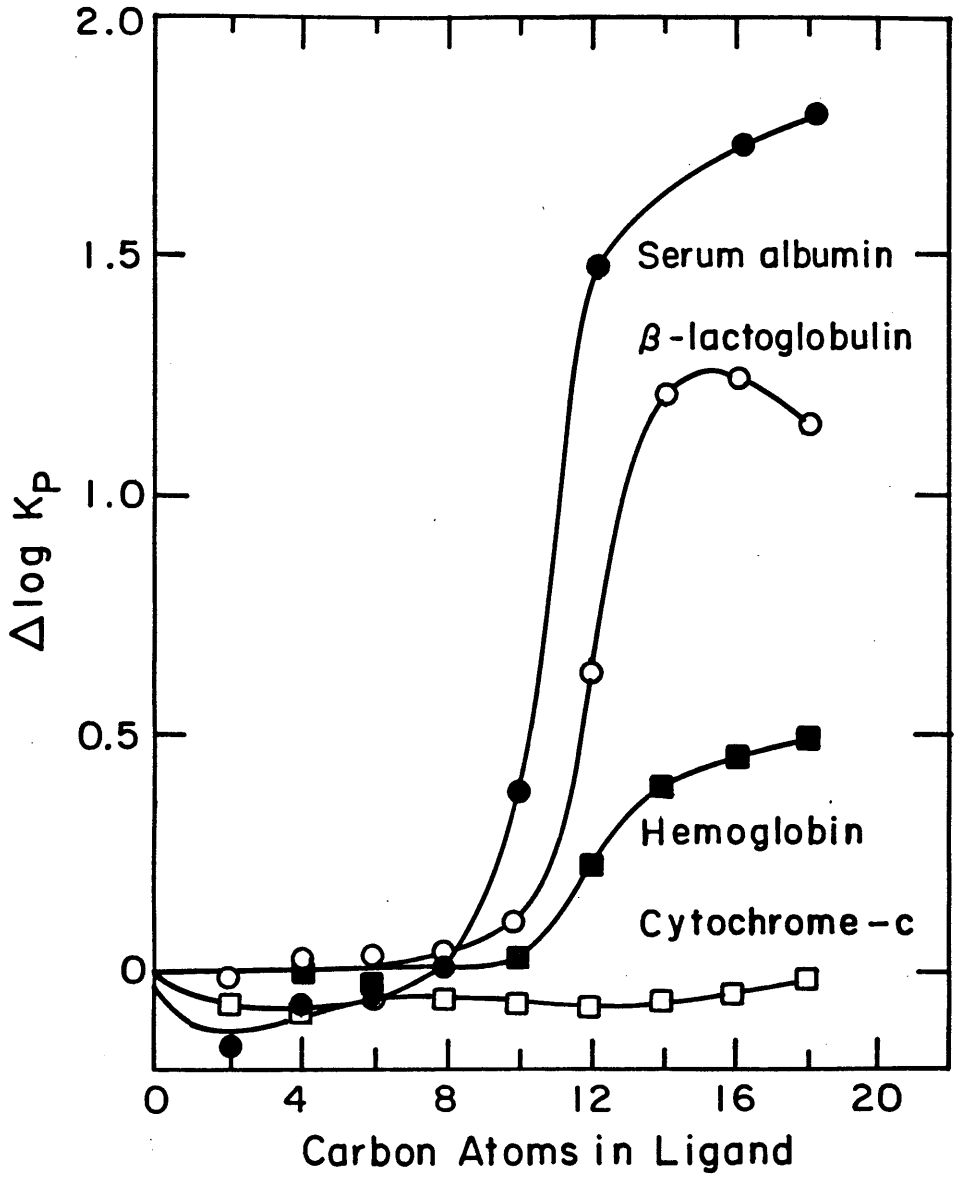

Figure 2.2 Effect of chain length (number of carbon atoms) of aliphatic ligand bound to PEO (6000 Daltons) on the partitioning of proteins. The difference in the logarithm of the protein partition coefficient with and without ligand, $\Delta \log K_p$, was measured in a system of 7% w/w PEO (6,000 Daltons) and 7% w/w dextran (500,000 Daltons), (Shanbhag and Axelsson, 1975).

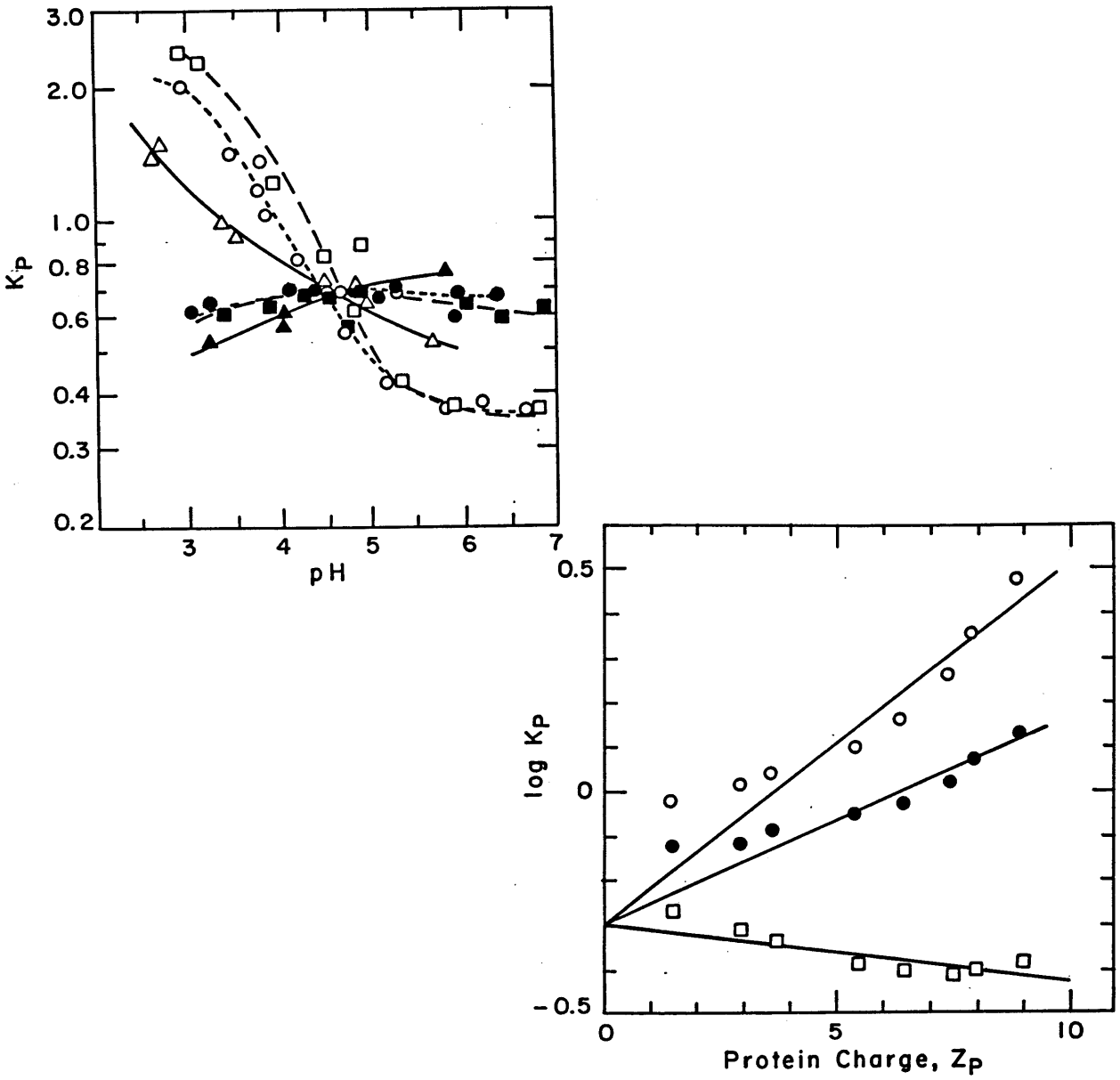

Figure 2.3 (a) Dependence of ovalbumin partition coefficient, K_p, on solution pH. Two-phase system composition: 4.4% w/w PEO (6,000 Daltons), 7.0% w/w dextran (500,000 Daltons), 0.1 - 0.6 M alkali chloride or 0.05 - 0.3 M alkali sulphate (with 0.01 M glycine or sodium phosphate) □ KCl, ○ NaCl, ▵ LiCl, ■ K_2SO_4, ● Na_2SO_4, ▲ Li_2SO_4 (Walter et al., 1972). (b) Relationship between the logarithm of the protein partition coefficient, K_p, and the net charge, z_p, of ribonuclease-a with 7.0% w/w PEO (8,000 Daltons) and 9.8% w/w dextran (500,000 Daltons). The system also contained 0.1 M KSCN (○), 0.1 M KCl (●), or 0.05 M K_2SO_4 (□) at 20°C (Johansson, 1974)

2.3.3 Polymer Molecular Weight

The molecular weights of the phase-forming polymers constitute important factors in determining the partitioning behavior of proteins (Husted et al., 1978; Albertsson, 1985; Albertsson et al., 1987; Forciniti et al., 1991a,b). An increase in the molecular weight of one of the polymers decreases the tendency of the proteins to partition to the phase which is rich in that polymer. For example, in Figure 2.4 the influence of a change in the molecular weight of PEO (in a two-phase aqueous PEO-dextran system) on the partition coefficients of a variety of globular proteins is presented. An increase of the PEO molecular weight from 3 000 Daltons to 10 000 Daltons produces a decrease in the protein concentration in the PEO-rich phase, as reflected in the decrease in the partition coefficient. A further increase of the PEO molecular weight beyond 10 000 Daltons resulted in a more gradual change of the protein partition coefficient. In interpreting the measurement presented in Figure 2.4, Albertsson et al. (1987) observed that in the PEO-dextran-water system the dependence of the protein partition coefficient on PEO molecular weight was small for small proteins having molecular weights around 10,000 Daltons, but increased almost linearly with polymer molecular weight up to proteins with molecular weights of 250,000 Daltons. An approximately inverse linear relationship between the logarithm of the protein partition coefficient and the phase polymer molecular weight was reported for bovine serum albumin, β-galactosidase, catalase, lactate dehydrogenase, cytochrome-c and ovalbumin (Albertsson et al., 1987).

An aspect not directly considered in the discussion above is that a change in the phase polymer molecular weight can, in general, alter the polymer compositions in the two coexisting polymer solution phases (Albertsson, 1985). Therefore, it is not always possible to disentangle the direct role of the polymer molecular weight from the other changes that can occur in the system. Note that Albertsson et al. (1987) chose experimental conditions far from the critical point of the two-phase system, and thus were able to minimise the changes in the compositions (wt%) of the two coexisting phases which can accompany changes in the polymer molecular weight.

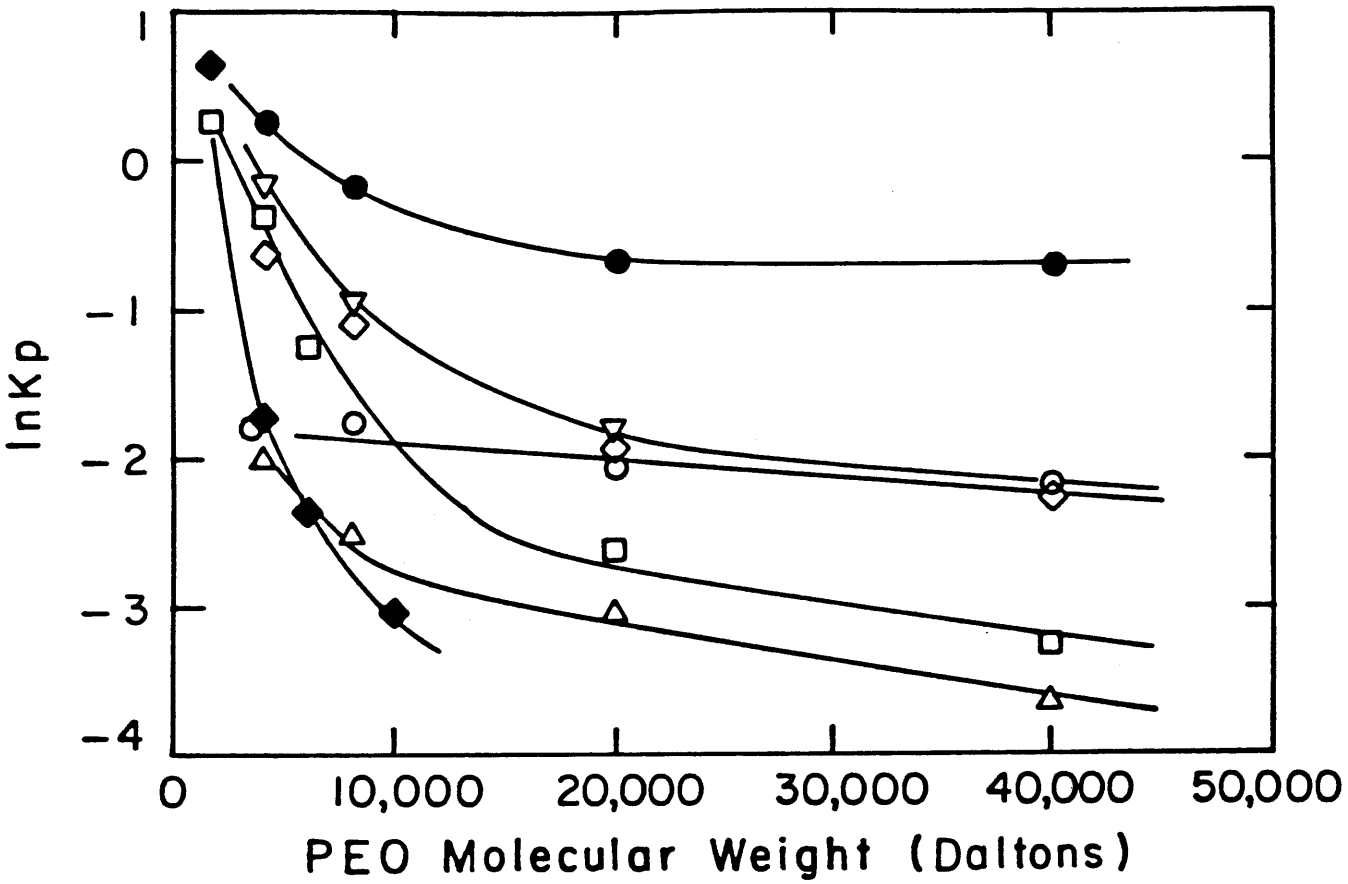

Figure 2.4 Dependence of the protein partition coefficient, K_p, on PEO molecular weight in a PEO-dextran-water system: (o) cytochrome c; (●) ovalbumin; ( ) bovine serum albumin; (▵) lactate dehydrogenase; (▽) catalase; (□) pullulanase; (◆) phosphorylase. (Hustedt et al., 1978; Albertsson et al., 1987)

2.3.4 Composition of the Coexisting Phases

An increase in the overall polymer concentration in the system can cause a more uneven distribution of the proteins between the phases (Albertsson, 1985; King et al., 1988; Baskir et al., 1989b). For example, as shown in Figure 2.5, as the weight fraction of PEO in the PEO-rich phase increases from 0.053 to 0.088, the partition coefficient of the protein chymotrypsinogen decreases from 0.30 to 0.07. Very close to the critical point of the phase diagram (the point at which the two coexisting phases become identical), the compositions of the phases in equilibrium are very similar, and therefore the protein partitioning is relatively even. Note that in Figure 2.5, the two-phase system with a PEO weight fraction of 0.053 in the PEO-rich phase is close to the critical point of the system. On the other hand, far from the critical point (corresponding to high weight fractions of PEO in the PEO-rich phase in Figure 2.5) the phase compositions differ greatly thus providing a strong driving force for the uneven partitioning of the proteins. It should be emphasized that changes in the phase compositions can also be induced by the addition of salts, or by changes in the molecular weights of the polymers, which in turn can affect the protein partitioning between the phases.

2.3.5 Salt Effects

The variation of salt type and concentration in two-phase aqueous polymer systems provides one of the most powerful means by which the selectivity and yield of the protein extraction can be manipulated. The richness of salt effects is due to the numerous mechanisms through which salts can affect the partitioning of proteins. Figure 2.6 shows the change in Kp as a function of KCl concentration (Albertsson and Nyns, 1961), illustrating the remarkable fact that very different partitioning behaviors can occur in the limits of low-salt concentrations (less than 0.1-0.2 moles of KCl per kg of phase system corresponding to log[KCl] being less than approximately -1.0 to -0.7) and high salt concentration (greater than 0.2 moles of KCl per kg of phase system or log[KCl]

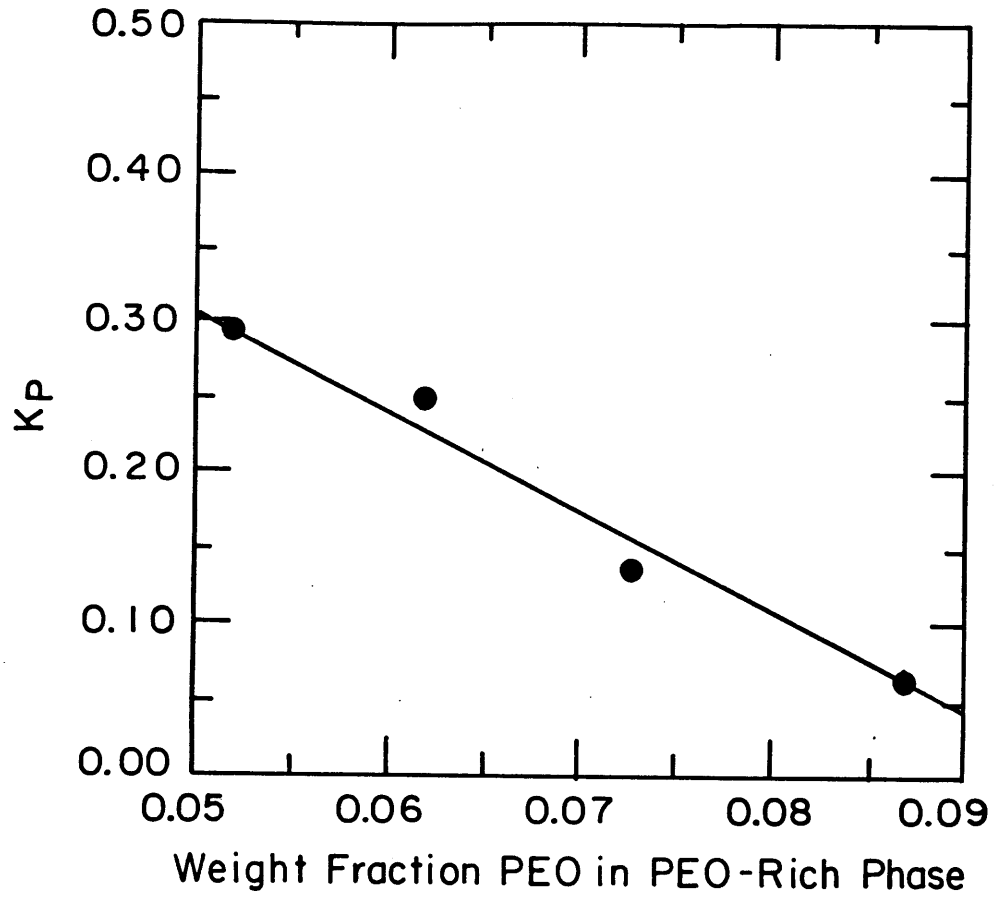

Figure 2.5 Predicted dependence of chymotrypsinogen partition coefficient (solid line) on polymer composition (% w/w) of coexisting phases in system PEO (7,500 Daltons), Polyvinylmethylether(PVME) (100,000 Daltons) at 20°C. The PEO-rich phase is the bottom phase. (Baskir et al., 1989)

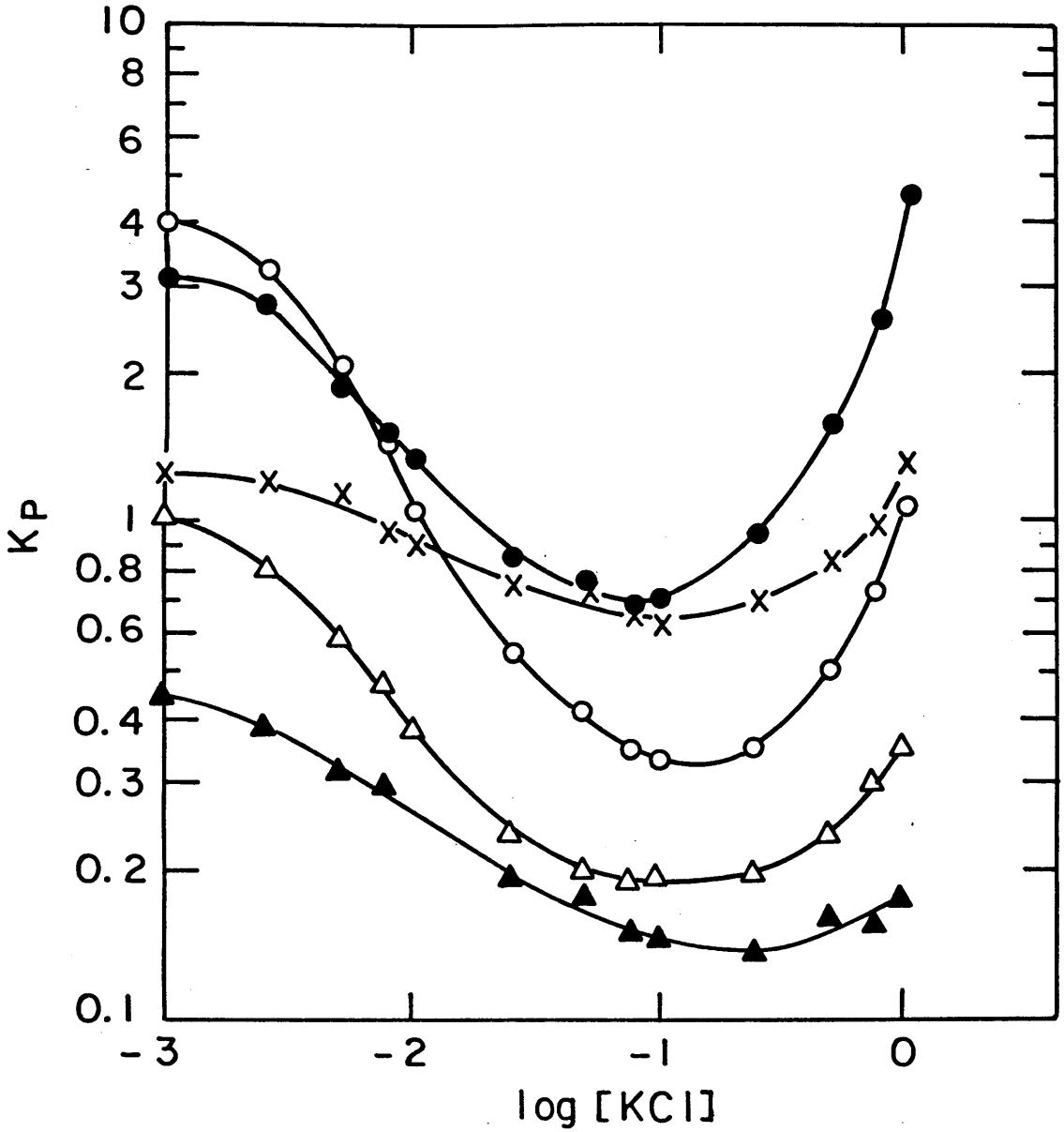

Figure 2.6 Partition coefficient, K_p, of five proteins with increasing KCl concentration (moles of KCl per kg of phase system). The phase system contained 4.4% w/w PEO (6,000 Daltons), 7% w/w dextran (500,000 Daltons), 0.005 M KH_2PO_4 and 0.005 M K_2HPO_4 at 20°C: (●) phycocyanin, (x) barley albumin, (○) phycoerythrin, (△) ceruloplasmin, (▲) serum albumin (Albertsson and Nyns, 1961).

being greater than -0.7). Below we discuss separately the low-salt and high-salt concentration regimes.

Low-Salt Concentrations.

Typically, salt concentrations in the range 0.1 M to 0.2 M have negligible effect on the compositions of the coexisting polymer solution phases (Zaslavsky et al., 1986, 1987 and 1988), and appear to have only a very small influence on the partition coefficient at the protein isoelectric points (pI) (Walter et al., 1972). In contrast, away from the pI, the specific type of salt in the system has a profound effect on the partitioning behavior of proteins (Albertsson and Nyns, 1961; Albertsson et al., 1970; Johansson, 1971; Walter et al., 1972; Sasakawa and Walter, 1972, 1974; Gelsema and De Ligny, 1982; Johansson, 1985). Generally, although not without exception (Zaslavsky et al., 1978, 1979, 1981, 1982 and 1983), the effect of salts at low concentrations has been discussed in terms of an apparent bulk-electrical potential difference established between the coexisting phases, which influences the partitioning behavior of charged proteins (Albertsson et al., 1970; Johansson, 1974; Brooks et al., 1984). Formally, the dependence of the partition coefficient on the electrical-potential difference can be simply understood as follows (Albertsson, 1985). The thermodynamic requirement for the diffusional equilibrium of a charged protein in the system results from the equality of the electrochemical potentials of the proteins in the top (t) and bottom (b) phases (Modell and Reid, 1983). These can be expressed as follows

$$\mu_p^t = \mu_p^{o,t} + kTlnc_p^t + kTln\gamma_p^t + z_p e\psi^t = \mu_p^b = \mu_p^{o,b} + kTlnc_p^b + kTln\gamma_p^b + z_p e\psi^b \qquad (2.2)$$

where μ_p^t and μ_p^b are the chemical potentials of the protein in the top and bottom phases, respectively, $\mu_p^{o,t}$ and $\mu_p^{o,b}$ are the chemical potentials of the protein in the corresponding

reference states of infinite protein dilution, γ_p^t and γ_p^b are the corresponding activity coefficients, z_p is the net charge of the protein (assumed to be the same in both phases as there exists negligible difference in pH between the two coexisting phases), e is the elementary charge, k is the Boltzmann constant, T is the absolute temperature and ψ^t and ψ^b are the electrostatic potentials in the top and bottom phases, respectively. Using Eq.(2.4), the partition coefficient, expressed as $\ln K_p = \ln(c_p^t/c_p^b)$, can be written as

$$\ln K_p = -\left(\frac{\Delta \mu_p^o}{kT} + \ln\left(\frac{\gamma_p^t}{\gamma_p^b}\right) + \frac{z_p e \Delta \psi}{kT} \right) , \qquad (2.3)$$

where

$$\Delta \mu_p^o = \mu_p^{o,t} - \mu_p^{o,b}, \ \textit{and} \ \ \Delta \psi = \psi^t - \psi^b \ . \qquad (2.4)$$

Equation (2.4) predicts a linear relationship between the logarithm of the protein partition coefficient, $\ln K_p$, and the product of the net charge of the protein, z_p, and the interphase potential difference, $\Delta\psi$. Under solution conditions such that the concentration of salt ions greatly exceeds the concentration of protein charges, the electrical potential difference between the two phases, $\Delta\psi$, will be independent of the partitioning of the protein in the system and determined by the salt type (Albertsson, 1985). Indeed, there are numerous experimental verifications of this prediction, an example being the partitioning of ribonuclease in the PEO-dextran-water system in the presence of a number of salts, as shown in Figure 2.3 (b) (Johansson, 1974), where the net protein charge is maniputed through changes in the solution pH. However, it is also important to note that deviations from this prediction are often found in the literature (Albertsson et al., 1970) as other factors, for example, the protein conformation, can also change with pH.

The existence of an interphase electrical potential arises from the tendency of cations and anions to distribute unequally between the coexisting phases owing to the different interactions between the ion types, the polymers and water in each phase (Albertsson, 1985). Note, however, that cations and anions cannot distribute

independently between the phases as this would lead to a violation of electroneutrality requirements. If one invokes the useful concept of an electrical potential difference between the two coexisting phases, the thermodynamic constraint of diffusional equilibrium leads to the equality of *electrochemical potentials* of each component present in each of the coexisting phases (Modell and Reid, 1983). The ions are then allowed to redistribute between the phases to ensure the electroneutrality of each phase. An alternative, but equivalent viewpoint, would be to consider ion-ion interactions on an equal footing with ion-polymer and ion-water interactions and to treat the system using the requirements of chemical equilibrium. In other words, the requirement of electroneutrality represents a convenient way to account for the interactions of the ions within the system.

To date, the precise nature of the interactions between ions, water and polymers is not well understood. In PEO-dextran-water-salt systems, for instance, Johansson (1970a,b, 1974) suggested that interactions between the ions and the dipoles present in the nonionic polymers may be a factor influencing the unequal affinity of the ions for each of the phases. Furthermore, the strength of these interactions increases with the polarizability of the anions and the charge-to-radius ratio of the cations. In the spirit of the so-called lyotropic series, the affinity of the alkali and halide ions for PEO should be $Li^+ > Na^+ > K^+$, and $I^- > Br^- > Cl^-$, which is indeed observed experimentally (Johansson 1970a,b, 1974). The electrical-potential difference created by the simple electrolytes present at 100-200mM is typically measured to be less than 7 mV (Brooks et al., 1984; King et al., 1988).

An additional complication arises with multivalent ions such as phosphates. These salts are often present as buffers to stabilize the solution pH and, therefore, the difference in the affinity of the ions for the phase forming polymers relates the solution pH to the electrical-potential difference between the coexisting phases (Kula et al., 1982; Bamberger et al., 1984). Furthermore, changes in the partitioning of proteins with phosphate ion concentration have been attributed to other mechanisms which are not directly related to changes in the interphase electrical-potential difference. This is discussed below.

High-Salt Concentrations.

The strong dependence of the protein partition coefficent on high salt concentrations is illustrated in Figure 2.7, where an increase in the sodium chloride concentration (moles of NaCl per kg of phase system) is seen to cause an increased protein affinity for (or decreased repulsion from) the phase rich in PEO, as reflected by the increase in the protein partition coefficient (Albertsson, 1985). In phase systems containing high salt concentrations, the effect of salts is generally attributed to the influence of the electric field of the ions on the water in the immediate vicinity of the ion (Bockris and Reddy, 1970), which may be complementary or antagonistic to the effects of the polymers and the proteins on the water. Consequently, these effects may be viewed as either a competitive or a synergistic influence on the structure of water in the system. Although the influence of simple salts on the structure of water has been the subject of many investigations (Bockris and Reddy, 1970), resulting in the classification of salts as so-called structure-making and structure-breaking ions, the influence of polymers and proteins on the precise structure of water appears unresolved. For example, both polymers and proteins contain polar regions and apolar regions, and although both regions impose constraints on the structure of water, their influence is fundamentally different. The apolar regions are unable to hydrogen bond to water and thus water will tend to form a cage-like structuring (clathrate) about these regions, maximizing hydrogen bonding with itself, whereas, polar regions may hydrogen bond preferentially with the water with or without disrupting the bulk water structure (Kjellander and Florin, 1981). As discussed in Section 2.2, the effect of salts on the interactions between the polymer components can have a pronounced effect on the phase behavior of protein-free two-phase aqueous polymer systems. This, in turn, will influence the partition of proteins through the effect of the phase composition on the protein partition coefficient. In addition, the presence of salts can influence the partitioning of proteins by modifying the effective intermolecular forces between the protein and the polymer coils, in an analogous manner to their influence on polymer-polymer interactions (see above). The effects of high salt concentrations are very specific to the type of salt

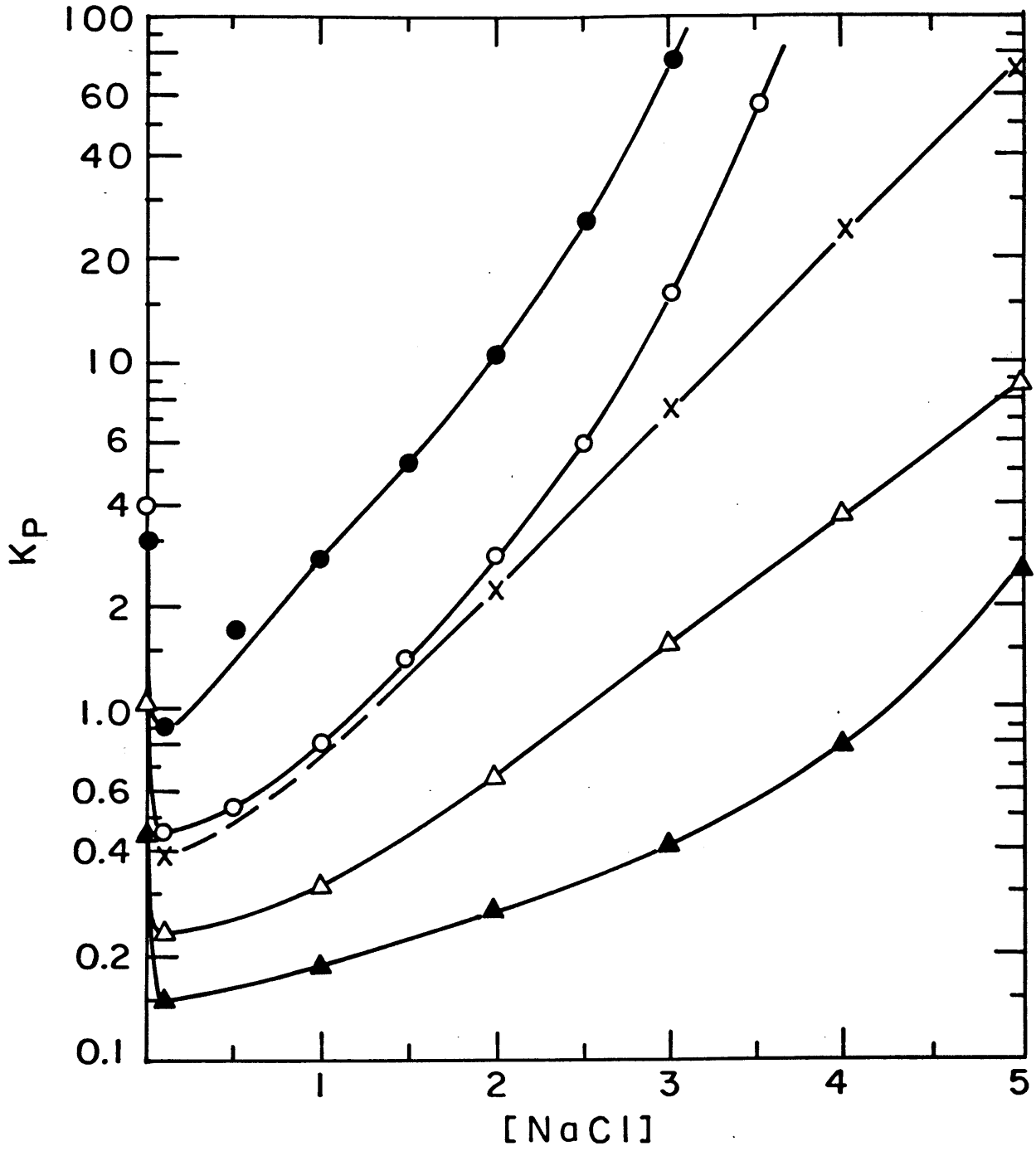

Figure 2.7 Partition coefficient, K_p, of five proteins in system 4.4% w/w PEO (6,000 Da), 7% w/w dextran, 0.005M KH_2PO_4, 0.005M K_2HPO_4 with increasing NaCl concentration (moles of NaCl per kg of phase system) at 20°C: (●) phycocyananin, (○) phycoerythrin, (x) γ-globulin, (△) ceruloplasmin, (▲) serum albumin (Albertsson, 1985).

used. For example, the addition of sodium phosphate to the PEO-dextran-water system decreases the concentration of dextran required to form a two-phase aqueous system, while the addition of an equivalent concentration of sodium chloride results only in a small change in the phase behavior (Bamberger et al., 1984).

2.3.6 Affinity Partitioning

A primary objective in the design of an aqueous two-phase polymer system for protein purification is to maximize the selectivity and yield of one of the phases for the protein of interest. In affinity partitioning, ligands having a particular affinity for specific proteins are covalently attached to one of the phase-forming polymers, which can provide the phase rich in that polymer with a high selectivity for the desired proteins. In general, the chemical nature of the ligand can take many forms, for example, short aliphatic hydrocarbon chains (Shanbhag and Johansson, 1974; Shanbhag and Axelsson, 1975; Johansson, 1976; Axelsson, 1978; Shanbhag and Johansson, 1979; Johansson and Shanbhag, 1984), triazine dyes (for example, Kopperschlager and Johansson, 1982; Johansson and Andersson, 1984a,b; Johansson et al., 1984; Cordes et al., 1987), metals (Suh and Arnold, 1990) and other ionic groups (Johansson, 1970b, 1973) have all been used as affinity ligands. The effect of the ligand presence on the partitioning behavior of proteins is generally characterised by $\Delta \ln K_p$, defined as

$$\Delta \ln K_p = \ln\left(\frac{K_{p,\max}}{K_p}\right) \qquad (2.5)$$

where $K_{p,\max}$ is the maximum protein partition coefficient measured in the presence of the ligand-bound polymer (see below), and K_p is the protein partition coefficient in the absence of ligands. Certain features of affinity partitioning are observed to be independent of the specific type of ligand attached to the polymers, such as the plateau (or maximum) in $\Delta \log K_p$ at high ligand-bound polymer concentrations illustrated in Figure 2.8 (Johansson and Andersson, 1984a,b). Other features of affinity partitioning,

such as the effect of salt type and concentration on $\Delta \ln K_p$, are specific to the particular ligand type (Johansson, 1970b, 1973; Johansson and Andersson, 1984a,b).

A class of ligands that has been thoroughly investigated is that based on triazine dyes used in the PEO-dextran-water-salt two-phase systems. Enhancements by factors of 10 to 500 in the partition coefficients of specific proteins from baker's yeast have been reported using these dyes, while other proteins were essentially unaffected by the presence of the ligand (Johansson and Andersson, 1984a). The enhancement in the partitioning was predominantly observed in the range where up to 2% w/w of the PEO-phase forming polymer bore ligands, while beyond 4% w/w ligand-bound PEO, little enhancement was observed. The presence of the plateau is generally attributed to saturation of the protein binding sites by the ligands bound to the polymers, although in some affinity partitioning systems (particularly those with aliphatic chain ligands) the self-association of the ligands at higher concentrations may also contribute to the plateau (Shanbhag and Axelsson, 1975; Shanbhag and Johansson, 1975, 1979). In the absense of ligands, an increase in the phase-polymer concentrations resulted in an increased partitioning of both the total protein and the target proteins away from the PEO-rich phase. In contrast, an increase in the phase-polymer concentration bearing the affinity ligands increased the partitioning of both total protein and target proteins to the PEO-rich phase up to 4% of the total PEO concentration. Beyond this concentration, a further increase in the phase polymer concentration resulted in a rejection of all proteins from the PEO-rich phase.

The role of the phase polymer in determing the protein affinity for the ligands was investigated by binding the ligands to both the PEO and dextran polymers. The effect of the ligand on the partition coefficient was more pronounced when confined to the lower dextran-rich phase, which was speculated to result from the presence of multiple ligands attached to each dextran coil. A decrease in the molecular weight of the polymer-bound dye has been observed to favour partitioning to that phase. This effect appears related to the steric interaction (repulsive) of the bulky polymer coil with the protein which accompanies the binding of the ligand to the protein. This steric interaction is stronger for ligands attached to higher molecular weight polymers.

The presence of salts modifies the affinity of the ligands (triazine dyes) for the proteins, with the effect dependent on the salt type. The addition of 150 mM KCl reduced the partition coefficient of glucose 6-phosphate dehydrogenase to the PEO-rich phase by a factor of almost 100 (Johansson and Andersson, 1984a). The effect of acetate was found to be more moderate than that of chloride, although in the presence of aromatic ions, such as benzylammonium ions, the effect was found to be comparable. Johansson and Joelsson (1987) further investigated this sensitivity to salt type in aqueous systems containing PEO and Procion Yellow HE-3G-bound dextran. In particular, the partitioning of the dye-bound phase polymer was found to occur to either the PEO-rich phase or to the dextran-rich phase, with partition coefficients values ranging from 0.02 to 28. With the partitioning of the proteins occuring to the dye-containing phase, the large changes in the partition coefficients of the proteins simply reflects the partitioning of the dye-bound polymer in the system.

An increase in temperature is found to decrease the value of $\Delta \ln K_p$ (Johansson and Andersson, 1984), presumably because the entropic penalties associated with forming a protein-ligand complex and confining the proteins to one phase are greater at higher temperatures, although the origin may also be related to factors such as the temperature-dependent conformations of the proteins and the influence of temperature on the properties of water. The addition of free ligands is found to reduce $\Delta \ln K_p$, as these ligands compete with the polymer-bound ligands for binding sites on the protein (Johansson and Andersson, 1984a,b)

To provide some insight into the influence of the triazine dyes as affinity ligands, Cordes et al. (1987) measured the binding constants of Cibacron blue 3GA and Procion red HE3b (coupled to monomethoxy-PEO-5000) with formate dehydrogenase (FDH). They observed that the binding of PEO-blue to formate dehydrogenase decreased with increasing PEO concentration, whereas the binding of PEO-red did not change. Furthermore, the binding constants appeared to be higher in dextran solution. In addition, it was observed that the binding of a second PEO-ligand to the protein was significantly weaker than that of the first. This was suggested to arise from the mutual steric interaction of the PEO coils attached to the ligands. From this study it is evident

that a complete understanding of affinity partitioning must account for the unequal binding strength of the ligands in each of the phases, multiple and unequal binding of ligands to the proteins, and the influence of the non-ligand carrying polymer on the binding of the ligands to the proteins.

Ligands comprising short hydrocarbon chains, typically 4-20 carbons per tail, have also been the subject of a number of investigations (Shanbhag and Johansson, 1974; Shanbhag and Axelsson, 1975; Johansson, 1976; Axelsson, 1978; Shanbhag and Johansson, 1979; Johansson and Shanbhag, 1984). Although many of the general features of the behavior of this ligand were common to those of the triazine dyes, some interesting departures were also noted. For example, a similar saturation behavior was observed with increasing polymer-bound ligand concentration as was observed when triazine dyes were used as ligands (Figure 2.8), although, in contrast to the triazine dyes, at still higher ligand-polymer concentrations $\Delta \ln K_p$ decreased (Shanbhag and Johansson, 1974). In addition, at constant ligand-bound polymer concentration, $\Delta \log K_p$ increased with the length of the hydrocarbon tail in a protein specific manner. However, at higher hydrocarbon tail lengths, $\Delta \log K_p$ decreased as shown in Figure 2.2 for β-lactoglobulin. Furthermore, the onset of saturation appeared to correspond to only a fraction of the total available protein binding sites of the protein being occupied. In general, the above observations are specific to the systems which use aliphatic chains as ligands, and suggest that ligand-ligand self-association may be an important consideration in understanding this type of affinity partitioning. The formation of micelle-like aggregates with increasing polymer-ligand concentration and hydrocarbon tail length appears to be consistent with the observed partitioning of proteins in these systems (Shanbhag and Johansson, 1979; Shanbhag and Axelsson, 1975).

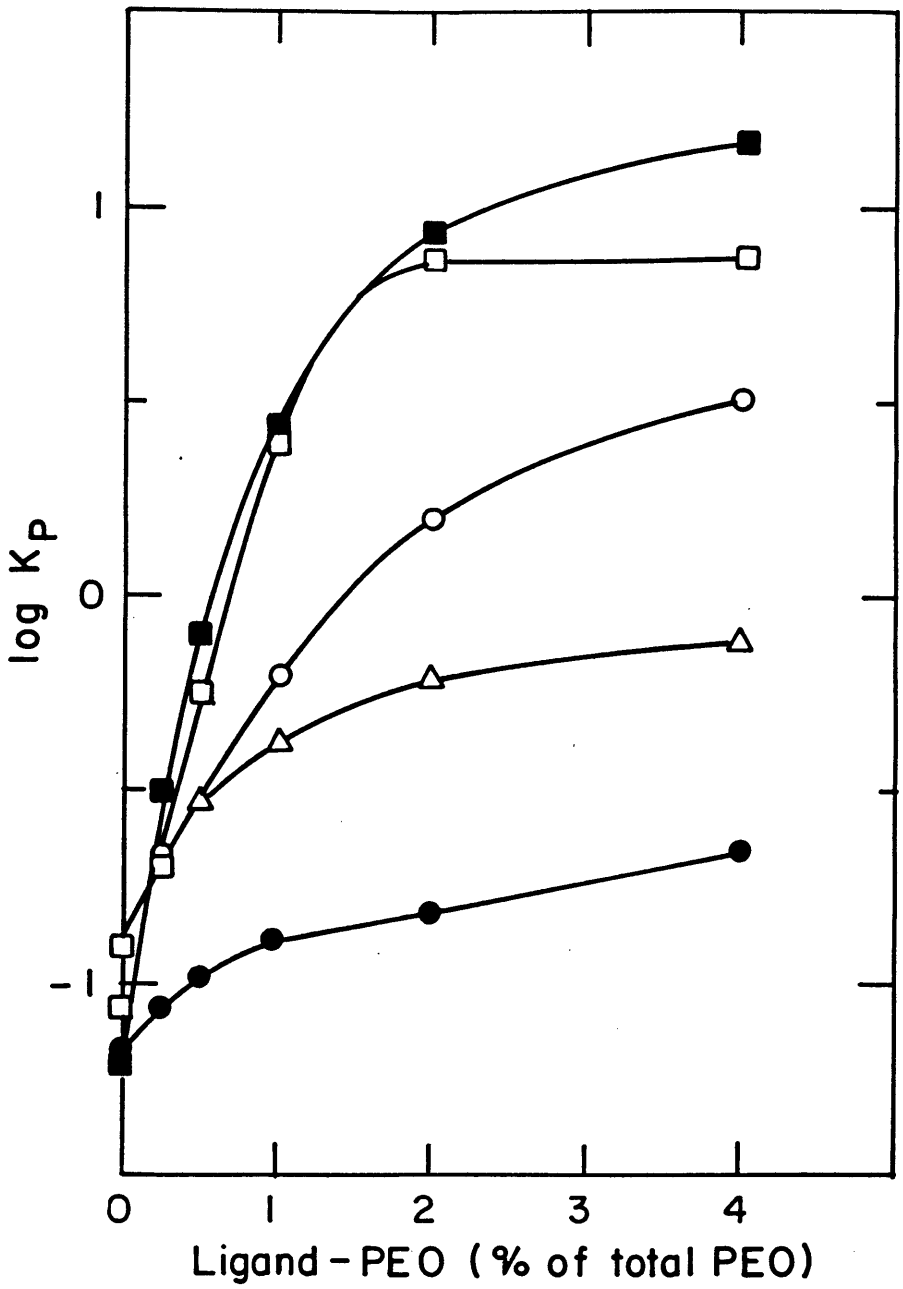

Figure 2.8 Logarithm of the partition coefficient of five proteins as a function of PEO-bound Cibacron Blue F3G-A concentration. System: 5% w/w total PEO (6,000 Daltons), 7% dextran (500,000 Daltons), 25 mM sodium phospahte buffer, pH 7.0, and yeast extract (10% of system). (△) total protein, (□) glucose-6-phosphate dehydrogenase, (○) 3-phosphoglycerate kinase, (●) alcohol dehydrogenase, (■) glyceraldehyde phosphate dehydrogenase (From Johansson and Andersson, 1984).

2.3.7 Charged Polymers

The partitioning behavior of proteins in aqueous two-phase polymer systems can be greatly affected by introducing charged groups onto the polymers (Johansson, 1970, 1973). In these two-phase systems, the strength of the electrostatic interaction between the polymer-bound charges and the protein-bound charges can be manipulated through changes in the solution pH and ionic strength. Figure 2.9 shows the pH dependence of the partitioning of hemoglobin between the two phases of the system containing water, dextran and the charged polymer trimethylamino-polyethylene oxide. The charged polymer was either a monovalent or divalent cation, depending on whether one or both ends of the polymer were derivatized. With increasing pH, the hemoglobin bears an increasing number of negative charges (and a decreasing number of positive charges) which results in the enhanced partitioning of the hemoglobin to the phase enriched in the positively charged polymer. In this system, the presence of low concentrations of inorganic salts can reduce the influence of the charged polymer on the protein partition coefficient by screening the electrostatic interaction between the polymer-bound charges and the protein-bound charges. One would expect that salt concentrations, which exceed the concentration of the charged polymers, could entirely swamp the effect of the charged polymer on the protein partition coefficient. In analogy to the action of ordinary salts, e.g., NaCl, the presence of the charged polymer can be considered to induce an electrical potential difference between the two-phases, since the polymer and its counter ions have different affinities for each of the two coexisting phases.

A novel polyelectrolyte system containing polyampholytes has recently been reported, with the partitioning of proteins in the system revealing a rich variety of behaviors (Hughes and Lowe, 1988). The polyampholytic phase-forming polymers were linear heteropolymers comprised of cationic and anionic derivatives of acrylic acid. As such, these polymers displayed a number of interesting properties. In particular, the net charge of the polymers was dependent on the solution pH, which in turn, affected the equilibrium phase behavior with nonionic polymers, polyampholyte solubilty, and the

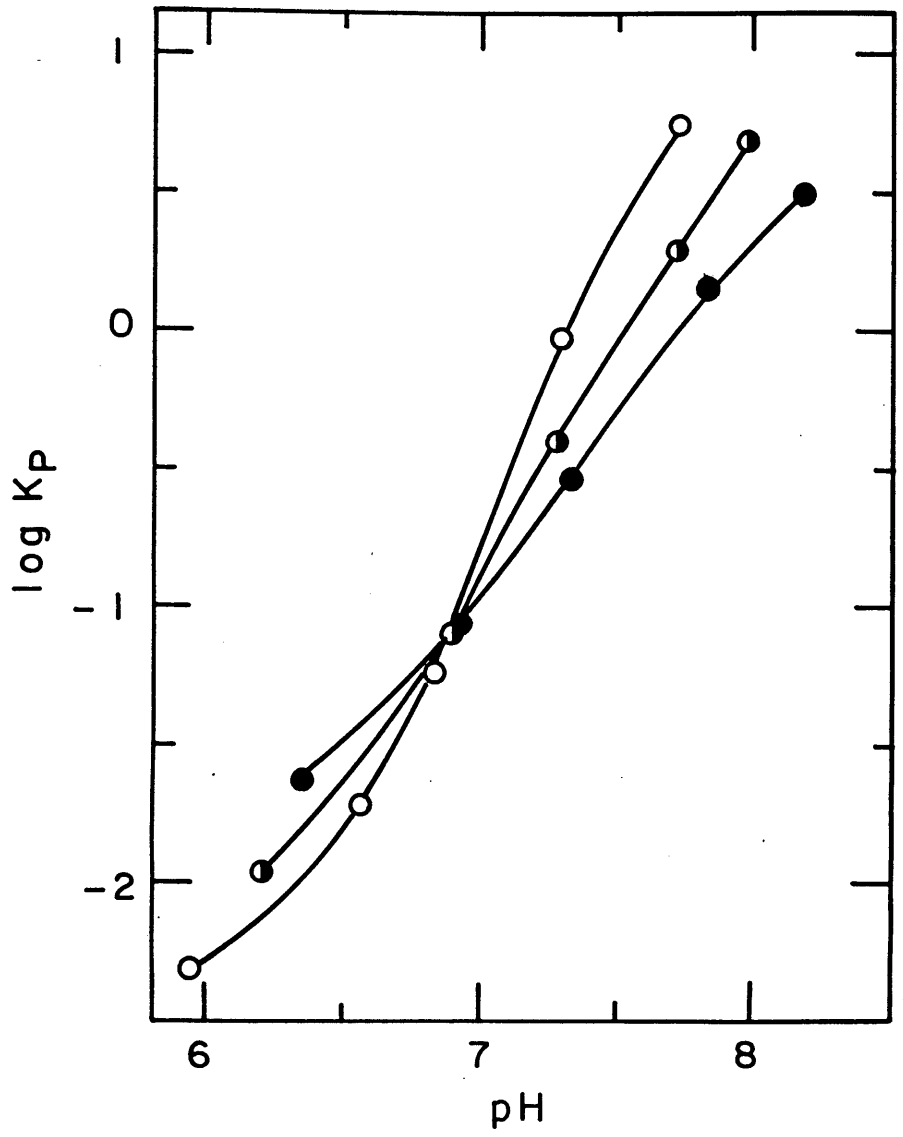

Figure 2.9 The partition coefficient of CO-hemoglobin in system 8% w/w trimethylamino-PEO, 8% w/w dextran (500,000 Daltons) with increasing potassium phosphate concentration. 2mM (○), 5mM (○), 10mM (●) (From Johansson et al., 1973).

partitioning behavior of proteins in these systems. In addition, as the conformations of the polyampholytes are sensitive to pH, the rheological properties of polyampholyte solutions are dependent on solution pH. Hughes and Lowe (1988) suggested that the partitioning of proteins in these systems appeared to be influenced primarily by electrostatic interactions between the polyampholytes and the protein charges, which could be manipulated by variation of solution pH, as well as the addition of salts to the system. One might also expect that the changing conformational properties, for example, flexibility of the polyampholyte coils, could be reflected in the protein partition coefficient. An interesting and potentially useful feature of this system is that protein recovery from the aqueous polyampholyte phases could be achieved by isoelectric precipitation of the polymers, while leaving the protein in solution.

Recently, a second investigation of the potential utility of synthetic polyampholytes as phase forming polymers in two-phase aqueous polymer systems has been reported (Patrickios et al, 1991). Aqueous solutions of the synthetic polyampholyte (acrylic acid : dimethylaminoethyl methacrylate : methyl methacrylate = 0.9 : 1 : 1) and poly(vinyl alcohol) were observed to phase separate into two coexisting polymer solution phases (of low viscosity) within a narrow pH range (less than 2 pH units) above the isoelectric point of the polyampholyte. Interestingly, with variations in pH, polyampholyte concentration, salt concentration and type, a variety of different equilibrium phases behaviors were observed in these systems, although, to date, no systematic investigation has been reported. For example, in contrast to the behavior of two-phase aqueous polymer systems containing polyelectrolytes, an increase in the salt concentration caused the concentration of polyampholyte in the polyampholyte-rich phase to decrease. With a further increase in salt concentration a phase inversion was observed. The partitioning behaviors of several proteins were investigated; the protein partitioning appeared to be governed by a competition of both electrostatic and non-electrostatic effects.

2.4 Theories of Protein Partitioning

2.4.1 General Thermodynamic Theories

In 1931, Bronsted proposed a theory for the partitioning of colloid-sized particles in liquid-liquid two-phase systems that has more recently formed the basis for several modern theories of partitioning in two-phase aqueous polymer systems (Bronsted, 1931; Bronsted and Warming, 1931). In particular, in studying the partitioning of As_2S_3 particles in the butanol-water two-phase system, Bronsted recognized that the distribution of colloidal species between two coexisting liquid phases is determined by a "potential energy" difference between these phases. In this spirit, he used the Boltzmann distribution to relate the concentrations of the partitioning colloid in the top and bottom phases, yielding the result

$$\frac{c_t}{c_b} = \exp\left(-\frac{\lambda}{kT}\right) \tag{2.6}$$

where c^t and c^b are the colloid concentrations in the top and bottom phases, respectively, λ is the difference in the colloid "potential energy" in the top and bottom phases, and k is the Boltzmann constant. For colloids of similar chemical composition, Bronsted suggested that the potential energy parameter, λ, should be proportional to the colloid molecular weight, M, namely,

$$\lambda=\lambda_o M \tag{2.7}$$

where λ_o reflects the potential-energy difference per unit mass, and depends not only on the nature of the colloid, but also on properties of the two-phase system, including its composition. The partition coefficient, K, can therefore be expressed as

$$\ln K = \ln\left(\frac{c^t}{c^b}\right) = -\frac{\lambda_o M}{kT} \tag{2.8}$$

Interestingly, this relationship between the logarithm of the partition coefficient and the molecular weight of the partitioning solute is consistent with the protein partition data shown in Figure 2.1. For globular non-hemoproteins it appears that λ_o, which accounts for differences in protein characteristics other than molecular weight, has a similar value for all the proteins partitioned. Since the volumes of globular proteins are approximately proportional to M, the success of Eq.(2.8) in describing the experimental partitioning results suggests that the volume of the proteins is an important factor in determining the nature of the interactions between the polymer solution phases and proteins. Such an interaction could be of the excluded-volume type, that is, the physical exclusion of the polymer coils from the volume occupied by the proteins. Alternatively, Bronsted (Bronsted, 1931; Bronsted and Warming, 1931), and later also Albertsson (1985), suggested that the surface area of the partitioned species may be the more relevant physical quantity with which to correlate the partitioning data. This would lead to an equation similar to Eq.(2.8), but with a $M^{2/3}$ dependency, rather than a linear one. Unfortunately, the scatter in the experimental measurements presented in Figure 2.1 does not permit distinction between these two-possible power-law dependencies on M. Note that if the partitioning is indeed predominantly a surface-dependent phenomenon, then it is somewhat surprising that proteins having such different surface compositions fall onto the same curve, unless, of course, the interactions between the polymers and the protein surface are very nonspecific. In this respect, an excluded-volume type interaction is non-specific, and thus appears a somewhat more plausible mechanism for the interactions with non-hemoproteins.

Bronsted and Warming (1931) also proposed a simple theory to describe the influence of the phase composition on the partitioning of colloidal species. They observed that colloids partitioned more unequally when the two-phase system was far from its critical point (the point in the phase diagram where the two-phases become identical). Recall that this is also observed when proteins are partitioned in two-phase aqueous polymer systems (see Section 2.3.4). Indeed, to reduce the degree of partitioning to measureable values, Bronsted and Warming (1931) performed partitioning experiments near the critical point of the two-phase system, and used temperature as a

convenient variable to manipulate the compositions of the two-coexisting phases and the distribution of the colloids between the phases. Assuming a quadratic relationship between the temperature and the phase compositions in the vicinity of the critical point (note that this is the simplest mathematical function that can describe the qualitative form of the binodal curve), Bronsted and Warming (1931) related the partition coefficient of the colloids to the phase compositions through the following simple expression

$$\ln K = -\frac{\lambda_1 M(c_2 - c_2^c)}{kT} \tag{2.9}$$

where c_2 and c_2^c are the concentrations of one of the phase forming components (denoted by 2) at the condition of interest and at the critical point (denoted by c), respectively. The formal similarity of Eq.(2.9) to several recent models of protein partitioning in two-phase aqueous polymer systems will be shown and discussed in Sections 2.4.2 and 2.4.3.

More recently, Gerson (Gerson, 1980; Gerson and Akit, 1980; Gerson and Scheer, 1980) suggested a thermodynamic framework to interpret the partitioning of cells in two-phase aqueous polymer systems in terms of the difference in their surface free energies in each phase as obtained from contact-angle measurements. The essence of the derivation is similar to that presented by Albertsson (1985) elsewhere. Gerson proposed that the chemical potential of a cell in a polymer-solution phase can be written as

$$\mu_{cell} = \mu^o_{cell} + kT\ln(\gamma_{cell}\, c_{cell}) + Af_{cell} + z_{cell}\, e\psi \tag{2.10}$$

where μ^o_{cell} is the standard-state chemical potential of the cells, γ_{cell} is the cell activity coefficient, c_{cell} is the cell concentration, A is the cell surface area, f_{cell} is the free energy per unit cell area at the cell-polymer solution interface, z_{cell} is the net cell charge (in units of elementary charge, e), and ψ is the electrical potential defined to reflect the affinity of ionic species for the solution relative to the standard state. At equilibrium, the cell chemical potentials should be equal in the top (t) and bottom (b) phases (Modell and Reid, 1983). Thus, use of Eq.(2.10) for both phases leads to the following expression for the partition coefficient of the cells

$$-kTlnK_{cell} = A\Delta f + z_{cell}\, e\Delta\psi + (\mu^{o,t}_{cell} - \mu^{o,b}_{cell}) + kT\ln\left(\frac{\gamma^{t}_{cell}}{\gamma^{b}_{cell}}\right) \qquad (2.11)$$

where $\Delta f = f^{t}_{cell} - f^{b}_{cell}$ and $\Delta\psi = \psi^{t} - \psi^{b}$. If the standard-state chemical potentials are chosen to be equal, and the solutions are sufficiently dilute in cells such that the ratio of the activity coefficients is close to unity, Eq.(2.11) simplifies to

$$-kTlnK_{cell} = A\Delta f + z_{cell}\, e\Delta\psi \qquad (2.12)$$

The proportionality between the logarithm of the cell partition coefficient, $\ln K_{cell}$, and the surface free energy difference per unit cell area, $\Delta\gamma$, predicted by Eq.(2.12), was verified by experimental measurements of the two quantities. It is interesting to compare Eq.(2.12) to Eq.(2.8) proposed by Bronsted (1931). In particular, with the net surface charge, z_{cell}, expressed as the product of a surface charge density, $\bar{z}_{cell}$, and cell area, A, that is, $z_{cell} = \bar{z}_{cell}A$, Eq.(2.12) can be written as

$$-kTlnK_{cell} = A(\Delta f + \bar{z}_{cell}\, e\Delta\psi) = \beta A \qquad (2.13)$$

where β is a constant characteristic of the specific cell type and two-phase polymer system considered, which is independent of the surface area of the cells. It is apparent that Eq.(2.13) differs from Eq.(2.8), with the surface area (proportional to $M^{2/3}$) in Eq.(2.13) replacing the volume (proportional to M) in Eq.(2.8). The fact that cell partition appears to be a surface-dependent phenomenon should not be taken to imply that the partition of much smaller proteins is also primarily surface dependent. Cells are significantly larger objects than the polymer coils (or the mesh size of a polymer solution of extensively interpenetrating polymer coils, see Chapter 3), and, therfore, at the length scale of an individual polymer coil the cell surface appears infinite in extent. In addition, it is likely that the size of the cell is much larger than the range of most forces acting between the cells and the polymer coils. Consequently, it is reasonable that the interactions of the cells with the polymer solution be characterized by the area of the cell

surface. In contrast, in protein systems, the polymer coils and the proteins have similar sizes, where this size can be comparable to the range of interactions, such as van der Waals, operating between the various components. Consequently, the interactions between proteins and polymers can also reflect the bulk characteristics of the components (as opposed to their surface properties only). In other words, it appears less likely that the interactions of proteins and polymers should be characterized solely by the areas of the components, that is, although Eq.(2.13) suggests that $M^{2/3}$ may be the more reasonable parameter with which to correlate cell partitioning data, this does not necessarily imply that one should also correlate protein partitioning data in the same manner.

It is relevant to mention the surface-thermodynamic model recently proposed by Boucher (1989) to describe the partitioning of particles between two liquid phases and their interface. In this model, the Gibbs adsorption equation was utilized, and the concept of an interfacial tension at the surface of the particles was invoked. In this respect, this approach is similar to that of Albertsson (1985) and Gerson (1980). Note that for proteins present in two-phase aqueous polymer systems, this interfacial free energy is likely to be a function of the radius of the proteins (due to curvature of the interface), as discussed in the preceeding paragraph.

4.4.2 Lattice Model Approaches

During the last forty years lattice models of polymer solutions (Flory, 1953; Huggins 1942) have provided a framework through which many of the features of polymer solution behavior can be understood qualitatively and, in a few instances, also quantitatively. The primary advantage of this approach is that the thermodynamic properties of a polymer solution can be related to molecular properties, for example, to the polymer molecular weight. Since the lattice model description of polymer solutions has been utilized in a number of cases to model the partitioning of proteins in two-phase aqueous polymer solutions, we will review briefly the essential features of this approach. For a more detailed review on the lattice modelling of polymer solutions, as well as

numerous extensions of the germinal theory proposed by Flory (1953) and Huggins (1942) see, for example, Cassassa (1976) and Flory (1970).

The free energy of a polymer solution is comprised of two contributions, the first arising from an *entropy* change associated with mixing polymers and solvent, and the second arising from an *enthalpy* change resulting from the formation of contacts between polymer coil segments and solvent. In a lattice model, these contributions to the free energy are estimated by modelling the polymer solution as a lattice, in which the volume of each lattice site is essentially determined by the size of the solvent molecules. A second characteristic feature of lattice theories is that the polymer is considered to be flexible at the length scale of the solvent molecules present in the system, and thus is treated as a catenation of statistical segments which are of the same size as the solvent molecules. Owing to the assumed flexibility of the polymer chain, each statistical polymer subunit possesses a certain degree of independence such that a series of consecutive segments along a polymer chain will trace out a path resembling a random walk. Consequently, the total number of configurations available to the polymer solution and its associated entropy can be conveniently enumerated using this lattice representation of the polymer solution, where a lattice site is occupied by either a solvent molecule or a statistical segment of the polymer. It should be noted that a necessary condition used in the evaluation of the entropy of mixing, as proposed by Flory (1953) and Huggins (1942), is that the polymer segments are randomly distributed over the volume of the solution. Clearly, such a situation is approximately realized only when the polymer coils are diffuse and extensively interpenetrating, and, even then, important correlations remain within the solution which are not accounted for in the lattice treatment (see below). The Flory-Huggins result for the entropy of mixing one polymer component and solvent is given by

$$\Delta S_M = -k(n_1 \ln\phi_1 + n_2 \ln\phi_2) \qquad \textbf{(2.14)}$$

where n_1 and n_2 are the numbers of solvent molecules and polymer coils present in the system, respectively, and ϕ_1 and ϕ_2 are the volume fractions of the respective species.

In general, the mixing of solvent and polymers produces an enthalpy change which, under conditions where the polymer segments and solvent are randomly distributed throughout the volume of the system, can be estimated using the following expression

$$\Delta H_M = q\Delta w_{12} n_1 \phi_2 = \chi kT n_1 \phi_2 \qquad (2.15)$$

where q is the number of nearest neighbours in the lattice, Δw_{12} is the energy change associated with the formation of a contact between statistical segments of species of types 1 and 2, and χ is the so-called Flory-Huggins interaction parameter (Flory, 1953; Huggins, 1942). Flory (1953) and Huggins (1942) emphasized the need to modify the physical interpretation of χ, which is defined in Eq.(2.15) solely as an enthalpy change. Clearly, the presence of an enthalpic interaction (in addition to excluded-volume type interactions) between the polymer segments and solvent implies some extent of local ordering among the interacting species. This ordering has not been accounted for explicitly in Eq.(2.14) or Eq.(2.15), and, therefore, χ is generally regarded as a free-energy parameter reflecting both enthalpic interactions and the local ordering in the polymer solution. In aqueous systems, where orientation-specific hydrogen bonding effects are important, χ is found to contain a large entropic component, and therefore the utilization of these lattice-type models to describe aqueous solutions is a controversial topic (Kjellander and Florin, 1981; Goldstein, 1984; Karlstrom, 1985; Sanchez and Balazs, 1989).

When modelling a real polymer system with a lattice-type approach, one is confronted with the task of determining how well the lattice represents the real system. From the outset, a lattice size must be assigned to the system. For aqueous polymer systems, the characterisitic size of a water molecule is about 3 Å, yet the appropriate statistical segment size for PEO in a lattice theory is thought to be approximately 10 Å (Flory, 1968), while for the dextran polymer the statistical segment size is likely to be even larger. Therefore, in assigning a lattice size to the real polymer solution a compromise must be made between satisfying the differing requirements of the polymer type and the solvent. Furthermore, such lattice approaches belong to the class of mean-

field theories where correlations and fluctuations in the polymer solution are neglected. This corresponds to distributing the polymer segments uniformly over the volume of the entire system. The extent to which this approximation is deleterious probably depends on the properties of interest. In Chapters 3 and 7, it is shown that the range of spatial correlations measured in PEO solutions utilizing neutron scattering (Cabane and Duplessix, 1982, 1987) is of the same magnitude as typical protein sizes, suggesting that these correlations may be important in describing the thermodynamics of protein partitioning in two-phase aqueous polymer solutions. As mentioned above, in view of the presence of orientation-specific hydrogen bonding in water, as well as volume changes which occur upon mixing polymers and water, the application of Flory-Huggins type lattice approaches to aqueous polymer solutions constitutes an interesting and controversial topic (Goldstein, 1984; Karlstrom, 1985; Sanchez and Balazs, 1989). While these considerations have been discussed extensively in the polymer solution literature, it is important to appreciate the approximations inherent in lattice models when applying them to protein partitioning in two-phase aqueous polymer systems.

The first attempts to understand protein partitioning in two-phase aqueous polymer systems in the context of a lattice-model approach utilized the Flory-Huggins framework (Flory, 1953; Huggins, 1942), treating the protein as a third polymer component (Brooks et al., 1985; Albertsson et al., 1987). As globular proteins are dense, compact, and often relatively rigid macromolecules, the treatment of the protein species as a diffuse random coil can lead, at best, to a qualitative account of the partitioning of proteins in two-phase aqueous polymer systems. Within this framework, the system was considered to contain four components: two phase-forming polymers, protein and solvent. Using the Flory-Huggins lattice theory (Flory, 1953; Huggins, 1942), the chemical potential of the protein, component p, was given by

$$\frac{\mu_p - \mu_p^o}{kT} = 1 + \ln\phi_p + \\ + r_p\left(-\phi_1 + \phi_2\left(\chi_{2p} - \frac{1}{r_2}\right) + \phi_3\left(\chi_{3p} - \frac{1}{r_3}\right) + \chi_{12}(\phi_1 - \phi_1\phi_2 - \phi_1\phi_3) - \chi_{23}\phi_2\phi_3\right) \qquad \textbf{(2.16)}$$

where it was assumed that $\chi_{12} = \chi_{13} = \chi_{1p}$. In Eq.(2.16), component 1 is the solvent, components 2 and 3 are the two polymer types, and r_i is the number of lattice sites occupied by species i. Using Eq.(2.16) for the protein in each coexisting phase, and demanding the equality of the protein chemical potentials in the top (t) and bottom (b) phases, one obtains the following expression for the equilibrium protein partition coefficient

$$lnK_p = r_p\left((\phi_1^t-\phi_1^b)(1-\chi_{1p})+(\phi_2^t-\phi_2^b)\left(\frac{1}{r_2}-\chi_{2p}\right)+(\phi_3^t-\phi_3^b)\left(\frac{1}{r_3}-\chi_{3p}\right)\right) \quad (2.17)$$

Note that terms which are second-order in the volume fraction of the various species were neglected in Eq.(2.17) as the volume fractions are typically around 0.10. The predictions of Eq.(2.17) are in qualitative agreement with measured protein partition coefficients, that is, the partitioning of proteins is predicted to become more unequal as the molecular weight of the protein, which is proportional to r_p, increases. This trend has been observed for a number of non-hemoproteins in the PEO-dextran-water two-phase system (Albertsson et al., 1987). In addition, Eq.(2.17) predicts the protein partitioning to be more one-sided as the compositions of the two coexisting phases become less similar, as represented by increasing values of ϕ_1^t - ϕ_1^b, ϕ_2^t - ϕ_2^b and ϕ_3^t - ϕ_3^b, and this prediction is also in general agreement with experimental observations. Furthermore, Eq.(2.17) predicts that a decrease in the molecular weight of one of the polymers should increase the partitioning of the protein to the phase rich in that polymer. This is generally observed in experiments (Hustedt et al., 1978) and, moreover, it has been observed that the effect of changing the polymer molecular weight is amplified by the size of the protein (Albertsson et al., 1987), as also predicted by Eq.(2.17). Thus, in general, Eq.(2.17) appears to be very successful in predicting the qualitative features of protein partitioning. This agreement may be fortuitous, however, as the origin of the predicted trends arises from the Flory-Huggins form of the entropy of mixing (Brooks et al., 1985). As emphasized above, since globular proteins are dense, compact, and often relatively rigid macromolecules, the treatment of the protein species as a diffuse

and random coil in the evaluation of the entropy of mixing raises some uncertainty in the result. As shown below, recent modelling approaches which treat the protein as an impenetrable hard sphere, rather than a diffuse coil, predict *qualitatively* different trends in the protein partition coefficient based solely on the entropy of mixing contribution (Baskir, 1987).

Recently, another model for protein partitioning in two-phase aqueous polymer systems, also based on the Flory-Huggins theory, has been proposed. Diamond and Hsu (1989) exploited an observed empirical relationship between the polymer compositions in each of the two coexisting phases in the PEO-dextran-water system in their analysis. Specifically, it was noted that the ratio

$$l = \frac{w_3^b - w_3^t}{w_2^b - w_2^t} \qquad \textbf{(2.18)}$$

was approximately constant for the two-phase aqueous polymer systems investigated. In Eq.(2.18), the symbol w_i^j is the weight fraction of the polymers in each of the coexisting phases and the subscripts and superscripts are the same as for Eq.(2.17). The ratio, l, in Eq.(2.18) corresponds to the slope of the equilibrium tie-lines of the binodals for each two-phase system, which is known to change only slightly with the overall compositions of the two-phase systems, although a dependence on the molecular weight of the phase-forming polymers is generally observed (see Section 2.2). This ratio, when determined for the phase systems investigated by Diamond and Hsu (1989) (dextran T-40 and PEO of molecular weights 3,400, 8,000 and 20,000 Daltons, respectively) was found to be -2.15,-2.09 and -1.60, respectively, for the three molecular weights considered. The approximation made by Diamond and Hsu (1989) was that this ratio is constant, independent of polymer molecular weight, which simplified the expression for the partition coefficient given in Eq.(2.17) as follows

$$lnK_p = k_o(w_2^b - w_2^t) \qquad \textbf{(2.19)}$$

where the parameter k_o is proportional to the molecular weight of the protein (see Eq.(2.17)), as well as reflecting interactions of the proteins with the polymers and water. Eq.(2.19) was found to represent dipeptide partitioning behavior well at pH 7.0. However, the partition coefficients of most proteins, with the exception of the smallest ones, were found not to conform to Eq.(2.19). In light of the approximations inherent in this equation, these observations are not unreasonable. Dipeptides are small molecules, similar to water molecules in their size, and may therefore be treated as a second type of solvent molecule in the system. In this respect, they may be realistically incorporated into the Flory-Huggins framework, and indeed the experimental results seem to support this expectation. On the other hand, the protein species consist of many amino acids, and, consequently, are very large compared to the solvent molecules. This in turn suggests that they cannot be treated as a second solvent species. Furthermore, as mentioned above, the representation of the globular proteins as random coiling species lacks a physical basis. Therefore, it is perhaps not surprising that the measured protein partition coefficients do not, in general, conform to Eq.(2.21). In addition, changes in the interactions between the salts (buffer) and the charged proteins, water and polymers, which have been observed experimentally to accompany changes in the concentrations of the polymers in each coexisting phase, can also affect the partitioning of the proteins. The dipeptides at pH 7.0 are zwitterionic and bear negligible net charge. Therefore, they may be less affected by the presence of the salts.

It is interesting to compare Eq.(2.19) and Eq.2.(9). Since k_o in Eq.(2.19) is proportional to the molecular weight of the protein (see Eq.(2.17)), it follows that Eq.(2.19) and Eq.(2.9) are formally equivalent. Bronsted and Warming (1931) characterized the concentration driving force in terms of the deviation in concentration from the concentration at the critical point, whereas Diamond and Hsu (1931) used the actual difference in concentration between the two coexisting phases.

A third lattice model for protein partitioning in two-phase aqueous polymer systems has been reported by Baskir et al. (1987, 1988 and 1989), who extended a self-consistent mean-field model for the adsorption of flexible polymers onto planar surfaces (Scheutjens and Fleer, 1979, 1980) to the case of a spherical geometry by confining the

polymer segments to a curved lattice determined by the shape and size of the protein (Figure 2.10). The protein was approximated as a rigid, impenetrable and spherical body of known size and with homogeneous surface properties, rather than as a random coiling polymer species. Each polymer solution phase was assumed to contain only one polymer type and water, and the protein was assumed to be sufficiently dilute that the partitioning of proteins is dominated by the interactions of isolated proteins and the polymer solution. In addition to the conventional polymer-solvent interaction parameter, χ, used in lattice models of polymer solutions, a polymer segment-protein surface interaction parameter, χ_s, was specified. This parameter characterizes the free-energy change that accompanies the displacement of solvent segments from the protein surface by a statistical polymer segment. A positive value of χ_s corresponds to an effective attractive interaction between the polymer segments and the protein surface. This lattice model approach resulted in a set of equilibrium chain conformations for the polymer, and an estimation of the free energy of the protein in the polymer solution phase.

The authors compared the lattice model predictions to measurements of the protein partition coefficents as a function of several polymer molecular weights, protein sizes and phase compositions in the PEO-dextran-water and PEO-PVME (poly(vinyl methyl ether))-water systems (Baskir et al., 1987, 1989b). A comparison of the experimental (filled circles) and model predicted values (solid curves) of the partition coefficient of pullulanase with PEO molecular weight is shown in Figure 2.11. In general, an attractive interaction free energy of approximately 0.2kT between a polymer segment and the protein surface was required to account for the experimental trends in the protein partition coefficient. It should also be noted that the authors did not treat explicitly the interactions of the salt (buffers), polymers and water, implying that this effect will be accounted for implicitly through the parameter χ_s. The authors speculated that the origin of the attraction between the polymer segments and the protein is hydrophobic in nature, although this seems inconsistent with the fact that χ_s for PEO (0.15) is significantly smaller than that for dextran (0.185), since PEO is generally considered to be the less hydrophilic of the two polymers (Albertsson, 1985). Note also that the predicted protein partition coefficient was found to be very sensitive to the value

of χ_s (Baskir et al., 1987).

By setting χ_s to zero, Baskir et al. (1987) evaluated the entropy change arising from the mixing of a hard sphere (the protein) and polymer coils, within in the context of the lattice model. This entropy change, and thus the predicted trends in the protein partition coefficient, are qualitatively different from those evaluated by Brooks et al. (1985) and Diamond and Hsu (1989), where the protein was represented as a random coil. For example, Baskir et al. (1987) predicted that for $\chi_s=0$ the entropy of mixing should be essentially independent of the polymer molecular weight while, in contrast, the Flory-Huggins form of the entropy of mixing predicts that the protein partition coefficient should decrease with increasing polymer molecular weight in the top phase (Brooks et al., 1985). Physically, it appears more reasonable to represent a globular protein by a hard sphere rather than a random coil, although the precise form of the entropy of mixing aqueous solutions of globular proteins and diffuse polymers appears unresolved (see Section 2.4.4).

A further interesting result of the model of Baskir et al. (1987) is the evaluation of the surface free energy of the proteins as a function of protein size, where it is reported that the Gibbs free energy of a protein is not proportional to the protein surface area until its radius is larger than approximately 60 Å. As most proteins are less than 60 Å in radius, the curvature of the protein surface appears to be important in describing its interaction with the surrounding polymer solution. This suggests that, in general, protein partitioning should not be characterized simply by the surface areas of the proteins, as discussed in Section 2.4.1.

2.4.3 Osmotic Virial-Expansion Approaches

The virial expansion-type approach for the description of protein partitioning in two-phase aqueous polymer systems is based on a generalization of the theory proposed by Edmonds and Ogston (1968) to describe the phenomenon of phase separation of aqueous solutions of macromolecules. The essence of the virial approach is to propose a mathematical expansion of the thermodynamic properties of the polymer

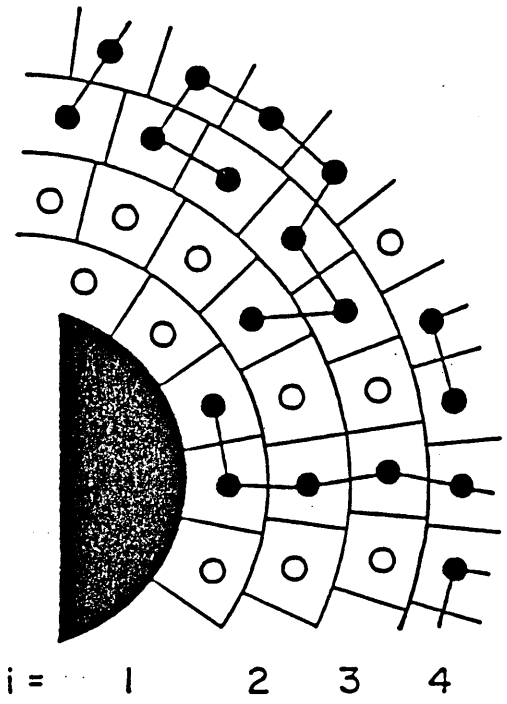

Figure 2.10 The lattice model for a protein in an aqueous polymer solution. The actual lattice is three dimensional (Baskir et al., 1987).

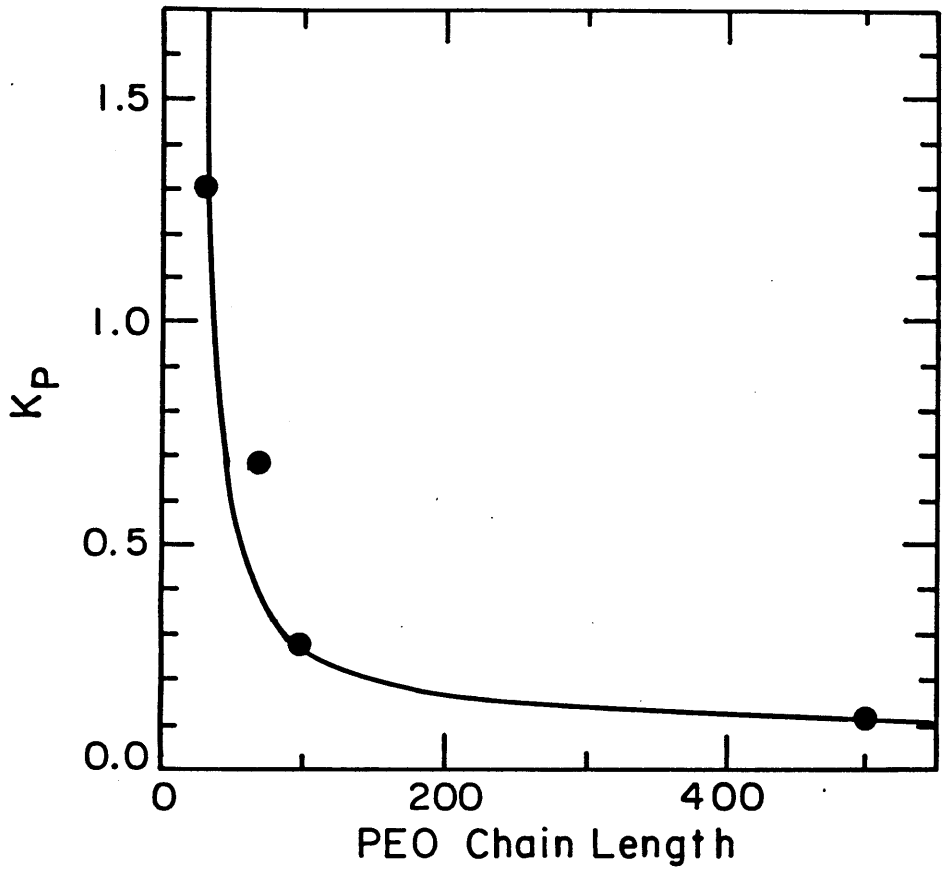

Figure 2.11 Predicted dependence of pullulanase partition coefficient (solid line) on PEO chain length in 12% w/w PEO (6,000 Daltons), 1% w/w dextran (500,000 Daltons) system. One unit of PEO chain length corresponds to 1 ethylene oxide repeat unit or 44 Daltons (Data of Hustedt et al., 1978; Model calculations of Baskir et al., 1987).

solution in terms of the concentrations of the polymers (McQuarrie, 1976). For example, the solvent chemical potential μ_1 (or, equivalently, the osmotic pressure), in a system containing three macromolecular species can be expressed as

$$\mu_1-\mu_1^o = -kTv_1\rho_1(m_2+m_3+m_p+\frac{a_{22}}{2}(m_2)^2+\frac{a_{33}}{2}(m_3)^2+\frac{a_{pp}}{2}(m_p)^2+ \\ +a_{23}(m_2m_3)+a_{2p}(m_2m_p)+a_{3p}(m_3m_p)+\ldots\ldots) \qquad (2.20)$$

where μ_1^o is the pure solvent chemical potential, v_1 is the pure solvent molar volume, ρ_1 is the solvent density, m_2, m_3 and m_p are the molalities of the two polymer types and the protein, respectively, and a_{ij} are the second virial coefficients of the i^{th} and j^{th} components. Equation (2.20) may be derived using statistical mechanics to provide a physical interpretation for the coefficients, a_{ij}. In *dilute* polymer solutions, the interaction coefficients, a_{ij}, reflect the pairwise interactions between polymer coils and proteins, i.e., a_{22} reflects the strength of the interaction between two polymer coils of type 2, a_{23} reflects the pairwise interaction between two polymer coils of type 2 and 3, and so on. The higher-order terms, not shown in Eq.(2.20), reflect the simultaneous interactions between three or more macromolecules in the solution. In general, for dilute solutions, the terms which are first-order and second-order in concentration describe the qualitative behavior of the solutions. To date, the virial-expansion approaches for protein partitioning in two-phase aqueous polymer systems have truncated the expansion at second-order in concentration. In the spirit of Eq.(2.20), King et al. (1988) and Forciniti and Hall (1990) have derived expressions for the chemical potentials of the two polymer types, protein and solvent in a two-phase aqueous polymer system. From these expressions, an equation for the partition coefficient of the proteins between the two aqueous polymer solution phases was derived to be

$$\ln K_p = \ln\left(\frac{m_p^t}{m_p^b}\right) = a_{2p}(m_2^b-m_2^t) + a_{3p}(m_3^b-m_3^t) + \frac{z_p e(\psi^b-\psi^t)}{kT} \qquad (2.21)$$

The last term was included by King et al. (1988) to account for the effect of electrostatic interactions in the system. In Eq.(2.21), under conditions of sufficient dilution, the coefficients a_{2p} and a_{3p} describe the strength of binary interactions between a protein and a polymer molecule. King et al. (1988) have reported an experimental determination of these coefficients, whereas Forciniti and Hall (1990) have attempted to calculate the coefficients from the molecular sizes of the proteins and the polymers. The virial model, Eq.(2.21), and the Flory-Huggins lattice model (Flory, 1953; Huggins, 1942), Eq.(2.17), both predict a similar dependence of the protein partition coefficient on the compositions of the two phases.

The interaction parameters, a_{ij}, in Eq.(2.21), were measured by King et al. (1988) using low-angle laser light scattering from buffered aqueous PEO-protein, dextran-protein, and PEO-dextran solutions under the same salt concentration and pH conditions as used in the two-phase aqueous polymer systems. A microelectrode was used to measure an electrical potential difference between the two phases caused by the presence of salts in the system, typically found to be less than 10mV. The experimentally determined interaction coefficients and electrical potential difference, when substituted into Eq.(2.21), gave a good prediction of the partition coefficient for several proteins with a variety of different salts and polymer concentrations. For example, for two different salt types, Figure 2.12 compares the experimentally measured and predicted partition coefficients of α-chymotrypsin as a function of the tie-line length in a PEO-dextran-salt system, defined as

$$b = [(w_3^t - w_3^b)^2 + (w_2^t - w_2^b)^2]^{1/2} \qquad (2.22)$$

Prediction of protein partition coefficients from the measured interaction parameters was often good, although an interpretation of the interaction parameters in terms of molecular properties of the proteins, polymers, salts and water was not reported. This has the disadvantage that measurements of the interaction coefficients, a_{ij}, are required for each polymer molecular weight, salt concentration, pH and protein type. In addition to enabling the prediction of protein partition coefficients, knowledge of the a_{ij}'s permitted

prediction of the binodals of the two-phase aqueous system.

Forciniti and Hall (1990) have also reported a theoretical treatment of protein partitioning in two-phase aqueous polymer systems using an osmotic virial-type expansion derived from a more fundamental consideration of statistical mechanics using the constant pressure solution theory of Hill (1957, 1959). Under certain assumptions, namely, those of a noninteracting solvent and an incompressible system, the derivation simplified to the Edmonds and Ogston theory (1962), the same theory which was used to provide the thermodynamic framework for the experimental approach of King et al. (1988). Forciniti and Hall (1990) investigated the dependence of the protein partition coefficients on the molecular weights of the protein and the polymers with the objective of exploring the role of excluded-volume interactions in protein partitioning. The coefficients were calculated using simple excluded-volume models for the polymer-protein interactions: the polymers were treated as impenetrable spheres, impenetrable cylinders or flexible coils. The protein was treated as an impenetrable sphere. The most successful of the three models was that in which the protein and dextran were treated as impenetrable spheres, and PEO was treated as an impenetrable cylinder, although none of the models could explain the dependence of protein partitioning on polymer molecular weight. Furthermore, the predicted trends in the protein partition coefficients were generally not of the correct order of magnitude, relative to experimental measurements. The authors concluded that excluded-volume interactions alone appear insufficient to account for observed protein partition coefficients, although for interactions between low molecular weight polymers and proteins, the characteristic size of the polymer coil with which to describe the polymer-protein interaction has not yet been identified (see Section 4.4) Furthermore, in Chapter 3 it will be shown that it is more appropriate to describe the protein-polymer interactions, for high molecular weight polymers, as interactions between proteins and a polymer net rather than identifiable polymers coil in the polymer solution. Note that the conclusion reached by Forciniti and Hall (1990), that excluded-volume interactions appear unable to account for protein partition coefficients, is also supported by Baskir et al. (1987).

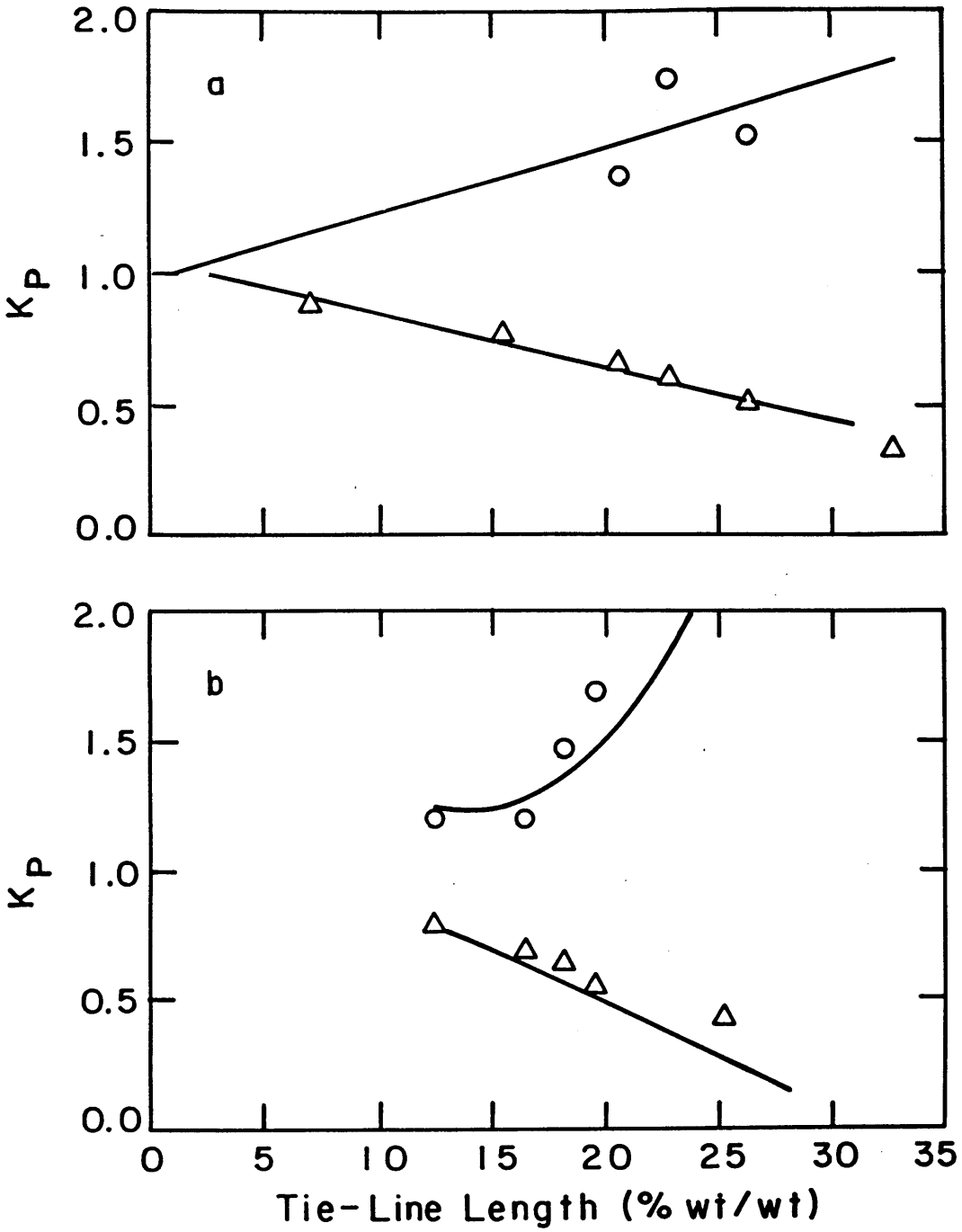

Figure 2.12 Comparison of measured (data points) and predicted (continuous lines) partition coefficients for α-chymotrypsin with increasing tieline length for system (a) PEO (3,350 Daltons), dextran (70,000 Daltons) salt and water, (b) PEO (8,000 Daltons), dextran (500,000 daltons), salt and water: (o) 50 mM KCl, (△) 50 mM KH_2PO_4 (King et al., 1988).

2.4.4 Models of Affinity Partitioning

Affinity partitioning is the enhanced partitioning of proteins resulting from the addition of a polymer derivatized with a ligand, that binds to certain receptor sites on proteins, to a two-phase system. The ligand may take various forms which include dyes, hydrophobic ligands, metals and other ionic groups (see Section 2.3.5). Despite these differences, certain features of affinity partitioning are universal and independent of the type of ligand, and may be understood using general thermodynamic models.

The first model for the action of polymer-ligand derivatives on the partition coefficients of proteins was reported by Flanagan and Barondes (1975). Using this model, they were able to account for the effect of the polymer-ligand concentration and number of protein receptor sites on the distribution of proteins between the two phases. Under the condition where only *one* ligand interacts with a protein, Flanagan and Barondes (1975) proposed the scheme presented in Figure 2.13. The generalization to n binding sites is straightforward, provided that the n sites are considered to be independent. The partition coefficient of the polymer-ligand-protein complex, K_p, is related to the free-energy change resulting from transferring the complex from the bottom phase to the top phase, ΔG_p, by

$$\Delta G_p = -kTlnK_p \tag{2.23}$$

Since the Gibbs free-energy change is solely a function of the thermodynamic state of the system, an equivalent process is one in which the polymer-ligand-protein complex dissociates in one phase, transfers between the phases and then reassociates in the other phase, as shown in Figure 2.12. The Gibbs free-energy for this process, ΔG_p, can be expressed as

$$\Delta G_p = -\Delta G_a^b + \Delta G_L + \Delta G_p^o + \Delta G_a^t \tag{2.24}$$

where the respective free-energy changes, ΔG_j^i are related to the equilibrium constants K_j^i through

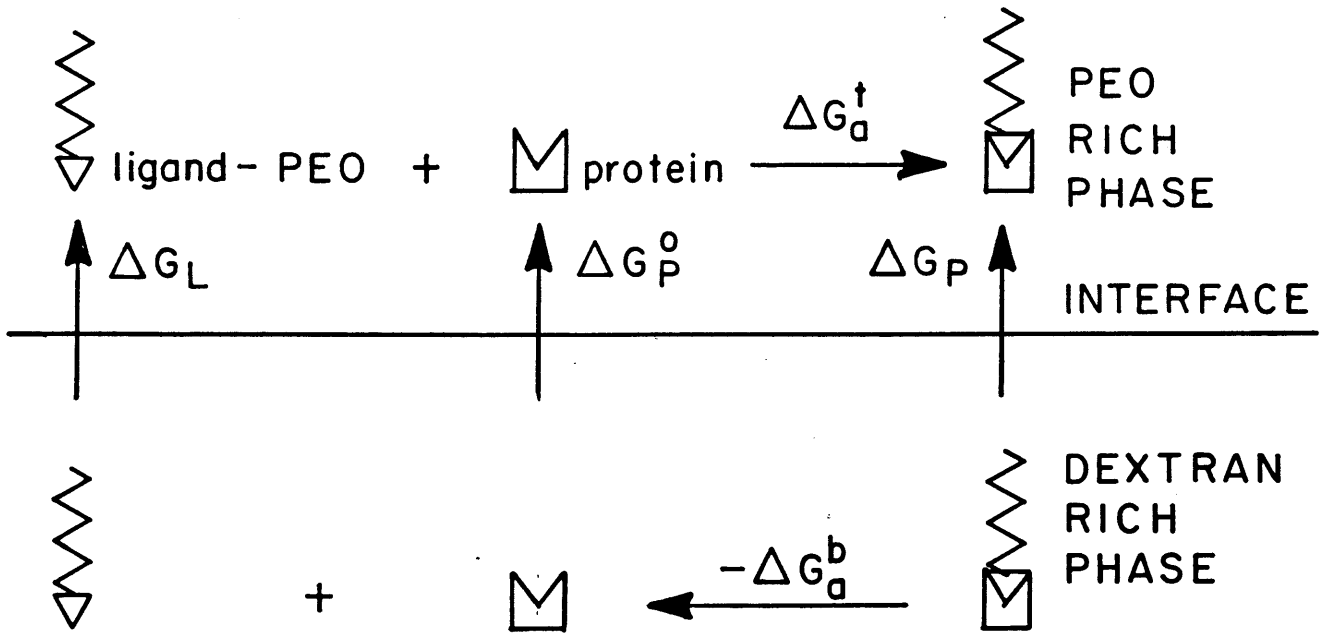

Figure 2.13 Schematic of interaction between protein and PEO-bound ligand in PEO-dextran system (Adapted from Flanagan and Barondes, 1975).

$$\Delta G_j^i = -kT\ln K_j^i \tag{2.25}$$

Note that K_a^t and K_a^b are the association constants for the proteins and ligands in the top and bottom phases, respectively. Eqs.(2.24) and (2.25) yield

$$K_p = K_p^o\left(\frac{K_L K_a^t}{K_a^b}\right) \tag{2.26}$$

For n binding sites per protein, Eq.(2.26) can be generalized to yield

$$K_p = K_p^o\left(\frac{K_L K_a^t}{K_a^b}\right)^n \tag{2.27}$$

To compare Eq.(2.26) with experimental measurements, the ligand-polymer species must be present in sufficient excess that all n sites on every protein are occupied by the ligands. In this limit, measurement of the distribution of proteins between the phases corresponds to a measurement of K_p. Furthermore, it is generally assumed that $K_a^t = K_a^b$, which corresponds to the association of the polymer-ligand and protein being equal in both phases. Under these conditions,

$$\ln\left(\frac{K_p}{K_p^o}\right) = n\ln K_L \tag{2.28}$$

The binding sites per protein, n, can be estimated from measurements of K_L, K_p and K_p^o. Comparisons with experimental measurements have revealed that this relationship yields rather low values of the number of ligands, n, bound to the proteins, as compared to the known number of active sites on the protein. Furthermore, n is generally determined to be noninteger.

Flanagan and Barondes (1975) recognized that at lower polymer-ligand concentrations, Eq.(2.26) will not be satisfied, as all ligand binding sites on the proteins will not be saturated with ligands. For the case where two ligands bind to each protein, the following expression for the overall partitioning of protein species (free and those complexed with the polymer ligand) was obtained,

$$K_p = K_p^o \left(\frac{1 + \frac{c_L^t K_L}{K_a^b}}{1 + \frac{c_L^t}{K_a^t}} \right)^2 \qquad (2.29)$$

where c_L^t is the ligand concentration in the top phase. This relationship was generalised by Brooks et al. (1985), and Cordes et al. (1987) for the interactions of n independent ligands per protein. The result is essentially identical to Eq.(2.29), except that the exponent 2 is replaced by n. A further refinement of the model allowed for two types of binding sites on the protein molecule, leading once again to a reasonable fit of the model to experimental data (Cordes et al., 1987).

Recently, an extension of the model of Cordes et al. (1987) has been reported for metal affinity partitioning (Suh and Arnold, 1990). In this model, the competition between the metal ligand (Cu(II)) and H^+ for the surface histidine residues of 4 different proteins was presented. The number of surface histidine sites on tuna cytochrome-C, *Candida krusei* cytochrome-C, horse hemoglobin, and whale myoglobin are 0, 2, 4 and 5, respectively. In contrast to other experimental investigations, a linear relationship was observed between $\Delta \log K_p$ and n, the number of surface histidines. This result suggests that the binding of each of the five polymers (PEO-5000) to whale myoglobin is independent of the presence of other bound polymers. In general, using other types of ligands, investigators have concluded that the number of bound polymers rarely exceeds 2.

To investigate the influence of factors such as polymer concentration, polymer molecular weight and protein size on the binding of ligands to proteins, Baskir et al. (1989a) have proposed a simple lattice model. In particular, they addressed the observations of Cordes et al. (1987), that generally (1) $\Delta \log K_p$ is not proportional to n, the number of binding sites on a protein, (2) the binding constants of the ligand-polymer are generally not equal in the two phases, (3) the binding may become weaker with increasing PEO concentration, and (4) the apparent number of binding sites, n, is frequently non-integral and can be less than unity. This model represents an extension of the earlier treatment by Baskir et al. (1987) for the partitioning of proteins in two-phase aqueous polymer systems in which the polymer concentration profile in the vicinity of the protein, in the absence of affinity ligands, was predicted. The extension to affinity partitioning assumes that the polymer-ligand is superimposed on, and has a negligible effect on, this concentration profile. The change in the free energy of a polymer-ligand as it is moved from the bulk polymer solution to the surface of the protein was calculated allowing for the interaction of only one polymer-ligand with the protein. As the length of the polymer tail attached to the ligand increased, the free energy of interaction was predicted to become less favorable. This corresponds to a decrease in $\Delta \ln K_p$ with increasing molecular weight of PEO, for a PEO-ligand which has been observed for some proteins, although for others there appears to be no influence of polymer molecular weight. As shown in Figure 2.14, an increase in the bulk polymer concentration (reported as the volume fraction of polymer in the bulk polymer solution, ϕ_2^*) was predicted to cause a decrease in the strength of the association between the polymer-ligand and the protein (characterized by $-\ln(K_a/K_a[\phi_2^*=0])$, where K_a is the binding constant for the association of the protein and ligand-bound polymer), consistent with measurements of the association of PEO-blue and formate dehydrogenase with increasing PEO concentration (Cordes et al., 1987). It was also predicted that the binding of a ligand-polymer may be enhanced by the presence of a polymer solution containing a different type of polymer than that used for the tail of the ligand, in agreement with the measurements of PEO-blue binding to formate dehydrogenase in dextran (Cordes et al., 1987).

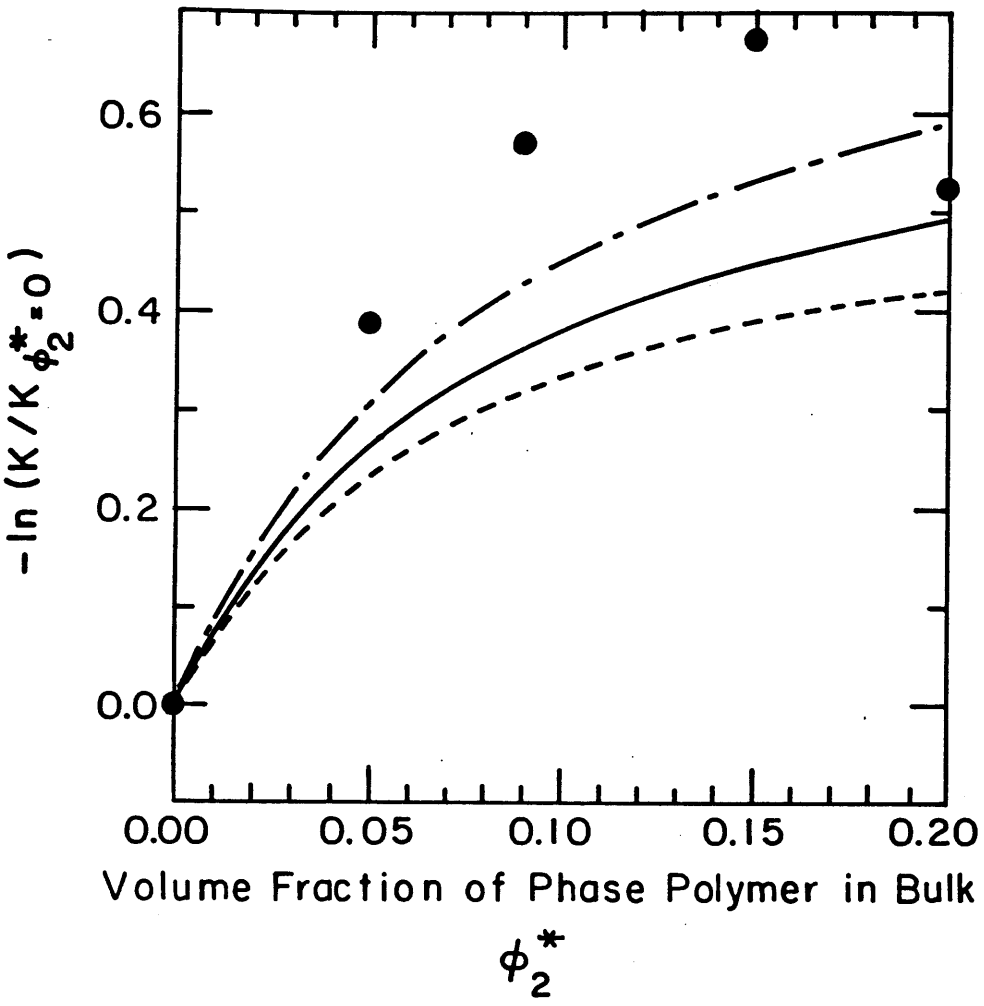

Figure 2.14 Predicted (curves) and experimental (data points) dependence of the formate dehydrogenase/PEO-blue association constant ($\ln K_a$) on the volume fraction of phase polymer (PEO) in the bulk polymer solution phase. $\chi_{t/s}$ is the polymer-ligand tail/protein surface interaction energy. Experimental data from Cordes et al. (1987), theoretical predictions from Baskir et al. (1989), -- - - -- - $\chi_{t/s}$=0.20, ------ $\chi_{t/s}$=0.175, - - - - $\chi_{t/s}$=0.15).

In general, the model proposed by Baskir et al. (1989a) for the binding of polymer-ligands to proteins suggests that, since the local environment about a protein may differ significantly from the bulk one, the binding constants of the polymer-ligands and the protein will in general vary with changes in the phase compositions, phase polymer types and polymer molecular weight. Although in the past these factors have been investigated experimentally, the model provides the first attempt at a molecular-level description of affinity partitioning processes, and provides possible explanations for a number of experimental observations. It must be emphasized, however, that this model implicitly incorporates the assumptions present in the lattice model discussed in Section 2.4, and as such suffers from similar deficiencies. Nevertheless, the good agreement between the model predictions and experimental results suggests that the dominant physical features of the affinity partitioning mechansim have been adequately captured.

2.5 Conclusions

In general, experimental investigations of protein partitioning in two-phase aqueous polymer systems have been successful in illuminating a wide variety of possible factors which can influence the distribution of proteins between two coexisting aqueous polymer solution phases. However, due to the large number of species present, and the complex nature of the individual species themselves, it has not always been possible to identify the precise mechanism(s) reponsible for specific partitioning behaviors. For example, experimental investigations have found that accompanying a change in the molecular weight of the phase forming polymers, there is an associated influence on the partitioning behavior of proteins in two-phase aqueous polymer systems. However, in order to rationalize the observed partitioning behavior, it is possible that one or more of a variety of mechanisms are responsible: Potential molecular-level mechanisms include the influence of polymer molecular weight on (i) the nature of the direct protein-polymer interactions, (ii) the polymer concentrations in the coexisting polymer solution phases, (iii) the Donnan equilibrium of charged species, and (iv) the nature of the protein-protein interactions in the polymer solution phases. Therefore, while existing experimental

investigations have been very useful in highlighting a *variety* of candidate mechanisms, it is evident that other experimental approaches are required in order to identify the *specific* mechanisms operating in these systems. In view of the ambiguity which is often associated with the interpretation of experimentally observed protein partitioning behaviors in two phase aqueous polymer systems, two important objectives of this thesis were,

(i) to consider carefully the potential coupling of mechanisms which influence partitioning of proteins in two-phase aqueous polymer systems. Specifically, in interpreting the influence of the phase-forming polymer molecular weight on the protein partition coefficient, we consider (a) the nature of protein-polymer interactions, (b) the nature of polymer-polymer interactions (including their influence on protein partitioning and the equilibrium of the coexisting polymer solution phases), (c) polymer-salt interactions, and (d) protein-protein interactions (which are mediated by the polymer solution phase).

(ii) to explore alternative experimental techniques with which to investigate aqueous solutions of proteins and polymers. In particular, we aimed to pursue experimental investigations in "one-phase" systems, since in single phase systems, the complications associated with the equilibrium of the coexisting polymer solution phases are removed. In this thesis we report (i) a small angle neutron scattering investigation (SANS) of aqueous solutions of PEO and bovine serum albumin and (ii) the partitioning of proteins between an aqueous solution and an entangled polymer solution using a diffusion cell with a semipermeable membrane.

In contrast to experimental investigations of protein partitioning in two-phase aqueous polymer systems, earlier theoretical formulations aimed at identifying the molecular-level mechanisms responsible for the experimentally observed partitioning behaviors have met with limited success. One factor which appears common to a number of the approaches is that insufficient consideration was given to the physical nature of the

system being described. In particular, the physical description must be reasonable from the view point of the protein, and thus approximations which have been successful in polymer-solution theories to predict thermodynamic properties of protein-free polymer solutions, can fail when applied to descriptions of the interactions of proteins and polymers in aqueous solutions. For example, simpler polymer solution theories neglect the correlations among polymer segments which arise from the excluded-volume interactions of the polymer coils in dilute polymer solutions, or the excluded-volume interactions of the polymer segments in extensively entangled polymer solutions. Accordingly, another central objective of this thesis was to address this issue and elucidate other aspects of the physical nature of the polymer solution which may be important in influencing protein partitioning. Specifically, three broad questions have been addressed:

(i) What factors constitute a *physical basis* for an understanding of protein partitioning? Specifically, how important are *geometry* and *energetics* in determining protein-polymer interactions?

(ii) Can we usefully apply *scaling concepts* from polymer physics (de Gennes, 1988) to rationalize the macroscopic consequences, such as protein partitioning behaviors, associated with different protein-polymer interaction mechanisms?

(iii) Can we reach a unified *theoretical description* of both the *molecular-level structure* and the *thermodynamic properties* of protein-polymer solutions, and verify both aspects using *experimental* methods?

In the following chapters of this thesis we address each of these objectives.

2.6 Literature Cited

Abbott, N.L.; Blankschtein, D.; Hatton, T. A., presented at the *6th International Conference on Partitioning in Aqueous Two-Phase Systems*, Assmannshausen, West Germany, **1989**.

Abbott, N.L., Blankschtein, D., Hatton, T. A., *Macromolecules*, **1991**, 24, 4334.

Albertsson, P.-Å., *Nature*, **1958**, 4637, 709.

Albertsson, P.-Å., *Partition of Cell Particles and Macromolecules*, Wiley, New York, N.Y. **1985**.

Albertsson, P.-Å.; Cajarville, A.; Brooks, D.E.; Tjerneld, F., *Biochimica et Biophysica Acta*, **1987**, 926, 87.

Albertsson, P.-Å.; Nyns, E. J., *Ark. Kemi*, **1961**, 17, 197.

Albertsson, P.-Å.; Sasakawa, S.; Walter, H., *Nature*, **1970**, 228, 1329.

Alexander, S., *J. Physique*, **1977**, 38, 977.

Ananthapadmanabhan, K.P.; Goddard, E.D., *J. Colloid Interface Sci.*, **1986**, 113, 294.

Ataman, M., *Colloid Polymer Sci.*, **1987**, 265, 19.

Ataman, M.; Boucher, E. A., *J. Poly. Sci. Poly. Phys. Ed.*, **1982**, 20, 1585.

Axelsson, C.-G., *Biochim. Biophys. Acta*, **1978**, 533, 34.

Bamberger, S.; Seaman, G.V.F.; Brown, J.A.; Brooks, D.E., *J. Colloid Interface Sci.*, **1984**, 99, 187.

Baskir, J.N.; Hatton, T.A.; Suter, U.W., *Macromolecules*, **1987**, 20, 1300.

Baskir, J. N., "Thermodynamics of the Separation of Biomaterials in Two-Phase Aqueous Polymer Systems", PhD Thesis, Massachusetts Institute of Technology, **1988**.

Baskir, J.N.; Hatton, T.A.; Suter, U.W., *J. Phys. Chem.*, **1989a**, 93, 969.

Baskir, J.N.; Hatton, T.A.; Suter, U.W., *J. Phys. Chem.*, **1989b**, 93, 2111.

Baskir, J.N.; Hatton, T.A.; Suter, U.W., *Biotechnol. Bioeng.*, **1989c**, 34, 541.

Bockris, J.O'M.; Reddy, A.K.N., *Modern Electrochemistry 1*, Plenum Press, New York **1970**.

Booth, F., *J. Chem. Phys.*, **1951**, 19, 391.

Booth, F., *J. Chem. Phys.*, **1955**, 23, 453.

Boucher, E.A.; Hines, P.M., *J. Poly. Sci.-Poly. Phys.*, **1976**, 14, 2241.

Boucher, E.A.; Hines, P.M., *J. Poly. Sci.-Poly. Phys.*, **1978**, 16, 501.

Boucher, E.A., *J. Chem. Soc., Faraday Trans. 1*, **1989**, 85, 2963.

Brooks, D.E.; Sharp, K.; Bamberger, S.; Tamblyn, C.H.; Seaman, G.V.F.; Walter, H., *J. Colloid Interface Sci.*, **1984**, 102, 1.

Brooks, D.E.; Sharp K.A.; Fisher, D., *Partitioning in Aqueous Two Phase Systems*, Walter, H.; Brooks, D.E.; Fisher, D., Eds, Academic Press, New York, **1985**.

Brönsted, J.N., *Z. Phys. Chem. Bodenstein-Festband*, **1931**, 155, 257.

Brönsted, J.N.; Warming, E., *Z. Phys. Chem. A.*, **1931**, 155, 343.

Cabane, B.; Duplessix, R., *J. Physique*, **1982**, 43, 1529.

Cabane, B.; Duplessix, R., *J. Physique*, **1987**, 48, 651.

Casassa, E.F., *J. Polymer Sci.*, **1976**, 54, 53.

Cohn, E.; Edsall, J., *Proteins, Amino Acids and Peptides as Ions and Dipolar Ions, ACS Monograph Series*, Reinhold Publishing Corporation, N.Y, **1943**.

Cordes, A.; Flossdorf, J.; Kula, M-R., *Biotechnol. Bioeng.*, **1987**, 30, 514.

Diamond, A.D.; Hsu, J.T., *Biotechnol. Bioeng.*, **1989**, 34, 1000.

Dobry, A.; Boyer-Kawenoki, F., *J. Poly. Sci.*, **1947**, 2, 90.

Edmond, E.; Ogston, A.G., *Biochem. J.*, **1968**, 109, 569.

Flanagan, S.D.; Barondes, S.H., *J. Biological Chem.*, **1975**, 250, 1484.

Florin, E.; Kjellander, R.; Eriksson, J.C., *J. Chem. Soc, Faraday Trans. 1*, **1984**, 80, 889.

Flory, P.J., *Statistical Mechanics of Chain Macromolecules*, Interscience, N.Y, **1968**.

Flory, P.J., *Disc. Faraday Soc.*, **1970**, 49, 7.

Flory, P. J., *Principles of Polymer Chemistry*, Cornell University Press, Ithaca, N.Y., **1953**.

Forciniti, D.; Hall, C.K., *ACS Symp. Ser.*, **1990**, 419, 53.

Forciniti, D.; Hall, C.K.; Kula, M.R., *Chem. Eng. Sci.*, **1991a**, in press.

Forciniti, D.; Hall, C.K.; Kula, M.R., *Biotechnol. Bioeng.*, **1991b**, in press.

Gelsema, W.J.; DeLigny, C.L., *Sep. Sci. and Technol.*, **1982**, 17, 375.

de Gennes, P.-G., *Scaling Concepts in Polymer Physics*, Cornell University Press, Ithaca, N.Y., **1979**.

Gerson, D.F., *Biochim. Biophys. Acta*, **1980**, 602, 269.

Gerson, D.F.; Akit, J., *Biochim. Biophys. Acta*, **1980**, 602, 281.

Gerson, D.F.; Scheer, D., *Biochim. Biophys. Acta*, **1980**, 602, 506.

Goldstein, R.E., *J. Chem. Phys.*, **1984**, 80, 5340.

Hill, T.L., *J. Am. Chem. Soc.*, **1957**, 79, 4885.

Hill, T.L., *J. Chem. Phys.*, **1959**, 30, 93.

Huggins, M.L., *Annal. N.Y. Acad. Sci.*, **1942**, 43, 1.

Hughes, P.; Lowe, C.R., *Enzyme Microb. Technol.*, **1988**, 10, 115.

Husted, H.; Kroner, H.K.; Stach, W.; Kula, M-R., *Biotechnol. Bioeng.*, **1978**, 20, 1989.

Johansson, G., *Biochim. Biophys. Acta*, **1970a**, 222, 387.

Johansson, G., *Biochim. Biophys. Acta*, **1970b**, 222, 381.

Johansson, G., *Proceedings of the International Solvent Extraction Conference*, **1971**, 2, 928.

Johansson, G., *Molec. Cell. Biochem.*, **1974**, 4, 169.

Johansson, G., *Biochim. Biophys. Acta.* **1976**, 451, 517.

Johansson, G., *J. Chromatogr.*, **1985**, 322, 425.

Johansson, G.; Andersson, M., *J. Chromatogr.*, **1984a**, 291, 175.

Johansson, G.; Andersson, M., *J. Chromatogr.*, **1984b**, 303, 39.

Johansson, G.; Andersson, M.; Akerlund, H.E., *J. Chromatogr.*, **1984**, 298, 483.

Johansson, G.; Joelsson, M., *J. Chromatogr.*, **1987**, 393, 195.

Johansson, G.; Kopperschläger, G.; Albertsson, P-Å., *Eur. J. Biochem.*, **1983**, 131, 589.

Johansson, G.; Shanbhag, V.P., *J. Chrom.*, **1984**, 284, 63.

Johansson, G.; Hartman, A.; Albertsson, P-Å., *Eur. J. Biochem.*, **1973**, 33, 379.

Kang, C.H.; Sandler, S.I., *Macromolecules*, **1988a**, 21, 3088.

Kang, C. H., Sandler, S. I., *Biotechnol. Bioeng.*, **1988b**, 32, 1158.

Karlstrom, G., *J. Phys. Chem.*, **1985**, 89, 4962.

Kern, R.J.; Slocombe, R.J., *J. Poly. Sci.*, **1955**, 15, 183.

Kern, R.J., *J. Poly. Sci.*, **1956**, 21, 19.

King, R.S.; Blanch, H.W.; Prausnitz, J.M., *AIChE Journal*, **1988**, 34, 1585.

Kjellander, R., Florin, E., *J. Chem. Soc., Faraday Trans. I*, **1981**, 77, 2053.

Kopperschläger, G.; Johansson, G., *Anal. Biochem.*, **1982**, 124, 117.

Kopperschläger, G.; Lorenz, G.; Usback, E., *J. Chromatogr.*, **1983**, 259, 97.

Kuboi, R.; Tanaka, H.; Komasawa, I., *Kagaku Kogaka Ranbunshu*, **1990**, 16, 1.

Kula, M-R.; Kroner, K.H.; Hustedt, H., *Advances in Biochemical Engineering*, **1982**, 24, 73.

Marques, C.M.; Joanny, J.F., *J. Physique*, **1988**, 49, 1103.

McQuarrie, D.A., *Statistical Mechanics*, Harper-Row, New York, **1976**.

Modell, M.; Reid, R.C., *Thermodynamics and Its Applications*, Prentice-Hall, N.Y., **1983**.

Perrau, M.B.; Iliopoulos, I.; Audebert, R., *Polymer*, **1989**, 30, 2112.

Pincus, P.A.; Sandroff, C.J.; Witten, T.A., *J. Physique*, **1984**, 45, 725.

Sanchez, I.C.; Balazs, A.C., *Macromolecules*, **1989**, 22, 2325.

Sasakawa, S.; Walter, H., *Biochemistry*, **1972**, 11, 2760.

Sasakawa, S.; Walter, H., *Biochemistry*, **1974**, 13, 29.

Scheutjens, J.M.H.M.; Fleer, G.J., *J. Phys. Chem.*, **1979**, 83, 1619.

Scheutjens, J.M.H.M.; Fleer, G.J., *J. Phys. Chem.*, **1980**, 84, 178.

Shanbhag, V.P.; Axelsson C-G., *Eur. J. Biochem.*, **1975**, 60, 17.

Shanbhag, V.P.; Johansson, G., *Biochem. Biophys. Res. Communications*, **1974**, 61, 1141.

Shanbhag, V.P.; Johansson, G., *Eur. J. Biochem.*, **1979**, 93, 363.

Sjoberg, A.; Karlstrom, G., *Macromolecules*, **1989**, 22, 1325.

Suh, S-S.; Arnold, F.H., *Biotech. Bioeng.*, **1990**, 35, 682.

Walter, H.; Sasakawa, S.; Albertsson, P.Å., *Biochemistry*, **1972**, 11, 3880.

Zaslavsky, B. Yu; Miheeva, L.M.; Mestechkina, N.M.; Pogorelov, V.M.; Rogozhin, S.V., *Febs Letters*, **1978**, 94, 77.

Zaslavsky, B.Yu; Miheeva, L.M.; Rogozhin, S.V., *Biochim. Biophys. Acta*, **1979**, 588, 89.

Zaslavsky, B.Yu; Miheeva, L.M.; Mestechkina, N.M.; Shchyukina, L.G.; Chlenov, M. A.; Kudrjashov, L.I.; Rogozhin, S.V., *J. Chromatogr.*, **1980**, 202, 63.

Zaslavsky, B.Yu; Miheeva, L.M.; Rogozhin, S.V., *J. Chromatogr.*, **1981**, 216, 103.

Zaslavsky, B.Yu; Mestechkina, N.M.; Miheeva, L.M.; Rogozhin, S.V., *J. Chromatogr.*, **1982**, 240, 21.

Zaslavsky, B.Yu; Mestechkina, N.M.; Rogozhin, S.V., *J. Chromatogr.*, **1983**, 260, 329.

Zaslavsky, B.Yu; Bagirov, T.O.; Borovskaya, A.A.; Gasanova, G.Z.; Gulaeva, N.D.; Levin, V.Yu; Masimov, A.A.; Mahmudov, A.V.; Mestechkina, N.M.; Niheeva, L.M. Osipov, N.N.; Rogozhin, S.V., *Colloid Polymer Sci.*. **1986**, 264, 1066.

Zaslavsky, B.Yu; Mahmudov, A.V.; Bagirov, T.O.; Borovskaya, A.A.; Gasanova, G. Z.; Gulaeva, N.D.; Levin, V.Yu; Mestechkina, N.M.; Miheeva, L.M.; Rodnikova, N. N., *Colloid Polymer Sci.*. **1987**, 265, 548.

Zaslavsky, B.Yu; Miheeva, L.M.; Aleschko-Ozhevskii, Y.Y.P.; Mahmudov, A.V.; Bagirov, T.O; Garaev, E.S., *J. Chromatogr.*, **1988**, 439, 267.

Chapter 3.

Novel Physical Pictures for Protein Partitioning in Two-Phase Aqueous Polymer Systems.

3.1 Introduction

In Chapter 2, a review of the existing theories for protein partitioning in two-phase aqueous polymer systems was presented. Here, we extract from Chapter 2 the extent to which the molecular natures of the proteins and the two-phase aqueous polymer systems were considered in earlier theoretical developments. In so doing, we aim to emphasize the fact that relatively little attention has been devoted in the past to developing a sound physical understanding of the molecular nature of these complex systems.

Brooks and coworkers (1985) and Albertsson and coworkers (1987) considered the molecular nature of two-phase aqueous polymer systems within the framework of the Flory-Huggins lattice model for polymer solutions (Flory, 1986; Huggins, 1941). In order to describe protein partitioning, the protein was approximated as a third flexible and linear polymer chain. On this basis, a qualitative interpretation of the dependence of the protein partition coefficient on protein size and on phase-forming polymer molecular weights was suggested. However, and as stated by these authors, some uncertainty exists in the conclusions reached due to the representation of relatively rigid and structured globular proteins as flexible and random coiling polymers (Brooks et al., 1985; Albertsson et al., 1987).

Alternatively, Forciniti and Hall (1990) explored the role of excluded-volume interactions on protein partitioning, at the protein isoelectric point, by calculating the second virial coefficients reflecting the protein-polymer interactions and treating the

protein as an impenetrable sphere and the polymers as either impenetrable spheres, cylinders or flexible coils. Implicitly, they assumed the polymer solution to contain identifiable polymer coils over the entire range of polymer molecular weights and concentrations encountered and did not consider the possibility of entanglement of the polymer coils into a mesh. In Chapter 3, we question the validity of this approximation and suggest that the high molecular weight polymers in the coexisting polymer solution phases of two-phase aqueous polymer systems *do* extensively entangle to form a polymer mesh. Within the polymer mesh the identities of individual polymer coils are lost, and the protein-polymer interactions become independent of the properties of the *polymer coils*, such as, their molecular weight. Accordingly, in entangled polymer solutions, we propose that it is not appropriate to describe the protein partitioning behavior in terms of protein-*polymer coil* interactions and therefore we suggest a mechanism which reflects the interactions of the proteins and a *polymer mesh.*

Baskir and coworkers (1987 and 1989) have extended a self-consistent mean-field model (Scheutjens and Fleer, 1979 and 1980) for the adsorption of flexible polymers onto planar surfaces to the case of a spherical geometry associated with the protein. In this model, the polymer segments are confined to a curved lattice determined by the spherical shape and size of the protein. In addition to the conventional polymer-solvent interaction parameters used in lattice models of polymer solutions (Flory, 1986; Higgins, 1941), a polymer segment-protein surface interaction parameter, χ_s, was introduced. The lattice-model approach predicts the average configurations of the polymer chains in the vicinity of the protein, as well as the chemical potential of the protein in the polymer solution phase. This approach, which has represented the most detailed molecular-level modelling attempt of protein partitioning in two-phase aqueous polymer solutions to date, contains a number of approximations in the physical description of the system. For example, it neglects fluctuations and correlations between polymer segments in the system, where the range can be larger or smaller than the protein size for the two-phase aqueous polymer systems considered in their work; that is, it assumes the polymer solution to be extensively interpenetrating over all molecular

weights of the polymers, and neglects correlations between polymer segments within the interpenetrating polymer network. In contrast, in the physical pictures developed in this chapter, we recognize that the solutions of low molecular weight polymers contain identifiable and singly dispersed polymer coils, and have explored the influence of such a scenario on the partitioning of proteins. Indeed, this region is of great interest since it is in this range of polymer molecular weights that the partition coefficient of the protein is most sensitive to the polymer molecular weight, as we show later. In addition, in solutions of high molecular weight polymers, where the identities of individual polymer coils are lost within a polymer network, we consider the existence of correlations within the polymer network arising from interactions between polymer segments and describe their influence on the partitioning of proteins.

In view of the rather simple and approximate physical foundations of the earlier theoretical formulations, in Chapter 3, we pursue a molecular description of the interactions of proteins and nonionic polymers with an emphasis on the development of physical pictures of these complex solutions. With this aim in mind, it is pertinent to note that, in general, the physics controlling the interactions between globular colloidal particles and flexible chain macromolecules is reflected in such diverse phenomena as the complexation of polymers and micelles (Tokiwa and Tsujii, 1973; Shirahama, 1974, Shirahama and Ide, 1976; Cabane, 1977; Cabane and Duplissex, 1982 and 1987; Goddard, 1986a,b); the polymeric stabilization and flocculation of gold sols (Heller and Pugh, 1956), ceramic particles (Woodhead, 1986), and other colloidal dispersions (Napper, 1983); and the stabilization, aggregation and precipitation of proteins (Gekko and Timasheff, 1981; Ingham, 1977 and 1978; Middaugh and Lawson, 1980). In the case of the adsorption of hydrophilic polymers onto the surfaces of ionic micelles in aqueous solutions, experimental measurements have revealed a variety of interesting physical pictures for these systems (Tokiwa and Tsujii, 1973; Shirahama, 1974, Shirahama and Ide, 1976; Cabane, 1977; Cabane and Duplissex, 1982 and 1987; Goddard, 1986a,b). For example, in dilute aqueous polymer solutions, anionic micelles adsorb onto a polymer coil giving rise to structures resembling beads on a necklace (Cabane and Duplessix, 1982). In addition, theory, particularly in the form of scaling

arguments, has complemented the experimental measurements and revealed important differences in the nature of polymer adsorption onto small globular colloids as compared to planar surfaces having infinite areas (Alexander, 1977; Pincus et al., 1984; Marques and Joanny, 1988).

The novel physical pictures which we have proposed are inspired, in part, by investigations of the interactions of nonionic polymers and micelles in aqueous solution (Tokiwa and Tsujii, 1973; Shirahama, 1974, Shirahama and Ide, 1976; Cabane, 1977; Cabane and Duplissex, 1982 and 1987; Goddard, 1986a,b). Ionic micelles and proteins can have similar shapes and sizes, and to some extent both micelles and proteins have charged surfaces and hydrophobic interiors. Based on this analogy, we reveal a variety of different physical pictures for aqueous polymer solutions containing globular proteins where pronounced differences exist which reflect the type, molecular weight and concentration of the polymer, the protein size, and the nature of the interactions between polymer segments and the protein.

For the various molecular-level pictures of aqueous polymer solutions containing proteins that we propose, in Chapters 4,5 and 6, we develop complementary statistical-thermodynamic models to describe the interactions of the polymers and the proteins, and discriminate between them by comparing the theoretical predictions with experimental trends. It is important to note that within the statistical-thermodynamic framework that relates the free energy of interaction between polymers and proteins to the protein partition coefficient, we have utilized simple geometric and scaling arguments (de Gennes, 1988) to capture the essential features of the interactions between polymers and proteins for each different physical picture proposed, as well as to obtain the various forms of the free energy of interaction. The essence of the scaling arguments is to capture the universal features characterizing the polymer-protein interactions. As such, the lack of cumbersome and complex computations permits us to concentrate on the underlying physical content of the formulation and *freely explore a variety of physical scenarios*.

The remainder of Chapter 3 is organized as follows. Section 3.2 presents our observations on some experimental protein partitioning data and highlights certain

correlations which exist between the protein partitioning behaviors, the protein properties, such as, protein size, as well as the properties of the two-phase systems, such as, polymer molecular weight. Section 3.3 discusses the applicability of polymer concepts in order to interpret the experimental observations presented in Section 3.2 and concludes that polymer concepts are applicable for the relatively low molecular weight poly(ethylene oxide) (PEO) considered. Using polymer concepts, Section 3.4 investigates the structure of the aqueous PEO-rich phase of an aqueous two-phase PEO-dextran system and reveals that the underlying structure of the PEO-rich phase undergoes a transition in nature with increasing PEO molecular weight. Specifically, a crossover from a PEO solution phase containing indentifiable polymer coils to a solution phase containing a polymer mesh (extensively entangled polymer coils) is proposed. Accompanying this proposition, a hypothesis is advanced which suggests that the protein partitioning behavior observed to accompany an increase in PEO molecular weight reflects this transition in the PEO solution structure. This hypothesis is subsequently supported in Section 3.5 by small angle neutron scattering (SANS) measurements from aqueous (D_2O) solutions which confirms the presence of the transition in the PEO-rich phase solution structure. In Section 3.6 we review structural studies of polymer-surfactant solutions and explore the analogy between the nature of a protein and that of micelles. This analogy is then combined with our description of the underlying structure of the PEO-rich phase to reveal novel physical pictures for protein partitioning in two-phase aqueous polymer systems in Section 3.7.

3.2 Experimental Observations

The measured partition coefficients, K_p, of a variety of globular proteins reported by Hustedt and coworkers (1978) and Albertsson and coworkers (1987) are presented in Figure 2.4 for the two-phase aqueous polymer system containing the polymers polyethylene oxide (PEO) and dextran. In this system, the top phase is rich in PEO and the bottom phase is rich in dextran. The response of the protein partition coefficients to changes in the molecular weight of PEO indicates the following three

features for these proteins in this system: (1) An increase in the molecular weight of PEO results in the partition of the proteins away from the top PEO-rich phase, and hence in a decrease in $\ln K_p$, (2) the protein response to the change in PEO molecular weight is greatest at PEO molecular weights below approximately 10,000 Daltons as reflected by the rapid decrease in $\ln K_p$ over this molecular-weight range, and (3) the response of the proteins to changes in PEO molecular weight is protein specific. Feature (3) is further reflected in Figure 3.1, where the change in the protein partition coefficient (per 4,000 Daltons PEO), $\Delta \ln K_p/\Delta M$, measured when the PEO molecular weight is varied from 4,000 Daltons to 8,000 Daltons (as shown by the circles) or from 20,000 Daltons to 40,000 Daltons (as shown by the diamonds) is given as a function of the hydrodynamic radii of the proteins. For example, in the region of low PEO molecular weight ($M_2 < 10{,}000$ Daltons), a doubling of the PEO molecular weight from 4,000 to 8,000 Daltons caused a change in the logarithm of the partition coefficient for ovalbumin (with a radius of 29Å) of 0.44kT per 4,000 Daltons of PEO. In contrast, for two-phase systems containing high molecular weight polyethylene oxide ($M_2 > 10{,}000$ Daltons), a change in the PEO molecular weight from 20,000 Daltons to 40,000 Daltons caused negligible change in the logarithm of the partition coefficient (per 4,000 Daltons change in PEO molecular weight). For all the proteins shown in Figure 3.1 it is apparent that this behavior is a general feature with the difference in partitioning between the low and high PEO molecular weight regions increasing with protein size.

For the systems in which the protein partition coefficients were measured by Albertsson and coworkers (1987), the weight fractions of each of the phase forming polymers in both the upper and lower phases are shown in Figure 3.2 (Albertsson, 1985). The constancy of the phase compositions over the range of PEO molecular weights investigated by Albertsson and coworkers (1987) suggests, to a first approximation, that the origin of trends measured in the protein partition coefficients with protein size and polymer molecular weight are not founded in variations of the phase compositions which may, in general, accompany changes in PEO molecular weight. Note that theinsensitivity of the phase compositions (%w/w) to the polymer molecular weight is due to the fact that the composition of the system is far from the critical-point composition. Furthermore,

it is evident from Figure 3.2 that each phase contains essentially only one type of polymer species. Typically, the concentration of the minor polymer species is less than 1% w/w.

Experimental observations such as those presented in Figures 2.4 and 3.1 motivated, in part, the philosophy behind our physical description of aqueous solutions and proteins and polymers. In particular, the correlation observed between the size of the proteins and their partitioning behavior suggests that geometry plays an important role in determining the protein partitioning behavior. Furthermore, it was apparent that the differences between the detailed chemical and physical natures of the proteins presented in Figure 2.4 are less important in determining their partitioning behaviors than are their common and averaged properties. The realization that a coarse-grained view of these systems, rather than an atom-by-atom account, may capture the essential nature of the interactions responsible for the partitioning behaviors of these proteins prompted the decision to pursue a scaling account (de Gennes, 1988; Alexander, 1977; Pincus et al., 1984; Marques et al., 1988) of protein partitioning. In addition, the formulation of a physical basis to account for the protein partitioning trends reported in Figures 2.4 and 3.1 was simplified by several experimental observations presented in Figure 3.2, namely, (i) negligible PEO was present in the dextran-rich phase, (ii) negligible dextran was present in the PEO-rich phase, and (iii) the *weight fractions* of PEO and dextran in the coexisting polymer solution phases were essentially constant over the range of PEO molecular weights investigated. Under these experimental conditions, the origin of the protein partitioning trends is traced to the influence of the PEO molecular weight on the PEO-rich phase. This simplification is discussed in more detail in Chapter 4. The impact of these simplifying observations on the development of physical pictures of protein partitioning is that we can focus our attention on the nature of the PEO-rich phase, and the protein-PEO interactions within the phase, in order to understand the protein partitioning behaviors presented in Figure 2.4.

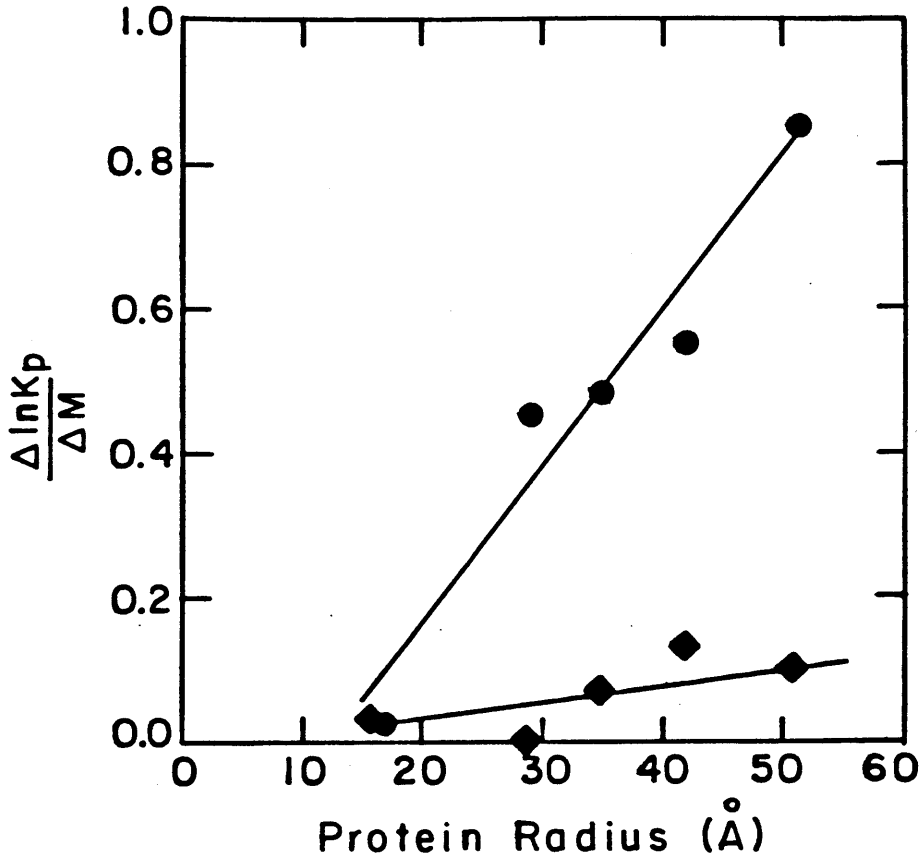

Figure 3.1 Change in protein partition coefficient (per 4,000 Daltons PEO), $\Delta \ln K_p / \Delta M_2$, with PEO molecular weight for five proteins; (o) 4,000 Daltons to 8,000 Daltons, (◇) 20,000 Daltons to 40,000 Daltons. The data are taken from Figure 2.4. In order of increasing size the proteins are: cytochrome-c, ovalbumin, bovine serum albumin, lactate dehydrogenase and catalase.

3.3 The Physical Nature of Aqueous Poly(Ethylene Oxide) (PEO) Solutions: Ordinary and Extraordinary Polymer Features

In the two-phase aqueous polymer systems of interest, the molecular weights of the PEO molecules are typically low, for example, Albertsson and coworkers (1987) used PEO molecular weights of 3,000 Daltons and above. We therefore examine the nature of PEO in a structured solvent such as water, and consider the applicability of polymer concepts to such species. PEO in the crystalline state possesses a helical structure (Tadokor et al., 1964). Upon dissolution in water, Raman (Koenig and Angood, 1970; Maxfield and Shepherd, 1975), infrared (Liu and Parsons, 1969) and nuclear magnetic resonance spectroscopies (Liu and Parsons, 1969; Liu and Anderson, 1970), as well as ultrasonic attenuation measurements (Hammes and Roberts, 1968) suggest the retention, to some extent, of the helical ordering present in crystalline PEO. Alternatively, investigations of high-molecular weight PEO in water using viscosity (Bailey et al., 1958; Beech and Booth, 1969; Molyneux, 1982), small-angle neutron scattering (SANS) and light scattering measurements (Cabane and Duplessix, 1982) reveal typical polymer-like behavior. For example, the exponent relating the polymer radius of gyration, R_g, to the molecular weight, M, is 0.62 and independent of the molecular weight for high molecular weight PEO (Cabane and Duplessix, 1982), as predicted by polymer scaling arguments (de Gennes, 1988). Therefore, one can conclude that high molecular weight PEO in water behaves as a quasi-random coil having some solvent-induced short-range order along the backbone of the polymer (Molyneux, 1982). For low-molecular weight PEO the evidence is less conclusive. There is an absence of appropriate SANS and light scattering data below PEO molecular weights of 10,000 Daltons, and the issue of partial coil drainage prevents the interpretation of viscosity data for low molecular weight polymers in terms of the polymer configuration (Beech and Booth, 1969; Bailey and Koleske, 1976). However, the elution of PEO in the molecular-weight range of 1,000 Daltons to 6,000 Daltons in water using size-exclusion chromatography was found to be only slightly affected by the addition of 6M guanidine (Ingham, 1977). As 6M guanidine disrupts hydrogen bonding in aqueous solution, this

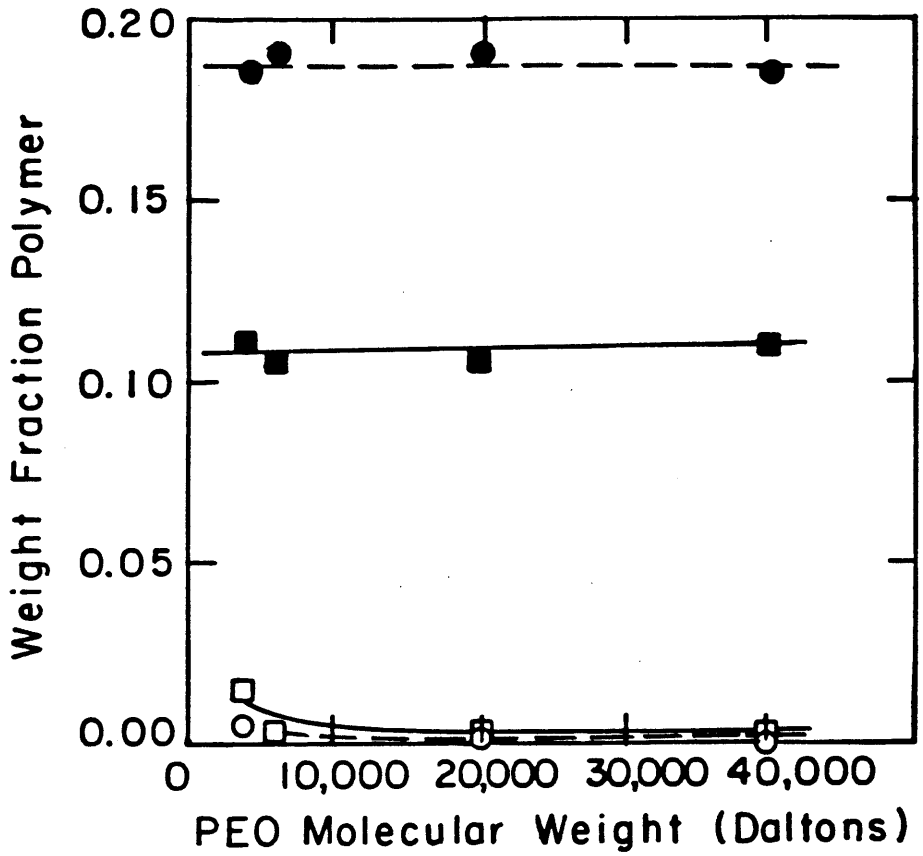

Figure 3.2 The weight fraction of PEO and dextran in the top and bottom phases as a function of PEO molecular weight; (●) dextran in bottom phase, (o) dextran in top phase, (■) PEO in top phase, (□) PEO in bottom phase. Data compiled from Albertsson, 1985).

suggests hydrogen bonding in aqueous solutions of low molecular weight PEO, at least, does not control the configuration of the polymer coils significantly. This observation, along with the flexibility of high molecular weight PEO, suggests that it is reasonable to treat PEO of molecular weight down to, at least, 3,000 Daltons using conventional polymer concepts.

3.4 The Structure of the PEO-Rich Solution Phase in Aqueous PEO-Dextran Two-Phase Systems

To elucidate the nature of the aqueous PEO solution comprising the top PEO-rich phase, we found it instructive to examine the PEO crossover concentration, c^*, as a function of PEO molecular weight, which can be estimated from

$$c^* = \frac{M}{\frac{4\pi}{3}R_g^3}, \qquad (3.1)$$

where M and R_g are the molecular weight and radius of gyration of the PEO polymer molecules, respectively (de Gennes, 1988). Eq.(3.1) defines the characteristic concentration of polymer mass within each polymer coil volume. Clearly, when the actual concentration of polymer in the solution exceeds this characteristic concentration, the coils are overlapping. In other words, the crossover concentration, c^*, is a polymer concentration characteristic of the region where the extensive overlap of polymer coils begins to occur. At polymer concentrations, c, much less than c^* the solution is dilute in polymer coils and consequently the identity of each individual polymer coil is preserved, and the solution properties reflect the identities of the individual polymer coils (Figure 3.3(a)). In contrast, when the polymer concentration is much greater than c^*, the polymer coils, no longer separated by regions of solvent, overlap and entangle with each other to form a continuous polymer web or net (Figure 3.3(b)). Within this web, the identities of the individual polymer coils are lost, and all thermodynamic properties

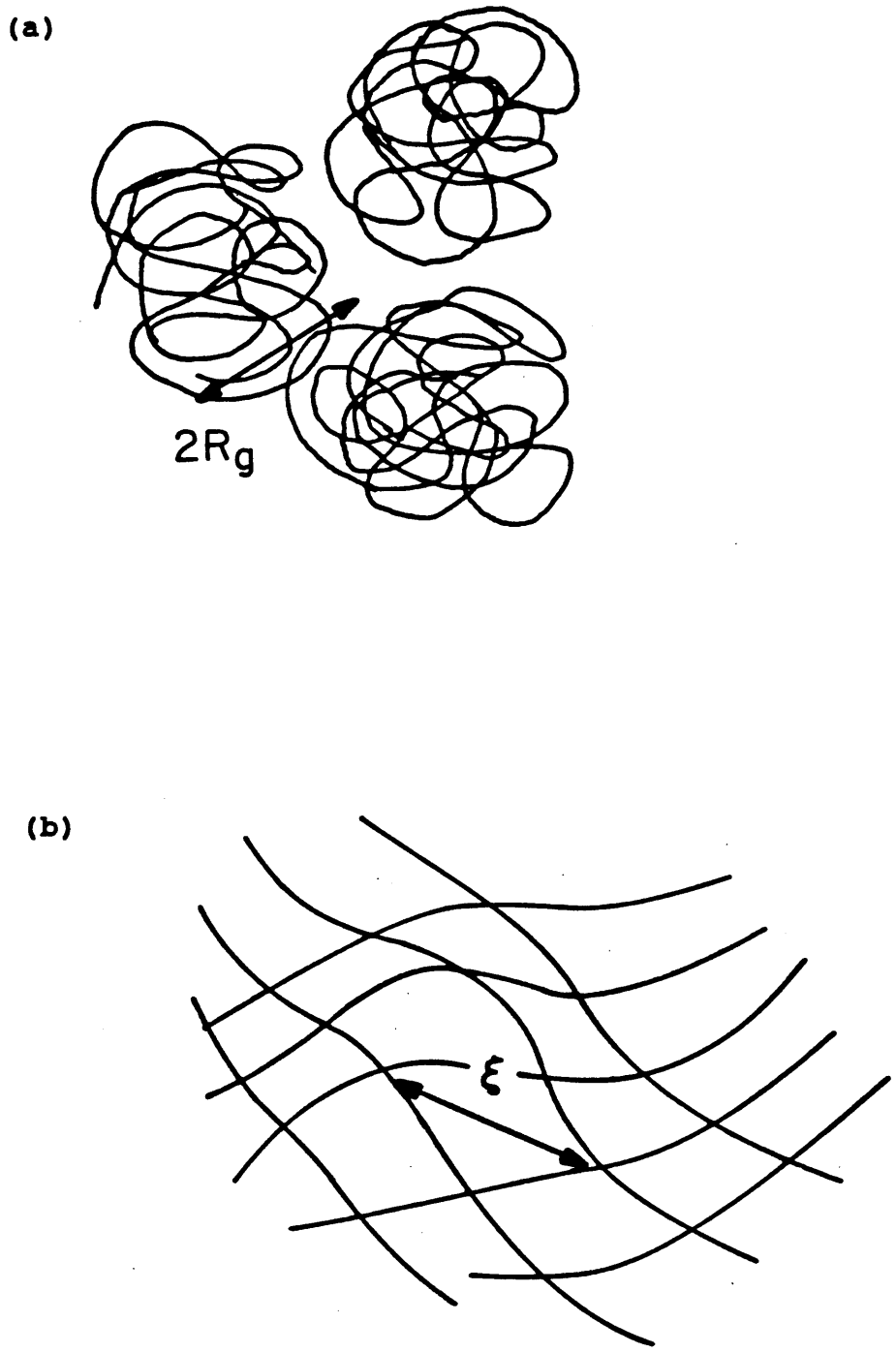

Figure 3.3 Polymer solution regimes: (a) $c \ll c^*$, (b) $c \gg c^*$

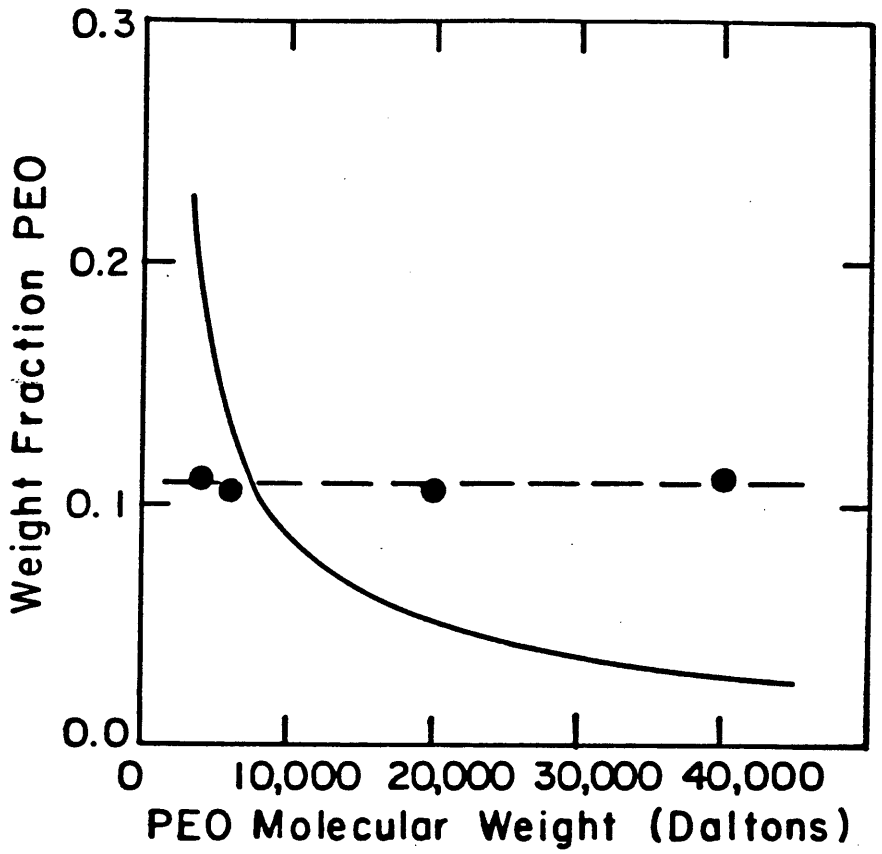

Figure 3.4 The polymer concentration, c^*, characterizing the transition from dilute to semidilute polymer solution regimes, evaluated from Eq.(3.1) as a function of PEO molecular weight (full line), and the measured PEO concentration, c, in the top PEO-rich phase, (•).

of the solution become independent of the molecular weight of the polymer coils. For aqueous solutions of PEO, the values of c^*, calculated from Eq.(3.1) as a function of polymer molecular weight, M, are reported as the full line in Figure 3.5. Also shown in Figure 3.4 is the measured PEO concentration in the top PEO-rich phase (data points with dashed line) for the systems in which the protein partition coefficients were measured by Albertsson (1985) and Albertsson and coworkers (1987). The two curves intersect in the vicinity of a PEO molecular weight of 10,000 Daltons, indicating that in going from a low to a high PEO molecular weight, the nature of the top PEO-rich solution phase undergoes a profound change in nature, as illustrated in Figure 3.4. This is an important observation, as it suggests that the change in the measured protein partition coefficents with increasing PEO molecular weight may, in fact, reflect the changing nature of the polymer solution in the top PEO-rich phase. This also suggests that the interactions of proteins and polymers will be quite different in the limits of low and high PEO molecular weights. Important objectives of this chapter are to characterize the changing nature of these interactions between proteins and polymers, and to investigate how these changes relate to the trends observed in the experimentally measured protein partition coefficients.

3.5 Neutron Scattering from Aqueous PEO Solutions

In Section 3.4, the importance of the theoretically predicted transition in the structure of the top PEO-rich phase (from singly dispersed polymer coils to an entangled polymer web) of the two-phase aqueous PEO-dextran system was outlined. In view of the important consequences of this prediction, the first objective of our neutron scattering investigation was to test experimentally the existence of such a transition over the range of PEO concentrations and molecular weights typically encountered in two-phase aqueous PEO-dextran systems. Here we present only the interpretation of the results of the experimental investigation, and their implcations on the development of physical pictures of protein-polymer interaction, and defer a detailed discussion of the technique of small angle neutron scattering and our experimental

methods to Chapter 7.

In general, the scattering of neutrons from flexible polymers dispersed in a low molecular weight solvent (such as D_2O) can be interpreted using the expression (Wilzius et al., 1983; Schaefer, 1984)

$$\frac{I_2(0)}{I_2(q)} = (1 + \xi^2 q^2) \qquad \textbf{(3.2)}$$

where the correlation length, ξ, may be interpreted as $R_g/3^{1/2}$ in the limit of vanishing polymer concentration (provided, $q < 3^{1/2}/R_g$), or as proportional to the polymer mesh or "blob" size (de Gennes, 1988), ξ_b, for entangled polymer solutions (provided $q < 1/0.35\xi_b$). More precisely, $\xi = 0.35\xi_b$ for an entangled polymer solution (Cabane and Duplessix, 1987).

In Figure 3.5, the logarithm of the correlation lengths for PEO in D_2O are presented as a function of the logarithm of the PEO volume fractions for a range of polymer molecular weights between 1 500 Da and 860 000 Da (data taken from Table 3.1). Several regimes corresponding to different solution behavior can be identified from an inspection of Figure 3.5. For the higher molecular weight polymers ($M_2 \gg 10\ 000$ Da), the ξ values are observed to collapse onto a universal curve (solid line) over the range of polymer volume fractions reported in Table 3.1. For these polymers, the magnitude of ξ is independent of polymer molecular weight, being solely a function of the polymer volume fraction. This observation is consistent with the existence of an entangled polymer mesh within which the identities of the individual polymer coils are lost (de Gennes, 1988).

In contrast to the universal behavior (molecular weight independence) observed for the high molecular weight polymers, the ξ values determined from the PEO samples having molecular weights of 1 500 Da, 4 000 Da and 9 000 Da were sensitive to the molecular weight of the polymer. The deduced ξ values were observed to increase with an increase in polymer molecular weight. This suggests that the structure of these solutions is sensitive to the sizes of the polymer coils, and is therefore indicative

Table 3.1 The polymer solution correlation length, ξ, deduced from SANS measurements for various molecular weights and volume fractions of PEO in D_2O.

PEO MOLECULAR WEIGHT (Da)	PEO VOLUME FRACTION	PEO SOLUTION CORRELATION LENGTH (Å)
860 000	0.008	45
	0.041	18
270 000	0.033	18
	0.067	12
160 000	0.054	13
	0.025	24
85 000	0.008	46
	0.047	15
	0.083	10
45 000	0.017	31
	0.083	10
	0.124	6.7
	0.039	16
21 000	0.025	23
	0.083	9.1
	0.124	6.3
	0.207	4.2
9 000	0.058	10
	0.097	8.4
	0.143	5.6
	0.167	4.6
	0.250	2.8

4 000	0.057	7.7
	0.097	6.0
	0.140	5.3
	0.125	5.6
	0.166	4.2
	0.250	2.5
1 500	0.057	5.3
	0.097	4.6
	0.140	3.9
	0.167	3.5
	0.250	2.5

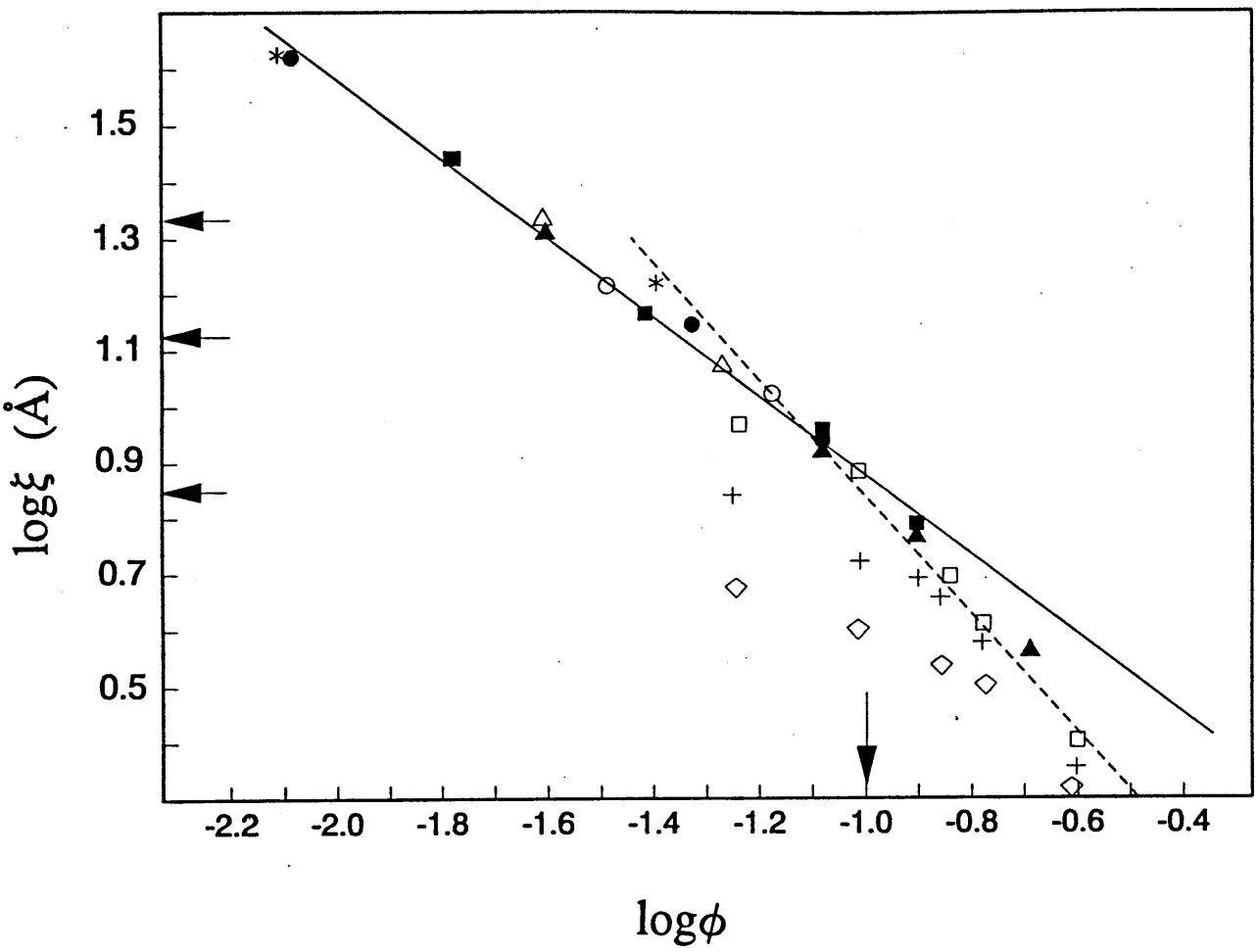

Figure 3.5 Logarithm of the static correlation length, $\log\xi$, as a function of the logarithm of the PEO volume fraction, $\log\phi$, deduced from SANS measurements of PEO in D_2O. Polymer molecular weights in Da: (*) 860 000, (o) 270 000, (▵) 160 000, (●) 85 000, (■) 45 000, (▲) 21 000, (□) 9 000, (+) 4 000, (◇) 1 500. See text for description of arrows.

of a polymer solution which contains identifiable polymer coils (Wiltzius et al., 1983; Schaefer, 1984). With decreasing polymer concentration, the ξ values for the low molecular weight polymers (1 500 Da, 4 000 Da and 9 000 Da) appear to be increasing towards a limiting value (dependent on the polymer molecular weight), which in the limit of vanishing polymer concentration should become equal to $R_g/3^{1/2}$ (see Chapter 7)). In Figure 3.5, on the ordinate axis, the correlation lengths evaluated according to $\xi = R_g/3^{1/2}$ are indicated by the horizontal arrows for PEO 1 500 Da, 4 000 Da and 9 000 Da, where R_g was determined from independent theoretical predictions which are reported in Chapter 6. The calculated ξ values (indicated by the arrows) appear to be in keeping with an extrapolation of the measured values of ξ to vanishing polymer concentration. Clearly, additional measurements are required at lower polymer concentrations to make a more precise comparison and reach a more definitive conclusion. At a fixed volume fraction of low molecular weight PEO, for example, $\log\phi = -1$, the value of ξ was observed to increase with molecular weight, but was always bounded by the ξ value of the solutions containing entangled high molecular weight PEO. The presence of the upper bound is consistent with the fact that with increasing molecular weight, the polymer coils entangle into a mesh. Within the entangled polymer mesh, the indentities of the individual polymer coils are lost and, therefore, the correlation length is observed to become independent of polymer molecular weight (de Gennes, 1988).

The central conclusion resulting from the experimental determination of the correlation lengths of aqueous PEO solutions is the confirmation of the occurrence of a transition in the polymer solution structure, from one containing identifiable polymer coils to one containing an entangled polymer network. In particular, beyond a PEO volume fraction of about 0.1 (see the vertical arrow in Figure 3.5), which is close to the concentration of PEO typically encountered in the PEO-rich phase of a two-phase aqueous PEO-dextran system, the onset of the molecular weight dependence of the correlation length occurs in the vicinity of a PEO molecular weight of about 10 000 Da. This is consistent with the hypothesis reported in Section 3.4 of a transition in the PEO-rich phase structure on the basis of experimentally observed protein partitioning (a thermodynamic property). It is important to note that the transition in the solution

structure is a gradual one, and in practice, much of the protein partitioning occurs in the crossover region (with reference to Figure 3.5, the crossover for a particular molecular weight of PEO can be defined as the range of polymer concentrations where the correlation length of the polymer solution is a function of both PEO molecular weight and volume fraction). This conclusion is not only relevant to past and future theoretical developments, but also impacted on our interpretation of the neutron scattering from polymer solutions containing proteins presented in Chapter 7. That is, for the 5.9% w/w PEO solution of molecular weight 8,650 Da (with BSA) that we investigate in detail below, we have adopted an analysis which describes the interactions between identifiable polymer coils and protein molecules (rather than an entangled polymer net interacting with protein molecules).

3.6 Structural Studies on Polymer-Surfactant Solutions: The Polymer-Micelle Analogy.

Although in Sections 3.4 and 3.5 we have established that individual polymer coils will be present in PEO solution phases of low PEO molecular weight, and an entangled PEO mesh will be present in PEO solution phases of high molecular weight (and concentration), the underlying physical nature of the polymer solution in the presence of proteins also depends, in part, on the relative strength of the interactions between the polymer coils and the globular protein molecules.

In Section 3.1, an analogy between interactions of proteins and polymers and interactions of ionic micelles and polymers was proposed. This analogy appears fruitful because the interactions of ionic micelles and polymers have been the subject of a number of experimental investigations (Tokiwa and Tsujii, 1973; Shirahama, 1974, Shirahama and Ide, 1976; Cabane, 1977; Cabane and Duplissex, 1982 and 1987; Goddard, 1986a,b). In particular, the structure of the aqueous polymer-micelle system containing PEO and sodium dodecylsulfate (SDS) anionic micelles has been studied in some detail by a variety of techniques including dialysis (Shirahama, 1974), conductivity (Tokiwa, 1973), surface tension (Jones, 1967), dye solubilization (Tokiwa, 1973),

nuclear magnetic resonance (Cabane, 1977), and small-angle neutron scattering (Cabane and Duplessix, 1982 and 1987). A conclusion supported by these experiments is the existence of a strong attraction between the anionic micelles and the PEO coils. More generally, it appears that interactions between polymers and micelles depend on the extent to which the polymer shields the micellar hydrocarbon cores from water, as well as on the magnitude of steric and electrostatic interactions between the polar surfactant head groups and the polymer segments (Nagarajan and Kalpacki, 1982). For example, the interaction of PEO with cationic micelles is found to be weaker than that with anionic micelles (Nagarajan and Kalpacki, 1982), and negligible interactions of PEO with nonionic micelles have been reported (Cabane, 1977). Therefore, by analogy, interactions of both the protein charges and the more hydrophobic amino acid residues with PEO may provide an attraction between the protein and the polymer segments. In proposing possible physical pictures of polymer-protein solutions we have catered for the existence of such attractive interactions.

Although the similarities of ionic micelles and proteins have been emphasized and will be exploited in our development of a physical basis for protein partitioning, we recognize that other properties of these two colloids differ from each other. For example, the structures of globular proteins are often stabilized by the formation of intramolecular covalent disulfide bonds which impart a degree of rigidity to the protein. In contrast, the assembly of surfactant molecules into a micellar structure is driven by purely physical forces and results in a less rigid assembly than a protein, and allows the continual exchange of surfactant molecules between micelles as well as surfactant monomers in solution. However, despite these difference, similarities in the nature of proteins and micelles do exist, and it is interesting, to consider, in general, the extent to which the understanding of well defined self-assembling systems can be translated to more complicated biological systems.

3.7 Novel Physical Pictures for Proteins in Polymer Solutions

We consider polymer solution phases rich in PEO having molecular

weights of less than approximately 10,000 Daltons as low molecular weight polymer solutions. In these solutions, for which $c < c^*$, the identities of the individual polymer molecules are preserved, and the important characteristic length scale to consider is the polymer coil size, described by its radius of gyration, R_g (see Figure 3.4(a)). For dilute solutions of PEO and water at ambient temperatures, excluded-volume interactions between the polymer segments cause the radius of gyration to scale as $M^{3/5}$ (Cabane and Duplessix, 1982, de Gennes, 1988). For the range of PEO molecular weights typically encountered in protein partitioning experiments, the polymer coil radius of gyration and the protein hydrodynamic radius have comparable sizes. Note, however, that the polymer can be larger or smaller than the protein, depending on the specific protein species and particular PEO molecular weight. Since the specific nature of the interactions between proteins and PEO appears unknown, we have explored a variety of possible physical pictures which differ primarily in the strength of the polymer coil interaction with the protein. Three pictures representing the nature of the interactions of proteins and low molecular weight PEO molecules are presented in Figure 3.6. The first picture, Figure 3.6(a), presents a scenario where the only interaction between the protein and the polymer coils is a physical excluded-volume interaction. That is, the free-energy change resulting from the introduction of a protein into the PEO solution arises solely as a consequence of the change in the number of configurations available to the system. The second picture, Figure 3.6(b), describes a scenario where a very weak attraction exists between the protein and polymer coils in addition to the excluded-volume interaction. Specifically, the attractive interaction is not strong enough to cause the collapse of the polymer coils onto the protein surface. Consequently, the polymer coils remain essentially undeformed in the vicinity of the protein surface. If the attractive interaction between the protein and the polymer coils increases in strength, the polymer coil will deform and actually adsorb onto the protein surface thus forming a polymer-protein complex. This third scenario is reflected in Figure 3.6(c). The deformation of the polymer from its relaxed configuration in the bulk solution, characterised by R_g, to a pancake-shaped configuration, characterised by thickness $D \ll R_g$, concentrates the polymer segments in the vicinity of the protein surface and thus increases the number of

contacts between each polymer coil and the protein surface. Limiting the extent of polymer adsorption are the loss of polymer conformations, as well as an increase in the excluded-volume interactions between the polymer segments present in the adsorbed layer.

In proposing physical pictures to describe the interactions of similar proteins and PEO in solutions *where the PEO coils have extensively entangled*, we have also considered the influence of steric and attractive interactions on the thermodynamic properties of these solutions. In Figure 3.7, we suggest four possible pictures for the interactions of globular protein molecules with an entangled polymer solution network. These scenarios reflect differences in the relative sizes of the polymer solution blob size, ξ_b, and the protein size, R_p, in addition to the strength of the attractive interactions between the polymer and protein molecules, which is characterized by ε, the energy change associated with bringing a single polymer segment from a solvated environment to the protein surface. For example, when R_p is less than ξ_b, and only steric interactions occur between the protein and the polymer segments, the protein behavior will be similar to that of an inert solvent species, capable of diffusing relatively unhindered through the polymer net (Figure 3.7(a)). While the protein is unaware of the mesh size of the polymer solution, depending on the relative size of the protein and the persistence length of the polymer chain, b, the protein may either interact independently with each polymer segment, $R_p \ll b$, or the protein may interact simultaneously with a group of correlated polymer segments within a volume roughly the size of the protein, $R_p \gg b$.

A rather different situation prevails when the protein size is much larger than the polymer blob size, that is when $R_p \gg \xi_b$. In this case, repulsive excluded-volume interactions between polymer strands belonging to the mesh and the impenetrable protein surface will cause a depletion of the polymer segments near the protein surface (Figure 3.7(b)). In view of the ability of the polymer segments to communicate the presence of the protein surface over distances corresponding to the correlation length of the polymer solution, the length scale of the depletion layer will be of order ξ_b. In this situation, since the radius of the protein is large compared to the correlation length of the polymer solution, the curvature of the protein surface does not play a dominant role in

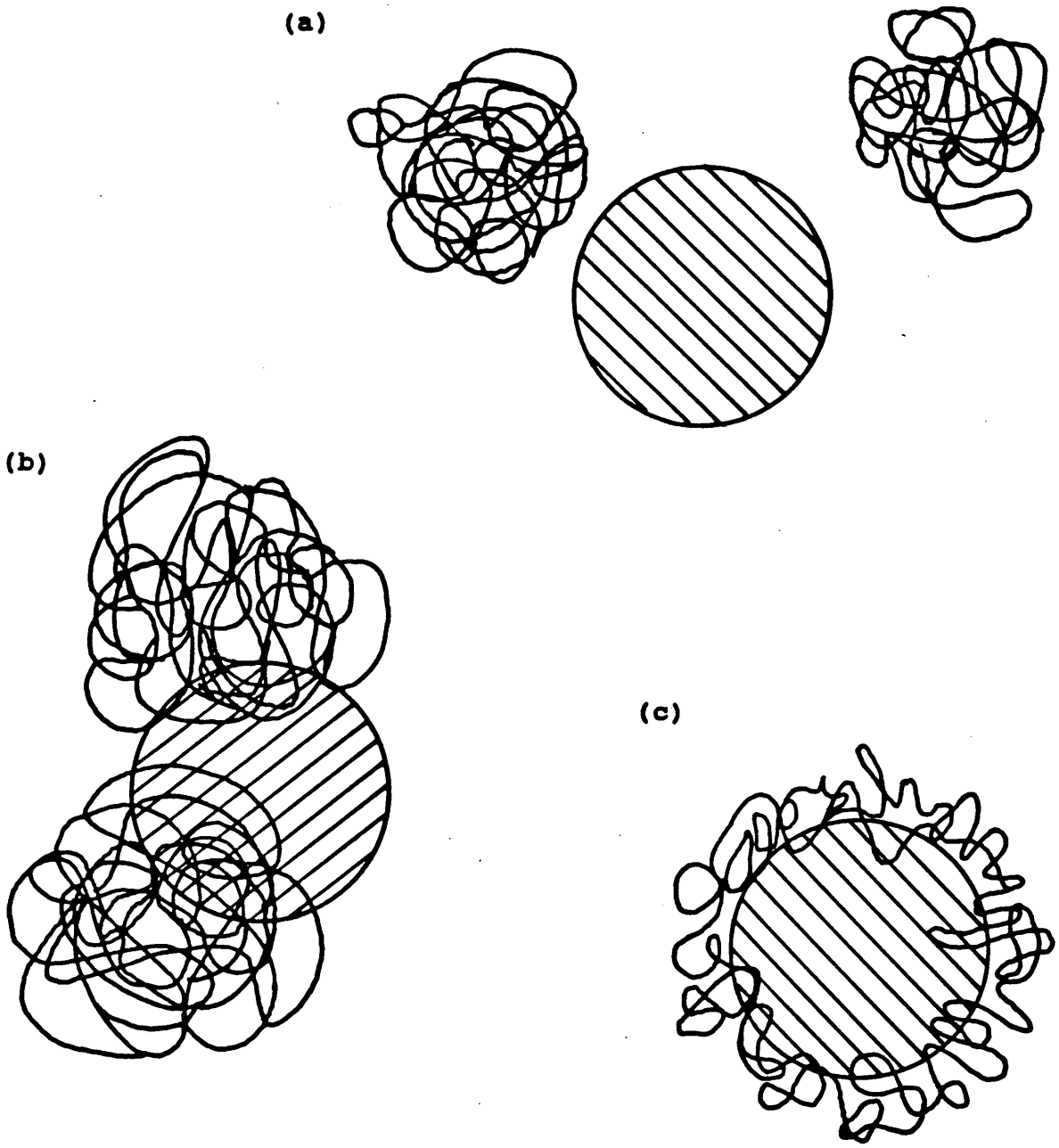

Figure 3.6. Three pictures representing the possible nature of the interactions between proteins and low molecular weight polymers: (a) Picture 1, physical exclusion only; (b) Picture 2, a weak attraction exists between the polymer and the protein in addition to physical exclusion; and (c) Picture 3, a stronger attraction between the polymer coils and the protein causes the formation of an adsorbed polymer layer about the protein.

determining the interactions of the protein and polymer network (other than to define the surface area of the protein).

One can also imagine scenarios where there are both steric and weak (perturbative) attractive interactions between the protein molecules and the polymers (Ingham, 1977). Under conditions such that the attraction is sufficiently weak, the structure of the solutions, as presented in Figures 3.7(a) and 3.7(b), are essentially preserved. In Chapter 5, we examine the influence of such weak attractions on the thermodynamic properties of entangled polymer solutions containing proteins.

In contrast to the case where there is a very weak attraction between the protein and polymer solution net, the presence of a stronger attraction will promote the decoration of the protein surface with an adsorbed layer of polymer, and consequently will induce a significant alteration of the structure of the polymer solution phase in the neighborhood of the protein. Scenarios corresponding to this situation are depicted in Figures 3.7(c) and 3.7(d). For polymer solution conditions where the polymer net size greatly exceeds the size of the protein, $\xi_b \gg R_p$, under the influence of strong attractive interactions between proteins and polymers, proteins may adsorb to the polymer net like beads on a necklace (Figure 3.7(c)). This regime is analogous to that investigated by Cabane and Duplessix (1982 and 1987) for a semidilute PEO solution complexing with SDS micelles. In this limit, where the protein is much smaller that the size of the polymer mesh (that is, much smaller than the range of the correlations between polymer segments) the nature of interactions between the polymers and proteins will be essentially independent of the polymer mesh size. That is, at the length scale of the protein (which is very small compared to the polymer mesh size), the nature of the polymer net is independent of the polymer concentration. This arises since the correlations between the polymer segments (that the protein feels) are determined by the excluded-volume interactions between polymer segments belonging to a local section of the polymer chain (intra-blob correlations) (de Gennes, 1988). The previous statements should not be interpreted to suggest that the partition coefficient of the protein will be independent of polymer concentration when $R_p \ll \xi_b$, since in this limit the concentration of polymer still determines the probability of a protein interacting with a strand of the polymer mesh.

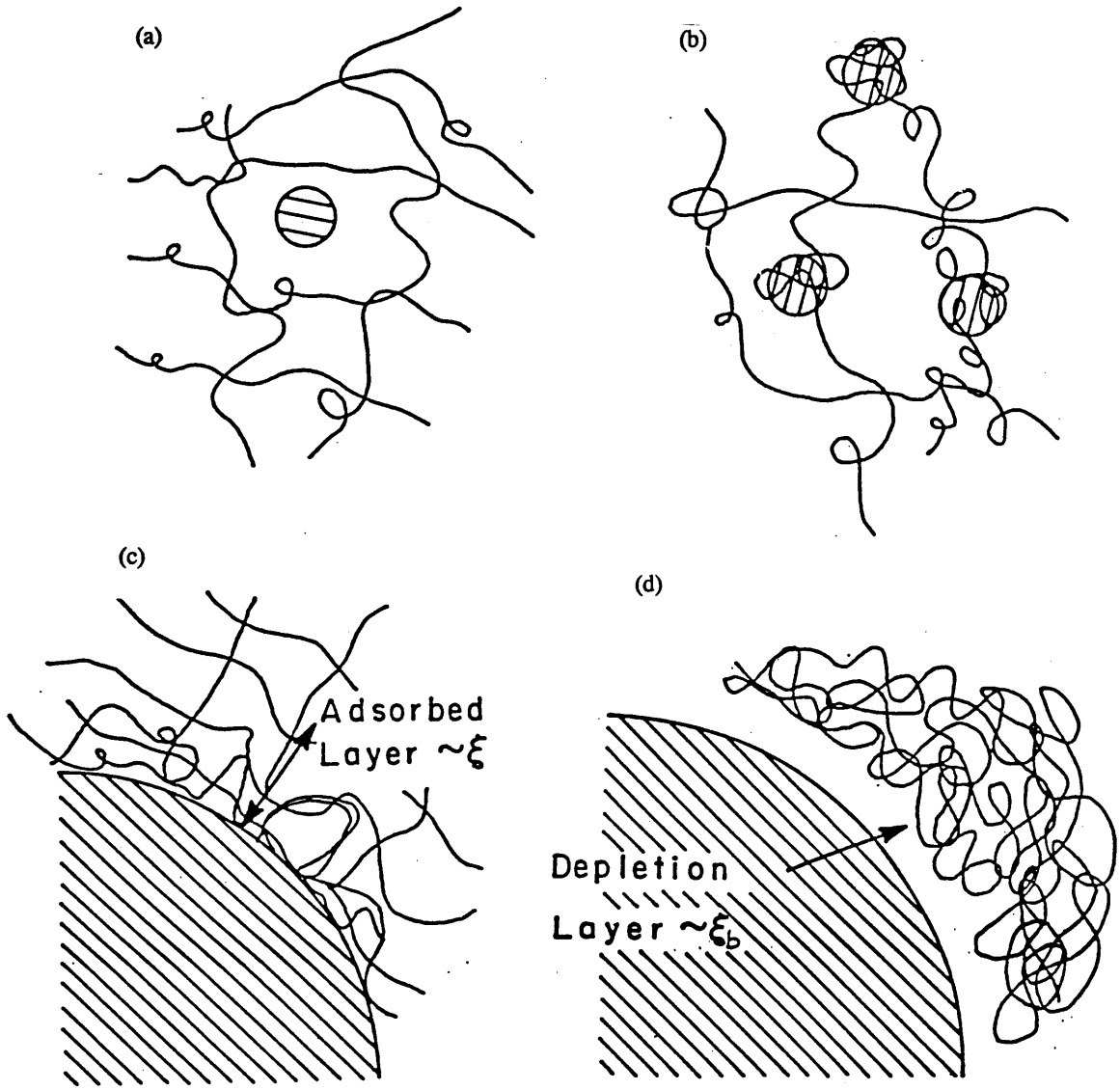

Figure 3.7 Possible pictures for the interactions of globular proteins and high molecular weight polymers: (a) very weak attraction or no attraction between the polymer mesh and the protein, and $R_p \ll \xi_b$; (b) very weak attraction or no attraction between the polymer mesh and the protein and $R_p \gg \xi_b$; (c) strong attraction between the polymer mesh and the protein, $R_p \ll \xi_b$; (d) strong attraction between the polymer mesh and the protein and $R_p \gg \xi_b$.

In the alternative limit, corresponding to the limit where the protein size greatly exceeds the polymer net size, $R_p \gg \xi_b$, the polymer strands will adsorbs to the surface of the protein, just as they would to a macroscopic and planar surface.

In the following Chapters, we examine the consequences of each of these physical scenarios on the thermodynamic properties, including the protein partition coefficient, of the aqueous solutions of proteins and polymers. Furthermore, through a comparison of the predicted and experimentally observed protein partitioning behaviors we show that one can distinguish between these possible pictures for the interactions of proteins and polymers.

3.8 Literature Cited

Albertsson, P.A., *Partition of Cell Particles and Macromolecules*; Wiley, New York, **1985**.

Albertsson, P.-A.; Cajarville, A.; Brooks, D.E.; Tjerneld, F., *Biochim. Biophys. Acta*, **1987**, 926, 87.

Alexander, S., *J. Physique*, **1977**, 38, 977.

Bailey, F.E.; Kucera, J.L.; Imhof, L.G., *J. Polym. Sci.*, **1958**, 32, 517.

Bailey, F.E.; Koleske, J.V., *Poly(ethylene oxide)*, Academic Press, New York, **1976.**

Baskir, J.N.; Hatton, T.A.; Suter, U.W., *Macromolecules*, **1987**, 20, 1300.

Baskir, J.N.; Hatton, T.A.; Suter, U.W., *J. Phys. Chem.*, **1989**, 93, 2111.

Beech, D.R.; Booth, C., *J. Poly. Sci.*, A-2, **1969**, 7, 575.

Brooks. D.E.; Sharp, K.A.; Fisher, D., Chapter 2, *Partitioning in Aqueous Two-Phase Systems*, Eds Walter, H; Brooks, D.E.; Fisher, D. Academic Press, New York, **1985**.

Cabane, B., *J. Phys. Chem.*, **1977**, 81, 1639.

Cabane, B.; Duplessix, R., *J. Physique*, **1982**, 43, 1529.

Cabane, B.; Duplessix, R., *J. Physique*, **1987**a, 48, 651.

Cabane, B., in *Surfactant Science Series*, Volume 22, Ed., R. Zana **1987**b.

Daoud, M.; Cotton, J.P.; Farnoux, B.; Jannink, G.; Sarma, G.; Benoit, H.; Duplessix, R.; Picot, C.; de Gennes, P.G., *Macromolecules*, **1975**, 8, 804.

Edwards, S.F., *Proc. Phys. Soc. London*, **1966**, 88, 265.

Flory, P.J., *Principles of Polymer Chemistry*, Cornell University Press, Ithaca and London, **1986**.

Forciniti, D.; Hall, C.K., *A.C.S Symposium Series*,**1990**, 419, 53.

Gekko, K.; Timasheff, S.N., *Biochem.*, **1981**, 20, 4667.

de Gennes, P.-G., *Scaling Concepts in Polymer Physics*, Cornell University Press, Ithaca, **1988**.

Glatter, O.; Kratky, O., *Small Angle X-Ray Scattering*, Academic Press, London, 1982.

Goddard, E.D., *Colloids and Surfaces*, **1986a**, 19, 255.

Goddard, E.D., *Colloids and Surfaces*, **1986b**, 19, 301.

Guinier, A.; Fournet, G., *Small Angle Scattering of X-Rays*, Wiley, New York, 1955.

Hammes, G.; Roberts, P.B., *J. Am. Chem. Soc.*, **1968**, 90, 7119.

Heller, W.; Pugh, T.L., *J. Chem. Phys.*, **1956**, 22, 1778.

Huggins, M.L., *J. Phys. Chem.*, **1941**, 9, 440.

Hustedt, H.; Kroner, K.H.; Stach, W.; Kula, M.-R., *Biotechnol. Bioeng.*, **1978**, 20, **1989**.

Ingham, K.C., *Arch. Biochem. Biophys.*, **1977**, 184, 59.

Ingham, K.C., *Arch. Biochem. Biophys.*, **1978**, 186, 106.

Jones, M.N., *J. Colloid and Interface Sci.*, **1967**, 23, 36.

Koenig, J.L.; Angood, A.C., *J. Poly. Sci.*, A-2 **1970**, 8, 1787.

Liu, K.-J.; Parsons, J.L., *Macromol.*, **1969**, 2, 529.

Liu, K.-J.; Anderson, J.E., *Macromol.*, **1970**, 3, 163.

Maxfield, J.; Shepherd, I.W., *Polymer,* **1975**, 16, 505.

Marques, C.M.; Joanny, J.F., *J. Physique*, **1988**, 49, 1103.

Middaugh, C.R.; Lawson, E.Q., *Anal. Biochem.*, **1980**, 105, 364.

Molyneux, P., *Water Soluble Synthetic Polymers; Properties and Behavior* 1, CRC Press, **1982.**

Nagarajan, R.; Kalpacki, B., *Microdomains in Polymer Solutions*, Editor P.Dubin, Plenum Press N.Y., **1982.**

Napper, D.H., *Polymeric Stabilization of Colloidal Dispersions*, Academic Press, London, **1983.**

Pincus, P.A.; Sandroff, C.J.; Witten, T.A., *J. Physique,* **1984**, 45, 725.

Schaefer, D., *Polymer*, 1984, 25, 387.

Scheutjens, J.M.H.M.; Fleer, G.J., *J. Phys. Chem.*, **1979**, 83, 1619.

Scheutjens, J.M.H.M.; Fleer, G.J., *J. Phys. Chem.*, **1980**, 84, 179.

Shirahama, K., *Colloid & Polymer Sci.*, **1974**, 252, 978.

Shirahama, K.; Ide, N., *J. Colloid Interface Sci.*, **1976**, 54, 450.

Tadokoro, H.; Chatani, Y,; Yoshihara, T,; Tahara, S,; Murahashi, S., *Makrol. Chem.* **1964**, 73, 109.

Tokiwa, F.; Tsujii, K., *Bull. Chem. Soc. Japan*, **1973**, 46, 2684.

Wiltzius, P.; Haller, H.R.; Cannell, D.S.; Schaefer, D.W., *Phys. Rev. Lett.*, **1983**, 51, 1183.

Woodhead, J.L., *J. Physique Colloque C1,* **1986**, 47, C1-3.

Chapter 4.

Proteins in Solutions of Identifiable Polymer Coils. I. Scaling-Thermodynamic Formulation

4.1 Introduction

In Chapter 3, novel molecular-level pictures for the interactions of globular proteins and flexible nonionic polymers in solution were proposed. In essence, certain protein partitioning behaviors were suggested to arise from changes in the polymer solution structure at length scales corresponding to the sizes of the protein molecules. Specifically, in the two-phase aqueous system containing poly(ethylene oxide) (PEO) and dextran, where an aqueous PEO-rich solution phase coexists with an aqueous dextran-rich solution phase, these novel physical pictures were based, in part, on a proposed transition in the nature of the PEO-rich phase, from the dilute to the entangled polymer solution regimes, with increasing PEO molecular weight. In systems containing a concentration of approximately 10% w/w low molecular weight PEO ($M_2 < 10\ 000$ Da), the solution is in the dilute regime in which individual polymer coils, which may be larger or smaller than the proteins, interact with the proteins. In contrast, in systems containing high molecular weight PEO ($M_2 \gg 10\ 000$ Da), the solution is in the entangled regime and the proteins interact with an entangled polymer mesh rather than with identifiable polymer coils. Depending on the protein size and the polymer concentration, the size of the polymer mesh can be larger or smaller than that of the protein molecule.

Here, we focus our attention on polymer solutions containing identifiable polymer coils. We aim to explore the nature of the free-energy change arising from the interactions of the protein and polymers in each of the physical scenarios proposed in Chapter 3 by developing scaling-thermodynamic formulations. A statistical-

thermodynamic framework is used to relate the free-energy change to the protein chemical potential and thus predict the associated protein partitioning behaviors. On the basis of these scaling arguments, we will demonstrate that although the physical exclusion of the proteins by the polymer coils contributes to the observed partitioning behavior, other interactions between polymers and proteins need to be considered to explain the observed partitioning trends. In particular, the influence of the PEO molecular weight on the partitioning behavior of the series of proteins (Albertsson et al, 1987; Hustedt et al, 1978), cytochrome-c, ovalbumin, bovine serum albumin, catalase, pullulanase and phosphorylase, is observed to be consistent with the presence of a weak attractive interaction (in addition to physical exclusion) between the protein molecules and the polymer coils. Finally, the presence of a strong attractive interaction between the proteins and polymers will be shown to be inconsistent with the partitioning behavior of the proteins reported in Figure 2.4.

The remainder of this chapter is organized as follows. In Section 4.2 a statistical-thermodynamic formulation is presented in order to relate the theoretically predicted free energy change arising from the interactions of the proteins and polymer coils to the experimentally measurable protein partition coefficient. Assuming that the sole contribution to the protein-polymer coil interaction arises from excluded volume interactions of the protein and polymer, Section 4.3 presents a derivation of the free energy of interaction and predicts the associated protein partitioning behavior. The importance of the polymer-polymer interactions on the protein partitioning behavior are emphasized and the influence of the solvent quality for the polymer is explored. At Θ-solvent conditions for the polymer, a picture which incorporates solely the excluded-volume interactions between the proteins and the polymer coils is unable to account for the influence of polymer molecular weight on K_p; at athermal-solvent conditions, where repulsive polymer-polymer interactions also influence the protein chemical potential, the predicted protein partition coefficient is shifted in a direction qualitatively consistent with experimental trends. In Section 4.4, for both athermal- and Θ-solvent conditions, the observed change in K_p is shown to be qualitatively consistent with the presence of a weak attraction between the polymer coils and the proteins. Finally, in Section 4.5, the

presence of a strong attraction between the polymer coils and the proteins, and associated formation of an adsorbed polymer layer at the surface of the proteins, can lead to a new partitioning behavior that has not yet been realized experimentally. In Section 4.6 we present our concluding remarks.

4.2 Statistical-Thermodynamic Framework

A thermodynamic formulation is required to relate the free-energy changes associated with the interactions between proteins and polymers to the experimentally accessible protein partition coefficient. Experimental measurements performed in the limit of vanishing protein concentration, namely, high protein dilutions, simplify the connection between the required free-energy changes and the protein partition coefficient, as it can be assumed that the proteins do not interact with each other significantly during measurement of the protein partition coefficient and thus may be assumed to be isolated from each other. As expected, in this limit, the protein partition coefficient is generally observed to become independent of protein concentration (Albertsson, 1985). This point is addressed further by experiment in Chapter 9 where measurements of the partition coefficients of ovalbumin are reported. In brief, over the range of ovalbumin concentrations from 0.2g/l to 2 g/l, the protein partition coefficient was observed to be independent of the ovalbumin concentration. Note that although the experimental conditions chosen reduce the influence of protein-protein interactions on the partition coefficient, we recognize that proteins can associate under certain conditions, particularly near their isoelectric point (Tanford, 1961). Furthermore, the presence of polymers may promote the association or dissociation of proteins depending on the polymer type and protein species (Middaugh and Lawson, 1980). Therefore, although the independence of the protein partition coefficient on protein concentration provides some justification for the assumed minor role of protein-protein interactions on protein partitioning, this topic warrants further investigation, particularly for those proteins which are known to self-associate. Another useful simplification that arises from the measurement of K_p at high protein dilution is that these low protein concentrations cause a negligible

perturbation to the two-phase equilibrium of the phase-forming polymers in the absence of the proteins. A typical protein concentration is 1 g/l (<0.1 mM) and thus the latter assumption appears reasonable and has been confirmed by experiments (Baskir, 1988). Finally, we consider each phase to contain water, protein and only one of the two polymers present in the system. Provided that the two-phase systems are far from their critical points, the concentration of the minority polymer is very low as is apparent from Figure 3.2, and hence this assumption appears very reasonable.

In general, the protein chemical potential in phase i (t or b) is given by

$$\mu_{p,i} = \mu^{o}_{p,i} + kTln(c_{p,i}\,\gamma_{p,i}) + z_{p,i}\,(\psi_i - \psi_o)\,, \tag{4.1}$$

where $\mu_p^{\circ}{}_{,i}$ is the standard-state chemical potential of the protein in phase i, $\gamma_{p,i}$ is the activity coefficient of the protein at concentration $c_{p,i}$, $z_{p,i}$ is the net protein charge in phase i, and ψ_i and ψ_o are the electrical potentials of phase i and a reference phase o, respectively. Note that the last term in Eq.(4.1) arises from the necessary presence of buffering salts in the system to control pH. The equilibrium distribution of proteins between two coexisting phases is determined by the equality of the chemical potentials in each phase, that is, by $\mu_{p,t}=\mu_{p,b}$. Furthermore, in the absence of significant protein-protein interactions (see discussions above), the protein activity coefficient in each phase is approximately unity. Using this information and Eq.(4.1), the protein partition coefficient is given by

$$lnK_p = \ln\left(\frac{c_{p,t}}{c_{p,b}}\right) = \left(\frac{\mu^{o}_{p,b} - \mu^{o}_{p,t}}{kT}\right) + \left(\frac{z_p\,(\psi_b - \psi_t)}{kT}\right), \tag{4.2}$$

where the net charge of the protein has been assumed to be independent of the phase in which the protein resides, that is $z_{p,t} = z_{p,b} = z_p$. This assumption is supported by the small pH difference between the two coexisting phases, as well as by the almost uniform partition of most salts between the phases (Albertsson, 1985). In general, experimental investigations have revealed that ψ_b- ψ_t can be influenced by the specific salt types in the

system, and the concentrations of the polymers in each of the coexisting phases (Albertsson, 1985; King et al., 1988). Since only very small changes are measured in the phase polymer compositions (% wt/wt) over the PEO molecular weight range of interest (see Figure 3.2), to a reasonable approximation, by examining changes in the protein partition coefficent with PEO molecular weight for a given salt (buffer) type and concentration, Eq.(4.2) suggests that one probes only those factors which affect the standard-state chemical potentials of the proteins. Note that an assumption implicit in the prior statement is that $\psi_b - \psi_t$ is not significantly influenced by the PEO molecular weight. This can be justified, in part, if one considers the interactions between salts and PEO to be short-ranged, that is, if salt interacts with PEO at the length scale of the polymer segments rather than the polymer coil size. Indeed, the precise nature of the interactions of nonionic polymers and salts remains to be elucidated although some experimental evidence (see below) supports our assertion. Under the above assumptions, the change in the protein partition coefficient accompanying changes in the PEO molecular weight reduces to

$$\Delta \ln K_p = \Delta \ln\left(\frac{c_{p,t}}{c_{p,b}}\right) = \left(\frac{\mu^o_{p,b,2} - \mu^o_{p,b,1}}{kT}\right) - \left(\frac{\mu^o_{p,t,2} - \mu^o_{p,t,1}}{kT}\right) \qquad \textbf{(4.3)}$$

Note that the symbol $\Delta \ln K_p$ denotes the change in the protein partition coefficient between two systems containing different PEO molecular weights, defined as states 1 and 2. We now return briefly to the assumptions leading to the cancellation of the electrical potential term in Eq.(4.3). If this is justified, the change in the protein partition coefficient predicted by Eq.(4.3), $\Delta \ln K_p$, should be independent of the salt type present in the system, which is indeed observed experimentally (see Chapter 9). In addition, since a very low concentration of PEO is present in the bottom dextran-rich phase, we assume that only the protein standard-state chemical potential term in the top PEO-rich phase changes with changes in PEO molecular weight. This further simplifies Eq.(4.3) yielding

$$\Delta \ln K_p = -\left(\frac{\mu^o_{p,t,2} - \mu^o_{p,t,1}}{kT} \right) \tag{4.4}$$

Eq.(4.4) is a central result which indicates that, under the assumptions detailed above, changes in the protein partition coefficient are essentially determined by the interactions of the protein in the top PEO-rich solution phase. Recall that the physical meaning of the protein standard-state chemical potential is the excess free-energy change upon introducing a single isolated protein from a polymer free solvent (where the center of mass of the protein is fixed) into a polymer solution phase. Note that the standard-state protein chemical potential is an excess free energy because the contribution arising from the ideal entropy of mixing the protein with the polymer solution is contained in the logarithmic term of Eq.(4.1) (with $\gamma_{p,i}=1$). In evaluating this free-energy change we have made an additional simplifying assumption regarding the proteins. That is, we have treated the proteins as rigid impenetrable spheres with homogeneous surface properties and have assumed that all properties of the protein may be uniformly averaged over the entire molecule. As previously mentioned, this simple view of the proteins is justified by the clear correlation between the protein partition coefficient and the characteristic protein size (see Figures 2.4 and 3.1), which suggests that other factors, for example, amino acid composition and distribution throughout the protein, may be less important than the protein size in determining the interactions with flexible polymers. It should be kept in mind, however, that proteins generally have rather inhomogeneous surface properties and possess structures which can breathe about a mean conformation. The incorporation of these additional protein properties into the description of protein-polymer interactions is likely to be necessary for any detailed quantitative treatment of these interactions.

4.3 Picture 1: The Mechanism of Physical Exclusion

The first picture, Figure 3.6(a), assumes that the sole contribution to the

free-energy change associated with introducing a protein into an aqueous PEO solution arises from the change in the number of configurations available to the system, in other words, a change in the entropy of the system. The precise meaning of the entropy of mixing in the present case is the entropy change resulting from mixing a single protein molecule, polymers and solvent relative to mixing polymers and solvent in the absence of the protein. Note that prior to mixing the protein with polymer and solvent, the protein is considered to be in a solvent phase, and therefore the protein is assumed not to change its state, for example, hydration characteristics and average configurational state, when mixed with the polymer and solvent. In contrast to Brooks and coworkers (1987) and Baskir and coworkers (1987 and 1989), the essential physics captured in our estimation of the entropy change is that polymer solutions of low PEO molecular weight do not consist of a web of entangled polymer, but rather contain individual, identifiable and non-overlapping coils, each characterized by a radius of gyration, R_g.

At constant temperature and volume, and therefore assuming negligible volume change upon mixing the protein and the polymers, the standard-state chemical potential of the protein is equal to the change in the Helmholtz free energy (Modell and Reid, 1983) of the system per protein introduced into the system, that is

$$\mu^o_{p,\,t,\,i} = \delta A^o_{p,\,t,\,i} \tag{4.5}$$

where $\delta A^o_{p,t,i}$ is the Helmholtz free-energy change upon introducing a single and isolated protein molecule into the top (t) PEO-rich solution phase at conditions i (i=1 or 2). For a change in the PEO molecular weight (denoted by the symbol Δ), and using Eq.(4.4), we find that,

$$\Delta ln K_p = -\left(\frac{\delta A^o_{p,\,t,\,2} - \delta A^o_{p,\,t,\,1}}{kT} \right) \tag{4.6}$$

In general, the change in the Helmholtz free energy can be expressed as (Modell and Reid, 1983)

$$\delta A^{o}_{p,t,i} = \delta U^{o}_{p,t,i} - T\delta S^{o}_{p,t,i} \tag{4.7}$$

where $\delta U_p^{\circ}{}_{,t,i}$ and $\delta S_p^{\circ}{}_{,t,i}$ are changes in internal energy and entropy, respectively. In Picture 1, no change in internal energy accompanies the transfer of a protein into the polymer solution phase. Thus, using Eqs.(4.6) and (4.7), the protein partition coefficient can be directly related to the change in the entropy, that is,

$$\Delta \ln K_p = \left(\frac{\delta S^{o}_{p,t,2} - \delta S^{o}_{p,t,1}}{k} \right) \tag{4.8}$$

The isothermal entropy of mixing the protein with the polymer solution is related to the number of configurations adopted by the various components of the solution through

$$\frac{\delta S^{o}_{p,t,i}}{k} = \ln \Omega_{N_p=1}(N_2, V, T) - \ln \Omega_{N_p=0}(N_2, V, T) \tag{4.9}$$

where $\Omega_{Np=1}$ and $\Omega_{Np=0}$ are the numbers of polymer solution configurations with and without the protein present, respectively, and N_2 is the number of polymer molecules in volume V.

Assuming that the number of ways of placing a polymer molecule in the volume V is proportional to the available free volume with a proportionality constant, A_2 (see Appendix 4 A), the number of configurations $\Omega_{Np=0}$ is given by (Tanford, 1961)

$$\Omega_{N_p=0} = \frac{A_2^{N_2}(V - U_1)(V - U_2) \ldots\ldots\ldots\ldots (V - U_{N_2})}{N_2!} \tag{4.10}$$

where U_j is the volume excluded by the j^{th}-1 polymer coils present in the system. Thus, V-U_j is the free volume available to the j^{th} polymer coil as it is placed sequentially in the volume V. For example, U_1=0, since the entire system volume V is available for the

placement of the first polymer coil. The factor $N_2!$ accounts for the indistinguishability of the polymer coils. The major difficulty in the evaluation of Eq.(4.10) is the assignment of excluded volumes U_j (Tanford, 1961; Ruckenstein and Chi, 1975). In the dilute polymer solution regime we assume that the excluded volumes are additive, that is, $U_j=(j-1)U_2$, where U_2 is the volume excluded by each polymer coil in the system. In that case, expanding the various natural logarithms appearing in $\ln\Omega_{Np=0}$ in terms of the expansion parameters $(j-1)U_2/V \ll 1$ to quadratic order yields

$$\ln\Omega_{N_p=0} = \ln(A_2^{N_2}) - \ln(N_2!) + N_2 lnV - \frac{U_2 N_2^2}{2V} - \frac{U_2^2 N_2^3}{6V^2} \qquad (4.11)$$

where the result $N_2(N_2-1) \simeq N_2^2$ for $N_2 \gg 1$ has been used.

We have extended the above approach to estimate the number of configurations of the polymer solution in which a protein molecule is dissolved. In general, the protein has a different size than each polymer coil. In the evaluation of the number of configurations, we place the N_p proteins (where $N_p=1$) in the volume V first, and follow it by the successive placement of the N_2 polymer coils. The logarithm of the number of configurations available to the solution, $\ln\Omega_{Np=1}$, is obtained by expanding the various natural logarithms in terms of the expansion parameters $U_2(j-1)/(V-U_pN_p) \ll 1$. To quadratic order this yields

$$\ln\Omega_{N_p} = \ln(A_2^{N_2} A_p^{N_p}) - \ln(N_2!) + N_2\ln(V - N_p U_p) + N_p lnV - \ln(N_p!)$$
$$- \frac{U_p N_p(N_p - 1)}{2V} - \frac{U_2 N_2^2}{2(V - N_p U_p)} - \frac{U_2^2 N_2^3}{6(V - U_p N_p)^2} \qquad (4.12)$$

where U_p is the volume excluded by the protein to the polymer coils, and A_p is the proportionality constant relating the fraction of the system volume accessible to the protein (free volume) to the possible configurations of the system when the protein is

introduced. Note, that for $N_p=0$, that is, with no protein present, Eq.(4.12) correctly reduces to Eq.(4.11). Setting $N_p=1$ in Eq.(4.12), corresponding to a single protein in the system, followed by the substitution of Eqs.(4.11) and (4.12) into Eq.(4.9) yields

$$\frac{\delta S^{o}_{p,t,i}}{k} = \ln(A_p V) + N_2 \ln\left(1 - \frac{U_p}{V}\right) - \frac{U_2 N_2^2 (\frac{U_p}{V})}{2V(1 - \frac{U_p}{V})} - \frac{U_2^2 N_2^3 (\frac{U_p}{V})(1 - \frac{1}{2}\frac{U_p}{V})}{3V^2(1 - \frac{U_p}{V})^2} \tag{4.13}$$

In Eq.(4.13) the term $\ln(A_pV)$, which depends on the magnitude of the system volume, V, describes the ideal mixing of the protein in a volume V. As this term is also accounted for in the second term of the protein chemical potential in Eq.(4.1), and therefore does not contribute to the standard-state chemical potential of the protein as defined in that equation, we subtract it from Eq.(4.13). In the dilute protein solution limit of interest to us, for which $U_p \ll V$, we can further expand Eq.(4.13) to leading order in U_p/V. Carrying out this expansion and substituting the resulting expression in Eq.(4.8) yields

$$\Delta \ln K_p = - \Delta\left(\frac{N_2 U_p}{V}\left(1 + \frac{N_2 U_2}{2V} + O\left(\frac{N_2 U_2}{V}\right)^2\right)\right) \tag{4.14}$$

Clearly, the truncation present in Eq.(4.14) produces an insignificant error provided that

$$\left[\frac{N_2 U_2}{V}\right]^2 << 1 \tag{4.15}$$

From Eq.(4.15) it is apparent that the validity of the truncation depends upon both the number density of polymer coils in the solution, N_2/V, and the strength of the polymer-polymer interactions, characterized by U_2, which depends upon the solvent conditions. Therefore, we consider two typical types of solvent conditions corresponding to the so-called athermal- and Θ-solvent conditions for the polymer (de Gennes, 1988). Athermal-solvent conditions prevail when there is no enthalpy change upon mixing polymer and solvent from the pure-component states. In the absence of an enthalpy change upon mixing, the interactions between polymer coils are strongly repulsive due to excluded-volume interactions. In the notation of Flory (1986) and Huggins (1941), this condition is characterised by $\chi=0$, where χ is the Flory-Huggins interaction parameter. The Θ-solvent condition corresponds to the presence of an effective attraction between polymer coils which exactly balances the repulsive excluded-volume interactions, and is characterized by $\chi=0.5$. PEO in water at ambient conditions lies between these two limits with a Flory-Huggins interaction parameter, χ, of typically 0.45 (Edmond and Ogston, 1968; Rogers and Tam, 1977). Consequently, by examining these two limits we hope to bound the behavior of the PEO-water (and salt) system.

In Picture 1, the polymer-protein interaction is characterized by U_p. For globular proteins which are relatively rigid (as compared to flexible random coiling polymers) and effectively impenetrable to the polymer, the assignment of the characteristic dimension of the protein needed to describe the exclusion of the polymer corresponds closely to the hydrodynamic radius of the protein. Furthermore, owing to the presence of relatively strong intramolecular forces within the protein it is unlikely that weak intermolecular interactions, for example, those with nonionic polymers, will cause large deformations of the protein structure. Indeed, the maintenance of enzymatic activity in most aqueous nonionic polymer solutions suggests, at the very least, the absence of changes in the protein structure associated with the active sites of the proteins (Albertsson, 1985; Walter et al., 1985). Contrasting this situation is the behavior of flexible and deformable polymers, where the average configuration of an *isolated* molecule reflects a delicate balance of the intramolecular forces. Furthermore, at finite concentrations, intermolecular interactions will also influence the polymer coil

configurations. That is, in polymer solutions of finite concentration, polymer coil configurations will reflect both intra- and inter-molecular interactions, effectively coupling these two factors. Note also that the average configurations of the flexible polymer coils associated with polymer-polymer interactions may differ from those associated with polymer-protein interactions as a result of the differing nature of the intermolecular interactions in the two cases. Specifically, for the interactions of globular proteins and flexible polymer coils, the characteristic dimension of the polymer coils for the description of the polymer-protein interaction will differ, in general, from that used to describe the polymer-polymer interactions. In particular, the former characteristic dimension will depend upon the relative sizes of protein and polymer. To illustrate this point the results of Hermans for excluded volumes are useful (Hermans, 1982; Hermans and Hermans, 1984). In the limit where the protein is much larger than the polymer, that is, $R_p \gg R_g$, the excluded volume arising from interactions between a polymer coil at Θ-solvent conditions and a spherical protein was determined to have the form (Hermans, 1982)

$$U_p = \frac{4\pi R_p^3}{3} + \left[\frac{4}{\pi}\right]^{1/2} S_p R_g \qquad \textbf{(4.16)}$$

where S_p is the surface area of the protein, and Eq.(4.16) is valid for $R_g/R_p < 0.41$. In the associated physical picture, the protein and polymer coil interact at their surfaces (where the polymer coil surface is defined by a sphere of radius R_g) since the protein is too large to penetrate to any significant extent into the polymer-coil volume. Alternatively, in the limit $R_g \gg R_p$, corresponding to the polymer coils being much larger than the protein, the excluded volume was determined to have the form (Hermans, 1982; Hermans and Hermans, 1984)

$$U_p = 4\pi R_p R_g^2 \qquad \textbf{(4.17)}$$

The difference in the functional form of Eq.(4.17) as compared to that of Eq.(4.16) reflects the fact that when the polymer coil increases in size as compared to the protein,

a significant number of polymer-coil configurations exist which permit the protein to diffuse unhindered into the volume occupied, on average, by the polymer coil. For the proteins reported in Figure 1 and for PEO in the molecular-weight range from 4,000 Daltons to 10,000 Daltons, the range of interest corresponds to $0.4 < R_g/R_p < 2.5$. Therefore, we are interested in the behavior of the excluded volume, U_p, in the region between the two limits treated by Eqs.(4.17) and (4.16).

Recently, Jansons and Phillips (1990) have reported the evaluation of the excluded volume over the complete range of relative polymer and impenetrable sphere sizes for Θ-solvent conditions. The excluded volume, U_p, was evaluated using the analogy between the flight of a diffusing particle and the statistics of ideal polymer coils (that is, polymer coils that possess no excluded volume and hence correspond to Θ-solvent conditions) and is given by

$$U_p = 4\pi R_p R_g^2 + 8(\pi)^{1/2} R_p^2 R_g + \frac{4\pi R_p^3}{3} \qquad \textbf{(4.18)}$$

Note that Eq.(4.18) correctly reduces to Eq.(4.17) or Eq.(4.16) in the appropriate limits of R_g/R_p, and will be used to characterize the excluded-volume interactions of polymer coils and proteins.

Case 1: Θ-Solvent

At Θ-solvent conditions for the polymer, the enthalpy of interaction between the polymer coils and solvent exactly balances the excluded-volume interactions between polymer coils implying that $U_2=0$. Therefore, Eq.(4.15) is always satisfied. Using the fact that $U_2=0$ in Eq.(4.14) yields

$$\Delta ln K_p = -\Delta \left[\frac{N_2 U_p}{V} \right] \qquad \textbf{(4.19)}$$

When comparing the prediction of $\Delta \ln K_p$ to the experimentally observed trends in the protein partition coefficient, it is important to note that the change in the polymer molecular weight occurs at constant weight fraction of the polymer solution phase. This fact was emphasized in Chapter 3. Therefore, accompanying a change in the polymer molecular weight is not only a change in the polymer coil size, but also changes in both the number concentration of polymer coils and the associated volume of the solution excluded by polymer coils. At constant weight fraction of polymer in the solution, the number of polymer coils per unit volume, N_2/V, scales with the number of polymer segments per polymer coil, N, as 1/(NV). However, since the volume of the system, V, is constant, for simplicity we omit the term V hereafter and use the scaling relation

$$\frac{N_2}{V} \sim \frac{1}{N} \tag{4.20}$$

For a polymer coil at Θ-solvent conditions, the radius of gyration scales as (Flory, 1986; de Gennes, 1988)

$$R_g \sim aN^{1/2} \tag{4.21}$$

where a is the characteristic size of a polymer segment. Substituting Eqs.(4.18), (4.20) and (4.21) into Eq.(4.19), the protein partition coefficient is predicted to have the form

$$\Delta lnK_p \sim -\Delta\left[4\pi R_p a^2 + 8\pi^{1/2} R_p^2 a N^{-1/2} + \frac{4\pi R_p^3 N^{-1}}{3}\right] \tag{4.22}$$

With the exponent of N constrained to negative values, the qualitative behavior of the experimentally determined protein partition coefficients shown in Figure 1 cannot be reproduced. Such a behavior requires that this exponent be greater than 0. To understand the behavior predicted by Eq.(4.22) we return to Eq.(4.19) which reflects two clear contributions. The first one arises from the term N_2/V, the number concentration

of polymer coils in the solution, which is a measure of the frequency of interaction between the protein and the polymer coils. The second one, U_p, the volume excluded by the protein from the polymer coils, is a measure of the strength of the polymer-protein excluded-volume interaction. It is the competition between these two factors that leads to the predicted behavior. An increase in the polymer molecular weight (recall that N is proportional to polymer molecular weight), at constant weight fraction of polymer in the solution, results both in a decreased frequency of interaction (since N_2/V decreases, see Eq.(4.20)) as well as in an increase in the strength of the excluded-volume interaction (since U_p increases, see Eqs.(4.18) and (4.21)). For Θ-solvent conditions the former factor dominates for small polymers, whereas for large polymers the two factors balance each other.

Case 2: Athermal-Solvent

For a polymer in an athermal solvent, the repulsive excluded-volume interactions between polymer coils causes U_2 to be greater than zero. Therefore, the validity of the truncation presented in Eq.(4.14) is not guaranteed and the condition in Eq.(4.15) must be satisfied to justify the truncation. Clearly, if Eq.(4.15) is satisfied, this constraint dictates that the second term in Eq.(4.15), which contains the influence of the polymer-polymer steric interactions (through U_2) on $\ln K_p$, cannot dominate the first term. Recall that the first term describes the contribution of the direct protein-polymer interaction to the protein chemical potential. In other words, because Eq.(4.15) must be satisfied to justify the truncation present in Eq.(4.14), it is not possible, in the context of the formalism developed so far, to predict protein partitioning behavior under conditions where polymer-polymer steric interactions dominate the form of the protein chemical potential. Nevertheless, it is of interest to examine the direction of the influence of polymer-polymer interactions on the partition coefficient of the protein (under conditions where Eq.(4.15) is satisfied) in addition to the infuence of the athermal-solvent conditions on the direct protein-polymer interaction. This will be done in the spirit of a scaling approach. For polymer coils in athermal solvents, the excluded

volume describing the interactions between equal sized polymer coils can be described using the polymer coil radius of gyration as (Tanford, 1961)

$$U_2 \sim a^3 N^{9/5} \tag{4.23}$$

where we have used the fact that $R_g \sim aN^{3/5}$ for a polymer coil in an athermal solvent (Flory, 1986; de Gennes, 1988). Note that U_2 is proportional to the spherical volume defined by R_g. To determine the form of the excluded volume which characterizes the interaction between the polymer coil in an athermal solvent and the protein we have adopted Eq.(4.18) suggested by Janson and Phillips (1990). Although Eq.(4.18) was derived for a Θ-solvent, we utilize it for polymer coils in an athermal solvent, using the appropriate scaling relation (shown above) to connect the polymer radius of gyration to the number of polymer segments per polymer coil. This approach for describing the qualitative features of polymer-protein interactions in an athermal solvent is supported by the Monte-Carlo calculations of U_p which are presented in Chapter 6. Substituting Eq.(4.18) (with $R_g \sim aN^{3/5}$ and U_2 given in Eq.(4.23)) and Eq.(4.20) into Eq.(4.14), and neglecting numerical prefactors, the following expression for $\Delta \ln K_p$ results

$$\Delta ln K_p \sim -\Delta \left[\left[4\pi R_p a^2 N^{1/5} + \frac{8\pi^{1/2} R_p^2 a}{N^{2/5}} + \frac{4\pi R_p^3}{3N} \right] \left(1 + p a^3 N^{4/5}\right) \right] \tag{4.24}$$

where p is an order unity numerical prefactor. Recall from the discussion above that the term $(1+pa^3N^{4/5})$ in Eq.(4.24) describes the influence of polymer-polymer interactions on the protein chemical potential and thus on the protein partition coefficient. The essence of the result in Eq.(4.24) may be summarized as

$$\Delta ln K_p \sim -\Delta\left(R_p^{\alpha} N^{\beta} N^{\gamma}\right) \tag{4.25}$$

where the exponents are constrained to lie in the limits $1<\alpha<3$, $-1<\beta<1/5$ and $0<\gamma<4/5$. In Eq.(4.25), the exponents α and β describe the influence of the protein size and polymer molecular weight, respectively, on $\Delta \ln K_p$ through direct polymer-

protein interactions, whereas γ captures the influence of the polymer molecular weight on $\Delta \ln K_p$ through polymer-polymer interactions. As noted earlier, the exponent of N must be greater than 0 to describe the experimental trends. Although this appears unlikely to result from β, as β decreases to -1 with decreasing N, it is important to note that the influence of the polymer-polymer interaction (through γ) is in the direction of the experimental trends in the protein partition coefficient. Indeed, the possibility that a more quantitative and detailed treatment of the entropy of mixing of protein and polymers may account entirely for the protein partition coefficient cannot be discarded. From this analysis it is evident that important features to be incorporated in future developments include the deformability and permeability of the polymer coils in the presence of the globular proteins, the partial permeability of the polymer coils to each other (which varies with the solvent condition), and the contributions of higher-order interactions between polymer coils and proteins. Work in this direction is in progress.

4.4 Picture 2: The Influence of Perturbative Weak Attractions

In the second picture, Figure 3.6(b), a weak attractive interaction between the polymer coils and the protein molecules is introduced to determine the influence of such weak attractions on the protein partition coefficient. Owing to the assumed weakness of the attraction we have treated it as a perturbation of the repulsive excluded-volume interactions considered in Section 4.3. Although in this chapter we have assumed the range of the attractive forces to be small relative to the size of the protein and polymer coils, we are aware that forces such as those of the van der Waals type can be significant between dense colloidal spheres and polymers and can act over length scales comparable to the typical dimensions of the protein and the polymer coils. Therefore, a more detailed treatment may consider the interactions of the entire protein molecule with the polymer coils, rather than the surface-type interactions of range a, the polymer segment size, characterized by an energy ε, considered below. Defined more precisely, ε is the local energy change (measured in units of kT) that accompanies the replacement of solvent at the protein surface by one polymer segment. Provided that ε is sufficiently

weak, the presence of the attraction will not significantly influence the frequency of contacts between a polymer coil and a globular protein (as compared to the random-mixing case). This is in contrast to the third picture to be treated in Section 4.5, where an increase in ε beyond a certain threshold value results in the extensive deformation of the polymer coil and the associated formation of an adsorbed polymer layer about the protein.

The contribution of the attraction between the polymer coils and the protein to the standard-state protein chemical potential, $\mu_p^{o,att}$, in the polymer solution can be considered to have the following form

$$\frac{\mu_p^{o,att}}{kT} \sim -\left(\frac{N_2 V_c}{V}\right)<m_s>\varepsilon \qquad (4.26)$$

Eq.(4.26) results from a consideration of binary interactions between the protein and the polymer coils. Note that although the contribution of the attraction between protein and polymer to the free energy of the solution is proportional to both the protein concentration, N_p/V, and polymer concentration, N_2/V, the protein chemical potential is only linear in N_2/V. The combined term $(N_2/V)V_c$ reflects the fact that in a dilute polymer solution the likelihood of contact between the polymer coils and the protein increases with both the polymer coil concentration, N_2/V, and the sizes of the protein and polymer coils, both of which are reflected in the term V_c. More specifically, with the center of mass of the protein fixed in space, V_c is the total volume traced out by the center of mass of the polymer coil for which the polymer coil has an attractive interaction energy $<m_s>\varepsilon$ with the protein. The term $<m_s>$ is the characteristic number of contacts between a polymer coil and a protein, averaged over all polymer configurations, for which at least one contact has occurred between the polymer coil and the protein. In the above formulation, the qualitative forms of V_c and $<m_s>$ depend upon the relative sizes of the protein and the polymer. We consider first a situation where the polymer coil size is either smaller or similar to that of the protein, that is, $R_g \leq R_p$, and subsequently show that our general treatment is also physically reasonable

in the limit $R_g \gg R_p$.

In the limit $R_g \leq R_p$, on average, very few configurations of the polymer chain permit the protein to penetrate the polymer-coil volume, which is characterized by R_g^3. For the case of interest here, where the range of the attractive interactions is of order a, V_c scales as $(R_g+R_p)^2 a$, the volume of a shell having an area of order $(R_g+R_p)^2$ and a thickness of order a. The term $<m_s>$ is estimated as

$$<m_s> \sim \rho^* A_c a \tag{4.27}$$

where ρ^* is the characteristic polymer-segment density at the protein surface, and A_c is the area of contact between the protein and the polymer coil, which depends, in general, on the sizes and deformability of both species. Since the attractive interaction is weak, the deformation of the polymer coil due to the attraction is considered to be small in the vicinity of the protein (in contrast to Picture 3), and thus the density of polymer segments at the protein surface will scale with the density of polymer segments within a polymer coil far from the protein surface. In particular, for athermal-solvent conditions (Θ-solvent conditions will be considered later)

$$\rho^* \sim \frac{N}{\frac{4\pi}{3}R_g^3} \sim \frac{N}{(aN^{3/5})^3} \sim \frac{1}{a^3 N^{4/5}} \tag{4.28}$$

When the protein and the polymer coil are similar in size, the curvature of the protein surface will reduce the available contact area for the polymer below that corresponding to an infinite planar surface. To account for this, we have estimated the contact area between the protein and the polymer coil, A_c, as R_{eff}^2, where R_{eff} is an effective radius between the protein and the polymer coil defined as

$$\frac{1}{R_{eff}} \sim \frac{1}{R_p} + \frac{1}{R_g} \tag{4.29}$$

Although other forms for the effective radius can be proposed, Eq.(4.29) is a

conveniently simple representation which also tends to a physically reasonable limit for $R_g \ll R_p$. In this latter limit, the number of contacts between the polymer coil and the protein is limited by the size of the polymer coil and naturally is independent of the protein dimension.

Using the above result for A_c in Eq.(4.26), along with Eqs.(4.27)-(4.29), the scaling form for the contribution of the attraction to the standard-state protein chemical potential for athermal-solvent conditions is given by

$$\frac{\mu_p^{o,\,att}}{kT} \sim -\left(\frac{N_2}{V}\right)\varepsilon R_p^2 a N^{2/5} \tag{4.30}$$

Although our treatment of Picture 2 includes a number of simplifications, the essence of the approach is supported by evaluations of $<m_s>$ using Monte-Carlo techniques to generate the configurations of a self-avoiding chain in the vicinty of a hard-sphere for $R_g \leq R_p$, the region of behavior accessible to the simulation (see Chapter 6). In particular, the scaling prediction that the contribution of the attraction to the protein standard-state chemical potential becomes more favorable with increasing polymer molecular weight (at constant N_2/V) for $R_g \leq R_p$ was verified, as was the predicted influence of the protein size on $<m_s>$.

Using Eqs.(4.4), (4.20) and (4.30), the contribution of the attractive interaction to the protein partition coefficient (for athermal-solvent conditions) is given by

$$\Delta ln K_p^{att} \sim \Delta\left(\frac{\varepsilon a R_p^2}{N^{3/5}}\right) \tag{4.31}$$

For θ-solvent conditions, Eqs.(4.26) to (4.29) lead to the same scaling form for $\Delta \ln K_p^{att}$ with the exception that the exponent of N in Eq.(4.31) changes from 3/5 to 1/2. Note that the contribution of the entropy of mixing (excluded-volume interactions) to the protein partition coefficient, for both athermal- and Θ-solvents, is the same as that

derived for Picture 1. In other words, Eq.(4.31) represents the contribution of the attraction between protein and polymers to the change in the protein partition coefficient and not the total change in the protein partition coefficient.

Equation (4.31) predicts two qualitative features of the protein partition coefficient, both of which are consistent with trends observed in experimental measurements of K_p (see Figures 2.4 and 3.1). First, with increasing polymer molecular weight, or equivalently with increasing N, the protein partition coefficient is predicted to decrease, in a manner consistent with Figure 2.4, and secondly the magnitude of this decrease in the protein partition coefficient is predicted to increase with protein size. This is also observed experimentally as shown in Figure 3.1. While allowance for a weak attraction between protein and polymer coils gives results that are consistent with experimental observations, this is not the case when the attraction is significantly stronger; as shown in Section 4.5 the presence of a stronger attraction produces a strikingly different behavior due to the formation of an adsorbed layer of polymer about the protein. For a hard sphere of radius b, Pincus and coworkers (1984) estimated the sticking energy necessary to form an adsorbed polymer layer around the sphere to be of order a/b (in units of kT), where a is the polymer segment size, and translational entropy effects associated with forming the adsorbed layer are neglected. This estimate corresponds to an ε value of order 0.1 (in units of kT) for typical protein and polymer segment dimensions encountered in protein partitioning in two-phase aqueous polymer systems, and may be considered to represent a bound between Pictures 2 and 3. In Section 4.5, we explore this latter scenario, and show that formation of an adsorbed polymer layer about the protein is qualitatively inconsistent with the measured protein partition coefficients presented in Figure 2.4. Finally, it is important to note that although the presence of a weak attraction between the polymer coils and the protein exerts an influence on the protein partition coefficient which is consistent with experimental measurements, without the precise numerical prefactor in Eq.(4.31) it is not possible to predict the relative magnitude of this contribution and that arising from the entropy of mixing to the protein partition coefficient.

It is also of interest to briefly consider the influence of the weak attraction

between the polymer coils and the protein in the alternative limit of $R_g \gg R_p$. In this limit, the polymer coil becomes penetrable to the protein and thus both V_c and $<m_s>$ exhibit a different behavior from that corresponding to the previous case $R_g \leq R_p$. The difference between the behaviors of V_c and $<m_s>$ in the limits $R_g \gg R_p$ and $R_g \leq R_p$ arises because of the difference in the ability of the protein to penetrate the polymer-coil volume. As discussed above, in the limit $R_g \leq R_p$, the protein is sufficiently large (in comparison to the polymer coil) so as to sample the average properties of the polymer coil. On the other hand, when $R_g \gg R_p$, the protein is so small as to only sample local domains within the polymer coil, the properties of which are independent of the overall polymer-coil configuration. Therefore, in the limit $R_g \gg R_p$, V_c becomes linear in N, corresponding to a long cylindrical shell of thickness *a* which encases the contour of the linear polymer chain, and consequently $<m_s>$ becomes independent of N. These observations combined with Eq.(4.26) predict that the contribution of the attraction to the protein chemical potential, in the limit of high polymer molecular weight, will be independent of the polymer molecular weight (at constant weight fraction of polymer). For this latter limit it is interesting to compare and contrast our approach to the treatment due to Alexander (1977), who has proposed scaling descriptions for the free energy of interaction between an impenetrable sphere and a single polymer coil in the presence of a weak attractive interaction. Note that Alexander (1977) was considering the limit of $N \to \infty$, where the entropy of mixing the sphere and polymer vanishes, and the sphere is located within the polymer coil with a probability approaching unity. The form proposed (Alexander, 1977) for the change in the free energy of the system upon introducing the sphere into the polymer system was

$$\frac{F_{att}}{kT} \sim -\frac{\varepsilon R_p^2}{a^2 N^{4/5}} \qquad (4.32)$$

for the polymer coil in an athermal solvent. Note that a direct and simple comparison of Eqs.(4.31) and (4.32) cannot be made as Eq.(4.32) is derived for a single polymer coil in solution. Consequently, in Eq.(4.32), accompanying an increase in polymer coil

molecular weight there must also be an increase in polymer weight fraction. In contrast, the polymer weight fraction remains constant in Eq.(4.31). Accordingly, it should be realized that the approaches leading to Eqs.(4.31) and (4.32) differ in the following ways. First, we have included a probability, $(N_2/V)V_c$, that the protein resides in the vicinity of the polymer coil, and have also accounted for the entropy contribution to the protein chemical potential arising from the mixing of polymers and protein (as described in Picture 1). Second, and perhaps more importantly, Alexander (1977) considers a scenario where the small spheres within the polymer coil experience the average density of segments within the coil, ρ^*. In other words, the spheres experience an average attractive field, associated with the average segment concentration, which decreases with N. In contrast, we consider spheres that are sufficiently small to penetrate the polymer-coil volume and experience a local interaction with polymer segments, which is independent of N, rather than sample the average properties of the entire polymer coil. It is important to note that this latter conclusion regarding the influence of the attractive interaction as N increases is consistent with the predicted independence of the excluded-volume interaction on N observed in the same limit (see Section 4.3). This is reasonable, since in this limit both the excluded-volume interactions and the attractions reflect the interactions of the protein with local polymer segments rather than with the entire polymer coil.

Although we have determined that the presence of a weak attraction is consistent with experimental observations, which is similar to the conclusion reached by Baskir and coworkers (1987 and 1989), it is important to appreciate the difference in the underlying physics treated in Picture 2 as compared to that incorporated by Baskir and coworkers (1987 and 1989). In particular, they did not treat the low molecular weight polymer solutions as dilute, and thus neglected the correlations between polymer-segments that arise because they belong to identifiable polymer coils in the polymer solution phases. Instead, the polymer segment concentration was smeared uniformly over the bulk solution volume and the polymer solution interaction with the protein was described in terms of a continuum of polymer segments rather than discrete polymer coils. In contrast, we suggest that the trends observed in the protein partition coefficient (see Figure 2.4) can

be a consequence of the existence of identifiable polymer coils in the solutions of low-molecular weight polymer. In Picture 2, it is precisely this changing nature of the polymer solution and the associated change in the extent of solution inhomogeneity on the length scale of the protein, that causes the attraction between the protein and the polymer to influence the protein partition coefficient in a manner consistent with trends observed experimentally. In such inhomogeneous polymer solutions, the protein is able to experience an environment that does not correspond to the macroscopic volume average, as assumed in the model of Baskir and coworkers (1987 and 1989). It is interesting to note that the presence of the very weak attraction between PEO coils and the proteins is consistent with observations of a very weak adsorption of proteins onto hydrogel surfaces (Lee and Ruckenstein, 1988).

4.5 Picture 3: A Protein-Polymer Coil Complex.

In this third scenario, as shown in Figure 3.6(c), the attractive interactions of the polymer segments and the protein are sufficiently strong to cause the collapse of the polymer coil into a pancake shape, with an associated spreading along the protein surface to form an adsorbed polymer layer. The adsorbed layer of polymer coils on the protein surface is characterized by a length scale D, the characteristic thickness of the adsorbed layer, and by m, the number or fraction of polymer coils contained within the adsorbed layer. Depending on the relative size of the polymer coil and the protein, more than one polymer may participate in the formation of the adsorbed layer ($m > 1$), one polymer may dominate the interaction with the protein ($m \sim 1$) or, in the limit of the polymer size being much larger than that of the protein, only a fraction of the polymer molecule may saturate the surface of the protein ($m \ll 1$). Previously, Alexander (1977) and Pincus and coworkers (1984) proposed scaling relations for the interactions of colloidal spheres with one polymer, and their work has provided the foundations for the generalized scaling analysis proposed for Picture 3.

We consider the free-energy expression describing the interactions of the polymers and the proteins to contain five physically distinguishable contributions. The

first arises from the formation of favorable contacts between the polymer segments and the protein. In contrast to Picture 2, the stronger attractive interaction between the protein surface and the polymer coil causes a change in the polymer segment concentration at the protein surface, as compared to that of the undeformed polymer in the bulk. This term, F_1, scales as

$$F_1 \sim -Nm\varepsilon f_c \tag{4.33}$$

where f_c is the fraction of polymer segments in the adsorbed layer at the protein surface. The fraction f_c has the following scaling form (Pincus et al., 1984),

$$f_c \sim \frac{3k_1 R_p^2}{(R_p + D)^3 - R_p^3} \tag{4.34}$$

where the constant, k_1, is an unknown order 1 prefactor, and R_p and D are measured in units of the polymer segment size a. In Eq.(4.34), f_c is estimated by assuming an approximately uniform segment density within the adsorbed layer, allowing for the spherical geometry of the protein. Relative to a planar geometry, corresponding to $R_p = \infty$, in Eq.(4.34) the curvature of the spherical protein reduces the value of f. Implicit in Eqs.(4.33) and (4.34) is the assumption that the adsorbed layer, containing, in principle, several polymer molecules, can be pictured locally as an entangled mesh of polymer. This seems physically reasonable for large high molecular weight polymers which are rather diffuse and may interpenetrate, but the generalization to low molecular weight polymers, which contain quite high polymer volume fractions, is less certain as they less readily form a homogeneous and entangled polymer mesh.

The second contribution to the free energy, F_2, accounts for the loss of configurational freedom accompanying the deformation of the polymer from a relaxed and unperturbed random-coil conformation far from the protein to a pancake-shaped configuration in the adsorbed layer. The essential scaling form of this contribution can be derived from at least two approaches. The first approach uses dimensional arguments

(de Gennes, 1988), combining the observation that the leading term of the entropy change will be linear in N along with the identification of the relevant length ratio R_g/D (de Gennes, 1988). The second approach uses random-flight statistics to describe the configurational freedom of ideal polymers (Cassasa, 1967). The precise exponents obtained from the two approaches can differ as the latter neglects the excluded-volume interaction between the polymer segments. In terms of the qualitative behavior shown by the protein partition coefficient, we found that the two approaches yielded the same predicted trends and thus we have arbitrarily adopted the exponent associated with the latter approach. The term F_2 scales as

$$F_2 \sim k_2 m \left(\frac{R_g}{D}\right)^2 \tag{4.35}$$

Once again, the evaluation of the precise numerical value of this term requires knowledge of the order unity prefactor, k_2.

Accompanying the formation of the adsorbed polymer layer, there is an increase in the extent of the repulsive excluded-volume interaction between the polymer segments. To evaluate this contribution we have used a simple scaling form based on a mean-field approximation for the interactions between polymer segments, as well as a description of the adsorbed polymer layer as a local entangled mesh of polymer solution (de Gennes, 1988). The form of this contribution to the free energy, F_3, is obtained by evaluating the work required to concentrate the polymer segments in the adsorbed layer against an osmotic pressure, π_p, due to the excluded-volume interactions between the polymer segments. This contribution is given by

$$F_3 = \int_{r=R_p}^{r=R_p+D} \pi_p \, d^3r \tag{4.36}$$

where the substitution of an expression for the osmotic pressure, namely,

$$\pi_p \sim \frac{\nu(mN)^2}{\left((R_p + D)^3 - R_p^3\right)^2} \tag{4.37}$$

yields

$$F_3 = \frac{k_3(mN)^2\nu}{2\left((R_p + D)^3 - R_p^3\right)} \tag{4.38}$$

Note that in Eq.(4.38) the parameter ν is the polymer-segment excluded-volume parameter, k_3 is an order 1 prefactor, and the term $mN/((R_p+D)^3-R_p^3)$ is the concentration of polymer segments within the adsorbed layer of thickness D. A reference term describing the extent of these same types of interactions in the unperturbed polymer solution is

$$F_4 = -\frac{9\sqrt{6}k_4\nu mN^{1/5}}{2\pi} \tag{4.39}$$

Equation (4.39) is also derived from Eq.(4.36), where the integral is performed over the volume of the polymer coil, characterized by R_g^3, with $R_g \sim aN^{3/5}$, rather than the volume of the adsorbed polymer layer as indicated in Eq.(4.36). Note that k_4 is an order unity prefactor. The summation of Eqs.(4.38) and (4.39) describes the change in the extent of polymer segment interactions in going from the unperturbed polymer-coil state to the state characterizing the adsorbed polymer layer on the protein surface.

The final contribution to the free energy of interaction arises from a change in the translational entropy of the system which accompanies the complexation of m polymer molecules with each protein, and the subsequent mixing of the complex with the remaining N_2-m free polymer coils in the polymer solution. The derivation of this term, F_5, which is presented in Appendix 4 A, is analogous to the development of the entropy of mixing in Section 4.3. The resulting expression is

$$F_5 = -mln\left(\frac{N_2 V_1^o}{V}\right) + \frac{N_2 U_p}{V}\left(1 + \frac{N_2 U_2}{2V}\right) - \frac{mN_2 U_2}{V}\left(1 + \frac{N_2 U_2}{2V}\right) \qquad (4.40)$$

In Eq.(4.40), where the molecular volume of water is denoted by V_1^o and U_p is the volume excluded by the protein-polymer complex, a simple physical interpretation can be ascribed to each of the terms. The first term accounts for the loss of configurations (states) accessible to the system, due to the m polymer coils complexing with the proteins, under hypothetical conditions such that excluded-volume interactions between polymers and between the protein-polymer complex and polymers are negligible, that is, $U_2=0$ and $U_p=0$, respectively. The last two terms account for the influence of these excluded-volume interactions on the free-energy term, F_5. Specifically, the second term accounts for a restriction on the configurations available to the system, as compared to the $U_p=0$ case, due to a fraction of the system volume, U_p/V, being excluded to polymer coils by the volume of the protein-polymer complex. Clearly, this reduction in the free volume of the system increases the free energy of the polymer solution. The last term describes the increased freedom experienced by the N_2-m free polymer coils remaining in solution which results from the removal of m polymer coils from solution to form the protein-polymer complex. That is, the complexation of the m polymer coils with the protein reduces the "cluttering" of the free polymer coils in solution.

The truncation present in Eq.(4.40) is similar to that discussed in Section 4.3, and the same considerations discussed at that stage apply here with the exception of the treatment for Θ-solvent conditions. To treat Θ-solvent conditions, in addition to setting $U_2=0$ in Eq.(4.40), and $\nu=0$ in Eqs.(4.37), (4.38) and (4.39), one must necessarily include the three-body interactions between polymer segments in the system (Pincus et al., 1984). The failure to include these interactions will result in the prediction of $m=\infty$, as there will be no mechanism to oppose the adsorption of increasing numbers of polymer molecules onto the protein surface. Due to this complication, which does not arise in the treatment of Θ-solvent conditions for Pictures 1 (no attraction) and 2 (weak attraction), we have not treated Θ-solvent conditions for

Picture 3. Rather, we have concentrated on the solvent conditions for which $U_2>0$, which is the relevant solvent condition for PEO in water. Furthermore, since the determination of the form of the free-energy change arising from the interactions of the protein and the polymers is not analytic, and involves the summation of five terms (see below), it is important to establish the correct magnitude for the entropy term. Using $\chi=0.45$, corresponding to PEO in water at 25°C (Edmond and Ogston, 1968; Rogers and Tam, 1977), and the Flory-Krigbaum (1982) theory to estimate the magnitude of U_2, it was determined that the truncation of the expansion in terms of N_2U_2/V at quadratic order (see Eqs.(4.11) and (4 A.1)) cannot be justified for polymer concentrations of 10% w/w and PEO molecular weights in the range 3,000 Daltons to 9,000 Daltons. Therefore, we have pursued an alternative semi-empirical approach, determining U_2 within the context of the existing theoretical framework through a comparison to independent experimental vapor-pressure data for aqueous PEO solutions (Haynes et al., 1989). That is, using Eq.(4.11), the chemical potential of water in an aqueous PEO solution can be derived (Tanford, 1961), and from this the vapor-pressure depression of aqueous PEO solutions can be evaluated (Haynes et al., 1989) as a function of U_2. Note that in the context of this approach, U_2 should not be strictly regarded as an excluded volume for binary interactions between polymers since it can also reflect higher-order interaction terms. A comparison of the predicted vapor-pressure depression of aqueous PEO solutions of approximately 10% w/w polymer with experimental measurements (Haynes et al., 1989), predicts a U_2 of similar magnitude to that obtained from the Flory and Krigbaum (1950) theory. Specifically, by interpolating between vapor-pressure depression data for aqueous PEO solutions having number average molecular weights, 3,800 Daltons and 9,000 Daltons, respectively, we predict that U_2 is given by the following empirical form

$$U_2 \sim 0.80\, N^{1.6} \qquad \textbf{(4.41)}$$

where U_2 is measured in units of the polymer segment volume a^3. Note that the exponent of N in Eq.(4.41) appears physically reasonable as it falls between the limits

of 3/2 and 9/5, expected for Θ- and athermal- solvent conditions, respectively. Although we have resorted to a semi-empirical treatment of polymer-polymer interactions, importantly, through a comparison to binary PEO-water vapor-pressure data we have established that our estimate of the magnitude of these interactions is accurate and will not lead to artifacts in predicted protein partitioning behavior. U_p, the excluded-volume characterizing the interactions of the protein-polymer complex and free polymer coils, was estimated using Eq.(4.18), where the protein radius R_p is replaced by the radius of the protein-polymer complex R_p+D.

The equilibrium free energy of interaction of the protein and the polymers is obtained by minimizing the total free energy, $\delta A^{\circ}_{p,t,i}$, obtained by summing the contributions F_1 to F_5, with respect to the number of polymers in the adsorbed layer, m, and the average characteristic equilibrium thickness of the adsorbed layer, D. A steepest gradient descent algorithm was used in the minimization process. Eq.(4.6) was used to relate the change in free energy, $\delta A^{\circ}_{p,t,i}$, to the protein partition coefficient, $\Delta \ln K_p$. The predicted dependence of $\Delta \ln K_p$ on polymer molecular weight, protein size and polymer segment-protein surface sticking energy was examined subject to the uncertainty in the order unity prefactors. Although variation of the numerical prefactors, k_1-k_4, yields quantitative changes in $\Delta \ln K_p$, the predicted qualitative behavior remains unchanged. For the purpose of the discussions that follow, we have assigned the order unity prefactors, k_1-k_4, the numerical values of 1.

The qualitative dependence of $\Delta \ln K_p$ on the number of polymer segments per coil, N, is shown in Figure 4.1. For a given polymer segment-protein surface sticking energy, ϵ, an adsorbed layer of polymer will form about the protein only above a critical polymer size, denoted by N^*. A polymer smaller than the critical size will not be confined to an adsorbed layer, and is free to diffuse about the bulk polymer solution. This is the scenario presented in Picture 2, see Section 4.4. The critical polymer size required to form an adsorbed layer increases with the decrease in the strength of the interaction between the polymer segments and the protein surface. For polymers larger than the critical polymer size, an increase in the polymer molecular weight, or equivalently in N, causes the protein to partition towards the polymer species. This is

a result of a more favorable interaction of polymer and protein with increasing polymer molecular weight.

The qualitative behavior predicted for $\Delta \ln K_p$ in Picture 3, depicted in Figure 4.1, is opposite to that observed in available experimental data for the partitioning of proteins shown in Figure 2.4 (recall that N is proportional to the polymer molecular weight). To date, the trends that we predict in Figure 4.1 for Picture 3 have not been observed experimentally in two-phase aqueous polymer systems. Indeed, it is interesting that the above scaling arguments predict that an enhanced interaction of the polymer segments and the partitioning colloids will produce a qualitatively different behavior from that traditionally observed. For example, in phase systems with flexible polyelectrolytes, electrostatic interactions of the charges residing on the polymer with those residing on the protein surface may be of sufficient strength to cause the confined adsorption of the polyelectrolyte onto the protein surface. Alternatively, the partitioning of solutes more hydrophobic than the hydrophilic proteins partitioned to date could provide a realization of the predictions of Picture 3. Such solutes may include, for example, the more hydrophobic proteins or gold sols.

4.6 Conclusions

In this chapter we have presented a new molecular-thermodynamic description for the interactions of globular proteins and flexible nonionic polymer coils which influence the partition of proteins in two-phase aqueous polymer systems. Polymer solution phases which contain identifiable polymer coils were considered. We have proposed descriptions for the free energy of interaction for each of the pictures suggested in Chapter 3 and related this quantity, through a statistical-thermodynamic framework, to the experimentally measured protein partition coefficient. To provide the connection between the molecular properties of the polymers and the thermodynamic parameters within the framework, we have utilized the results of scaling arguments. For our purposes, a scaling approach appears to provide a useful qualitative description of the protein partition coefficient, and suggests qualitatively different trends in the protein

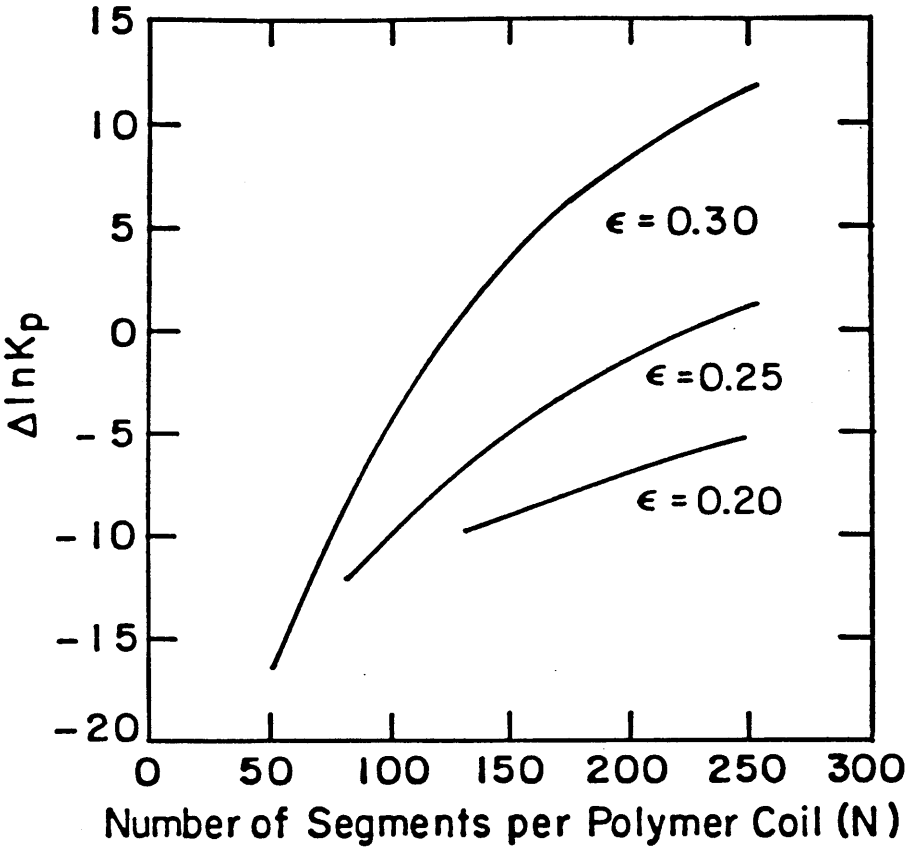

Figure 4.1 Predicted behavior of protein partition coefficient for Picture 3 with increasing polymer size, N, for sticking energy values ε=0.20, 0.25, 0.30 and R_p=10a. Note that the order unity prefactors, k_1-k_4, were assigned the numerical values of unity in Figure 4.1, although this should not be taken to suggest that the predictions are quantitative. For details, see Section 4.5.

partition coefficient with polymer molecular weight for the three scenarios investigated. Although our description of Picture 2 can at best be qualitative when using the scaling relations (without known numerical prefactors) the statistical-thermodynamic framework presented is suitable for the development of a more detailed description. Specifically we have concluded that at Θ-solvent conditions for the polymer, a picture which incorporates solely the excluded-volume interactions between the proteins and the polymer coils is unable to account for the influence of polymer molecular weight on K_p; at athermal-solvent conditions, where repulsive polymer-polymer interactions also influence the protein chemical potential, the predicted protein partition coefficient is shifted in a direction qualitatively consistent with experimental trends. For both athermal- and Θ-solvent conditions, the observed change in K_p is found to be qualitatively consistent with the presence of a weak attraction between the polymer coils and the proteins. The presence of a strong attraction between the polymer coils and the proteins, and associated formation of an adsorbed polymer layer at the surface of the proteins, can lead to a new partitioning behavior that has not yet been realized experimentally.

In this chapter we have not speculated in detail on the origin of the weak attraction incorportated in Picture 2, although we have discussed briefly the influence of the range of the attraction. In particular, when dealing with such small colloidal systems, where the role of van der Waals interactions may be important, the concept of a polymer interaction with the *surface* of the protein may not be appropriate. That is, the influence of the volumes and geometries of the interacting bodies on the interaction, as well as the possible long-range nature of the forces may be important. Also, we have not treated in detail the potentially important role of water in protein partitioning. Such considerations may be important in proposing a more detailed statistical-thermodynamic description of Picture 2. Indeed, within the framework of the equation of state/Monte-Carlo approach reported in Chapter 6, it is found that the apparent strength of the attractive interaction between a polymer segment and protein molecule is an increasing function of the protein size.

It is further evident from this scaling-thermodynamic approach that there is a clear need for alternative experimental studies to provide independent evidence for

the existence of weak attractive interactions between this class of proteins and PEO. To this end, measurements using light scattering and neutron scattering, analogous to those performed in the anionic surfactant-polymer systems, may be illuminating. Along these lines, a small angle neutron scattering investigation of aqueous solutions of PEO and bovine serum albumin is presented in Chapter 7.

Although many improvements of the current developments outlined in this chapter are readily evident, the Chapter 4 establishes a physically sound statistical-thermodynamic framework on which these developments may be founded. Furthermore, the qualitative predictions of the protein partition coefficients suggest a direction for a more detailed description of the interactions influencing protein partitioning in two-phase aqueous polymer systems. Specifically, it is evident that future theoretical formulations should include (1) the influence of the deformability and permeability of the polymer coils on their interactions with globular proteins, (2) the partial permeability of polymer coils to each other (which varies with the solvent quality), and (3) the contributions of higher-order interactions between polymer coils and proteins. With these considerations in mind, in Chapter 6, we develop an Equation of State/Monte-Carlo formulation to predict the thermodynamic properties of aqueous solutions containing PEO and proteins.

Appendix 4 A

The derivation of the entropy of mixing term, F_5, presented in Section 4.4 starts with Eq.(4.11) and a modified form of Eq.(4.12), where the latter is altered to account for the reduction in the number of free polymer coils in the system from N_2 to N_2-m. In addition, substituting $N_p=1$ on the right-hand side of Eq.(4.12) yields

$$\ln\Omega_{N_p=1} = \ln(A_2^{N_2-m}A_p) - \ln((N_2-m)!) + (N_2-m)\ln(V - U_p) + lnV - \frac{U_2(N_2-m)^2}{2(V - U_p)} - \frac{U_2^2(N_2-m)^3}{6(V - U_p)^2} \quad \textbf{(3.A1)}$$

where U_p is the volume excluded by the protein-polymer complex (that is, the protein and m adsorbed polymer coils) to the polymer coils. Subtracting Eq.(4.11) from Eq.(4.A1) leads to the translational-entropy change accompanying the mixing of the protein-polymer complex and the remaining N_2-m polymers, ΔS_{mix}, where

$$\frac{\Delta S_{mix}}{k} = -m\ln(A_2V) + \ln(A_pV) - N_2\ln(1 - \frac{m}{N_2}) + m\ln(N_2 - m) - m + (N_2-m)\ln(1-\frac{U_p}{V}) + \frac{U_2N_2^2}{2V} - \frac{U_2(N_2-m)^2}{2V\left(1-\frac{U_p}{V}\right)} + \frac{U_2^2N_2^3}{6V^2} - \frac{U_2^2(N_2-m)^3}{6V^2\left(1-\frac{U_p}{V}\right)^2} \quad \textbf{(3.A2)}$$

Expanding Eq.(4.A2) to leading order in the expansion parameters, U_p/V ($<<1$) and m/N_2 ($<<1$), yields

$$\frac{\Delta S_{mix}}{k} = -m\ln(\frac{A_2V}{N_2}) + \ln(A_pV) - \frac{N_2U_p}{V}\left(1 + \frac{N_2U_2}{2V}\right) + \frac{mN_2U_2}{V}\left(1 + \frac{N_2U_2}{2V}\right) \quad \textbf{(4.A3)}$$

In Eq.(4.A3), the term $\ln(A_pV)$ represents the entropy of mixing a single protein in a volume V in the absence of free polymers. As the quantity of interest is the deviation in the entropy of mixing from that in the absence of polymer-protein excluded-volume interactions, this term is subtracted from Eq.(4.A3) (see also Section 4.3).

In order to evaluate the entropy of mixing from Eq.(5.A3), the value of A_2 must be determined. Recall that A_2 is defined as follows: if $V-U_t$ is the free volume accessible to a polymer coil upon placement in the system, where U_t is the total system volume that is excluded by the other molecules in the system, then $A_2(V-U_t)$ is the number of ways to place the center of mass of the polymer coil in the available system volume, $V-U_t$. We have defined A_2 as

$$A_2 = \frac{1}{V_1^o} \qquad \textbf{(4.A4)}$$

where V_1^o is the molecular volume of the solvent. That is, we assumed that the volume of a solvent molecule defines an imaginary lattice of cells each of which can accomodate the center of mass of a polymer coil. Note that A_2 is independent of the polymer-coil size, and that the influence of the polymer-coil size on the configurations available to the system is reflected through the free volume available to the polymer coil. Using Eq.(4.A4) in Eq.(4.A3), subtracting $\ln(A_pV)$ from Eq.(4.A3) (as discussed above), and recognizing that $F_5=-\Delta S_{mix}^{ex}/k$ leads to Eq.(4.40) in Section 4.5.

4.7 Literature Cited

Albertsson, P.A., *Partition of Cell Particles and Macromolecules*, Wiley, New York, **1985**.

Albertsson, P.-A.; Cajarville, A.; Brooks, D.E.; Tjerneld, F., *Biochim. Biophys. Acta*, **1987**, 926, 87.

Alexander, S., *J. Physique,* **1977**, 38, 977.

Baskir, J.N.; Hatton, T.A.; Suter, U.W., *Macromolecules,* **1987**, 20, 1300.

Baskir, J.N.; Hatton, T.A.; Suter, U.W., *J. Phys. Chem.*, **1989**, 93, 2111.

Baskir, J.N. *Ph.D. Thesis*, Massachusetts Institute of Technology, **1988**.

Brooks. D.E.; Sharp, K.A.; Fisher, D., Chapter 2, *Partitioning in Aqueous Two-Phase Systems*, Eds Walter, H; Brooks, D.E.; Fisher, D. Academic Press, New York, **1985**.

Cassasa, E.F., *J. Polymer Sci.*, **1967**, B5, 773.

Edmond, E.; Ogston, A.G., *Biochem. J.*, **1968**, 109, 569.

Flory, P.J., *Principles of Polymer Chemistry*, Cornell University Press, Ithaca and London, **1986**.

Flory P.J.; Krigbaum W.R., *J. Chem. Phys.*, **1950**, 18, 1086.

de Gennes, P.-G., *Scaling Concepts in Polymer Physics*, Cornell University Press, Ithaca and London, **1988.**

Gerson, D., *Biochim. Biophys. Acta*, **1980**, 602, 281.

Haynes, C.A.; Beynon, R.A.; King, R.S.; Blanch, H.W.; Prausnitz, J., *J. Phys. Chem.*, **1989**, 93, 5612.

Hermans, J., *J. Chem. Phys.*, **1982**, 77, 2193.

Hermans, J.J.; Hermans, J., *J. Polymer Sci.*, **1984**, 22, 279.

Huggins, M.L., *J. Phys. Chem.*, **1941**, 9, 440.

Hustedt, H.; Kroner, K.H.; Stach, W.; Kula, M.-R., *Biotechnol. Bioeng.*, **1978**, 20, **1989**.

Jansons, K.M.; Phillips, C.G., *J. Colloid Interface Sci.*, **1990**, 137, 75.

King, R.S.; Blanch, H.W.; Prauznitz, J.M., *AIChE Journal*, **1988**, 34, 1585.

Lee, S.H.; Ruckenstein, E., *J. Colloid Interface Sci.*, **1988**, 125, 365.

Middaugh, C.R.; Lawson, E.Q., *Anal. Biochem.*, **1980**, 105, 364.

Modell, M.; Reid, R.C., *Thermodynamics and its Applications*, Second Ed., Prentice-Hall, London, **1983**.

Pincus, P.A.; Sandroff, C.J.; Witten, T.A., *J. Physique*, **1984**, 45, 725.

Rogers, J.A.; Tam, T., *Can. J. Pharm. Sci.*, **1977**, 12, 65.

Ruckenstein, E.; Chi, J.C., *J. Chem. Soc. Faraday Trans*, II **1975**, 71, 1690.

Tanford, C., *Physical Chemistry of Macromolecules*, Wiley, New York, **1961**.

Walter, H.; Brooks, D.E.; Fisher, D., Eds, *Partitioning in Aqueous Two-Phase systems*, Academic Press, New York, **1985**.

Chapter 5.

Proteins in Entangled Polymer Solutions. II. A Scaling-Thermodynamic Formulation

5.1 Introduction

The influence of the polymer solution structure on the partitioning of proteins in two-phase aqueous polymer systems was investigated in Chapter 3. Experimentally observed protein partitioning behaviors were proposed to arise from changes in the underlying structure of the polymer solution which occur at length scales corresponding to the sizes of the protein molecules. Specifically, in the two-phase aqueous polymer system containing poly(ethylene oxide) (PEO) and dextran (Albertsson, 1985), molecular-level pictures of protein-polymer interactions were advanced based on a proposed transition in the nature of the PEO-rich phase, from a solution containing individually dispersed PEO coils to an entangled PEO solution, with increasing PEO molecular weight. Observations on experimental data (Abbott et al., 1991a) (which were reported in Chapter 3) are consistent with this prediction, since the partitioning behavior of proteins in two-phase aqueous PEO-dextran systems is sensitive to polymer molecular weight in the limit of low PEO molecular and insensitive to the polymer molecular weight in the limit of high PEO molecular weights (Abbott et al., 1991a). While the proposed transition in the polymer solution structure was intially advanced on the basis of theoretical estimates for the crossover and observations regarding the partitioning behavior of certain proteins in two-phase aqueous polymer systems (Abbott et al., 1991a), the presence of the crossover was subsequently confirmed by small angle neutron

scattering measurements from aqueous (D_2O) PEO solutions (Abbott et al., 1991c).

In Chapter 4, for proteins in polymer solutions containing *identifiable polymer coils*, statistical-thermodynamic descriptions, utilizing scaling concepts from polymer physics (de Gennes, 1988), were developed for each physical scenario presented in Chapter 3 and the associated protein partitioning behaviors were predicted (Abbott et al., 1991a). It was concluded that although the physical exclusion of the protein by the polymer coils contributes to the observed partitioning behavior, other interactions also play a significant role. In particular, the influence of the PEO molecular weight on the partitioning behavior of a series of hydrophilic proteins was observed to be consistent with the presence of a weak attractive interaction between the protein molecules and the polymer coils (Abbott et al., 1991a). In Chapter 6, a more quantitative evaluation of the protein partition coefficient, using a combined Equation of State/Monte-Carlo approach is presented. This approach corroborates the important role of non-steric interactions between the proteins and PEO. These more precise calculations suggested the presence of a weak attractive interaction energy which increased with protein (characteristic) size, R_p, where $17\text{Å} < R_p < 51\text{Å}$, from order 0.01kT to 0.1kT (per polymer segment at the protein surface) (Abbott et al., 1991b). Finally, in Chapter 7 we show that the measurement and interpretation of the intensity of neutrons scattered at small angles (SANS) from bovine serum albumin ($R_p = 35\text{Å}$) in PEO solutions containing identifiable polymer coils is also consistent with the existence of a weak attractive interaction between BSA and PEO (in addition to a repulsive steric interaction) (Abbott et al., 1991c).

While a somewhat unified picture of the interactions between proteins and polymers in solutions containing identifiable polymer coils appears to be emerges from Chapters 3, 4, 6 and 7, the alternative scenario, where the polymer coils are extensively entangled in solution also requires attention. The central aim of the present Chapter (along with Chapter 8) is to provide an account for the interactions of protein molecules and entangled polymer solutions which complements our descriptions of protein-polymer coil interactions presented in Chapter 4.

While the partitioning of proteins between entangled polymer solution

phases can be studied using two-phase aqueous polymer systems, several factors introduce ambiguity into the interpretation of the results. First, the partitioning behavior of proteins in two-phase aqueous polymer systems reflects the *relative interactions* between the proteins and *two* coexisting polymer solution phases. Second, the independent control of the polymer concentration in only one of the two coexisting phases of a two-phase aqueous polymer system is not possible. Therefore, in order to overcome these limitations, in Chapter 8 we report the results of an alternative experimental technique, which does not suffer these limitations. Specifically, we report the measurement of the partitioning of proteins between an entangled polymer solution phase and an aqueous polymer-free phase using a diffusion cell (see Figure 8.1 in Chapter 8). In contrast to the two-phase aqueous polymer systems, such an experimental set-up allows us to study the interactions of the proteins and a *single* entangled polymer solution phase. Therefore, in proposing a scaling-thermodynamic theory for proteins in entangled polymer solutions we focus our attention on predicting the partitioning behavior of proteins in the diffusion cell experiments. While the partitioning of proteins in two-phase aqueous polymer systems appears very similar to the partitioning of proteins in a diffusion cell, we demonstrate that the subtle difference in experimental set-up has important consequences on the partitioning behavior. The origin of this non-trivial difference lies in the fact that the mechanical membrane of the diffusion cell can support a pressure difference (the osmotic pressure) between the two compartments. In contrast, in two-phase aqueous polymer systems both phases are at the same pressure.

In order to interpret the protein partition coefficients measured using the diffusion cell, in the spirit of our prior treatment of protein-polymer interactions in dilute polymer solutions (Abbott et al., 1991a, b, and c), we have (i) utilized the molecular-level pictures for the interactions of proteins and entangled polymer solutions presented in Chapter 4, (ii) developed scaling-thermodynamic theories for each picture, and (iii) predicted the associated protein partitioning behavior. In Chapter 8 we compare the theoretical predictions with protein partitioning trends observed experimentally in the diffusion cell experiments.

We have chosen to focus our attention on the interactions of certain

globular hydrophilic proteins and PEO since the partitioning of these species has been the subject of previous investigations in two-phase aqueous polymer systems containing PEO as one of the "phase-forming" polymers (Saskawa and Walter, 1970 and 1972; Walter et al., 1972; Zaslavsky et al., 1983; Albertsson et al., 1987; Johansson, 1985; Diamond and Hsu, 1989 and 1990). In order to elucidate the character of the interactions between PEO and the proteins in aqueous solution, an appreciation of the physical nature of the polymer solution is required. Specifically, the length scales which characterize the aqueous PEO solutions and which are used to describe the interactions between PEO and proteins, must be identified. At polymer concentrations, c, much less than c^* (where c^*, is a polymer concentration characteristic of the region where the extensive overlap of polymer coils begins to occur), the solution is dilute in polymer coils and consequently the identity of each individual polymer coil is preserved (de Gennes, 1988). However, in contrast, when the polymer concentration is much greater than c^*, the polymer coils overlap and become entangled to form a transient polymer solution web or mesh (de Gennes, 1988). Within this mesh, the identities of the individual polymer coils are lost and *all* thermodynamic properties of the solution are independent of the molecular weight of the polymer coils. For polymer solutions containing extensively entangled polymer coils, the characteristic length scale of the polymer solution, that is the mesh size (blob size) of the polymer web or mesh, ξ_b, no longer reflects the identities of the individual polymer coils, but instead is determined by the total volume fraction of polymer in solution. This mesh size, which is also a measure of the range of correlations between polymer segments in the solution, scales with polymer volume fraction, ϕ, as (de Gennes, 1988)

$$\xi_b \sim a\phi^{-3/4} \qquad \textbf{(5.1)}$$

Note that Eq.(5.1) can be derived by requiring that the polymer-coil radius (characterized by R_g) and the blob size (ξ_b) be equal at the cross-over polymer concentration, c^*. For aqueous (D_2O) solutions of PEO, an analysis of small angle neutron scattering measurements was consistent with a value of $a \simeq 4$Å (Abbott et al., 1991c; Cabane and

Duplessix, 1987). The range of polymer volume fractions encountered in two-phase aqueous polymer systems containing PEO is typically 0.05 to 0.15, and thus using Eq.(5.1), the corresponding ξ_b values in an entangled aqueous PEO solution are 40Å to 20Å, respectively (Abbott et al., 1991c). Significantly, this web size is comparable to the sizes of small proteins partitioned in these systems. For example, the hydrodynamic radius of cytochrome-c is about 20Å (see Table 8.3). This is an important observation since, when the blob size of the entangled PEO solution is comparable to the size of a protein, the correlations and fluctuations among the polymer segments over distances of order ξ_b can influence the nature of the interactions between the polymer and the protein.

While the relative sizes (i.e., the *geometries*) of the polymer blob, ξ_b, and the protein radius, R_p, play a significant role in determining the nature of protein-polymer interactions, the *energetic* interactions between the polymer segments and the protein molecules can also be important. In Chapter 3, our treatment of the influence of attractive interactions between PEO coils and proteins was motivated, in part, by an analogy between the physical nature of spheroidal micelles (Cabane and Duplessix, 1987 and 1982; Cabane, 1977) and protein molecules (Abbott et al., 1991a) and the way in which they interact with PEO coils in aqueous solutions. On the basis of this analogy, it was concluded that attractive interactions between proteins and PEO can also influence the properties of aqueous protein-PEO solutions (for example, protein partitioning behavior). Here, we continue this analogy and consider the influence of attractive interactions (of differing strengths) between the proteins and extensively entangled PEO in aqueous solution (in addition to the influence of geometry). It is also relevant to point out that accompanying the investigations of polymer-micelle interactions (Cabane and Duplessix, 1987 and 1982; Cabane, 1977), a number of scaling-type theoretical descriptions were developed which pointed out that important differences exist between the nature of polymer adsorption onto planar and curved surfaces (Alexander, 1977; de Gennes, 1979; Pincus et al., 1984; Marques and Joanny, 1988). These scaling descriptions are developed further here, and then incorporated into a statistical-thermodynamic theory of protein partitioning in entangled polymer solutions, which is presented in Section 5.

Finally, we mention that a number of investigations exist on the hindered diffusion of globular objects through polymer networks (Lin and Phllies, 1982, 1984a and b); Ullmann et al., 1985; Phillies et al., 1985; Brown and Rymden, 1986). Indeed, just as thermodynamic properties are influenced by the relative sizes of the globular species and the polymer solution correlation length (in addition to their energetic interactions with the net), the hindered diffusion of a globular species through the net is influenced by similar factors. Although in this chapter we consider issues related to the equilibrium properties of proteins in entangled polymer solutions, the study of the hindered diffusion of proteins through the entangled polymer solutions complements this report.

The remainder of this chapter is organized as follows. In Section 5.2 we present and discuss a statistical-thermodynamic framework that relates the predicted thermodynamic properties of solution of proteins and entangled polymers to the experimentally measureable protein partition coefficient. In the Sections, 5.3 to 5.8 we present scaling-thermodynamic arguments for each of the physical scenarios presented in Figure 3.7 and predict the associated protein partitioning behavior in a diffusion cell experiment (see Chapter 8.). Finally, in Section 5.9 we present our concluding remarks.

5.2 Statistical-Thermodynamic Framework

In the limit of vanishing protein concentration, the interactions between the protein molecules themselves are very infrequent, and the equilibrium partition coefficient of the protein is simply related to the free-energy change associated with the transfer of the protein between the top (PEO-free) and bottom (PEO solution) compartments of the diffusion cell. Accordingly, the partition coefficient of the protein, K_p, can be expressed as (see Chapter 4)

$$\ln K_p = \ln\left[\frac{c_{p,t}}{c_{p,b}}\right] = \left[\frac{\mu^o_{p,b}(T,P+\Pi,\phi) - \mu^o_{p,t}(T,P)}{kT}\right] + \left[\frac{z_p e\,(\psi_b - \psi_t)}{kT}\right] \qquad \textbf{(5.2)}$$

where $\mu^{o}_{p,i}$ is the standard-state chemical potential of the protein in phase i (top (t) or bottom (b)), Π is the osmotic pressure of the polymer solution in the bottom compartment, and $c_{p,i}$ is the protein concentration in phase i. The physical interpretation of the protein standard-state chemical potential is the free-energy change upon taking the protein from a polymer-free solvent phase at temperature, T, and pressure, P, and introducing it into a solution with a composition, temperature and pressure, corresponding to the conditions in either the top or the bottom compartments of the diffusion cell.

It is relevant to point out that an important difference exists between Eq.(5.2) and the thermodynamic framework of Chapter 4, where the partitioning of proteins between the two coexisting polymer solution phases of a two-phase aqueous polymer system was considered (Abbott et al., 1991a). The difference in these two situations influences our definition of the standard-state protein chemical potential. In two-phase aqueous polymer systems, proteins are partitioned across a *planar liquid-liquid interface* between the two coexisting polymer solution phases which are at the same pressure. In contrast, in the diffusion cell experiment, the mechanical membrane which separates the top and bottom compartments *can* support a pressure difference. This pressure difference, which corresponds to the osmotic pressure of the polymer solution, determines that the pressures in the protein standard states, as defined by Eq.(5.2), are no longer the same. Interestingly, this subtle difference between the experimental systems can lead to rather significant differences in the predicted protein partitioning behaviors (see Section 5.5).

The macroscopic electrical potential term in Eq.(5.2) (the last term) accounts for the Donnan-type potential associated with the diffusional equilibrium of charged species (proteins and electrolytes) between the two compartments of the diffusional cell (Albertsson, 1985; Johansson, 1985; Bamberger et al., 1984; Brooks et al., 1984). The origin of the potential difference is the interactions of the salt ions and PEO and, thus, the effect is ion specific (Albertsson, 1985; Johansson, 1985; Bamberger et al., 1984; Brooks et al., 1984). As discussed in Chapter 8, this term predicts that the partitioning of proteins in the diffusion cell experiments will be sensitive to the types of

ions present. In view of the relatively small influence that (sodium) sulphate and chloride salts have on the partitioning of cytochrome-c, as reported in Figure 8.2, it appears that the contribution of the last term in Eq.(5.2) to the protein partition coefficient, K_p, is not dominant at these low PEO concentrations. In particular, we have estimated the maximum magnitude of the electrical potential difference to be around 0.2mV (see Chapter 8). Accordingly, for the range of PEO concentrations, ϕ, considered in Chapter 8, we can simplify Eq.(5.2) to

$$\ln K_p = \left[\frac{\mu^o_{p,b}(T,P+\Pi,\phi) - \mu^o_{p,t}(T,P)}{kT} \right] \qquad \textbf{(5.3)}$$

In order to evaluate the difference in the standard-state protein chemical potential, $\mu^o_{p,b}(T,P+\Pi,\phi)-\mu^o_{p,t}(T,P)$, it is useful to consider the reversible isothermal process where a protein is transferred from a solvent phase at pressure P, to a polymer solution phase at pressure $P+\Pi$. We consider that $\mu^o_{p,b}(T,P+\Pi,\phi)-\mu^o_{p,t}(T,P)$ contains two identifiable contributions, ΔG_p and ΔG_2, with relative magnitudes which depend on the solution conditions, as discussed below. First, accompanying the introduction of the protein into the polymer solution, interactions between the proteins and polymers (which can be steric and energetic) constrain the movement of the protein, and an entropic penalty, arising from the loss of the translational freedom of the proteins, is incurred. The corresponding free-energy change is denoted ΔG_p. The second contribution, which mirrors ΔG_p, arises from the influence of the same interactions (between proteins and polymers) on the configurational and translational freedom of the polymer. This contribution is denoted ΔG_2. Clearly while, these two contributions to $\mu^o_{p,b}(T,P+\Pi,\phi)-\mu^o_{p,t}(T,P)$ are coupled through the nature of the interactions between the protein and polymer, it turns out (as shown below) that depending on the solution conditions, only one of the two contributions tends to dominate. For polymer concentrations (and protein sizes) such that $R_p/\xi_b \ll 1$, ΔG_p dominates the standard-state protein chemical potential, while in the limit, $R_p/\xi_b \gg 1$, the contribution ΔG_2 dominates. In keeping with the division of the protein standard state chemical potential into two contributions, we

consider the evaluation of the protein partition coefficient for each of the physical pictures as,

$$\ln K_p = \left[\frac{\mu^o_{p,b}(T,P+\Pi,\phi) - \mu^o_{p,i}(T,P)}{kT} \right] = \left[\frac{\Delta G_p + \Delta G_2}{kT} \right] \qquad \textbf{(5.4)}$$

It is relevant to briefly compare Eq.(5.4) with the spirit of our previous statistical-thermodynamic description of protein solutions containing identifiable polymer coils (see Chapter 4 for details), namely,

$$\Delta ln K_p = -\Delta \left[\left[\frac{N_2 U_p}{V} \right] + U_p \left[\frac{N_2^2 U_2}{2V} + O \left[\frac{N_2^3 U_2^2}{V^2} \right] \right] \right] \qquad \textbf{(5.5)}$$

where N_2/V is the number density of polymer coils in solution, U_p is the excluded-volume describing the steric interactions of the protein and polymer *coils*, and U_2 is the excluded-volume describing the steric interactions of two polymer coils. Note that Eq.(5.5) was derived under conditions where only steric interactions occur between the protein and polymers coils (Abbott et al., 1991a). In order to compare Eq.(5.5) with Eq.(5.4), the term N_2U_p/V, which describes the volume fraction of solution excluded from the proteins by the polymer coils, is identified with ΔG_p in Eq.(5.4). The terms $U_p[...]$ in Eq.(5.5) are identified with ΔG_2 in Eq.(5.4). Specifically, the terms in the square bracket are the nonideal portion of the polymer solution osmotic pressure. These terms, when multiplied by the volume of solution excluded to the polymer coils by the protein, U_p, describe the (excess) free energy change ΔG_2 in Eq.(5.4). Finally, it is interesting to note that ΔG_2 vanishes at the Θ-solvent conditions for the polymer (in contrast to ΔG_p which remains at a non-zero value).

5.3 Steric Interactions ($\varepsilon=0$) with Small Proteins ($R_p \ll \xi_b$)

Figure 3.7(a) corresponds to solution conditions where the protein size, R_p, is much smaller than the blob size of the polymer solution, ξ_b. First we evaluate ΔG_p, and subsequently show that, in the limit $R_p \ll \xi_b$, this term is much larger than ΔG_2. In Figure 3.7(a) the only interaction between the polymers and proteins occurs because they can not occupy the same physical space (there is no attraction, $\varepsilon=0$, where ε is the energy change upon bringing a single polymer segment from bulk solution to the protein surface (in units of kT)). Since the protein is much smaller than the typical distance between the polymer strands within the entangled polymer mesh, the probability of the protein interacting simultaneously with two strands of the polymer net is very low. Therefore, and as shown below, the fraction of the solution phase which is excluded from a protein molecule will be proportional to the volume fraction of polymer in solution. Statistical-thermodynamic considerations equate the (volume) fraction of the solution excluded to the protein, U_p, with $\Delta G_p/kT$, that is, $\Delta G_p/kT=U_p$ (Tanford, 1961). Physically, $1-U_p$ is the average probability of finding space in the solution which is accessible to the protein. This "free-volume" fraction in the solution decreases with an increase in the polymer concentration. Depending upon the relative sizes of the protein, R_p, and the polymer persistence length, b, the functional dependence of the excluded-volume, U_p, on the protein radius, R_p, can vary. Here we focus on the case relevant to the interactions of PEO and globular protein molecules where the size of the protein is large compared to the persistence length of the polymer chain. When $R_p \gg b$, the polymer chain "appears" flexible to the protein and the interactions between the polymer segments and the protein molecule are not independent. That is, a significant probability exists, which increases with the protein size, that two or more polymer segments belonging to the same local chain length will simultaneously interact with the protein. Specifically, the protein will interact with sections of the polymer strands which have sizes similar to R_p. The number of polymer segments, n_a, within a local section of a polymer strand, with a size (radius of gyration) equal to the protein size is,

$$n_a \sim \left[\frac{R_p}{a}\right]^{5/3} \tag{5.6}$$

Since, by definition, these "protein-sized blobs" of polymer chain interact independently with the protein molecules, the total volume excluded from the protein per protein-sized blob is of order R_p^3. To evaluate the volume fraction of the solution which is excluded from the protein by the blobs, the number of protein-sized blobs in solution (per unit volume of solution), N_a, is required. This can be estimated as $N_a \sim \phi/(a^3 n_a)$ and leads to the result

$$\frac{\Delta G_p}{kT} \sim N_a R_p^3 \sim \frac{\phi R_p^3}{a^3 n_p} \sim \phi \left[\frac{R_p}{a}\right]^{4/3} \qquad a \ll R_p \ll \xi_b \tag{5.7}$$

Equation (5.7) can be compared to the simpler case where the polymer chain is rigid on the length scale corresponding to the size of the protein molecule. For the case of rigid polymer chains ($R_2 \ll b$), all polymer segments interact independently with the protein molecule, and therefore the volume fraction of solution excluded from the protein, U_p, can be estimated by considering the interactions of a rod (the polymer chain) and sphere (protein), that is, $U_p = \phi(R_p/a)^2$. The exponent of R_p in Eq.(5.7), 4/3, which is smaller than the corresponding exponent in the case of the rigid polymer chain, 2, reflects the fact that when the polymer chain becomes flexible on a length scale compared to the protein size, the protein will simultaneously interact, on average, with several polymer segments. In particular, the number of simultaneous interactions increases with the protein size as $R_p^{2/3}$, and thus the sensitivity of U_p to the size of the protein decreases, as compared to the case when the polymer chain is stiff on the length scale of the protein and the polymer segments interact independently with the protein. A form similar to Eq.(5.7) has been previously derived by de Gennes using a slightly different argument (de Gennes, 1979).

In order to predict the protein partition coefficient using Eq.(5.4), we also require an estimate of ΔG_2, which accounts for the influence of the protein-polymer interactions on the translational and configurational freedom of the polymer. It turns out, as shown below, that this term is negligible in the limit $R_p \ll \xi_b$. The term ΔG_2 can be estimated by considering the work done to introduce a protein into the polymer solution against the osmotic pressure of the polymer, that is, $\Delta G_2 = U_2 \Pi$, where U_2 is the volume of the solution that is excluded from the polymer by the protein. It should be understood that, in general, the volume U_2 does not correspond to the molecular volume of the protein species, however, in the limit $R_p \ll \xi$, U_2 is of the order the protein size. While the configurational freedom of the polymer chains is reduced in the vicinity of the protein surface (which results in the exclusion of the polymer from the vicinity of the protein surface), at distances beyond (order) R_p from the protein surface, the polymer can "feel" the edges of the protein and thus experiences the freedom it has in bulk solution. Consequently, the polymer is excluded from a volume of the solution of order R_p^3 (this contrasts to the situation $R_p \gg \xi_b$ (described below), where the polymer is depleted from a volume of order ξ_b^3 about the protein). Scaling relations for the osmotic pressure of the polymer solution, π_p, which account for the existence of correlations between monomers, predict the osmotic pressure scales as (de Gennes, 1988)

$$\Pi_p \sim \frac{kT}{\xi_b^3} \tag{5.8}$$

where ξ_b^3 is the effective concentration of "blobs", each of which behaves independently to each other, in the polymer solution. Therefore, using Eq.(5.8) for the osmotic pressure of the polymer solution and $U_2 \sim R_p^3$, ΔG_2 can be evaluated as,

$$\frac{\Delta G_2}{kT} = U_2 \Pi \sim \left[\frac{R_p}{\xi_b} \right]^3 \tag{5.9}$$

Clearly, in the limit, $R_p/\xi_b \ll 1$, this term is negligible as compared to Eq.(5.7) (which

are of order $(R_p/\xi_b)^{4/3}$). Therefore, using Eqs.(5.4) and (5.7), and the result $\Delta G_p \gg \Delta G_2$, the protein partitioning behavior, in the limit $R_p \ll \xi_b$, is predicted as

$$lnK_p \sim \varphi \left[\frac{R_p}{a}\right]^{4/3} \qquad a \ll R_p \ll \xi_b \tag{5.10}$$

5.4 Steric and Weak Attractive Interactions ($\varepsilon \ll 1$) with Small Proteins ($R_p \ll \xi$)

In view of the significant role that attractive protein-polymer interactions (in addition to steric interactions) play in determining the thermodynamic properties of proteins in solutions which contain identifiable PEO coils (Abbott et al., 1991a, b, and c), it is also relevant to examine the influence of such weak attractions on the partition coefficients measured in the diffusion cell experiments (with entangled PEO solutions). To evaluate the influence of the attractions, we have made a number of simplifying assumptions (which are consistent with those previously made when treating the interactions of protein and PEO solutions containing identifiable polymer coils (Abbott et al., 1991a, b, and c)); the attractive interactions between polymer segments and protein molecules are short-ranged (with a range on the order the polymer segment size, *a*); the distribution of polymer segments in the vicinity of the protein molecule is not significantly perturbed by weak attractive interactions (see Figure 3.7(a)). With these assumptions in mind, the influence of the perturbative weak attractive interaction can be estimated from the number of polymer segments, N^*, found, on average, within a distance *a* of the protein surface. That is,

$$\frac{\Delta G_p^{att}}{kT} = \varepsilon N^* \tag{5.11}$$

Recall ε is the energy change upon bringing a single polymer segment from bulk solution to the protein surface (in units of kT).

When the protein is large compared to the persistence length of the polymer chain, one must consider the interaction of N_a "protein-sized polymer blobs" (each containing n_a polymer segments) with the protein molecule (see Eq.(5.6) and the accompanying text). This physical situation is analogous to the interaction of N_a polymer *coils* (each with n_a statistical segments) with protein molecules which was considered in Chapter 4. That is, for a solution of N_a polymer coils which interact with the protein with energy ε (per polymer segment contact), the influence of an attractive interaction on the protein partition coefficient can be written as,

$$\ln K_p \sim - N_a \varepsilon R_p^2 a n_a^{2/5} \qquad \textbf{(5.12)}$$

Eq.(5.12) was derived previously by considering a balance of two opposing effects (Abbott et al., 1991a). First, when a protein and polymer molecule collide, the density of polymer segments that is "felt" by the protein molecule scales with the density of polymer segments within a polymer coil having its unperturbed average configuration (which decreases as $a^{-3}n_a^{-4/5}$ with increasing polymer size (de Gennes, 1988)). Second, with each collision, the number of polymer segment contacts made with the protein will be proportional to the available surface area of the protein, R_p^2, and the "surface area" of the polymer coil, defined by $R_g^2 \sim a^2 n_a^{6/5}$. Finally, Eq.(5.12) also accounts for the probability of a collision occuring between a protein molecule and a polymer blob, which is proportional to the number of protein-sized polymer blobs in solution, N_a. To use Eq.(5.12) for solutions of extensively entangled polymer coils, we subsitute, $N_a = \phi / a^3 n_a$ and Eq.(5.6) into Eq.(5.12), to yield the influence of an attractive interaction on ΔG_p as

$$\frac{\Delta G_p^{att}}{kT} \sim - \frac{\phi \, \varepsilon R_p}{a} \qquad \textbf{(5.13)}$$

Substituting Eqs.(5.7) and (5.13) into Eq.(5.4), along with the condition $\Delta G_p \gg \Delta G_2$, yields

$$lnK_p = \phi \left[\frac{R_p}{a} \right]^{4/3} \left[1 - k_1 \varepsilon \left[\frac{a}{R_p} \right]^{1/3} \right] \qquad \textbf{(5.14)}$$

It is relevant to compare Eq.(5.13) to an equivalent equation which can be obtained using a different form for N^*, derived previously by de Gennes (1979), namely

$$\frac{\Delta G_p^{att}}{kT} \sim - \varepsilon \phi \left[\frac{R_p}{a} \right]^{1/3} \qquad \textbf{(5.15)}$$

The difference between Eq.(5.15) and Eq.(5.13) appears because in the evaluation of Eq.(5.13) we attempted to include the fact that when a protein-sized polymer blob and a protein molecule collide, the strength of the interaction will depend on the number of polymer segment contacts. As mentioned above, we have predicted that the number of contacts scales as $n_a^{6/5-4/5}=n_a^{2/5}$. If this term is omitted from Eq.(5.12), Eq.(5.13) returns to Eq.(5.15).

5.5 Steric Interactions ($\varepsilon=0$) with Large Proteins ($R_p \gg \xi$)

For the scenario (Figure 3.7(b)) where the protein size is large compared to the polymer solution mesh, ξ_b, the interactions between the polymer network and the protein molecules are intimately related to the the relative size of protein and the polymer correlation length. In this situation, we will show that the dominant contribution to the protein partition coefficient is the term ΔG_2 (in Eq.(5.4)). Recall, ΔG_2 is the free energy change in transferring a protein from a solvent phase at pressure P into a polymer solution phase at pressure $P+\Pi$. It is evaluated as the reversible isothermal work done in order to exclude the polymer from the protein volume and the polymer depletion layer at the protein surface, denoted as U_2, against the osmotic pressure of the polymer solution, Π (de Gennes, 1979). This can be estimated as

$$\Delta G_2 = U_2 \Pi \sim (R_p + \xi_b)^3 \Pi \qquad (5.16)$$

where the depletion of the polymer extends a distance ξ_b from the protein surface (see Chapter 3). Using Eq.(5.8) in Eq.(5.16), a scaling form for ΔG_2 can be estimated as (Alexander, 1977)

$$\frac{\Delta G_2}{kT} \sim \left(\frac{R_p}{\xi_b}\right)^3 \sim \left(\frac{R_p}{a}\right)^3 \phi^{9/4} \qquad a \ll \xi_b \ll R_p \qquad (5.17)$$

To estimate the magnitude of ΔG_p in the limit $R_p \gg \xi_b$, it is useful to reconsider the evaluation of ΔG_p for the limit $R_p \ll \xi_b$. Equation (5.7) predicts that for the limit $R_p \ll \xi_b$, where polymer segments interact with the polymer segments independently, $\Delta G_p \sim \varphi$. On the other hand, as the ratio R_p/ξ_b increases, polymer segments will simultaneously exclude the protein, and thus volume excluded (from the protein) *per polymer* will decrease. Therefore, Eq.(5.7) also forms an upper bound on the magnitude of ΔG_p for $R_p \gg \xi_b$. By rewriting Eq.(5.7) in the form

$$\Delta G_p \sim \left(\frac{R_p}{\xi_b}\right)^{4/3} \qquad (5.18)$$

and comparing it with Eq.(5.17) it becomes apparent that in the limit $R_p \gg \xi_b$, ΔG_2 is much larger than ΔG_p. Accordingly, in the limit $R_p \gg \xi_b$, the partition coefficient of the protein can be written as

$$\ln K_p \approx \left(\frac{R_p}{a}\right)^3 \phi^{9/4} \qquad (5.19)$$

It is interesting to contrast Eq.(5.19) with the prediction for the partitioning of proteins between two phases at constant pressure, such as the partitioning of proteins in two-phase aqueous polymer systems containing entangled polymer solution phases. In such a

situation, the work done in transferring a protein molecule from one phase to the other corresponds to the work done against the osmotic pressure in forming (only) the depletion layer about the protein. Specifically, the volume of the protein is not included in the excluded volume since the same pressure is exerted on this volume in both phases. Accordingly, from a simple modification to Eq.(5.16) that excluded the protein volume from U_2, $\ln K_p$ is predicted to have the form

$$lnK_p \sim \phi^{3/2}\left[\frac{R_p}{a}\right]^2 \qquad \textbf{(5.20)}$$

A comparison of Eq.(5.20) with Eq.(5.19) shows the rather different exponents that relate the concentration of polymer and protein size with the protein partition coefficient for two subtly different experimental situations.

5.6 Steric and Weak Attractive Interactions ($\varepsilon \ll 1$) and Large Proteins ($R_p \gg \xi$)

In the spirit of previous scaling arguments (de Gennes, 1988 and 1979), we have proposed the following extension of Eq.(5.19) to account for the influence of weak attractive interactions between the polymer segments and the protein surface (Figure 3.7(b)). Specifically, the attractive interactions between the polymer segments and the protein surface are insufficient to deform the polymer strands extensively in the vicinity of the protein (for the case $\varepsilon=0$). Provided that $\varepsilon \ll 1$, this scenario appears reasonable (unless $n_s\varepsilon > 1$, where n_s is the number of surface contacts). Under these conditions, de Gennes (1988) suggested that the concentration of polymer segments at the surface may be estimated by assuming the equality of the osmotic pressures in the bulk and at the surface. Assuming that the osmotic pressure is proportional to the concentration of polymer segments at the surface, ϕ_s, equating the osmotic pressure at the surface to the bulk osmotic pressure, π_p, and using Eq.(5.8) one obtains the simple result

$$\phi_s \sim \phi^{9/4} \tag{5.21}$$

If the introduction of the very weak attractive interaction between the polymer segments and the protein does not significantly perturb ϕ_s, substituting $N^* = (R_p/a)^2 \phi_s$ into Eq.(5.11) leads to the following form for the influence of attractive interactions on the protein partition coefficient measured using the diffusion cell

$$\frac{\Delta G_2^{att}}{kT} \sim -\left(\frac{R_p}{a}\right)^2 \varepsilon \ \phi^{9/4} \tag{5.22}$$

In Eq.(5.22), the number of contacts between the protein molecule and the polymer segments is proportional to the surface area of the protein, R_p^2. The form of the protein partition coefficient which incorporates both repulsive steric and weak attractive interactions between the protein molecule and polymers is obtained by summing Eq.(5.19) and Eq.(5.22).

$$lnK_p = \phi^{9/4} \left[\frac{R_p}{a}\right]^3 \left[1 - k_2 \varepsilon \frac{a}{R_p}\right] \tag{5.23}$$

5.7 Strong Attractive Interactions ($n_s\varepsilon \gg 1$) and Small Proteins ($R_p \ll \xi_b$)

In Figure 3.7(c), we have depicted a situation where a protein-polymer complex has formed under the influence of a strong attractive interaction between the polymer and protein. In view of the findings of Chapter 4, which predicted protein-polymer complexation in dilute polymer solutions to be inconsistent with the observed partitioning behaviour of certain hydrophilic proteins in two-phase aqueous polymer systems containing low molecular weight PEO, it appeared unlikely that the scene depicted in Figure 3.7(c) would predict the partitioning behavior of the same hydrophilic proteins (interacting with semidilute PEO solutions) used in the diffusion cell experiment.

However, a recent diffusion cell measurement (Cleland and Wang, 1991) (see Chapter 8), which was based on the same experimental technique developed in this chapter, found a partitioning behavior for the hydrophobic protein intermediate (a partially refolded protein), carbonic anhydrase, which is qualitatively different from the results in Figure 2 and which cannot be accounted for by the scenarios depicted in Figures 3.7 (a) and (b) (Cleland and Wang, 1991). Indeed, as we show below, the partitioning behavior of the carbonic anhydrase intermediate is qualitatively consistent with the scene depicted in Figure 3.7(c).

Following the experimental observations of complexation between anionic micelles and semidilute PEO solution networks (Cabane and Duplessix, 1987), a number of theoretical attempts have been reported to describe the free energy change when small spheres and flexible polymers form complexes (Alexander, 1977; de Gennes, 1979; Pincus et al., 1984; Marques and Joanny, 1988). Due to the similar geometries of the micelle and protein, these results serve as a useful foundation for the description of protein interactions with semidilute polymer solutions (for the case where protein-polymer complexation occurs). In view of the rather complete descriptions for the form of the free energy of interaction which are available elsewhere, here, we shall only briefly summarize the pertinent results (Alexander, 1977; de Gennes, 1979; Pincus et al., 1984; Marques and Joanny, 1988).

When the protein molecule is sufficiently small compared to the polymer mesh size, only one strand of the polymer net will complex with the protein. Under the influence of a strong attractive interaction between the protein and polymer segments, polymer will adsorb to the surface of the protein molecule. The adsorption of the polymer chain to the protein surface severely restricts the configurations available to the polymer chain and an entropic penalty is associated with the loss of configurational freedom. The formation of a dense adsorbed polymer layer is opposed further by repulsive excluded volume interactions between polymer segments which increase with the concentration of polymer in the adsorbed layer. Accordingly, we consider three contributions to the free energy change, F_o/kT, which accompany the formation of a protein-polymer complex, namely (Alexander, 1977; de Gennes, 1979; Pincus et al.,

1984; Marques and Joanny, 1988),

$$\frac{F_o}{kT} \approx -\frac{\varepsilon Na}{D} + \frac{k_3 a^2 N}{6D^2} + \frac{k_4 g_2 N^2 a^3}{4\pi R_p^2 D} \tag{5.24}$$

where N is the number of polymer segments within the adsorbed polymer layer of thickness D which envelopes the protein, $g_2=1-2\chi$, where χ is the Flory-Huggins constant (Flory, 1986; Huggins, 1941), and k_3 and k_4 are order 1 numerical constants. In Eq.(5.24), the first term describes the contribution to the free energy of interaction that arises from the formation of favorable contacts between the polymer segments and the protein. Assuming a uniform density of polymer segments in the adsorbed polymer layer, the ratio a/D is the fraction of polymer segments in the adsorbed layer that contact the protein. The second term captures the entropic penalty incurred by the polymer chain when it is confined to the adsorbed layer. It can be thought of as an elastic energy. Note that the second term is only strictly correct for an ideal chain, and therefore, for the sake of simplicity, in Eq.(5.24) we make an approximation. The last term in Eq.(5.24) captures the work done in concentrating the polymer segments into the adorbed layer against their repulsive excluded volume interactions. If Eq.(5.24) is minimized with respect to N and D, the equilibrium number of polymer segments in the adsorbed polymer layer, N^*, and the free energy of complexation, F^*/kT can be derived as

$$N^* \sim \frac{R_p^2 \varepsilon}{k_4 g_2 a^2} \tag{5.25}$$

and

$$\frac{F^*}{kT} \approx -\frac{k_5 \varepsilon^3 R_p^2}{a^2 g_2} \tag{5.26}$$

where k_5 is a numerical constant which is evaluated as

$$k_5 \sim \frac{1}{k_3 k_4} \tag{5.27}$$

Below, we sketch a scheme which relates the predicted free energy change upon complexation, F^*/kT (see Eq.(5.26)), to the experimentally measureable protein partition coefficient, $\ln K_p$. To simplify the analysis, we assume that F^*/kT is the dominant contribution to the protein chemical potential, and in doing so we neglect terms such as the entropy of mixing the protein and polymer species. Since in general, for complexation to occur, $F^*/kT \gg 1$, this approximation does not appear limiting. The free energy of binding, F^*/kT, describes the protein-polymer binding equilibrium

$$[c_p] + [N^*] \rightleftharpoons [c_p N^*] \tag{5.28}$$

where $[c_p]$ is the concentration of unbound protein in solution, $[N^*]$ is the concentration of polymer domains which contain N^* polymer segments (each domain can be thought of as a potential binding site of a protein molecule) and $[c_p N^*]$ is the concentration of protein-polymer complexes in the solution. The equilibrium constant, K_1, which describes the complexation is defined by

$$K_1 = \frac{[c_p N^*]}{[c_p][N^*]} \tag{5.29}$$

Equation (5.29) is related to the free energy of complexation by $F^* = -kT\ln K_1$. The experimentally measureable quantity, the protein partition coefficient in a diffusion cell experiment, is related to the concentrations of the species in Eq.(5.30) as

$$K_p = \frac{[c_p]}{[c_p N^*] + [c_p]} \tag{5.30}$$

Eqs.(5.28) to (5.30), when combined with the polymer conservation statement

$$[N^*]_o = [N^*] + [c_p N^*] \tag{5.31}$$

where $[N^*]_o$ is the total concentration (bound and unbound) of protein complexation sites on the polymer, predict the protein partition coefficient as

$$K_p = \frac{1 + K_l[c_p]}{K_l[N^*]_o + 1 + K_l[c_p]} \tag{5.32}$$

Eq.(5.32) is a useful equation since K_l and $[N^*]_o$ are related to the physical properties of the system, such as the protein size, R_p, by the scaling relations in Eqs.(5.25) and (28), and $[c_p]$ and K_p are experimentally measureable quantities.

In Chapter 8, we compare the form of the protein partition coefficient predicted by Eq.(5.32) to that observed for the partitioning of the hydrophobic protein intermediate, carbonic anhydrase (Cleland and Wang, 1991).

5.8 Strong Attractive Interactions ($n_s\varepsilon \gg 1$) with Large Proteins ($R_p \gg \xi_b$)

When the protein is much larger than the polymer mesh size, as depicted in Figure 3.7(d), the protein surface behaves as a macroscopic body with an area for adsorption which is defined by the protein surface area. This scenario has been studied in detail by a number of theoretical methods, including the use of scaling techniques . In view of the rather detailed and exhaustive prior treatments, and absence of any directly relevant protein partitioning data, we simply refer the reader to the following selection of papers on the topic of polymer adsorption at macroscopic surfaces (de Gennes, 1976; Scheutjens and Fleer, 1979 and 1980; de Gennes, 1981; Cohen-Stuart et al., 1986; Bouchaud and Daoud, 1987; Fleer et al., 1988; Douglas, 1989; Auvray and Cotton, 1987; de Gennes, 1987).

5.9 Conclusions

In two-phase aqueous polymer systems containing high molecular weight polymers, the coexisting solution phases contain entangled webs of polymer, within which the identities of the individual polymer coils are lost. In such two-phase aqueous polymer systems, the partitioning of proteins is insensitive to the molecular weight of the polymers but is sensitive to their concentration. The physical nature of the interactions of globular proteins and entangled polymer solutions depends on the relative sizes of the polymer solution net, ξ_b, and the protein dimensions, R_p, in addition to the strength of energetic interactions between the protein and the polymer, ε (per polymer segment at the protein surface). For the various scenarios, scaling-thermodynamic theories were developed to predict the form of protein chemical potential in entangled polymer solutions. Through a thermodynamic framework, the thermodynamic properties of the solution are related to the experimentally measureable protein partition coefficient. Rather different protein partitioning behaviors were predicted for the different physical scenarios developed in Chapter 3. In order to eliminate the ambiguity associated with interpreting the partitioning of proteins in *two-phase* aqueous polymer systems, where the concentrations of the phase-forming polymers are coupled through the polymer solution equilibrium, the partitioning of proteins across a semipermeable membrane is considered. In Chapter 8, the scaling predictions for the protein partitioning behavior are compared to experimental measurements using a diffusion cell.

5.10 Literature Cited

Abbott, N.L.; Blankschtein, D.; Hatton, T.A. *Macromolecules* **1991a**, 24, 4334.

Abbott, N.L.; Blankschtein, D.; Hatton, T.A. *Macromolecules* **1991b**, submitted.

Abbott, N.L.; Blankschtein, D.; Hatton, T.A. *Macromolecules*, **1991c**, submitted.

Albertsson, P.A. *Partition of Cell Particles and Macromolecules*; Wiley, New York, **1985**.

Albertsson, P.A.; Cajarville, A.; Brooks, D.E.; Tjerneld, F. *Biochim. Biophys. Acta*, **1987**, 926, 87.

Albertsson, P.-A.; Cajarville, A.; Brooks, D.E.; Tjerneld, F. *Biochim. Biophys. Acta*, **1987**, 926, 87.

Alexander, S., *J. Physique*, **1977**, 38, 977.

Auvray, L.; Cotton, J.P., **1987**, 20, 202.

Bamberger, S.; Seaman, G.V.F.; Brown, J.A.; Brooks, D.E., *J. Colloid Interface Sci.*, **1984**, 99, 187.

Bouchaud, E.; Daoud, M., *J. Physique*, **1987**, 48, 1991.

Brooks, D.E.; Sharp, K.; Bamberger, S.; Tamblyn, C.H.; Seaman, G.V.F.; Walter, H., *J. Colloid Interface Sci.*, **1984**, 102, 1.

Brown, W.; Rymden, R., *Macromolecules*, **1986**, 19, 2942.

Cabane, B.; Duplessix, R. *J. Physique* **1987**, 48, 651.(26)

Cabane, B., *J. Phys. Chem.*, **1977**, 81, 1639.

Cabane, B.; Duplessix, R. *J. Phys.*, **1982**, 43, 1529.

Cleland, J.L.; Wang, D.I.C., PhD Thesis, Massachusetts Institute of Technology, **1991**.

Cohen-Stuart, M.A.; Cosgrove, T.; Vincent, B., *Adv. Colloid Interface Sci.*, **1986**, 24, 143.

de Gennes, P.-G. *Scaling Concepts in Polymer Physics*; Cornell University Press, Ithaca

and London, **1988.**

de Gennes, P.G., *Comptus Rendus Acad. Sci.*, **1979**, 288, 359.

de Gennes, P.G., *J. Physique*, **1976**, 37, 1445.

de Gennes, P.G., *Macromolecules*, **1981**, 14, 1637.

de Gennes, P.G., *Adv. Colloid Interface Sci.*, **1987**, 27, 189.

Diamond, A.D.; Hsu, J.T., *Biotechnol. Bioeng.*, **1989**, 34, 1000.

Diamond, A.D.; Hsu, J.T., *AIChE J.*, **1990**, 36, 1017.

Douglas, J.F. *Macromolecules*, **1989**, 22, 3707.

Fleer, G.J.; Scheutjens, J.M.H.M.; Cohen-Stuart, M.A., *Colloids and Surfaces*, **1988**, 31, 1.

Flory, P.J. *Principles of Polymer Chemistry*; Cornell University Press: Ithaca N.Y., **1986.**

Huggins, M.L. *J. Phys. Chem.* **1941**, 9, 440.

Hustedt, H.; Kroner, K.H.; Stach, W.; Kula, M.R., *Biotechnol. Bioeng*, **1978**, 20, 1989.

Johansson, G.; *J. Chromatography*, **1985**, 322, 425.

Lin, T.H.; Phillies, G.D.J., *J. Phys. Chem.*, **1982**, 86, 4073.

Lin, T.H.; Phillies, G.D.J., *J. Colloid Interface Sci.*, **1984a**, 100, 82.

Lin, T.H.; Phillies, G.D.J., *Macromolecules.*, **1984b**, 17, 1686.

Marques, C.M.; Joanny, J.F., *J. Phys. France*, **1988**, 49, 1103.

Phillies, G.D.J.; Ullmann, G.S.; Ullmann, K.; Lin, T.H., *J. Chem. Phys.*, **1985**, 82, 5242.

Pincus, P.A.; Sandroff, C.J.; Witten, T.A., *J. Physique*, **1984**, 45, 725.

Sasakawa, S.; Walter, H., *Nature*, **1970**, 223, 329.

Sasakawa, S.; Walter, H., *Biochemistry*, **1972**, 11, 2760.

Scheutjens, J.M.H.M.; Fleer, G.J., *J. Phys. Chem.*, **1979**, 83, 1619.

Scheutjens, J.M.H.M.; Fleer, G.J., *J. Phys. Chem.*, **1980**, 84, 178.

Tanford, C. *Physical Chemistry of Macromolecules*; Wiley: New York, **1961**.

Ullmann, G.S.; Ullmann, K.; Linder, R.M.; Phillies, G.D.J., *J. Phys. Chem.*, **1985**, 89, 692.

Walter, H.; Sasakawa, S.; Albertsson, P.A., *Biochemistry*, **1972**, 11, 3880.

Zaslavsky, B.Y.; Mestechkina, N.M.; Rogozhin, S.V., *J. Chromatography*, **1983**, 260, 329.

Chapter 6.

Proteins in Solutions of Identifiable Polymer Coils. II. Equation-of-State/Monte-Carlo Approach

6.1 Introduction

The important role of the interactions between polymers and proteins in determining the protein partitioning behavior in phase-separated aqueous polymer systems was emphasized in Chapter 4. In particular, the influence of these interactions on the free energy of mixing proteins and polymers was examined in the context of a scaling-thermodynamic formulation. In the course of that work many of the more general issues associated with the evaluation of the free energy of mixing macromolecules were encountered. Specifically, the need to consider the potential coupling of interactions *between* macromolecules and interactions *within* macromolecules was discussed. The purpose of the present chapter is two-fold: (i) to address many of the important and unresolved issues related to the free energy of mixing globular proteins and flexible linear polymers in aqueous solution which were identified in Chapter 4, and (ii) to shed light on the more general problem of the role of deformability and penetrability in evaluating the free energy of colloidal systems, where the deformability of the particles arises from the coupling of intra- and inter colloid interactions.

An important contribution to the free energy of mixing solutions which contain colloids and flexible polymers arises from the translational and configurational degrees of freedom available to these macromolecular species (Tanford, 1961; Flory, 1986; de Gennes, 1988). Specifically, the translational degrees of freedom arise from the many positions that the centers of mass of the species can assume, while the

configurational degrees of freedom reflect the different conformations that the flexible macromolecules can adopt for a fixed position of their centers of mass. In all macromolecular systems, the existence of a variety of interactions, for example, weak attractive interactions of the van der Waals type, or strong repulsive steric (excluded-volume) interactions, restricts the translations and the configurations which can be sampled by the species within the system. While the translations are influenced by the interactions between macromolecules, the nature of these interactions can, in general, also reflect their internal configurational states. It follows, therefore, that the configurations of macromolecules can also reflect, in general, a balance of the interactions *within* and *between* species. However, when there are strong cohesive interactions within macromolecules (and particles) and only weak interactions between species, their configurational states (the shapes) are only weakly perturbed by interparticle interactions. An example of a system where there *is* a clear separation of the intra- and inter-particle interactions is a solution of gold or silica sols where the individual sols are held together by short-ranged, yet very strong "chemical" forces (metallic or covalent bonds, respectively), and only weak van der Waals interactions exist between the sols (Wilcoxen et al., 1989; Lin et al., 1989). In contrast, many other colloidal systems exhibit rather weak interactions within the colloidal particles. In that case, the configurational state of the colloidal particles is greatly influenced by both the interactions within the particles and between particles. An example of such a system is a micellar solution containing aggregates of surfactant molecules (micelles) (Israelachvili et al., 1976; Puvvada and Blankschtein, 1990; Chenalier and Zemb, 1990). In this case, the "physical" forces, such as, hydrophobic forces, which are responsible, in part, for the self-assembly of the surfactant molecules into fluid-like and deformable aggregates, are similar in nature and strength to the interactions occurring between micellar aggregates. Indeed, the wide variety of shapes and sizes of micelles that are observed experimentally in surfactant solutions reflects, in general, the delicate nature of the balance between intra- and inter- micellar interactions.

Another class of systems in which the above mentioned considerations are important is aqueous solutions containing globular proteins and flexible linear polymers

(Albertsson, 1986; Walter et al., 1985; Sutherland and Fisher, 1989). Changes in the configurational state of flexible linear polymers in response to variations in solution conditions, such as, polymer concentration, have been documented both experimentally and theoretically (de Gennes, 1988; Cotton et al., 1972; Farnoux et al., 1975; Daoud et al., 1975). For example, the average radius of gyration of a polymer coil within an entangled polymer network decreases with increasing polymer concentration (Cotton et al., 1972; Farnoux et al., 1975; Daoud et al., 1975). Indeed, under certain conditions, a concentration dependent collapse of the chain to a globular state is observed (Momii et al., 1991). Similarly, proteins are delicately folded linear polypeptide chains having average conformations which generally reflect a balance between the "physical" and "chemical" forces acting within the polypeptide chain, as well as the interactions occurring between the polypeptide chain and its surrounding environment (Dill and Alonso, 1988). For example, upon addition of anionic surfactant molecules, such as, sodium dodecyl sulphate, or other denaturants, such as urea, to an aqueous protein solution, a protein will typically undergo a gross conformational change from a highly structured and compact globular state to a more expanded and tenuous random-coil conformation (Tanner et al., 1982; Guo et al., 1990).

For the sake of brevity, the reader is referred to two recent reviews of previous theoretical work dealing with protein partitioning in two-phase aqueous polymer systems (Baskir et al., 1989; Abbott et al., 1990). Below we summarize only the essential points needed for the theoretical developments presented in this chapter.

As was discussed in Chapter 4, in the poly(ethylene oxide) (PEO)-dextran-water two-phase system, a transition occurs in the nature of the top PEO-rich phase, from a solution of identifiable polymer coils to a solution of extensively interpenetrating polymers, with increasing PEO molecular weight (Abbott et al., 1991). Solutions of the former type, that is, "dilute" polymer solutions, consist of singly dispersed polymer coils separated from each other, on average, by domains of pure solvent (Tanford, 1961; Flory, 1986; de Gennes, 1988). In contrast, the solutions of high molecular weight PEO contain polymer coils which overlap extensively and entangle to form a transient polymer mesh (Tanford, 1961; Flory, 1986; de Gennes, 1988). Within this mesh, in contrast to

the "dilute" polymer regime, the identities of the individual polymer coils are lost and properties of the solution, such as the osmotic pressure, become independent of polymer molecular weight. Interestingly, in the two-phase aqueous PEO-dextran system, the transition in the underlying structure of the PEO-rich solution phase, bought about by an increase in PEO molecular weight, was accompanied by large changes in the partitioning behavior of a variety of globular proteins. Specifically, the protein partition coefficient, defined as the ratio of the protein concentrations in the top and bottom phases, respectively, was observed in experiments (Hustedt et al., 1978; Albertsson et al., 1987) to decrease with an increase in the molecular weight of PEO in the system. However, for sufficiently high molecular weights of PEO, where the PEO was extensively entangled, the protein partition coefficient was observed to be independent of the PEO molecular weight, reflecting the fact that the protein "lost sight" of the PEO coils within the entangled polymer mesh (Abbott et al., 1991a). Furthermore, it was observed that the ability of a protein to sense the transition in the underlying solution structure correlated with the size of the protein species. That is, large proteins, for example, catalase, exhibited large changes in their partition coefficients, whereas small proteins, such as cytochrome-c, were insensitive to changes in the structure of the solution (Abbott et al., 1991a). For the purpose of the present chapter we confine our treatment to polymer solutions in the "dilute" regime, since it is in this regime that one observes the greatest sensitivity of the protein partition coefficient to changes in the PEO molecular weight (Abbott et al., 1991a). In Chapters 5 and 8, we discuss the rather different situation of proteins interacting with entangled polymer solutions (Abbott et al., 1991b).

In a typical PEO-rich solution phase which contains low molecular weight PEO ($M < 10\ 000$ Da), the individual polymer coils which interact with the protein may be larger or smaller than protein molecules (Abbott et al., 1991a). It is important to point out that this situation is in sharp contrast with the extensively-studied case where a colloid, for example, a silica sol, interacts *sterically* with a flexible polymer that is significantly smaller in size than the sol (Vrij, 1976; de Hek and Vrij, 1981; Vincent et al., 1979; Patel and Russel et al., 1989a and b; Dey and Hirtzel, 1991). In that case, the polymer coil and sol are essentially impenetrable to each other, so that, in effect, one

can represent the steric interaction potential between the two particles as a simple hard-sphere repulsion (Vrij, 1976; de Hek and Vrij, 1981; Vincent et al., 1979, Patel and Russel, 1989a and b; Dey and Hirtzel, 1991). The range of this steric repulsion is given by the sum of the globular colloid radius and the polymer radius of gyration, R_g (Vrij, 1976; de Hek and Vrij, 1981; Vincent et al., 1979; Patel and Russel, 1989a and b; Dey and Hirtzel, 1991). In contrast, in the protein partitioning case, where the polymer-coil size can become large compared to the size of the globular protein, the polymer coil can no longer be represented effectively as an impenetrable sphere of size R_g since an increased number of polymer-coil configurations allows the protein to penetrate the volume occupied, on average, by the polymer (Abbott et al., 1991a). In order to model this interesting situation, and at the same time be able to exploit some of the available useful results for hard-sphere systems, we have chosen to generalize the conventional treatment of excluded-volume hard-sphere interactions. Specifically, we have represented the polymer coil as an effective hard-sphere whose size reflects the permeability of the polymer coil towards the protein. In other words, due to the penetrable and diffuse nature of the polymers, one expects that as the polymer molecular weight increases, the *effective hard-sphere size* associated with the polymer should increase more slowly than that corresponding to a rigid impermeable particle. It is this new physical situation, dealing with excluded-volume interactions between particles possessing different degrees of penetrability, which does not appear to have received much attention in the past, but which is essential to the treatment of protein partitioning in two-phase aqueous polymer systems, that we address in this chapter. Indeed, in Section 6.6 we show that if the penetrability of the polymer coil to the protein is neglected, within the framework of our theoretical development, *qualitatively* different trends in the protein partition coefficient are predicted.

In Chapter 4 it was shown that under certain experimental conditions (Abbott et al., 1991a), the change in the logarithm of the protein partition coefficient, $\Delta \ln K_p$, accompanying a change in PEO molecular weight, can be related simply to the standard-state chemical potential of the protein, $\Delta \mu^{\circ}_{p,t}$, in the top (t) PEO-rich polymer solution phase, that is,

$$\Delta \ln K_p = - \frac{\Delta \mu^o_{p,t}}{kT} , \qquad (6.1)$$

where k is the Boltzmann constant, and T is the absolute temperature. The standard-state chemical potential of the protein in the top phase corresponds to the free-energy change upon introducing a single protein molecule into the top polymer solution phase from a phase containing pure solvent. Therefore, this term captures the effects of the direct interactions of the protein with the polymers, as well as the influence of polymer-polymer interactions on the protein. Note that protein-protein interactions are not considered because in the limit of vanishing protein concentration, corresponding to the experimental conditions (Hustedt et al., 1978; Albertsson et al., 1987), they make a negligible contribution to the observed partitioning behavior. Mathematically-simple geometric and scaling arguments were developed to probe the *qualitative* form of the standard-state protein chemical potential, and thus the protein partition coefficient, arising from protein-polymer and polymer-polymer interactions (Abbott et al., 1991a). A rather interesting picture emerged which suggested that change in the partition coefficients of proteins, which is observed to accompany a change in the PEO molecular weight, reflects a delicate balance of several competing factors. These factors can be readily understood with reference to the following equation (Abbott et al., 1991a),

$$\Delta \ln K_p = - \frac{\Delta \mu^o_{p,t}}{kT} = - \Delta \left[\frac{N_2 U_p}{V} \left(1 + \frac{N_2 U_2}{2V} + O\left[\left(\frac{N_2 U_2}{V} \right)^2 \right] \right) + \frac{k_1 \varepsilon a R_p^2}{N^{3/5}} \right] \qquad (6.2)$$

where N_2/V is the number density of polymer coils in solution, U_p is the excluded volume characterizing the steric interactions between a protein and a polymer coil, U_2 is the polymer-polymer effective excluded volume, ε is the local energy change (measured in units of kT) that accompanies the replacement of solvent at the protein surface by one polymer segment, N is the number of polymer segments per coil (which

is proportional to the polymer molecular weight, M_2), a is the size of a polymer segment, R_p is the radius of the protein, and k^i is an order unity numerical constant. The first term in Eq.(6.2), N_2U_p/V, describes the influence of steric interactions between proteins and polymers on $\Delta \ln K_p$, and results from a competition between the number density of polymer coils in the solution, N_2/V, (which decreases with increasing PEO molecular weight, M_2, at a constant weight fraction of PEO; $N_2/V \sim 1/M_2$) and the magnitude of the repulsive steric interaction between a protein and a polymer coil, U_p (which increases with the molecular weight of the PEO; the functional dependence of U_p on the PEO molecular weight is $U_p \sim M_2^{\alpha}$, where α is dependent on the relative size of the protein and PEO coil). It turns out, that with increasing molecular weight of PEO, due to the increasing permeability of the polymer coils to the proteins, the exponent α is constrained to the range, $0 < \alpha < 1$. Specifically, in the limit when the polymer coil is much larger than the protein, $\alpha \rightarrow 1$, which reflects the ability of the protein to readily penetrate the volume occupied on average by the polymer coil, and interact with the entire *length* of the polymer chain within the coil. By combining the predicted influence of a change in PEO molecular weight on both U_p and N_2/V, it is evident that the term $U_pN_2/V \sim M_2^{\alpha-1}$ decreases with increasing PEO molecular weight, M_2. That is, with reference to Eq.(6.2), the effect of this term on the predicted protein partitioning behavior is *opposite* to the trend observed experimentally.

In Eq.(6.2), the bracketed expansion in terms of N_2U_2/V, describes the influence of polymer-polymer interactions on the standard-state chemical potential of the proteins. Physically, this influence on the standard-state protein chemical potential can be understood, to first order in N_2U_2/V, by considering the competing influences of a change in the PEO molecular weight on the number density of polymer coils in solution, N_2/V, and the polymer-polymer excluded volume, U_2. As discussed above, at a constant weight fraction of PEO within the PEO-rich polymer solution phase, $N_2/V \sim 1/M_2$. However, in contrast to the protein-polymer excluded volume, U_p, the functional dependence of the polymer-polymer excluded-volume on PEO molecular weight is $U_2 \sim M_2^{\alpha}$, where $\alpha \simeq 9/5$. The reason for the rather different form of the polymer-polymer excluded-volume, as compared to the protein-polymer excluded-volume, is that

in the former case, the *two* polymer coils are of equal size at all molecular weights of PEO, and therefore, the exponent $\alpha \simeq 9/5$ is only weakly molecular weight dependent. Combining the influence of a change in PEO molecular weight on both N_2/V and U_2, the predicted functional dependence is $N_2U_2/V \sim M_2^{\alpha-1}$, which increases with the molecular weight of PEO. Therefore, the influence of the polymer-polymer interactions is to increase the standard-state protein chemical potential in a manner which is consistent with the experimentally observed influence of a change in PEO molecular weight on the protein partition coefficient (Abbott et al., 1991a). However, within the framework of the scaling-thermodynamic approach presented in Chapter 4, due to (i) the truncation of the expansion in Eq.(6.2) at second order in the expansion parameter, N_2U_2/V, (ii) the unknown values of the polymer-polymer excluded-volume, U_2, and (iii) the additional influence of polymer-polymer excluded-volume effects (within a polymer coil) on the magnitude of the protein-polymer excluded-volume, U_p, it became evident that in order to evaluate the precise influence of the protein-polymer and polymer-polymer interactions on the predicted protein partitioning behavior, a more quantitative approach was required. Nevertheless, from a consideration of the first two terms in Eq.(6.2), it is apparent that the predicted influence of an increase in PEO molecular weight results from a delicate balance reflecting the opposing influences of the protein-polymer and polymer-polymer interactions on the standard-state protein chemical potential.

In view of the possibility that steric effects alone could not predict the observed protein partitioning behavior, the last term in Eq.(6.2) was introduced to examine the influence of a weak attractive interaction between the protein molecules and the PEO coils on the standard-state chemical potential of the protein. For the sake of brevity the reader is referred to Chapter 4, where a detailed discussion of this term is presented and the possible physical origins of the attraction are discussed. However, it is pertinent to mention that while the attractive interaction between a PEO coil and protein molecule was shown to increase with increasing PEO molecular weight, when the opposing influence of the decreasing number density of polymer coils was included, N_2/V, an increase in the standard-state protein chemical potential was predicted. It is noteworthy that this trend in the standard-state protein chemical potential is consistent

with that observed experimentally (Hustedt et al., 1978; Albertsson et al., 1987). Although the realization that weak attractive interactions between PEO coils and certain proteins may be important in determining the protein partitioning behavior, in order to estimate the strength of the attraction required to account for the observed partitioning behavior, the *additive* effects of steric and attractive interactions on the protein chemical potential, that is, all three terms of Eq.(6.2), must be included. As discussed above, due to approximations present within Eq.(6.2), such a *quantitative* prediction was beyond the scope of Chapter 4. There, the aim was not to provide a detailed quantitative account of the protein partitioning problem but rather establish a sound physical description of these systems which can be used as a basis for more detailed theoretical formulations. In this spirit, using Chapter 4 as the foundation, here we present a more quantitative account of protein partitioning in two-phase aqueous polymer systems.

Each of the issues outlined above is addressed and, in particular, we develop a quantitative account of protein-polymer and polymer-polymer interactions, including the relative importance of their contributions to the standard-state protein chemical potential. We reveal that very weak attractive interactions can have a marked effect on the *qualitative nature* of the predicted protein partitioning behavior. In these evaluations, by combining liquid-state (McQuarrie, 1976; Carnahan and Starling, 1969; Carnahan and Starling, 1970) and dilute polymer solutions theories (Flory and Krigbaum, 1950; Zimm et al., 1953; Orofino and Flory, 1957), along with a simple Monte-Carlo evaluation (Wall and Mandel, 1975; Hermans, 1982; Hermans and Hermans, 1984), we include (1) the influence of the deformability and permeability of the polymer coils on their interactions with globular proteins, (2) the partial permeability of polymer coils to each other (which varies with the solvent quality), and (3) the contributions of higher-order interactions between polymer coils and proteins. In addition, we investigate the influence of the protein shape on the partitioning behavior of proteins. Specifically, we evaluate the influence of deviations from sphericity (ellipsoidal shape) on the predicted standard-state protein chemical potential.

The remainder of the chapter is organized as follows. In Section 6.2, a general thermodynamic framework that relates thermodynamic quantities at constant

solvent chemical potential to those at constant pressure is developed. Within this framework, using an equation of state for a binary-hard sphere mixture, the chemical potentials of the hard spheres are evaluated. In Section 6.3, the components of the hard-sphere mixture are identified with the protein and polymers, and the effective hard-sphere interaction potentials describing steric protein-polymer and polymer-polymer interactions are evaluated. Subsequently, in Section 6.4, within the thermodynamic framework at constant pressure, the protein chemical potential in solutions containing flexible linear polymer molecules is evaluated. The dependence of the standard-state protein chemical potential on polymer molecular weight, as well as on protein shape and size is also reported. In Section 6.5, the additional effect of weak attractive protein-polymer interactions on the protein chemical potential is evaluated. In Section 6.6, we discuss our findings and compare our predictions with earlier thermodynamic formulations for protein partitioning in two-phase aqueous polymer systems.

6.2 Thermodynamic Framework

As discussed in Chapter 4, under judiciously chosen experimental conditions, the change in the protein partition coefficient with PEO molecular weight, can be simply related to the standard-state chemical potential of the protein (see Eq.(6.1)) (Abbott et al., 1991a). Since the system pressure is held constant in the experimental measurement of the protein partition coefficients, we present here an evaluation of the chemical potentials of the protein and PEO in an ensemble at constant pressure. For the evaluation of the thermodynamic properties of solutions containing solvent, salts, polymers and proteins we treat the species as incompressible, and approximate the solvent in the presence of salts as a structureless continuum (the approximation made in treating the solvent as a continuum is justified by the large size of the proteins and polymers as compared to that of the solvent molecules). The present treatment contrasts with that presented in Chapter 4, where a simplifying approximation was made, and the protein chemical potential was evaluated holding constant the solvent chemical potential (Abbott et al., 1991a). A comparison of the predicted standard-state protein chemical

potential at constant pressure, P, with that at constant solvent chemical potential, μ_1, is presented and further discussed in Section 6.6.

In Appendix 6.A, a derivation is given of a general thermodynamic framework relating the chemical potential of species i in an incompressible solvent at constant pressure, to that at constant solvent chemical potential. This development is particularly useful because it enables us to make use of some existing analytical results for the chemical potentials of hard-sphere mixtures which were derived at constant solvent chemical potential (Jansen et al., 1986a). It is noteworthy that in the protein partitioning case, the evaluation of the protein and polymer chemical potentials is simplified considerably by the fact that we are concerned with the limit of vanishing protein concentration, namely, $\phi_p \to 0$ (Abbott et al., 1991a). In this limit, with the understanding that the polymer chemical potential, μ_2, becomes independent of protein concentration, it is shown in Appendix 6.A that the following condition must be satisfied

$$\left[\frac{\partial \mu_p}{\partial \phi_2}\right]_{T,P,\phi_p} = (1 - \phi_2)\left[\frac{\partial \mu_p}{\partial \phi_2}\right]_{T,\mu_1,\phi_p} \qquad \textbf{(6.3)}$$

Equation (6.3) is a central result that is used to evaluate changes in the protein chemical potential at constant pressure from changes in the protein chemical potential occurring at constant solvent chemical potential. The latter quantity has been previously evaluated for hard-sphere systems (Jansen et al. 1986a).

We present an evaluation of the protein chemical potential at constant pressure using a description of the system in terms of effective hard-sphere sizes. This approximate representation of the system is justified in view of the following considerations. First, it is emphasized that we account for the deformability and penetrability of the polymer coils (both for polymer-polymer and for polymer-protein interactions) through the careful choice of the effective hard-sphere sizes of both polymers and proteins (see Section 6.3). Second, we realize that, in general, equations of state for simple hard-sphere systems will not be sufficient to describe complex

systems, such as protein-polymer mixtures. This is due to the fact that different effective hard-sphere sizes will be required to describe the polymer hard-sphere size associated with polymer-polymer interactions and that associated with polymer-protein interactions. That is, such mixtures belong to the class of so-called non-additive hard-sphere systems (Flory, 1968). However, because our aim is to describe the standard-state chemical potential of the protein in the limit of vanishing protein concentration, which is the relevant limit for the protein partitioning behavior considered here, it is not neccessary to resort to equations of state for non-additive hard-sphere systems. This follows because one can adjust the effective hard-sphere size of the protein species such that the same polymer effective hard-sphere size can be used both for polymer-polymer and polymer-protein interactions. Although, in general, this approach will not predict correctly the contribution of protein-protein interactions to the protein chemical potential, this contribution is insignificantly small in the limit of vanishing protein concentration considered in this paper. Finally, we emphasize that in our theoretical formulation the effective protein and polymer hard-sphere sizes should not be identified with the actual physical sizes of these species.

With the above considerations in mind, and with the excluded-volume interactions between proteins and polymer coils, as well as between the polymer coils themselves, represented in terms of effective hard-sphere sizes, we have utilized an equation of state for a binary mixture of hard spheres at constant solvent chemical potential, as well as Eq.(6.3), to evaluate the protein chemical potential at constant pressure (Jansen et al., 1986a). Under conditions of constant solvent chemical potential, Jansen and coworkers (1986a) derived the following expression for the chemical potential of component p (the protein, in our case) in a binary hard-sphere mixture of components p and 2 (the polymer in our case)

$$\left[\frac{\mu_p}{kT}\right]_{T,\mu_1} = \left[\frac{\mu_p^o}{kT}\right]_{T,\mu_1} + \ln\left[\frac{\phi_p}{1-\xi_3}\right] + \sigma_p^3\eta_o + 3\sigma_p^2\eta_1 + 3\sigma_p\eta_2 + 3\sigma_p^2\eta_1\eta_2 + \frac{9}{2}\sigma_p^2\eta_2^2 + 3\sigma_p^3\eta_2^3 \qquad \textbf{(6.4)}$$

where the parameters η_k and ξ_k are defined by

$$\eta_k = \frac{\xi_k}{1 - \xi_3} \tag{6.5}$$

and

$$\xi_k = \phi_2 \sigma_2^{k-3} + \phi_p \sigma_p^{k-3} \tag{6.6}$$

where k=0,1,2, and 3, and ϕ_2 and ϕ_p are the volume fractions of the polymer and protein, respectively. In Eq.(6.4), μ_p° is the standard-state chemical potential of the protein at a constant solvent chemical potential, and in Eqs.(6.6) and (6.4), σ_2 and σ_p are the effective hard-sphere diameters of the polymer coils and the protein molecules, respectively. Using Eqs.(6.5) and (6.6) in Eq.(6.4), then substituting the resulting Eq.(6.4) in Eq.(6.3), and finally integrating (in the limit of vanishing protein concentration, $\phi_p \to 0$) from $\phi_2=0$ to ϕ_2, yields the following useful result

$$\begin{aligned}\left[\frac{\mu_p}{kT}\right]_{T,P,\phi_2,\phi_p\to 0} - \left[\frac{\mu_p}{kT}\right]_{T,P,\phi_2\to 0,\phi_p\to 0} &= \frac{9}{2}r_\sigma^3 - \frac{9}{2}r_\sigma^2 \\ + \phi_2\left[1 + \frac{9}{2}r_\sigma^2\right] + \frac{\phi_2^2}{1-\phi_2}\left[3r_\sigma^3 + \frac{9}{2}r_\sigma^2\right] &+ 3\frac{\phi_2^3}{(1-\phi_2)^2}r_\sigma^3 \\ + \ln(1-\phi_2)\left(-4r_\sigma^3 + 6r_\sigma^2 - 3r_\sigma\right) + \frac{1}{(1-\phi_2)}\left[-6r_\sigma^3 + \frac{9}{2}r_\sigma^2\right] &+ \\ \frac{3}{2(1-\phi_2)^2}r_\sigma^3\end{aligned} \tag{6.7}$$

where $r_\sigma = \sigma_p/\sigma_2$. In Eq.(6.7), $\mu_p(T,P,\phi_2,\phi_p\to 0)$ corresponds to the standard-state protein

chemical potential in a polymer solution phase having an effective hard-sphere polymer volume fraction ϕ_2, and $\mu_p(T,P,\phi_2 \rightarrow 0,\phi_p \rightarrow 0)$ corresponds to the standard-state chemical potential of the protein in a polymer-free solvent phase. The difference between these two is equal to $\mu^{\circ}_{p,t}$ in Eq.(6.1) and Chapter 4 (Abbott et al., 1991a).

To utilize Eq.(6.7) in Eq.(6.1), in order to predict the change in the logarithm of the protein partition coefficient, $\Delta \ln K_p$, the two length scales σ_2 and σ_p, need to be evaluated. Recall that σ_2 is the effective hard-sphere diameter of the polymer, which reflects the deformability and penetrability associated with the polymer-polymer excluded-volume interactions, and σ_p is the effective hard-sphere diameter of the protein, which reflects the deformability and penetrability associated with protein-polymer excluded-volume interactions.

6.3 Effective Hard-Sphere Potentials for Steric Interactions

The topic of polymer-polymer interactions in solutions of identifiable polymer coils has received considerable experimental and theoretical attention over the last few decades (Flory and Krigbaum, 1950; Zimm et al., 1953; Orofino and Flory, 1957; Flory, 1968). Our approach utilizes the classical theories of Flory (1968) to calculate the radius of gyration of isolated polymer coils (PEO), and Flory and Krigbaum (1950) to calculate the equivalent hard-sphere diameters corresponding to the effective excluded-volume interactions between two polymer coils. The theoretically calculated polymer-coil radius of gyration (Flory, 1968) is substantiated through a comparison with the radius of gyration of an isolated PEO coil obtained using neutron-scattering and light-scattering measurements (Cabane and Duplessix, 1982). To assess the validity of the characterization of polymer-polymer interactions using an effective hard-sphere potential over the range of polymer concentrations encountered in two-phase aqueous polymer systems. That is, we have compared available vapor-pressure measurements of aqueous PEO solutions (Haynes et al., 1989) with predicted vapor-pressure values based on the use of the theoretically-calculated effective polymer hard-sphere diameters.

The classical theory of Flory (1968) yields the following expression for the

polymer-coil radius of gyration

$$R_g = \alpha \left[\frac{c_\infty l^2 n}{6} \right]^{1/2} \tag{6.8}$$

where c_∞ is the characteristic ratio of the PEO chain (see below), l^2 is the mean-square length of each bond comprising the repeat units of PEO, n is the number of bonds per polymer coil, and α is the Flory expansion parameter. In Eq.(6.8), the characteristic ratio describes the intrinsic stiffness of the polymer chain, which arises from the fact that neighboring bonds along the polymer chain are correlated in their orientations due to restrictions on the bond angles between them. The characteristic ratio of the PEO chain can be defined at the Θ-solvent conditions for the polymer, namely (Flory, 1968)

$$c_\infty = \frac{<r^2>_o}{nl^2} = 4.1 \pm 0.4 \ , \tag{6.9}$$

where $<r^2>_o$ is the mean square end-to-end length of the polymer coil at Θ-solvent conditions. The literature value of the characteristic ratio reported in Eq.(6.9) was determined from viscosity measurements in aqueous salt solutions at 35°C (Flory, 1968). The Flory expansion parameter, α in Eq.(6.8), describes the swelling of the polymer coil due to the repulsive excluded-volume interactions which occur between the polymer-coil segments, and can be evaluated from (Flory, 1968)

$$\alpha^5 - \alpha^3 = \frac{27 v_{sp}^2 M_o^{3/2} (1-2\chi) M_2^{1/2}}{2(2\pi)^{3/2} c_\infty^{3/2} l^3 v_1^o N_A} \tag{6.10}$$

where v_{sp} is the specific volume of the polymer, M_o is the molecular weight of a polymer bond, M_2 is the molecular weight of the polymer coil, v_1^o is the molar volume of the solvent, χ is the Flory-Huggins interaction parameter, and N_A is Avogadro's Number. Inspection of Eq.(6.10) shows that the strength of the excluded-volume interactions

between polymer coils is mediated by the solvent quality, as characterized by the term, $1-2\chi$. Under the conditions of sufficiently high polymer molecular weight, M_2, and sufficiently good solvent quality ($\chi < 0.5$), the polymer coil will be extensively swollen, that is, $\alpha \gg 1$, and Eq.(6.10) predicts that $\alpha \sim M_2^{1/10}$. Substituting this result into Eq.(6.8) yields the well-known result (Flory, 1986; de Gennes, 1988), $R_g \sim M_2^{3/5}$ (note that for PEO, $3n = M_2/44$). Using Eqs.(6.9) and (6.10) with the following literature values for the physical parameters which characterize PEO in water at 25°C, $\chi = 0.45$ (Edmond and Ogston, 1968; Rogers and Tam, 1977), $l = 1.46$ Å (Flory, 1968), $M_o = 44/3$ g/mole, $v_1^o = 18$ cm^3/mole and $v_{sp} = 0.83$ cm^3/g (Cabane and Duplessix, 1987), in Eq.(6.8), the radius of gyration of PEO was calculated as a function of PEO molecular weight. In Table 6.1, the theoretically predicted PEO radius of gyration, R_g, is compared as a function of PEO molecular weight to the radius of gyration data extrapolated from neutron scattering and light scattering measurements for PEO in water (Cabane and Duplessix, 1982). As can be seen, a good agreement exists between the theoretical and experimental values of the polymer radius of gyration.

The Flory-Krigbaum theory (1950) estimates the *effective volume* excluded by one polymer coil to another, which reflects, in essence, two competing contributions. The first arises from the *actual physical* exclusion of one polymer coil by another, such that two polymer-coil segments cannot occupy the same physical space. The second has an enthalpic origin and reflects energetic interactions (mediated by the solvent) between the polymer-coil segments. In particular, an enthalpic contribution arising from attractive energetic interactions between the polymer coils will tend to reduce the effective volume excluded by one polymer coil to another, and at the so-called Θ-solvent condition, the net excluded volume is zero (Flory, 1968). The general expression for the excluded volume, U_2, is given by

$$U_2 = \frac{v_{sp}^2 M_2^2}{v_1^o N_A}(1 - 2\chi)\left[1 - \frac{X}{2!2^{3/2}} + \frac{X^2}{3!3^{3/2}} - \ldots\right] \qquad \textbf{(6.11)}$$

where the expansion parameter X is defined by

M_2 (Da)	Predicted R_g (Å)	Measured R_g (Å)	R_{22}^{HS} (Å)
3 000	20.4	18.9	11.4
4 000	23.9	22.6	13.8
5 000	27.1	26.0	16.0
6 000	29.9	29.1	18.0
7 000	32.6	32.0	19.9
8 000	35.1	34.7	21.7
9 000	37.5	37.4	23.5
10 000	39.8	39.9	25.1

Table 6.1. Comparison of the predicted PEO radius of gyration, R_g, and measured R_g from neutron and light scattering measurements (Cabane and Duplessix, 1982), as a function of PEO molecular weight, M_2. Also presented are the predicted effective hard-sphere radius of PEO, R_{22}^{HS} as a function of PEO molecular weight, M_2.

$$X = 2(\alpha^2 - 1) \tag{6.12}$$

At Θ-solvent conditions for the polymer, $\chi=0.5$, $\alpha=1$, and, as is evident from Eqs.(6.11) and (12), both $U_2=0$ and $X=0$. The effective hard-sphere radius of a polymer coil characterizing polymer-polymer interactions, R_{22}^{HS}, is calculated by equating the expression for the excluded volume, U_2, in Eq.(6.11) with the following well-known expression (Tanford, 1961) for the excluded volume between two hard spheres,

$$U_2 = \frac{32\pi(R_{22}^{HS})^3}{3} \tag{6.13}$$

The predicted R_{22}^{HS} values as a function of PEO molecular weight, M_2, are also presented in Table 6.1. Owing to the possible effect of polymer-polymer interactions on the average configuration of the polymer coils (Cotton et al., 1972; Farnoux et al., 1975; Daoud et al., 1975), one can, in general, expect the effective hard-sphere polymer radius to exhibit a concentration dependence as the polymer concentration increases. As this aspect of the polymer-coil behavior was not incorporated in our description of the effective polymer-coil hard-sphere radius, a comparison between the measured vapor pressure of PEO in water (Haynes et al., 1989) and a theoretical prediction, which explicitly incorporates the effective hard-sphere radius of the polymer, was made to assess the range of validity of our approximate treatment in terms of concentration-independent R_{22}^{HS}.

To compute the vapor pressure of an aqueous solution of PEO, we have used the following well-known result (Modell and Reid, 1983)

$$a_1 = \frac{P_1}{P_1^o} \tag{6.14}$$

where a_1 is the solvent activity, P_1° is the vapor pressure of pure water, and P_1 is the vapor pressure of an aqueous PEO solution. The activity of the solvent is related to the

osmotic pressure of the aqueous PEO solution by (Modell and Reid, 1983)

$$RT \ln a_1 = -v_1^o \Pi \tag{6.15}$$

where v_1° is the partial molar volume of the solvent, and Π is the solution osmotic pressure. We have evaluated the osmotic pressure of the polymer solution using the Carnahan-Starling equation of state for a monodisperse hard-sphere system (Carnahan and Starling, 1969 and 1970). This description of the polymer solution in terms of effective hard-sphere sizes, is consistemt with our previous description of the polymer-polymer interactions used to evaluate the protein chemical potential in a polymer solution. Accordingly, the osmotic pressure of the PEO solution can be calculated as (Carnahan and Starling, 1969 and 1970)

$$\frac{\Pi}{kT} = \frac{N_2}{V} \frac{(1 + \phi_2 + \phi_2^2)}{(1 - \phi_2)^3} \tag{6.16}$$

where N_2/V is the number density of PEO coils in the solution, and ϕ_2 is the effective hard-sphere volume fraction occupied by the polymer coils in solution ($\phi_2 = 4\pi N_2 (R_{22}^{HS})^3/3V$). Substituting Eqs.(6.15) and (6.16) into Eq.(6.14) leads to the desired result which relates the vapor-pressure depression to the effective hard-sphere volume fraction of PEO in solution, that is,

$$\frac{P_1}{P_1^o} = \exp\left[\frac{-v_1^o N_2 (1 + \phi_2 + \phi_2^2)}{V (1 - \phi_2)^3}\right] \tag{6.17}$$

In evaluating the vapor-pressure depression predicted by Eq.(6.17), and subsequently comparing it with the experimental measurements reported by Haynes and coworkers (1989), one must consider the influence of polymer-size polydispersity in the polymer samples used in the experiments. Specifically, the PEO samples used in the vapor-pressure measurements (Haynes et al., 1989) had number-average molecular

weights of 3 790 Da and 9 037 Da, and weight-average molecular weights of 3 860 Da and 11 800 Da, respectively. Since the osmotic pressure of a polydisperse system reflects the number-average properties (Modell and Reid, 1983), in computing the effective hard-sphere radius of the polymer coils the number-average molecular weights were used. From Table 6.1, an interpolation of the appropriate molecular weights to 3 790 Da and 9 037 Da yields effective PEO hard-sphere radii (R_{22}^{HS}) of 13.5Å and 23.5Å, respectively. In Figure 6.1, the predicted vapor-pressure depression of the aqueous PEO solutions, is compared to experimental measurements. For the PEO sample corresponding to a number-average molecular weight of 3 790 Da, the reasonable agreement between the calculated (solid line) and experimental (●) vapor pressures of the PEO solutions shown in Figure 6.1 suggests that the essential nature of the polymer-polymer interactions has been captured effectively. Unfortunately scatter in the experimental data points prevents a more precise comparison between the theoretical prediction and experimental measurements of the vapor-pressure depression. However, the general agreement suggests that such a description of the polymer-polymer interactions will provide a reasonable estimation for their contribution to the protein standard-state chemical potential and associated protein partition coefficient. For the larger PEO having a molecular weight of 9 037 Da, the comparison of theory (dotted line) and experiment (■), shown in Figure 6.1, indicates that a significant difference exists beyond PEO weight fractions of approximately 0.1. This difference may reflect a transition in the underlying structure of the PEO solution, from one composed of singly dispersed polymer coils to one characterized by an entangled polymer coils, that can occur with either increasing PEO weight fraction or molecular weight (de Gennes, 1988). Significantly, and as reported (Abbott et al., 1991a) in Chapter 4, aqueous solutions of PEO having a molecular weight of approximately 10 000 Da will undergo such a transition in the vicinity of PEO weight fraction of approximately 0.1. With this in mind, it is very reasonable that our description of the 9 037 Da PEO solution as one composed of separate polymer coils becomes inappropriate above PEO weight fractions of around 0.1. PEO of molecular weight 3 790 Da undergoes a similar transition in the nature, but at a significantly higher PEO weight fraction of approximately 0.2 (or more).

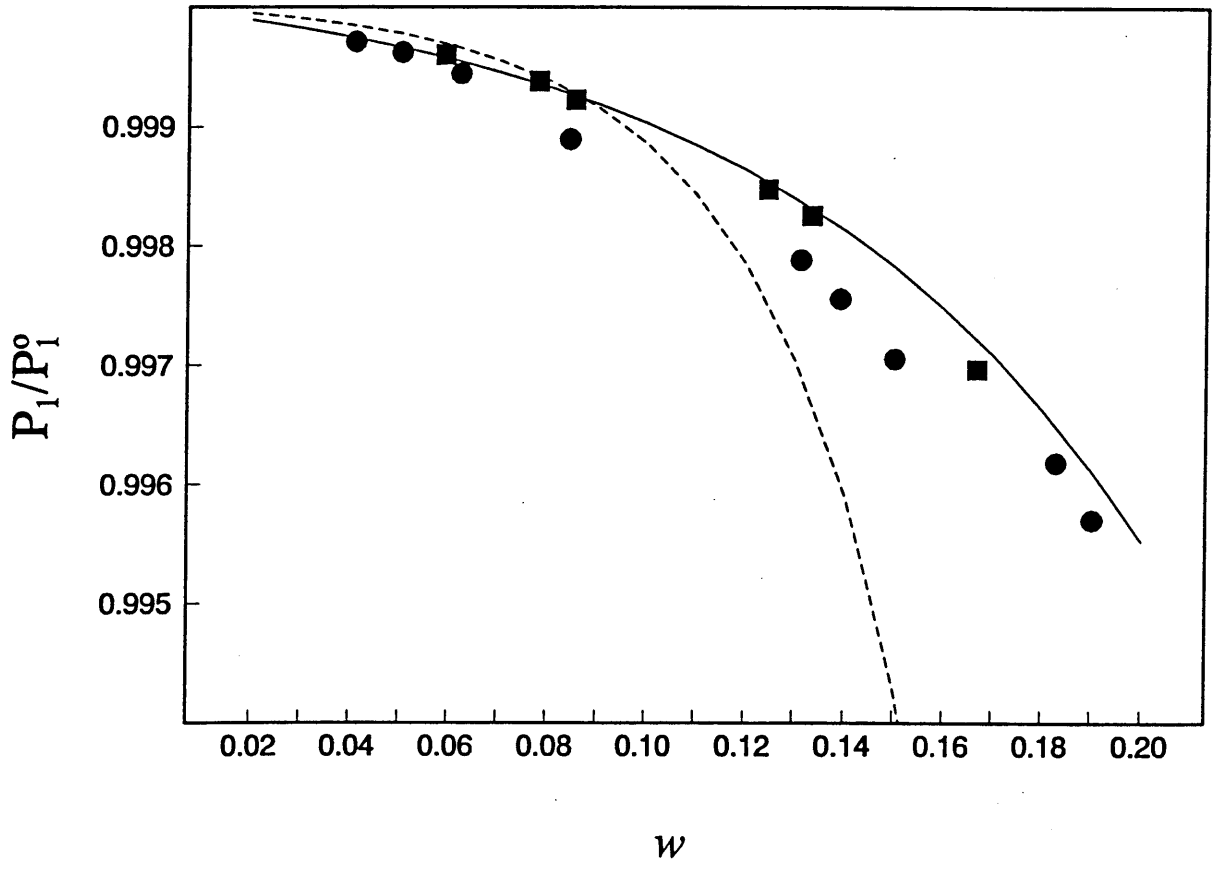

Figure 6.1. Comparison of predicted and experimental vapor-pressure depression, P_1/P_1^o, of aqueous PEO solutions as a function of PEO weight fraction, w: 3 790 Da (solid line), (●); 9 037 Da (dotted line), (■).

In summary, over the range of solution conditions consistent with the description of the aqueous PEO solution as one containing singly-dispersed polymer species, the agreement between the theoretical predictions and the experimental vapor-pressure measurements is very reasonable. This suggests that the contribution of polymer-polymer interactions to the protein chemical potential is described adequately. It is noteworthy that this conclusion is supported by neutron scattering measurements which will be reported in Chapter 7 (Abbott et al., 1991c).

The second important type of interaction that must be characterized in order to predict the protein chemical potential in aqueous PEO solutions is the direct polymer-protein interaction. First, we consider excluded-volume interactions occuring between the protein and the polymer, and subsequently, in Section 5, we consider the influence of other interactions (attractions). The steric interaction in this case is rather more interesting than the polymer-polymer one described earlier, since it involves two unlike species: a rather flexible, deformable and penetrable polymer coil, and a relatively impenetrable, globular and structured protein molecule. At Θ-solvent conditions for the polymer, where the configurations of a polymer chain can be described in analogy with Brownian motion, the solution of the diffusion equation yields the following analytical expression for the excluded volume arising from the interaction of a flexible chain and an impenetrable sphere (Jansons and Phillips, 1990)

$$U_p = 4\pi R_p R_g^2 + 8(\pi)^{1/2} R_p^2 R_g + \frac{4\pi R_p^3}{3} \qquad \textbf{(6.18)}$$

Equation (6.18) is not strictly applicable in the case of PEO in water, where solvent conditions at 25°C are better than Θ-solvent conditions (Cabane and Duplessix, 1982; Edmond and Ogston, 1968; Rogers and Tam, 1977; Cabane and Duplessix, 1987), since additional correlations between polymer segments will influence the nature of the excluded-volume interaction between the entire polymer coil and the protein. However, consideration of this equation proves illuminating since some qualitative features of the equation are common to the two cases of Θ-solvents and good solvents. In particular,

from an inspection of Eq.(6.18), it can be seen that when the polymer coil is much larger than the protein, that is, $R_g \gg R_p$, the excluded volume scales as $R_p R_g^2$. This contrasts to the opposite limit where $R_p \gg R_g$, and the excluded volume scales with R_p^3. The different functional forms of U_p in the two limits $R_p \ll R_g$ and $R_p \gg R_g$ reflects the difference in the deformability and penetrability of the protein as compared to the polymer. It is this feature of the interaction that we have attempted to capture in our evaluation of the protein-polymer excluded-volume away from the Θ-solvent conditions. To account for the swelling of the PEO chains, which arises from the interactions between PEO segments in the same coil, a simple Monte-Carlo method was developed to estimate this excluded volume contribution (Wall and Mandel, 1975; Hermans, 1982; Hermans and Hermans, 1984). Although qualitatively one may expect the excluded volume to be similar to that corresponding to the Θ-solvent case, the purpose of the present work is to provide a somewhat more quantitative determination of the protein chemical potential in a polymer solution. Accordingly, the steric interaction between the polymer coil and the protein was evaluated using a reptation method (Wall and Mandel, 1975) to generate the configurations of the polymer coil (on a cubic lattice) in the vicinity of the protein (modelled as a hard sphere or ellipsoid). The excluded volume is evaluated as (Hermans, 1982; Hermans and Hermans, 1984)

$$U_p = V_p^o \left[\frac{N}{<m>} \right] \qquad \textbf{(6.19)}$$

where N is the number of statistical polymer segments per polymer coil, V_p° is the molecular volume of the protein, and $<m>$ is the number of statistical polymer segments which simultaneously overlap the protein volume, averaged over an ensemble of polymer-coil configurations generated using the Monte-Carlo method. Eq.(6.19) can be understood intuitively using the following simple argument. If all N statistical polymer segments on the chain interact *independently* with the protein, the excluded volume, U_p, would be equal to NV_p° (the polymer segment volume is very small compared to the protein volume) (Tanford, 1961). However, the polymer segments are

not independent since they belong to the same polymer chain, and therefore, their positions are correlated. The result of the polymer chain connectivity is that if a single polymer segment interacts with the protein, because it belongs to a polymer coil, there will be, in all likelihood, other polymer segments interacting simultaneously with the protein. This implies a *reduction* of the excluded volume NV_p^o by the factor $<m>$. In addition to providing a quantitative evaluation of the excluded volume, an additional advantage of this general method is that it is not constrained to linear polymer architectures or spherical protein geometries. An account of non-spherical (ellipsoidal) protein geometries will also be given in this chapter.

To ensure the correct generation of an unbiased sample of polymer configurations, as shown in Figure 6.2, the root-mean-square end-to-end length of the polymer coil, $<R^2>^{1/2}$, was evaluated as a function of the number of polymer-coil segments, N. The data points represent the average of 10 independent runs, each consisting of $200N^2$ attempted polymer-segment moves, and the error bars extend a standard deviation on either side of the average. The solid line is a linear fit to the data points and was used to determine the exponent relating $<R^2>^{1/2}$ to N. The value determined was 0.587 ± 0.018, and is consistent with the expected value of approximately 3/5 for a self-avoiding polymer coil in three dimensions (Flory, 1986; de Gennes, 1988).

To determine the scaling prefactor that relates the dimensions of the lattice-generated polymer coil to the actual size of the PEO coils in aqueous solution, a correspondence between the size of a lattice segment and a PEO segment (*a*) must be established. In essence, the number of bonds along the PEO chain that corresponds to the statistical-segment size is determined by the polymer flexibility, that is, c_∞ (Flory, 1968). Consistent with the known flexibility of PEO ($c_\infty = 4.1$) (Flory, 1968), we assume that 4 bonds of the PEO chain constitute one statistical segment of the simulated polymer chain. Accordingly, the number of statistical polymer segments within the polymer chain is $N = n/c_\infty$. The size of a statistical segment was determined by requiring that the radii of gyration of the statistical chain (with N polymer segments) equal the radius of gyration of the PEO chain. In order for the dimensions of the simulated chains (see Figure 6.2)

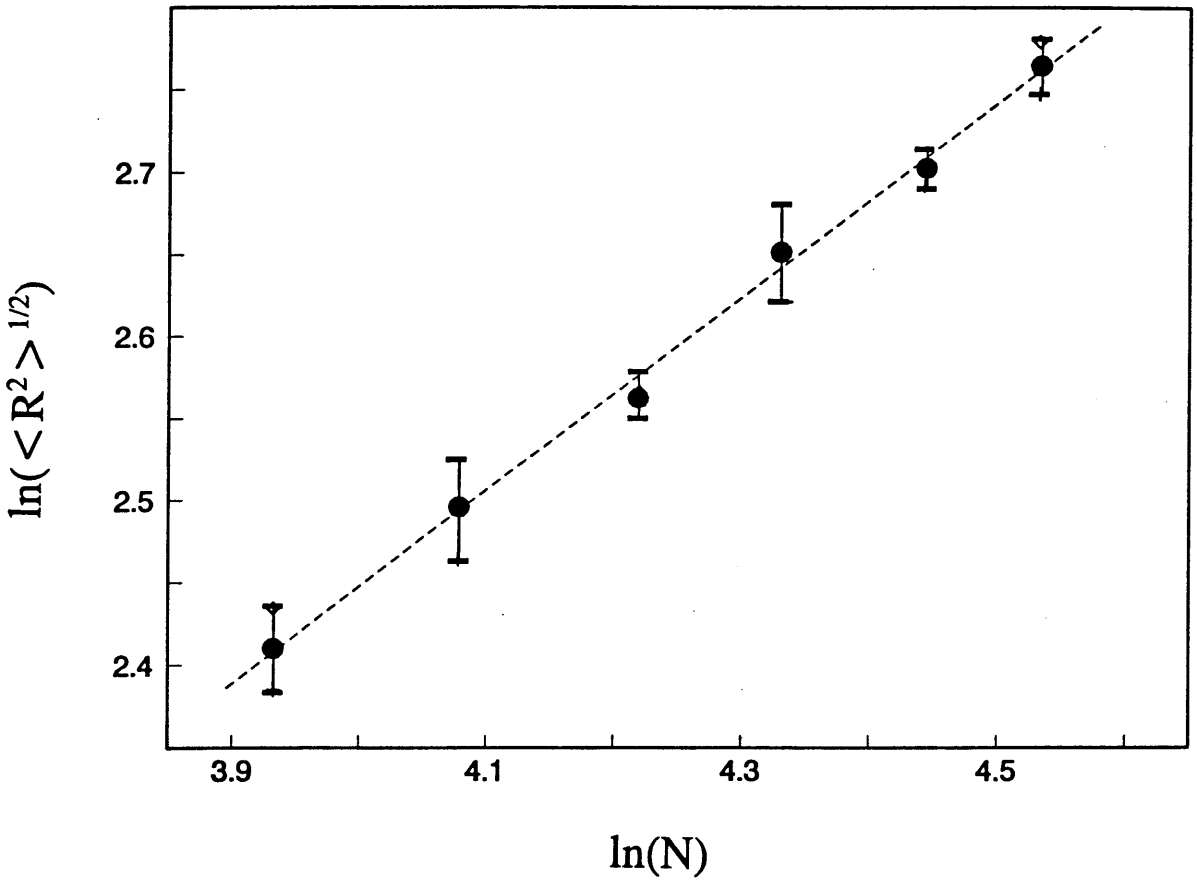

Figure 6.2. Logarithm of the root-mean-square end-to-end length of polymer coil, $\ln(\langle R^2 \rangle^{1/2})$, as a function of the logarithm of the number of polymer segments per coil, ln(N). The error bars extend one standard deviation either side of the mean value, and the line of best fit is shown.

to equal the measured PEO chain dimensions (Table 6.1), a statistical-segment length corresponding to 4 Å was determined. Note that although the solvent condition for PEO in water does not correspond to the athermal conditions of the simulation, the departure of the solvent conditions from athermal is incorporated by choosing the effective statistical-segment size to be 4 Å (de Gennes, 1988).

The excluded volume characterizing the polymer-protein interactions, evaluated according to Eq.(6.19), is presented in Figure 6.3 as a function of PEO molecular weight. The results are presented for three spherical protein sizes, corresponding to cytochrome-C (R_p=19 Å), ovalbumin (R_p=29 Å) and catalase (R_p=52 Å), for the range of PEO molecular weights between 3 000 Da to 5 500 Da. From an inspection of Figure 6.3 it can be seen that the excluded volume increases both with protein size and PEO molecular weight.

Using the excluded-volume data presented in Figure 6.3, and the spherical (physical) size of a protein, the effective hard-sphere radius of the polymer coil (associated with excluded-volume interactions with a protein), R_{2p}^{HS}, can be evaluated from (Tanford, 1961)

$$U_p = \frac{4\pi(R_p + R_{2p}^{HS})^3}{3} \qquad \textbf{(6.20)}$$

The predicted variation of R_{2p}^{HS}, with PEO molecular weight is shown in Figure 6.4. Owing to the deformable and penetrable nature of the polymer coil, R_{2p}^{HS} changes both with the size of the protein molecule and the polymer molecular weight. Note that R_{2p}^{HS} is, in general, different from R_{22}^{HS}, and that for a fixed polymer molecular weight, R_{2p}^{HS} increases with increasing protein size. This trend reflects the fact that with an increase in the protein size, there will be a decrease in the number of polymer configurations which permit the protein to penetrate the volume occupied, on average, by the polymer coil. Furthermore, for a fixed protein size, as is also reflected in Figure 6.4, an increase in polymer molecular weight results in an increase in the effective hard-sphere radius of the PEO coil. For small proteins, the increase in the effective polymer size is less than

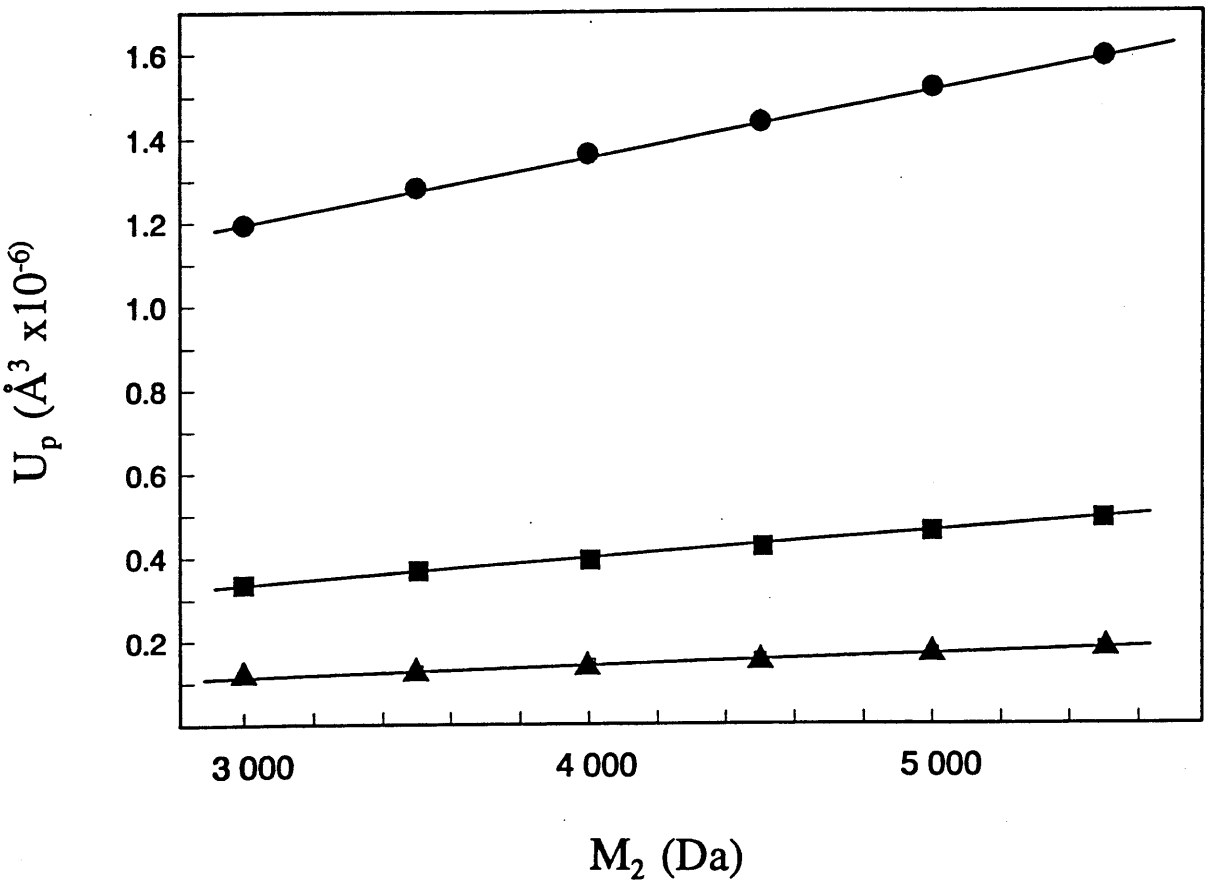

Figure 6.3. Predicted excluded-volume of polymer and protein, U_p, as a function of PEO molecular weight, M_2; (▲) cytochrome-C, R_p=19Å; (■) ovalbumin, R_p=29Å; (●) catalase, R_p=52Å.

for the large proteins. This is, once again, because the fraction of the average polymer volume which is accessible to the protein increases with decreasing protein size. In Figure 6.4, for the purpose of comparison, we also show the effective hard-sphere radius of a PEO coil associated with polymer-polymer interactions (taken from Table 6.1). It is interesting to observe that this effective radius is always smaller than the effective hard-sphere size of the polymer coil used to characterize polymer-protein interactions. In other words, for the range of protein sizes investigated, the polymers are more permeable to each other than to the protein species.

While the above discussion of R_{2p}^{HS} illuminates the nature of polymer-protein interactions, it is necessary to further develop the above result in order to incorporate the protein-polymer and polymer-polymer potentials into a thermodynamic framework which can predict the standard-state protein chemical potential. In Section 3 we developed a generalized hard-sphere representation of the polymer-protein solution, and in so doing, we implicitly assumed the same polymer coil effective hard-sphere size to describe both polymer-polymer and polymer-protein interactions. The essential complication arises from the fact that, as reported in Figure 6.4, different effective hard-sphere polymer sizes are required to describe polymer-polymer interactions (R_2^{HS}) and polymer-protein interactions (R_{2p}^{HS}). However, with a change in polymer molecular weight, rather than attributing changes in the protein-polymer excluded-volume to the effective hard-sphere size of the polymer (R_{2p}^{HS}), one can distribute these changes between an effective hard-sphere protein size, and an effective polymer hard-sphere size. In particular, for our purposes it is advantageous to use the same polymer effective hard-sphere radius to characterize the polymer for both protein-polymer and polymer-polymer interactions, that is, R_{22}^{HS} (since this is required for the thermodynamic analysis). Accordingly, using the excluded-volumes from Figure 6.4 and the effective hard-sphere radii of the polymer coils that characterize the polymer-polymer interactions (R_{22}^{HS}) from Table 6.1, an effective hard-sphere radius of the protein molecules, R_p^{eff}, can be evaluated by rewriting Eq.(6.20) in the form

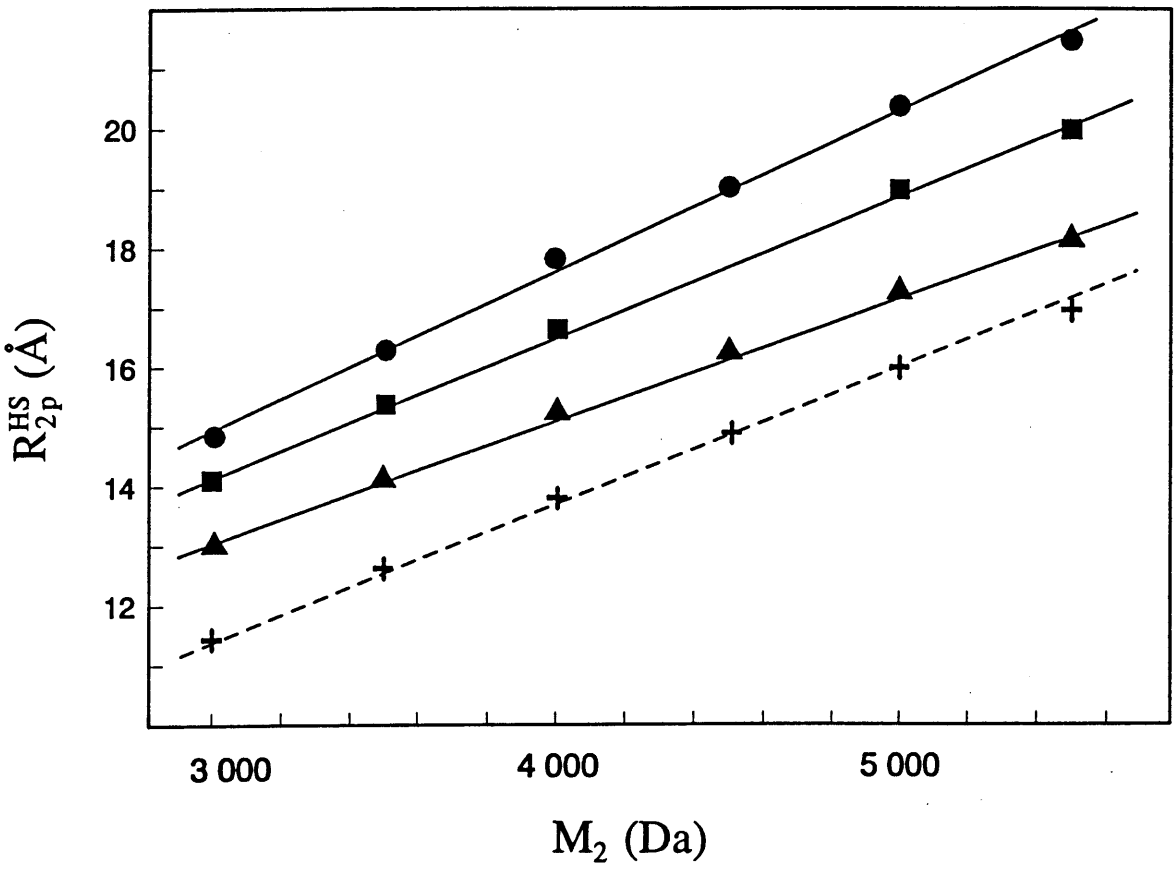

Figure 6.4. Predicted effective hard-sphere radius of PEO coil, R_{2p}^{HS}, associated with the excluded-volume interaction with protein, as a function of PEO molecular weight, M_2: (▲) cytochrome-C, R_p=19Å; (■) ovalbumin, R_p=29Å; (●) catalase, R_p=52Å. Also shown is the effective hard-sphere radius of a PEO coil, R_{22}^{HS}, associated with the excluded-volume interaction with another polymer coil having the same molecular weight (+).

$$U_p = \frac{4\pi}{3}(R_p^{eff} + R_{22}^{HS})^3 \qquad \textbf{(6.21)}$$

The ratio of the effective protein size to the actual protein size, R_p^{eff}/R_p, evaluated according to the above description as a function of PEO molecular weight, is presented in Figure 6.5. In Figure 6.5, it is evident that the protein size used in Eq.(6.21) is a function of the polymer molecular weight. For a small protein like cytochrome-c, an increase in PEO molecular weight results in a decrease in the effective protein radius. This prediction follows naturally from the results presented in Figure 6.4, and may be understood in terms of the increasing penetrability of the polymer coils towards small proteins at the higher PEO molecular weights (de Gennes, 1988). Perhaps a less expected result is the observed increase in the effective protein radius with PEO molecular weight observed for the large proteins. For large proteins, such as catalase, the effective hard-sphere size of the polymer used to characterize the protein-polymer interactions (R_{2p}^{HS}) is more sensitive to polymer molecular weight than is the effective hard-sphere size of the polymer coil used to characterize the polymer-polymer interactions (R_{22}^{HS}). This can be seen from a careful inspection of Figure 6.4.

It should always be kept in mind that the effective hard-sphere size of the protein used in Eq.(6.7) for the protein chemical potential reflects the nature of both protein-polymer and polymer-polymer interactions. That is, $\sigma_p=2R_p^{eff}=2(R_p+R_{2p}^{HS}-R_{22}^{HS})$. Clearly, this approach will only be successful in the limit of vanishing protein concentration, where interactions between proteins have a negligible effect on the protein chemical potential. It is also quite clear that this approach cannot be easily generalized to higher protein concentrations, where protein-protein interactions may play an increasingly important role in determining the protein partitioning behavior.

6.4 Evaluation of the Standard-State Protein Chemical Potential

In order to evaluate the standard-state protein chemical potential using the effective hard-sphere sizes evaluated in Section 6.3, we identify R_{22}^{HS} with $\sigma_2/2$ and R_p^{eff}

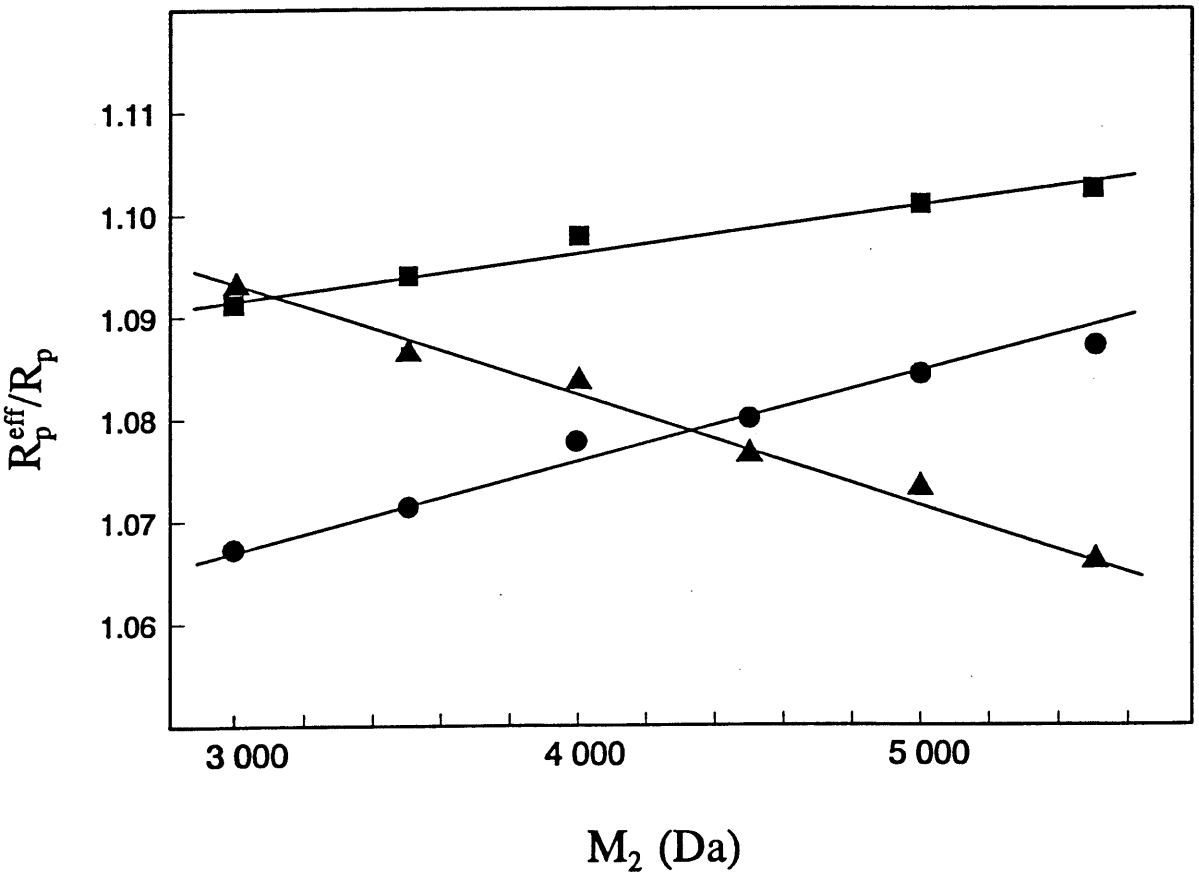

Figure 6.5. Predicted ratio of the effective hard-sphere protein and physical protein radii, R_p^{eff}/R_p, as a function of PEO molecular weight, M_2: (▲) cytochrome-C, R_p=19Å; (■) ovalbumin, R_p=29Å; (●) catalase, R_p=52Å.

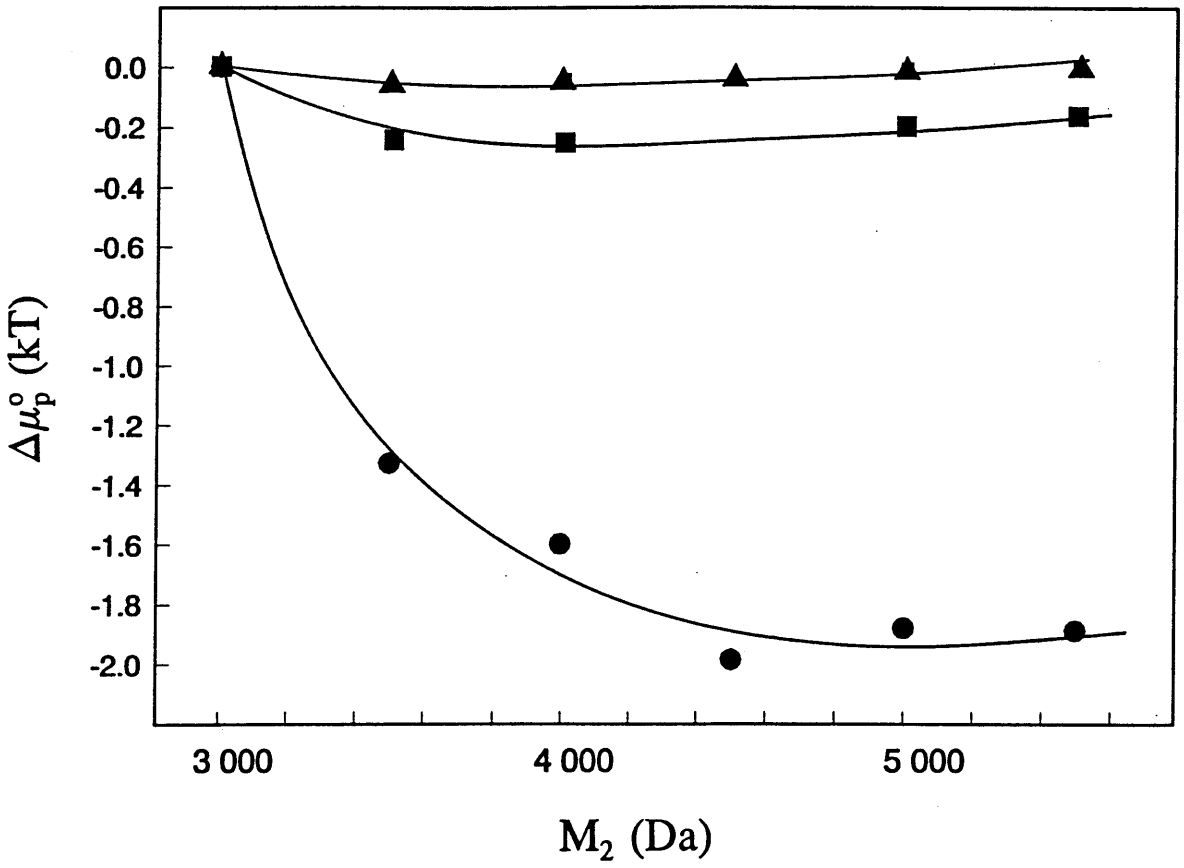

Figure 6.6. Predicted standard-state protein chemical potential in a 10% w/w aqueous PEO solution, relative to that in a solution of PEO 3 000 Da, $\Delta\mu_p^o$, as a function of PEO molecular weight, M_2: (▲) cytochrome-C, R_p=19Å; (■) ovalbumin, R_p=29Å; (●) catalase, R_p=52Å.

with $\sigma_3/2$ in Eq.(6.7). Figure 6.6 presents a prediction of the change in the standard-state protein chemical potential as a function of PEO molecular weight for three proteins of differing size, and for solution conditions corresponding to 10% w/w PEO in water (as discussed in Chapter 4, this PEO concentration is typical of that encountered in the top PEO-rich phase of a two-phase aqueous polymer system containing PEO and dextran) (Abbott et al., 1991a). For the smallest protein species, cytochrome-c, a negligible change in the standard-state protein chemical potential is predicted to accompany changes in PEO molecular weight from 3 000 Da to 5 500 Da, subject to the statistical uncertainty introduced by the evaluation of the protein-polymer excluded volume using the Monte-Carlo method. The change in the chemical potential is amplified by the protein size. For example, the prediction for the change in the standard-state chemical potential of catalase, (●), shows a statistically significant decrease to accompany an increase in PEO molecular weight. On the basis of Eq.(6.1), it is evident that this decrease in the standard state protein chemical potential translates into a predicted increase in the protein partition coefficient with increasing PEO molecular weight. This result is in direct contrast to the trends observed experimentally, where increasing PEO molecular weight resulted in a decrease in the protein partition coefficient (Hustedt et al., 1978; Albertsson et al., 1987). Therefore, within the approximations of the thermodynamic formulation presented in this chapter, it appears that on the basis of entropy alone (steric interactions) it is not possible to account for the observed partitioning behavior of proteins in the PEO-dextran two-phase aqueous polymer system.

One approximation in the above treatment is the representation of the protein molecules as spherical bodies. Indeed, many proteins are rather more ellipsoidal in shape with ratios of the major and minor axes of approximately 3 (Creighton, 1984; Peters, 1985). To assess the role of the more detailed protein geometry on the partitioning behavior, we have investigated the influence of introducing asymmetry in the protein shape. The Monte-Carlo method developed for the evaluation of the protein-polymer interactions is well suited for this investigation, and geometries more intricate than ellipsoidal ones could also be treated readily.

Figure 6.7 shows the influence of the protein shape on the change in the

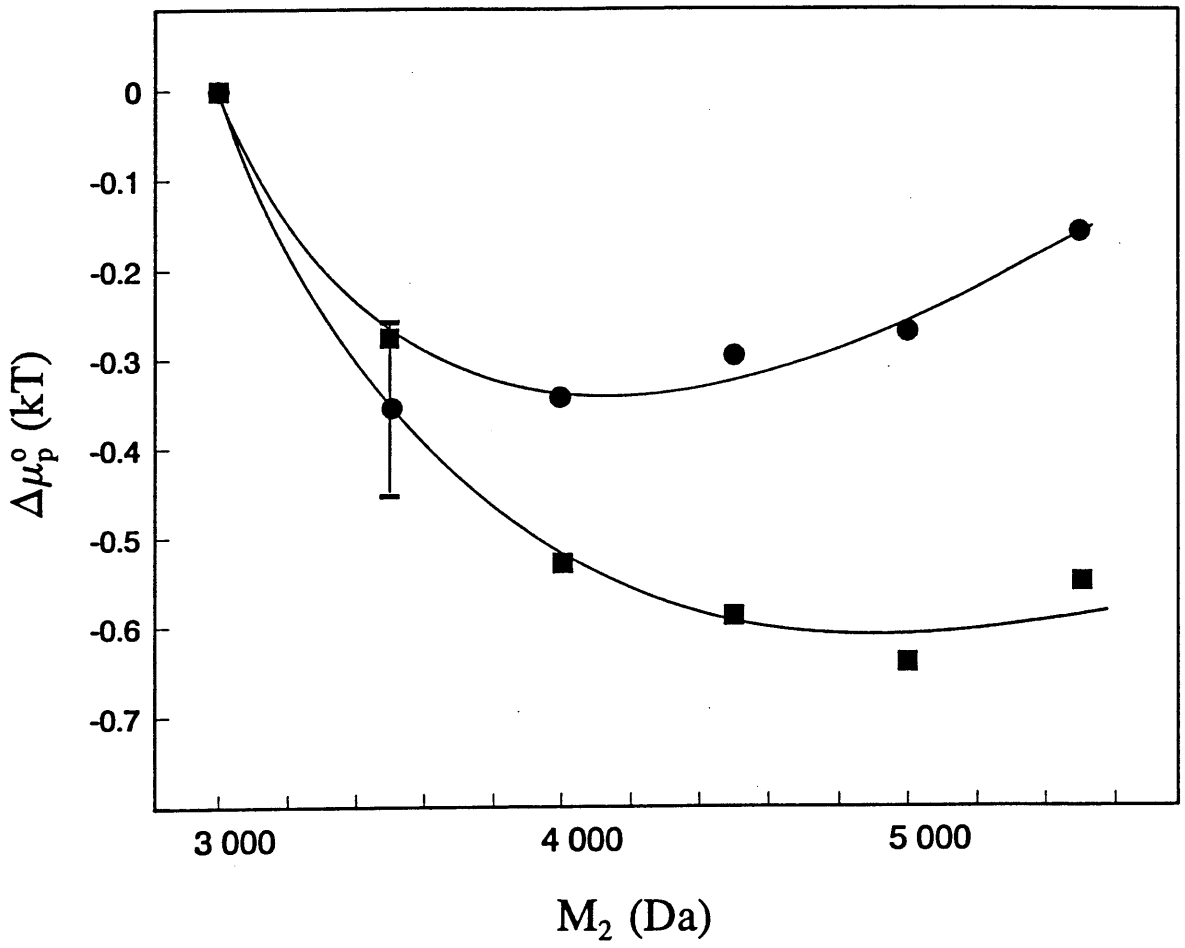

Figure 6.7. Predicted effect of protein shape asymmetry on the standard-state protein chemical potential in a 10% aqueous PEO solution, relative to that in a solution of PEO 3 000 Da, $\Delta\mu_p^o$, as a function of PEO molecular weight, M_2. The protein volume corresponds approximately to bovine serum albumin. (■) sphere with radius of 35Å; (●) ellipsoid with a semimajor axis of 79Å and a semiminor axis of 23Å.

standard-state protein chemical potential predicted to accompany a change in PEO molecular weight. Keeping the volume of the protein constant (which, for the sake of illustration, corresponds to the volume of a BSA molecule), the aspect ratio of the protein was varied from 1.0 to 3.5 (Creighton, 1984; Peters, 1985). Interestingly, it appears that an increase in the asymmetry of the protein will increase the change in the standard-state protein chemical potential. Physically, this arises because an increase in the aspect ratio of the protein causes an increase in the magnitude of the excluded volume characterizing the protein-polymer interactions. The relatively large magnitude of this effect, as seen in Figure 6.7, suggests that for a more accurate and quantitative prediction of protein partitioning in two-phase aqueous polymer systems it will be necessary to account for the nonspherical shape of most proteins.

6.5 Attractions and the Standard-State Protein Chemical Potential

In Chapter 4, in addition to revealing the (competing) contributions of steric protein-polymer and polymer-polymer interactions to the standard-state protein chemical potential, the important role of weak short-range attractive interactions between the protein and the polymer segments was examined (Abbott et al., 1991a). For this purpose, qualitative scaling-type arguments were used. The conclusion of that investigation was that weak attractive interactions influence the standard-state protein chemical potential in a manner that is consistent with trends observed experimentally. The primary aims of the following section is (1) to assess the validity of the scaling-type arguments through a simple Monte-Carlo calculation, and (2) to determine the strength of attractive interactions that would be sufficient to account for the experimentally observed influence of PEO molecular weight on the protein partition coefficient.

The treatment of the attractive interactions between the protein and the polymer-coil segments utilizes a hard-sphere perturbation approach (McQuarrie, 1976), which has been successful in describing the influence of weak attractions on the equilibrium phase behavior and light scattering properties of other colloidal systems (Jansen et al., 1986a, b, and c). This approach relies on the fact that for systems with weak interactions, the

attractive contribution to the osmotic pressure remain of order ρ^2, where ρ is the number density of a species in solution, up to quite high number densities (we consider the validity of this approximation in Appendix 6.B) (Jansen et al., 1986a, b, and c). To second order in number density, the osmotic pressure, Π, for a solution containing a mixture of species can then be written as (McQuarrie, 1976)

$$\Pi = \Pi_{hs} + \sum_{i,j} B_{i,j}^{att} \rho_i \rho_j \qquad \textbf{(6.22)}$$

where Π_{hs} is the hard-sphere contribution to the osmotic pressure, ρ_i is the number density of species i, and B_{ij}^{att} is the attractive portion of the second-virial coefficient for species i and j, defined as

$$B_{i,j}^{att} = \frac{1}{2}\int (1 - e^{-V_{i,j}^{(1)}(r)}) \, d^3r \qquad \textbf{(6.23)}$$

where $V_{ij}^{(1)}(r)$ is the contribution of the attractive interaction to the potential of mean force between species i and j which are separated by a distance r. In the notation of statistical mechanical perturbation theory, $V_{ij}^{(1)}(r)$ is the perturbation potential relative to a reference potential (which, in our case, is the pure hard-sphere system treated in Section 6.4).

Under the constraint of constant solvent chemical potential, the contribution of attractive interactions of the form given in Eq.(6.22) to the chemical potential of species i in a mixture of j species is given by (Jansen et al., 1986a)

$$\left[\frac{(\mu_i^o)^{att}}{kT} \right]_{\mu_1} = 2 \sum_j B_{i,j}^{att} \rho_j \qquad \textbf{(6.24)}$$

For a mixture of proteins (species p) and polymers (species 2) dispersed in a solvent (species 1) at vanishing protein concentration ($\rho_p \to 0$), Eq.(6.24) for i=p reduces to

$$\left[\frac{(\mu_p^o)^{att}}{kT}\right]_{\mu_1} = 2\, B_{2p}^{att}\, \rho_2 \qquad \textbf{(6.25)}$$

Recall that the solvent, species 1, does not appear explicitly in Eq.(6.25) since it is treated in the continuum approximation. However, the solvent properties *do* influence the protein chemical potential, that is, B_{2p}^{att} is a function of the solvent quality, since all interactions in the solution are mediated by the solvent. It is interesting to note that the expression in Eq.(6.25) is identical to that derived in Chapter 4 (Abbott et al., 1991a). Here, however, we wish to evaluate the protein chemical potential at constant pressure (rather than at constant solvent chemical potential, see Appendix 6.A). This can be achieved readily by combining Eq.(6.3), which relates changes in the chemical potential at constant pressure to those at constant solvent chemical potential, and Eq.(6.25), which describes the influence of the attraction on the protein chemical potential at constant solvent chemical potential. The resulting expression for the contribution of the attractive interactions to the protein chemical potential at constant pressure is given by (Jansen et al., 1986a)

$$\left[\frac{(\mu_p^o)^{att}}{kT}\right]_{P} = 2\, B_{2p}^{att}\, \rho_2 - B_{2p}^{att}\, V_2\, \rho_2^2 \qquad \textbf{(2.26)}$$

where $V_2=4\pi(R_{22}^{HS})^3/3$.

Whereas in Chapter 4 the attractive crossed-virial coefficient, B_{2p}^{att}, was estimated using simple scaling-type arguments, here we report a more quantitative evaluation using a Monte-Carlo method. Since B_{2p}^{att} describes the interactions between a deformable and penetrable polymer coil and an impenetrable sphere, the evaluation of this quantity required that we account for the influence of both repulsive excluded-volume and attractive interactions on the configurations that are sampled by the polymer coil when residing in the vicinity of the protein. We approximate this evaluation by the

integral,

$$B_{2p}^{att} = \frac{1}{2}\left\langle \int_0^\infty \left(1 - e^{\frac{-V_{2p}^{(1)}(r)}{kT}}\right) d^3r \right\rangle \approx \frac{1}{2}\int_0^\infty \left(1 - e^{\left\langle \frac{-V_{2p}^{(1)}(r)}{kT} \right\rangle}\right) d^3r \qquad \textbf{(6.27)}$$

where the angular brackets denote a weighted average over all possible polymer configurations that (i) do not intersect the volume occupied by the protein and (ii) satisfy the constraint that the centers of mass of the polymer coil and the protein be separated by a distance r. In order to evaluate B_{2p}^{att} we have used the approximation presented in Eq.(6.27), where the averaging is performed over the interaction potential, rather than over the entire integral. This approximation, which greatly reduces the effort involved in evaluating the integral, is a good one provided that $V_{2p}^{(1)}(r)/kT \ll 1$. In Appendix 6.B, we show that this constraint is generally satisfied for our use of Eq.(6.27). For a short-range contact-type interaction between the polymer-coil segments and the protein (as was treated in Chapter 4 and is investigated here), this average can be simply evaluated as

$$-\frac{\langle V_{2p}^{(1)}(r)\rangle}{kT} = \frac{\sum^{\{C\}} m_s \varepsilon e^{m_s \varepsilon}}{\sum^{\{C\}} e^{m_s \varepsilon}} \qquad \textbf{(6.28)}$$

where the summations are over a representative sample of the polymer configurations, {C}, such that the two criteria mentioned above are satisfied, m_s is the number of contacts between the polymer coil and the protein for a given polymer-coil configuration and ϵ is the energy change upon bringing a polymer coil segment from infinity to the protein surface (ε is defined to be positive for an attractive interaction). In view of the conditions for which the perturbation approach is valid, that is, for weak long-range attractions (McQuarrie, 1976; Jansen et al., 1986a, b, and c), it is interesting to note that despite the short-range attractive nature of the interactions between the polymer *segments* and the protein, the interaction potential between the polymer *coil* and the protein, as

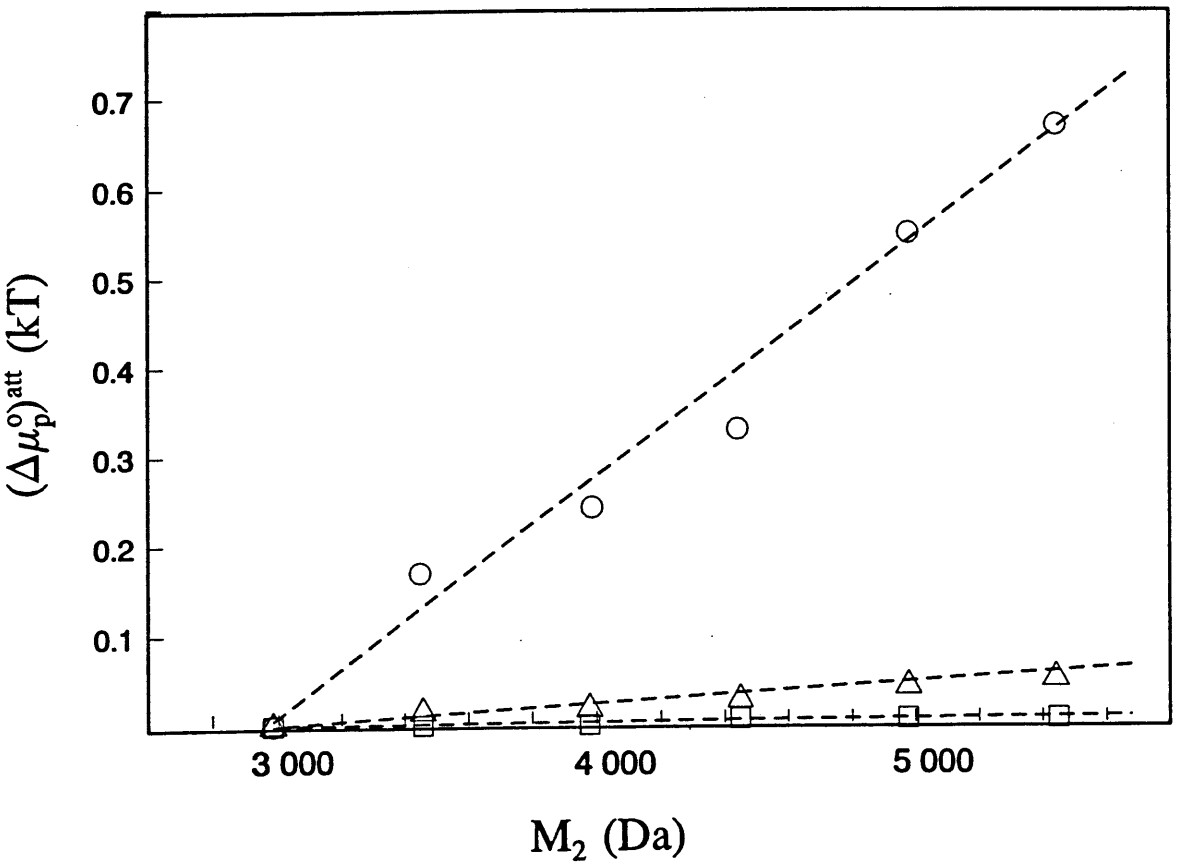

Figure 6.8. Predicted contribution of the protein-polymer attraction to the standard-state protein chemical potential in a 10% w/w aqueous PEO solution, relative to a solution of PEO 3 000 Da, $(\Delta\mu_p^o)^{att}$, as a function PEO molecular weight, M_2, and for ovalbumin (R_p=29Å). Polymer segment-protein interaction energies; (□) 0.001kT, (▵) 0.01kT, (○) 0.1kT.

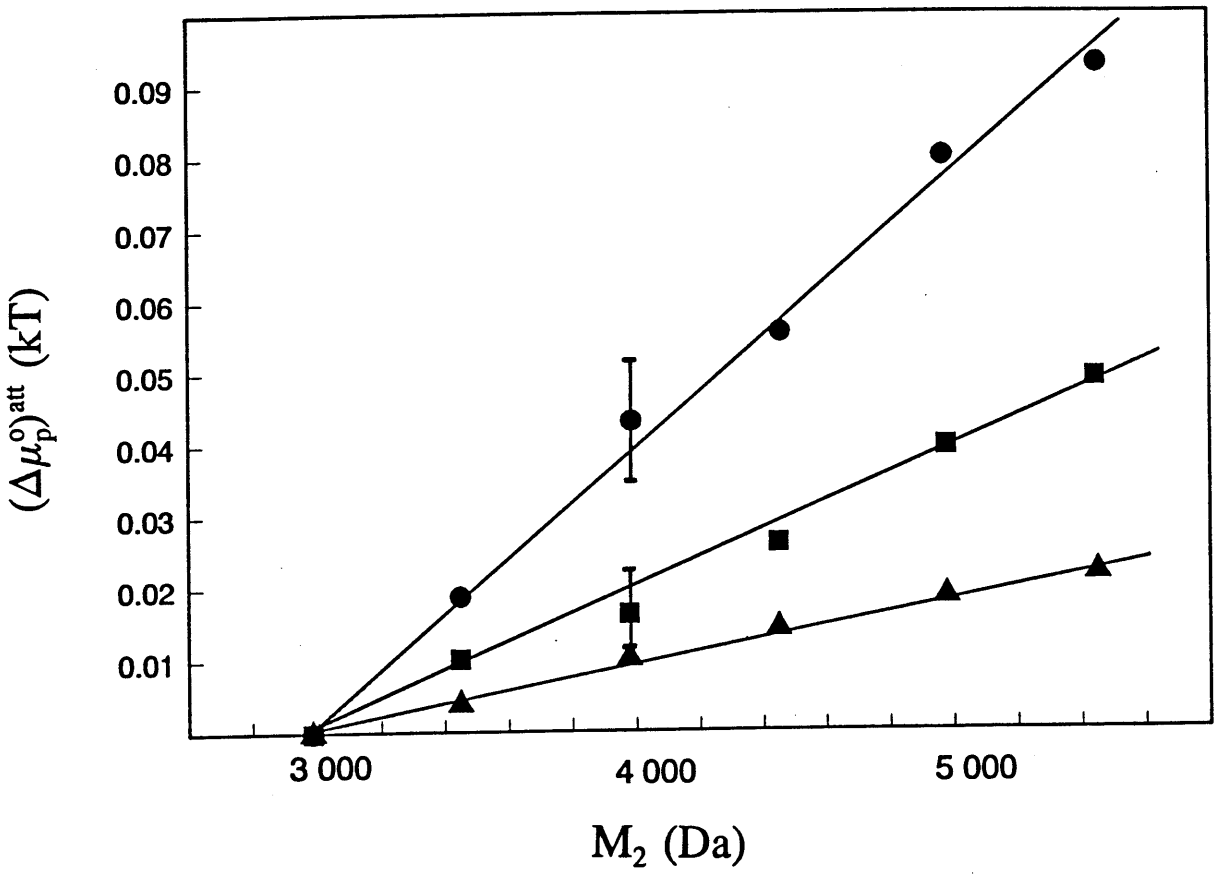

Figure 6.9. Predicted contribution of the protein-polymer attraction to the standard-state protein chemical potential in a 10% w/w aqueous PEO solution, relative to a solution of PEO 3 000 Da, $(\Delta\mu_p^o)^{att}$, as a function PEO molecular weight, M_2. Polymer segment-protein surface interaction energies: 0.01kT; (▲) cytochrome-C, R_p=19Å; (■) ovalbumin, R_p=29Å; (●) catalase, R_p=52Å.

evaluated in Eq.(6.28), is slowly varying and long-ranged. Finally, it is relevant to mention that the above framework is also suitable for exploring the influence of different types of interactions potentials on the predicted protein partitioning behavior.

In Figure 6.8, the contribution of the attractive interactions between the polymer-coil segments and the protein to the standard-state protein chemical potential at constant pressure, evaluated according to Eqs.(6.26), (6.27) and (6.28), is presented. The quantity reported is the change in the standard-state protein chemical potential accompanying an increase in PEO molecular weight, for a fixed protein size corresponding to that of ovalbumin (R_p=29 Å), and 3 different interaction energies (ϵ=0.001, 0.01 and 0.1 kT). It is evident that an increase in PEO molecular weight results in an increase in the chemical potential of the protein, and that the increase is magnified by the strength of the attractive interaction. Figure 6.9 illustrates the influence of protein size on the change in the standard-state protein chemical potential with an increase in PEO molecular weight. For the 3 spherical proteins investigated (R_p=17, 29 and 51 Å), the effect of protein size is also to magnify the change in the protein standard-state chemical potential. Using Eq.(6.1), it can be seen that the predicted increase in the standard-state protein chemical potential translates to a decrease in the protein partition coefficient with an increase in PEO molecular weight. This prediction is consistent with experimental investigations of protein partitioning in the two-phase aqueous PEO-dextran system which found that the influence of an increase in PEO molecular weight is to decrease the protein partition coefficient (Abbott et al., 1991a; Hustedt et al., 1978; Albertsson et al., 1987).

The numerical evaluations of the influence of attractive interactions on the standard-state protein chemical potential can be compared to the result of the simple scaling argument reported in Chapter 4 (Abbott et al., 1991a). In particular, for the condition, $R_p \approx R_g$, it was reported that (Abbott et al., 1991a)

$$\left[\frac{\mu_p^o}{kT}\right]^{att} \sim -\frac{\varepsilon\, a\, R_p^2}{N^{3/5}} \qquad \textbf{(6.29)}$$

and for higher molecular weights, where $R_g > R_p$, the exponent on N was predicted to decrease to zero (Abbott et al., 1991a). For comparison, our numerical results for ovalbumin predict an N exponent of 0.45 ± 0.05 for $\varepsilon = 0.001$ as well as $\varepsilon = 0.01$, and 0.40 ± 0.05 for $\varepsilon = 0.10$ and, therefore, are in satisfactory agreement with the simple scaling theory (Abbott et al., 1991a). Very similar exponents were determined for two other protein sizes, corresponding to cytochrome-C ($R_p = 17$Å) and catalase ($R_p = 51$Å).

Combining the contributions of both the excluded-volume interactions (see Section 6.2) and attractive interactions (described above) to the predicted standard-state protein chemical potential for ovalbumin, it was determined that an attractive interaction of strength between 0.01 and 0.05 kT per polymer segment can predict the experimentally observed change in the protein partition coefficient with PEO molecular weight. For catalase, an attractive interaction of approximately 0.20 to 0.30 kT is required, and for cytochrome-C an attractive interaction of only (approximately) 0.01 kT is needed. Thus, on the basis of this theory, it appears that there may be a correlation between the size of the protein and the strength of the attractive interaction required to account for the change in the protein chemical potential with PEO molecular weight. This observation is suggestive of an attractive interaction between the polymer segments and the protein molecules, where the polymer segments are interacting with the bulk of the protein instead of solely its surface. Van der Waals-type interactions are of this nature (Israelachvili, 1985), although it is not clear that they are of sufficient strength to explain the partitioning of the larger proteins, for example, catalase. Although the precise origin of the attractive interaction is unknown, it is interesting to note that their magnitudes are consistent with neutron scattering measurements of BSA in aqueous PEO solutions which are to be reported in a future publication (Abbott et al., 1991c). Finally, it is relevant to consider the relative contributions of the attractions and the steric repulsions to the total interaction between the protein and the polymer. In Table 6.2, the two contributions, B_{2p}^{HS} and B_{2p}^{att}, to the second-virial coefficient describing the protein-(ovalbumin, $R_p = 29$Å) PEO interactions are presented as a function of the PEO molecular weight for $\varepsilon = 0.01$kT and 0.1kT. From the comparison presented in Table 6.2 it is evident that, despite the presence of the attractive interaction, the *net* interaction between

the protein and the polymer is repulsive. For an attractive interaction of around ε=0.05kT (the approximate strength of attraction required to predict the partitioning behavior of ovalbumin), interpolation of the results for ε=0.01kT and ε=0.1kT suggests that the second virial coefficient is approximately 80% of the value calculated for purely steric interactions.

6.6 Discussion

In Section 6.3 we evaluated the effective hard-sphere radius of a PEO coil, R_{2p}^{HS}, in order to describe the steric interaction of a PEO coil with a globular protein molecule. Specifically, in evaluating, R_{2p}^{HS}, we accounted for the increase in the penetrability of the coil to the protein as the PEO molecular weight was increased. Consequently, this approach contrasts with previous descriptions of polymer-colloid interaction in which the polymer-coil radius of gyration, R_g, was used to describe the steric interaction of a flexible polymer and a rigid colloid (Vrij, 1976; de Hek and Vrij, 1981; Vincent et al., 1979; Patel and Russel, 1989a and b; Dey and Hirtzel, 1991). In order to assess the importance of taking into account the penetrability of the PEO coil, rather than simply using the polymer-coil radius of gyration, in Figure 6.10 we have presented the standard-state protein chemical potential calculated using either R_g or R_{2p}^{HS} to characterize the polymer in the evaluation of the protein-polymer interaction. From an inspection of Figure 6.10, where the predicted changes in the protein (ovalbumin, R_p=29Å) standard-state chemical potential as a function of PEO molecular weight are presented, it can be seen that *qualitatively* different trends in the standard-state protein chemical potential are predicted. The characterization of the polymer-protein interaction using the polymer-coil radius of gyration, R_g, is seen to predict an *increase* in the standard state protein chemical potential as a function of polymer molecular weight. In contrast, when the protein-polymer interaction is characterized using R_{2p}^{HS} (see Section 6.3), a *decrease* in the protein standard-state chemical potential is predicted. The difference between the two predictions arises because the former characterization of the polymer coil does not correctly take into account the increase in the penetrability of the

M_2 (Da)	ε (kT)	B_{2p}^{HS} (Å^3)	$-B_{2p}^{att}$ (Å^3)	$-B_{2p}^{att}/B_{2p}^{HS}$
3 000	0.01	167 500	4 940	0.03
3 500		182 800	5 430	0.03
4 000		199 400	6 050	0.03
4 500		216 200	6 400	0.03
5 000		230 900	6 610	0.03
5 500		246 000	6 790	0.03
3 000	0.10	167 500	76 050	0.45
3 500		182 800	83 490	0.46
4 000		199 400	93 920	0.47
4 500		216 200	101 730	0.47
5 000		230 900	104 580	0.45
5 500		246 000	109 000	0.44

Table 6.2. Predicted contributions of steric repulsions, B_{2p}^{HS}, and attractions, B_{2p}^{att}, to the second virial coefficients of PEO and ovalbumin as a function of PEO molecular weight, M_2, and strength of attraction, ε.

polymer coil (to the protein) as the polymer molecular weight is increased. This comparison demonstrates the importance of accounting for the penetrability of the polymer coil in order to correctly describe the thermodynamic properties of solutions containing globular proteins and flexible polymer coils.

In Section 6.2, a theoretical framework to determine the chemical potential of a protein in a polymer solution phase was presented for the conditions of constant solution temperature and pressure. In view of the previous evaluation of the protein chemical potential at constant solvent chemical potential (Abbott et al., 1991a) (Chapter 4), it is pertinent to examine to what extent these different thermodynamic ensembles influence the predicted protein partitioning behavior. Physically, the two approaches to the evaluation of the protein chemical potential differ as follows. In Chapter 4, an ensemble at constant temperature and volume was used and accordingly, upon introduction of the protein species into the system (at constant system volume) a change in the pressure of the system will occur (Abbott et al., 1991a). In the context of the formulation used to evaluate the protein chemical potential, this pressure change, which will manifest itself as a change in the molar and excluded volumes of the species in the system, was neglected (Abbott et al., 1991a). This approximation is equivalent to the evaluation of the protein chemical potential in a solution where the chemical potential of the solvent remains constant upon the introduction of the protein species. Although this neglect of the pressure change would appear to become negligible as the size of the system is made arbitrarily large (and vanishes as 1/L, where L is a measure of the system size), in evaluating the chemical potential of the protein, we actually evaluate the change in the free energy of the entire system (that is, we integrate over all L), such that the effect of the pressure change does not vanish (Modell and Reid, 1983). In this paper we have made no such approximations and have derived the protein chemical potential at constant T and P. To assess the practical significance of the current development, in Figure 6.11 the predicted standard-state chemical potential of a spherical protein (ovalbumin, R_p=29Å) at constant solvent chemical potential and at constant pressure is presented as a function of PEO molecular weight. From Figure 6.11 it is apparent that, for the prediction of rather subtle changes in the protein chemical potential, the difference

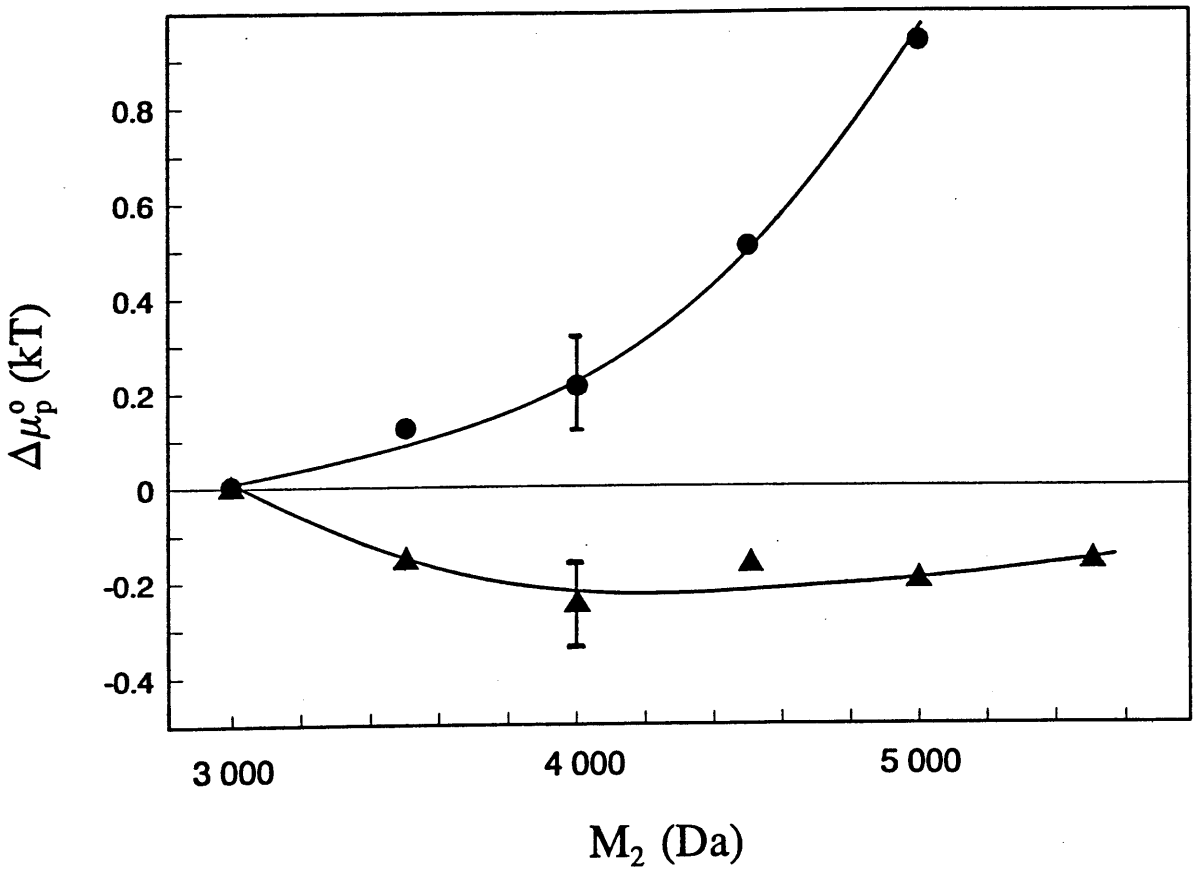

Figure 6.10. Predicted change in the standard-state protein chemical potential in a 10% w/w aqueous PEO solution, relative to a solution of 3 000 Da, $\Delta\mu_p^\circ$, as a function of PEO molecular weight, M_2, for ovalbumin (R_p=29Å, ε=0): (●) protein-polymer interaction characterized by R_g, (▲) protein-polymer interaction characterized by R_{2p}^{HS}.

between the two approaches can lead to *qualitatively* different predictions of the protein chemical potential. Note that the quantities being compared in Figure 6.11 are $\mu_p(\phi_2, \phi_p \to 0, T, \mu_1)$-$\mu_p(\phi_2 \to 0, \phi_p \to 0, T, \mu_1)$ and $\mu_p(\phi_2, \phi_p \to 0, T, P)$-$\mu_p(\phi_2 \to 0, \phi_p \to 0, T, P)$. It is apparent that the change in the protein chemical potential at constant T and μ_1 is always greater than that at constant T and P. This difference can be understood with reference to the imaginary experiment presented in Figure 6.12 (see also Appendix 6.A). A process involving the introduction of species into the right compartment of the cell at constant solvent chemical potential, will result in a higher pressure (P+Π) within the cell as compared to the same process conducted at constant P. In the latter case, following the introduction of impermeable solutes into the right compartment there will be a decrease in the solvent chemical potential. This will be reflected in a decrease in the pressure (P-Π) within the left compartment of the cell. It is essentially this difference in pressure between the two systems, which corresponds to the osmotic pressure of the solution, which is responsible for the difference between the chemical potentials $\mu_p(\phi_2, \phi_p \to 0, T, \mu_1)$-$\mu_p(\phi_2 \to 0, \phi_p \to 0, T, \mu_1)$ and $\mu_p(\phi_2, \phi_p \to 0, T, P)$-$\mu_p(\phi_2 \to 0, \phi_p \to 0, T, P)$.

A second and important difference between the present development and the earlier scaling-thermodynamic treatment is in the accounting of higher-order interactions. In particular, with reference to Eq.(6.2), a truncation was made in an expansion which produces an insignificant error only when $(N_2U_2/V)^2 \ll 1$. As was discussed in Chapter 4, near Θ-solvent conditions for the polymer and for very dilute polymer solutions, this constraint is readily satisified (Abbott et al., 1991a). However, at polymer concentrations, N_2/V, typically encountered in two-phase aqueous polymer systems, is not (typically) satisfied (Abbott et al., 1991a). Consequently, the incorporation of higher-order interactions was a significant advance in the evaluation of the standard-state protein chemical potential. It is interesting that errors introduced by the two approximations in Chapter 4, and discussed above, tend to cancel each other. That is, the correct evaluation of the protein chemical potential at constant T and P, as compared to that at constant T and μ_1, results in a lower protein chemical potential, while the incorporation of the higher-order interactions tends to increase the predicted protein chemical potential.

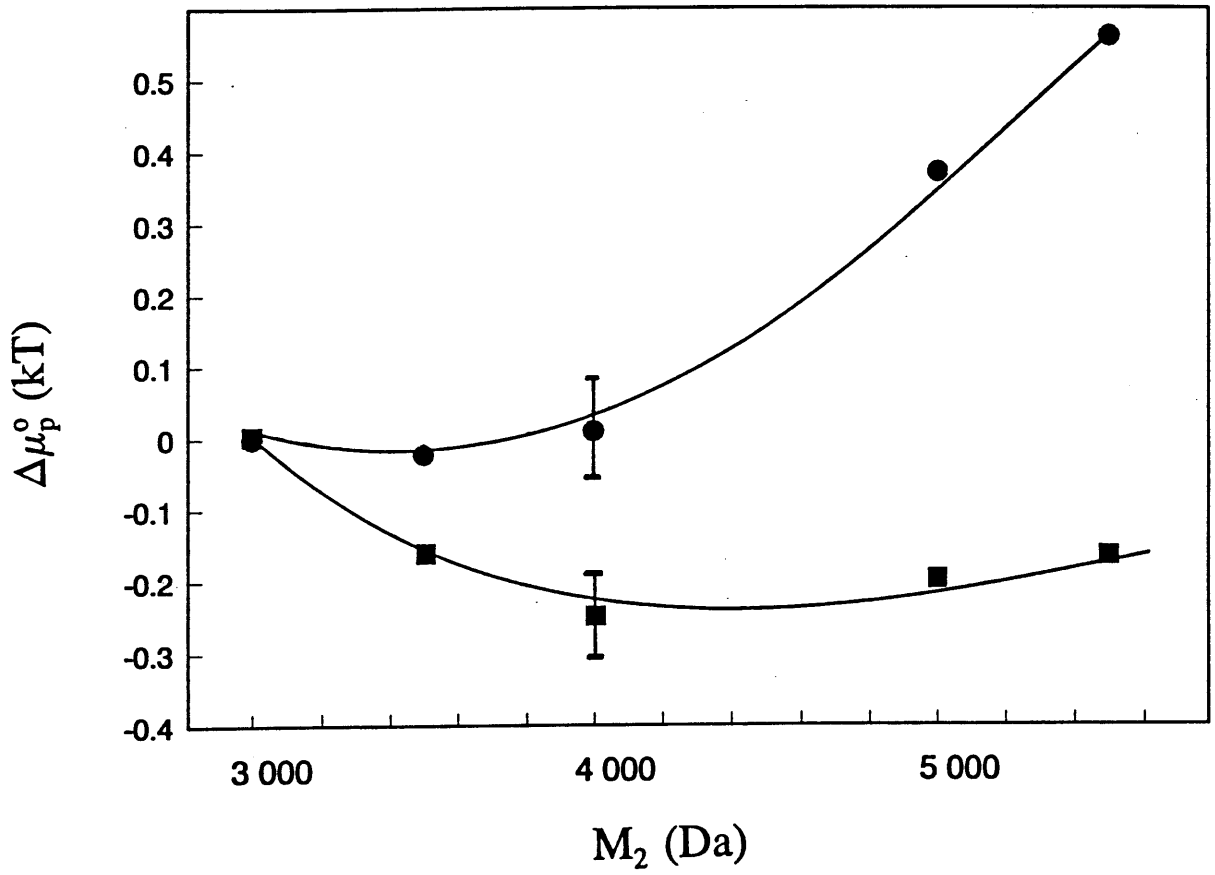

Figure 6.11. Comparison of standard-state protein chemical potential in a 10% w/w aqueous PEO solution, relative to a solution of 3 000 Da, $\Delta\mu_p^\circ$, at constant pressure (■) and at constant solvent chemical potential (●), as a function of PEO molecular weight, M_2: R_p=29Å, ε=0.

Finally, a few comments are in order to connect our conclusions with the suggestions of previous workers. First, our conclusions appear consistent with that of Forciniti and Hall (1990), who examined (using a virial expansion which was truncated at second order) the steric interactions between proteins and polymers (modelling both species for a variety of different geometries), and concluded that the influence of polymer molecular weight on the protein partition coefficient could not be accounted for by steric interactions alone. In addition, our conclusions regarding the presence of weak attractive interactions between the proteins studied and PEO are similar to those based on the lattice model results of Baskir and coworkers (1987 and 1989), who also included an attractive interaction between the protein and the polymer. However, the mechanism through which the attraction influences the protein partitioning behavior is rather different in the two cases. Specifically, our approach recognizes the existence of identifiable polymer coils in the polymer solution phase, and describes the interactions of *polymer coils* with the proteins. Baskir and coworkers considered the polymer solution phase to be a homogeneous polymer solution with a uniform concentration of polymer segments throughout the bulk polymer solution phase (Barkir et al., 1987 and 1989). In contrast, in our description of protein partitioning, we have proposed that it is precisely this transition from the dilute to the entangled polymer solution regimes (with increasing PEO molecular weight) which is the underlying cause of the observed protein partitioning behavior accompanying a change in PEO molecular weight.

In concluding, we have presented a new formulation for the free energy of mixing solutions of proteins and identifiable polymer coils, and have used it to describe experimental observation on the partitioning of proteins in two-phase aqueous PEO-dextran systems. The physical situation we have treated was based on our previous scaling-thermodynamic approach, which revealed that in two-phase aqueous polymer systems containing low-molecular weight PEO, identifiable PEO coils in the PEO-rich solution phase interact with the protein molecules. In the free-energy formulation presented in this paper, we have emphasized the importance of including the penetrable and deformable nature of the polymer in the description of the polymer-polymer and protein-polymer interactions. Furthermore, we have demonstrated that the inclusion of

these considerations can lead to qualitatively different predictions of protein partitioning behavior. Within the framework of the thermodynamic formulation presented, we have concluded that (1) the deformability and penetrability of the polymer coils to the proteins is an essential feature of protein-polymer interactions, (2) direct steric interactions between hydrophilic proteins (considered here) and PEO coils cannot account for the observed influence of PEO molecular weight on the protein partitioning behavior, (3) the contributions of interactions between PEO coils, which are a function of PEO molecular weight, represent an important influence on the observed protein partitioning behavior observed to accompany a change in PEO molecular weight, (4) the presence of weak attractive interactions, of strength 0.01kT to 0.1kT, are consistent with the observed influence of PEO molecular weight on the protein partitioning behavior, (5) deviations of the protein shape from spherical symmetry can significantly influence the predicted protein partitioning behavior, and (6) evaluation of the protein chemical potential at constant solvent chemical potential, rather than at constant pressure, can lead to qualitatively incorrect predictions in the observed protein partitioning behavior. While the above conclusions are based on the evaluation of the predicted protein partitioning behavior (a thermodynamic property of the system), in a Chapter 7 we describe the interpretation of neutron scattering measurements (which reflect the average correlations in the solution) of solutions containing PEO and proteins, and which lead to similar conclusions (Abbott et al., 1991c).

Appendix 6.A

The derivation of Eq.(6.3) is best described with reference to Figure 6.12 which depicts an imaginary cell divided by a membrane which partitions a pure solvent compartment (left compartment) from a compartment which contains solvent and two types of solute macromolecular species (right compartment). In what follows, the solvent will be denoted as component 1, and the solute species as components 2 and 3. Later, components 2 and 3 will be identified as the polymer and protein, respectively. The volume fraction of component i is ϕ_i (i=1,2,3) in the right compartment. The system

is maintained at constant temperature, T. Since the membrane (dotted line) is only permeable to the solvent, the pressure, P, in the right compartment is different from the pressure, P′, in the left compartment. In view of the semipermeable nature of the membrane, the pressure difference across the membrane corresponds to the osmotic pressure, Π, of the macromolecular solution, that is,

$$P' + \Pi(T\ ,\ P\ ,\phi_2\ ,\ \phi_3\ ) = P \tag{6.A1}$$

Note that to define the intensive state of a three-component single-phase system, the Gibbs phase rule requires that 4 intensive and independent state variables be specified (for example, T, P, ϕ_2, ϕ_3) (Modell and Reid, 1983).

Consider the system in Figure 6.12 constrained in such a way that in the right compartment the total pressure, P, is held constant. The Gibbs-Duhem equation for the right compartment is given by

$$N_1 d\mu_1(T,\ P,\ \phi_2,\ \phi_3) + N_2 d\mu_2(T,\ P,\ \phi_2,\ \phi_3) + N_3 d\mu_3(T,\ P,\ \phi_2,\ \phi_3) = 0 \tag{6.A2}$$

where N_i and μ_i (i=1,2,3) are the number of molecules and the chemical potential of component i, respectively (Modell and Reid, 1983). In addition, under conditions of solvent diffusional equilibrium between the two compartments, changes in the solvent chemical potentials in each compartment must be equal, that is,

$$d\mu_1(T,\ P,\ \phi_2\ ,\ \phi_3) = d\mu_1'(T,\ P'\ ) \tag{6.A3}$$

Furthermore, since the left compartment contains pure solvent, it follows that, at constant temperature, changes in the pure solvent chemical potential can only result from changes in the pressure, P′, of the left compartment. That is,

$$d\mu_1'(T,\ P'\ ) = \left[\frac{\partial \mu_1'(T,\ P'\ )}{\partial P'}\right]_T dP' \tag{6.A4}$$

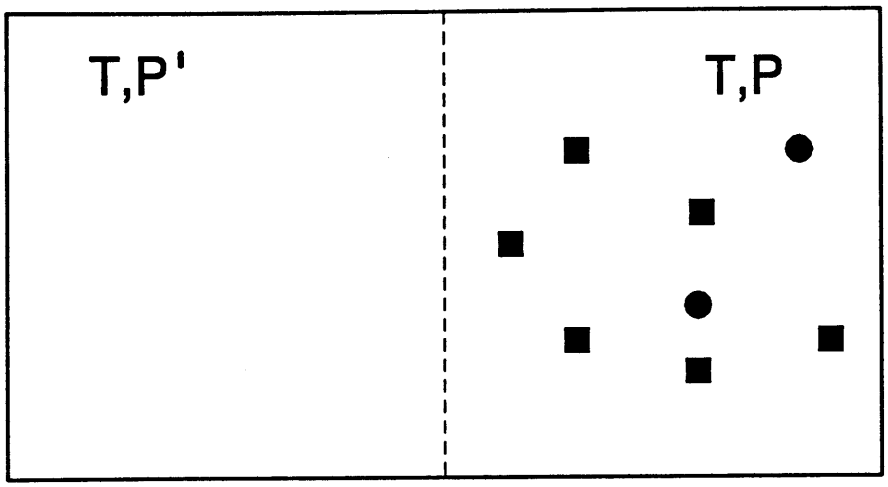

Figure 6.12. Schematic of an imaginary cell, divided by a membrane (dotted line) which partitions a pure solvent compartment (left compartment) from a compartment containing solvent and two types of solute macromolecular species.

Finally, expressing the Gibbs free energy of the left compartment, at constant temperature, as

$$dG'(T, P', N_1')_T = V'dP' + \mu_1'dN_1' \qquad \textbf{(6.A5)}$$

leads to the Maxwell relation

$$\left[\frac{\partial \mu_1'(T\ ,\ P')}{\partial P'}\right]_{T,N_1'} = \left[\frac{\partial V'}{\partial N_1'}\right]_{T,P'} = V_1^o \qquad \textbf{(6.A6)}$$

where V_1^o is the molecular volume of the pure solvent in the left compartment (Modell and Reid, 1983). In view of Eqs.(6.A3), (6.A4) and (6.A6) it follows that

$$d\mu_1(T, P, \phi_2, \phi_3,) = V_1^o dP' \qquad \textbf{(6.A7)}$$

At constant P, Eq.(6.A1) implies that $dP' = -d\Pi(T, P, \phi_2, \phi_3)$. Using this result in Eq.(6.A7), and subsequently inserting the resulting expression for $d\mu_1$ in Eq.(6.A2) yields

$$N_2 d\mu_2(T, P, \phi_2, \phi_3) + N_3 d\mu_3(T, P, \phi_2, \phi_3) = N_1 V_1^o d\Pi(T, P, \phi_2, \phi_3) \qquad \textbf{(6.A8)}$$

Differentiating Eq.(6.A8) with respect to ϕ_2, at constant T, P and ϕ_3 yields

$$N_2\left[\frac{\partial \mu_2}{\partial \phi_2}\right]_{T,P,\phi_3} + N_3\left[\frac{\partial \mu_3}{\partial \phi_2}\right]_{T,P,\phi_3} = N_1\ V_1^o\left[\frac{\partial \Pi}{\partial \phi_2}\right]_{T,P,\phi_3} \qquad \textbf{(6.A9)}$$

In general, the osmotic pressure in the right compartment is a function of temperature, T, pressure, P, and the volume fractions, ϕ_2 and ϕ_3. For the case of incompressible solutes and constant temperature, T, assumed in this derivation, the osmotic pressure in

the righthand side of Eq.(6.A9) becomes a functional of only ϕ_2 and ϕ_3. Therefore, since the osmotic pressure is independent of both the system pressure and the solvent chemical potential,

$$\left[\frac{\partial\Pi(\phi_2,\,\phi_3)}{\partial\phi_2}\right]_{T,P,\,\phi_3} = \left[\frac{\partial\Pi(\phi_2,\,\phi_3)}{\partial\phi_2}\right]_{T,\,\mu_1,\,\phi_3} \qquad \textbf{(6.A10)}$$

In view of Eq.(6.A10), and utilizing volume fraction units ($\phi_i = N_i V_i^o/V$, where V is the volume of the right compartment), Eq.(6.A9) leads to the central result that

$$\frac{\phi_2}{V_2^o}\left[\frac{\partial\mu_2}{\partial\phi_2}\right]_{T,\,P,\,\phi_3} + \frac{\phi_3}{V_3^o}\left[\frac{\partial\mu_3}{\partial\phi_2}\right]_{T,\,P,\,\phi_3} = \phi_1\left[\frac{\partial\Pi}{\partial\phi_2}\right]_{T,\,\mu_1,\,\phi_3} \qquad \textbf{(6.A11)}$$

where V_2^o and V_3^o are the molecular volumes of components 2 and 3, respectively. The importance of Eq.(6.A11) rests in the fact that it relates the chemical potentials of the macromolecules at constant pressure, P, (the left-hand side of Eq.(6.A11)) to a thermodynamic property of the same system at constant solvent chemical potential, μ_1. An equivalent expression to Eq.(6.A11) can be obtained by differentiating Eq.(6.A8) with respect to ϕ_3, rather than ϕ_2, at constant ϕ_2, T, P.

To evaluate the right-hand side of Eq.(6.A11), it is useful to consider an alternative constraint imposed on the system shown in Figure 6.12 where now the pressure P′ in the left compartment is held constant (along with the temperature). Under these conditions, in view of Eq.(6.A4), the solvent chemical potential in the left compartment, $\mu_1'(T,P')$, is constant. In that case, Eq.(6.A3) implies that

$$d\mu_1(T,\,P,\,\phi_2,\,\phi_2) = d\mu_1'(T,\,P') = 0 \qquad \textbf{(6.A12)}$$

In addition, at constant P′, Eq.(6.A1) implies that the pressure change in the right compartment, dP, is equal to the osmotic pressure change, dΠ, that is

$$dP = d\Pi(T,\ P,\ \phi_2,\ \phi_3) \tag{6.A13}$$

For the right compartment, under isothermal conditions, and using Eq.(6.A12), the Gibbs-Duhem equation takes the following form (Modell and Reid, 1983)

$$N_2 d\mu_2(T,\ P,\ \phi_2,\ \phi_3) + N_3 d\mu_3(T,\ P,\ \phi_2,\ \phi_3) = VdP \tag{6.A14}$$

Substituting Eq.(6.A13) in Eq.(6.A14) and utilizing volume fraction units, leads to the result

$$\frac{\phi_2}{V_2^o} d\mu_2(T,\ P,\ \phi_2,\ \phi_3) + \frac{\phi_3}{V_3^o} d\mu_3(T,\ P,\ \phi_2,\ \phi_3) = d\Pi(T,\ P,\ \phi_2,\ \phi_3) \tag{6.A15}$$

Differentiating Eq.(6.A15) with respect to ϕ_2 at constant T, μ_1 and ϕ_3 yields

$$\frac{\phi_2}{V_2^o}\left[\frac{\partial \mu_2}{\partial \phi_2}\right]_{T,\ \mu_1,\ \phi_3} + \frac{\phi_3}{V_3^o}\left[\frac{\partial \mu_3}{\partial \phi_2}\right]_{T,\ \mu_1,\ \phi_3} = \left[\frac{\partial \Pi}{\partial \phi_2}\right]_{T,\ \mu_1,\ \phi_3} \tag{6.A16}$$

Multiplying Eq.(6.A16) by ϕ_1, and substituting the resulting expression for $\phi_1(\partial\Pi/\partial\phi_2)_{T,\ \mu 1,\ \phi 3}$ in the right-hand side of Eq.(6.A11), yields

$$\frac{\phi_2}{V_2^o}\left[\frac{\partial \mu_2}{\partial \phi_2}\right]_{T,\ P,\ \phi_3} + \frac{\phi_3}{V_3^o}\left[\frac{\partial \mu_3}{\partial \phi_2}\right]_{T,\ P,\ \phi_3} = \frac{\phi_1\ \phi_2}{V_2^o}\left[\frac{\partial \mu_2}{\partial \phi_2}\right]_{T,\ \mu_1,\ \phi_3} + \frac{\phi_1 \phi_3}{V_3^o}\left[\frac{\partial \mu_3}{\partial \phi_2}\right]_{T,\ \mu_1,\ \phi_3} \tag{6.A17}$$

The equivalent expression to Eq.(6.A17), which accounts for the variation of the chemical potentials with respect to the volume fraction of component 3, is given by

$$\frac{\phi_2}{V_2^o}\left[\frac{\partial \mu_2}{\partial \phi_3}\right]_{T,\,P,\,\phi_2} + \frac{\phi_3}{V_3^o}\left[\frac{\partial \mu_3}{\partial \phi_3}\right]_{T,\,P,\,\phi_2} = \frac{\phi_1\,\phi_2}{V_2^o}\left[\frac{\partial \mu_2}{\partial \phi_3}\right]_{T,\,\mu_1,\,\phi_2} + \frac{\phi_1 \phi_3}{V_3^o}\left[\frac{\partial \mu_3}{\partial \phi_3}\right]_{T,\,\mu_1,\,\phi_2} \tag{6.A18}$$

With the knowledge of the chemical potentials μ_2 and μ_3 at constant solvent chemical potential that is, the terms on the right-hand sides of Eqs.(6.A17) and (6.A18), these two equations provide coupled differential equations whose solution yields expressions for the chemical potentials, μ_2 and μ_3, as a function of compositions, ϕ_2 and ϕ_3, at constant pressure, P, and temperature, T.

To connect the formulation presented above to the protein partitioning problem, we identify component 2 with the polymer species and component 3 with the protein species. Accordingly, component 3 is renamed as component p. It is noteworthy that in the protein partitioning case, the solution of Eqs.(6.A17) and (6.A18) for the protein and polymer chemical potentials is simplified considerably by the fact that we are concerned with the limit of vanishing protein concentration, namely, $\phi_p \to 0$ (Abbott et al., 1991a). Therefore, we do not need to solve Eq.(6.A18) since this equation describes the dependence of the protein and polymer chemical potentials on protein concentration. Furthermore, in Eq.(6.A17), the polymer chemical potential, μ_2, becomes independent of protein concentration, that is, in the limit of vanishing protein concentration, the contribution of the protein to the osmotic pressure is negligible, as compared to polymer contribution. Thus, in Eq.(6.A17), the terms describing the polymer chemical potential are independent from the terms involving the protein, while the protein chemical potential *is* dependent on the polymer presence (since this determines the osmotic pressure of the solution). Therefore, Eq.(6.A17) yields the two equations,

$$\frac{\phi_2}{V_2^o}\left[\frac{\partial \mu_2}{\partial \phi_2}\right]_{T,P,\phi_p} = \frac{\phi_1\,\phi_2}{V_2^o}\left[\frac{\partial \mu_2}{\partial \phi_2}\right]_{T,\mu_1,\phi_p} \qquad \textbf{(6.A19)}$$

and

$$\frac{\phi_p}{V_p^o}\left[\frac{\partial \mu_p}{\partial \phi_2}\right]_{T,P,\phi_p} = \frac{\phi_1\phi_p}{V_p^o}\left[\frac{\partial \mu_p}{\partial \phi_2}\right]_{T,\mu_1,\phi_p} \qquad \textbf{(6.A20)}$$

Note that Eq.(6.A19) can be derived by considering simply a two component system containing polymer and water. The solution of Eq.(6.A19) provides the polymer chemical potential at constant pressure. However, since our interest is in the influence of the polymer concentration on the protein chemical potential, we need solve only Eq.(6.A20). Equation (6.A20) can be rewritten as

$$\frac{1}{(1-\phi_2)}\left[\frac{\partial \mu_p}{\partial \phi_2}\right]_{T,P,\phi_p} = \left[\frac{\partial \mu_p}{\partial \phi_2}\right]_{T,\mu_1,\phi_p} \qquad \textbf{(6.A21)}$$

where the approximation, $\phi_1=1-\phi_2-\phi_p=1-\phi_2$, valid for vanishing protein concentrations, has been used. Equation (6.A21) is a central result that will be used in Section 2 to evaluate changes in the protein chemical potential at constant pressure from changes in the protein chemical potential occurring at constant solvent chemical potential (see Eq.(6.3)). Specifically, the usefulness of Eq.(6.A21) results from the fact that the term on the right-hand side has been evaluated previously from an equation of state for the case of hard-sphere mixtures (Jansen et al., 1986a).

Appendix 6.B

In Section 6.5, in calculating the influence of attractive interactions on the

standard-state protein chemical potential using a perturbation approach, the following approximation was made to derive Eq.(6.27)

$$\langle \exp(-\beta V_{ij}^{(1)}) \rangle = 1 + \langle -\beta V_{ij}^{(1)} \rangle + O\left(\langle \beta^2 V_{ij}^{(1)2} \rangle\right) \qquad \textbf{(6.B1)}$$

where the truncation of the expansion in $\beta V_{ij}^{(1)}$ ($\beta = 1/kT$) is valid when $-\beta V_{ij}^{(1)} \ll 1$. In order to assess the validity of this truncation, the theory of Barker and Henderson (1967) was used to estimate the size of the term of order $(\beta V_{ij}^{(1)})^2$. In order to justify the truncation at order $\beta V_{ij}^{(1)}$, it can be readily shown that the following constraint must be satisfied (McQuarrie, 1976).

$$-\frac{1}{2}\frac{\int_0^\infty \langle (\beta V_{ij}^{(1)}(r))^2 \rangle \, d^3r}{\int_0^\infty \langle \beta V_{ij}^{(1)}(r) \rangle \, d^3r} \ll 1 \qquad \textbf{(6.B2)}$$

The denominator in Eq.(6.B2) was evaluated using the Monte-Carlo scheme described in Section 6.5, and the term $<V_{ij}^{(1)}(r)^2>$ in the numerator was readily calculated by an analogous technique (see Section 6.5) from the summation

$$\langle (\beta V_{2p}^{(1)}(r))^2 \rangle = \frac{\sum^{\{C\}} (m_s \varepsilon)^2 e^{(m_s \varepsilon)^2}}{\sum^{\{C\}} e^{(m_s \varepsilon)^2}} \qquad \textbf{(6.B3)}$$

In Table 6.3, for a spherical colloid with a 37Å radius (the size of bovine serum albumin) and a polymer chain with 147 statistical segments (the size of PEO 8,650 Da), the ratio defined by Eq.(6.B2) is presented for a range of interaction strengths ε. For this relatively large protein and PEO molecular weight, it is evident that provided that the interaction strength is less than approximately 0.1kT per polymer segment

interaction with the protein, the error introduced in the truncation of Eq.(6.B1) is relatively small. For attractive interactions stronger than 0.1kT, a significant error (>20%) can result, although the qualitative features are expected to remain the same. For the smaller molecular weights of PEO investigated in other sections of this paper the truncation error will be less.

Polymer Segment Interaction Strength ε	Truncation Error
0.01	0.02
0.03	0.05
0.05	0.08
0.07	0.13

Table 6.3. Truncation error evaluated using Eq.(6.B2) as a function of the strength of the attraction between a polymer segment and a protein, ε, for bovine serum albumin (R_p=37Å) and PEO 8 650 Da.

6.7 Literature Cited

Abbott, N.L.; Blankschtein, D.; Hatton, T.A. *Bioseparation*, **1990**, 1, 191.

Abbott, N.L.; Blankschtein, D.; Hatton, T.A. *Macromolecules*, **1991a**, 24, 4334.

Abbott, N.L.; Blankschtein, D.; Hatton, T.A. *Macromolecules*, **1991b**, submitted.

Abbott, N.L.; Blankschtein, D.; Hatton, T.A. *Macromolecules*, **1991c**, submitted.

Albertsson, P.A. *Partition of Cell Particles and Macromolecules*; Wiley: New York, **1986**.

Albertsson, P.-A.; Cajarville, A.; Brooks, D.E.; Tjerneld, F. *Biochim. Biophys. Acta*, **1987**, 926, 87.

Barker, J.A.; Henderson, D., *J. Chem. Phys.*, **1967**, 47, 2856.

Baskir, J.N.; Hatton, T.A.; Suter, U.W., *Macromolecules*, **1987**, 20, 1300.

Baskir, J.N.; Hatton, T.A.; Suter, U.W. *Biotechnol. Bioeng.*, **1989a**, 34, 541.

Baskir, J.N.; Hatton, T.A.; Suter, U.W., *J. Phys. Chem.*, **1989b**, 93, 2111.

Cabane, B.; Duplessix, R. *J. Phys.*, **1982**, 43, 1529.

Cabane, B.; Duplessix, R. *J. Phys.*, **1987**, 48, 651.

Carnahan, N.F.; Starling, K.E.; *J. Chem. Phys.*, **1969**, 51, 635.

Carnahan, N.F.; Starling, K.E.; *J. Chem. Phys.*, **1970**, 53, 600.

Chevalier, Y.; Zemb, T. *Rep. Prog. Phys.* **1990**, 53, 279.

Cotton, J.P.; Farnoux, B.; Jannink, G. *J. Chem. Phys.* **1972**, 57, 290.

Creighton, T.E. *Proteins: Structures and Molecular Properties*, Freeman: New York, **1984**.

Daoud, M.; Cotton, J.P.; Farnoux, B.; Jannink, G.; Sarma, G.; Benoit, H.; Duplessix, R.; Picot, C.; de Gennes, P.G. *Macromolecules*, **1975**, 8, 804.

de Gennes, P.-G. *Scaling Concepts in Polymer Physics*; Cornell University Press: Ithaca N.Y., **1988**.

de Hek, H.; Vrij, A. *J. Colloid Interface Sci.* **1981**, 84, 409.

Dey, D.; Hirtzel, C.S. *Colloid Polym. Sci.*, **1991**, 269, 28.

Dill. K.A.; Alonso, D.O.V. *Protein Structure and Protein Engineering*, **1988**, 39, 51.

Edmond, E.; Ogston, A.G. *Biochem. J.*, **1968**, 109, 569.

Farnoux, B.; Daoud, M.; Decker, D.; Jannink, G.; Ober, R.; *J. Phys.* **1975**, 36, L-35.

Flory, P.J. *Principles of Polymer Chemistry*; Cornell University Press: Ithaca N.Y., **1986**.

Flory, P.J.; Krigbaum, W.R. *J. Chem. Phys.*, **1950**, 18, 1086.

Flory, P.J. *Statistical Mechanics of Chain Molecules*, Wiley: New York, **1968**.

Forciniti, D.; Hall, C.K., *ACS Symp. Ser.* **1990**, 419, 53.

Guo, X.H.; Zhao, N.M.; Chen, S.H.; Teixeira, J.; *Biopolymers*, **1990**, 29, 335.

Haynes, C.A.; Beynon, R.A.; King, R.S.; Blanch, H.W.; Prausnitz, J. *J. Chem. Phys.*, **1989**, 93, 5612.

Hermans, J. *J. Chem. Phys.*, **1982**, 77, 2193.

Hermans, J.J; Hermans, J. *J. Polym. Sci.*, **1984**, 22, 279.

Hustedt, H.; Kroner, K.H.; Stach, W.; Kula, M.-R. *Biotechnol. Bioeng.*, **1978**, 20, **1989**.

Israelachvili, J.N.; Mitchell, D.J.; Ninham B.W. *J. Chem. Soc. Faraday Trans. II*, **1976**, 72, 1525.

Israelachvili, J.N. *Intermolecular and Surface Forces with Applications to Colloidal and Biological Systems*, Academic Press: London, **1985**.

Jansen, J.W.; de Kruif, C.G.; Vrij, A. *J. Colloid Interface Sci.*, **1986a**, 114, 471.

Jansen, J.W.; de Kruif, C.G.; Vrij, A. *J. Colloid Interface Sci.*, **1986b**, 114, 481.

Jansen, J.W.; de Kruif, C.G.; Vrij, A. *J. Colloid Interface Sci.*, **1986c**, 114, 492.

Jansons, K.M.; Phillips, C.G.; *J. Colloid Interface Sci.*, **1990**, 137, 75.

Lin, M.Y.; Lindsay, H.M.; Weitz, D.A.; Ball, R.C.; Klein, R.; Meakin, P. *Nature*, **1989**, 339, 360.

McQuarrie, D.A. *Statistical Mechanics*, Harper & Row: New York, **1976.**

Modell, M.; Reid, R.C. *Thermodynamics and Its Applications*, Prentice-Hall: New Jersey, **1983**.

Momii, T.; Numasawa, N.; Kuwamamoto, K.; Nose, T. *Macromolecules*, **1991**, 24, 3964.

Orofino, T.A.; Flory, P.J. *J. Chem. Phys.*, **1957**, 26, 1067.

Patel, P.D.; Russel, W.B. *J. Colloid Interface Sci.* **1989a**, 131, 192.

Patel, P.D.; Russel, W.B. *J. Colloid Interface Sci.* **1989b**, 131, 201.

Peters, T. *Adv. Protein Chem.*, **1985**, 37, 161.

Puvvada, S.; Blankschtein, D., *J. Chem. Phys.* **1990**, 92, 3710; and references cited therein.

Rogers, J.A.; Tam, T. *Can. J. Pharm. Sci.*, **1977**, 12, 65.

Sutherland, I.A.; Fisher, D., *Separations using Aqueous Two-Phase Systems*; Plenum, New York, **1989**.

Tanford, C. *Physical Chemistry of Macromolecules*; Wiley: New York, **1961**.

Tanner, R.E.; Herpigny, B.; Chen, S.-H.; Rha, C.K. *J. Chem. Phys.*, **1982**, 76, 3866.

Wall, F.T.; Mandel, F., *J. Chem. Phys.*, **1975**, 63, 4592.

Walter, H.; Brooks, D.E.; Fisher, D., *Partitioning in Aqueous Two-Phase Systems*; Academic Press: New York, **1985**.

Wilcoxen, J.P.; Martin, J.E.; Schaefer, D.W. *Phys. Rev. A* **1989**, 39, 2675.

Vincent, B.; Luckham, P.F.; Waite, F.A. *J. Colloid Interface Sci.* **1979**, 73, 508.

Vrij, A. *Pure & Appl. Chem.*, **1976**, 48, 471.

Zimm, B.H.; Stockmayer, W.H.; Fixman, M. *J. Chem. Phys.*, **1953**, 21, 1716.

Chapter 7.

A Small Angle Neutron Scattering Investigation of Proteins in Aqueous Polymer Solutions

7.1 Introduction

In Chapter 3, the nature of protein-polymer interactions was explored through the development of novel molecular-level pictures for the structure of polymer solution phases. Accompanying the development of the novel molecular-level pictures for the interactions between proteins and polymers in solution, complementary scaling-thermodynamic descriptions were advanced for each physical scenario to predict the associated protein partitioning behaviors (Chapter 4). On the basis of these scaling arguments, it was concluded that although the physical exclusion of the proteins by the polymer coils contributes to the observed partitioning behavior, other interactions between polymers and proteins need to be considered to explain the observed partitioning trends. In particular, the influence of the PEO molecular weight on the partitioning behavior of the series of proteins (Hustedt et al., 1978; Albertsson et al., 1987), cytochrome-c, ovalbumin, bovine serum albumin, catalase, pullulanase and phosphorylase, was observed to be consistent with the presence of a weak attractive interaction (in addition to physical exclusion) between the protein molecules and the polymer coils (Abbott et al., 1991a). In Chapter 6, the thermodynamic properties of polymer solution phases containing globular proteins were investigated further using a more quantitative evaluation of the steric and non-steric (attractive) interactions between proteins and polymers (Abbott et al., 1991b). Specifically, the protein-polymer interactions were evaluated using a simple Monte-Carlo scheme which included the influence of both repulsive steric and short-ranged attractive interactions. The

experimental trends in the protein partitioning behavior were reproduced by allowing for a weak attractive interaction energy, ε, which appeared to increase with protein size, R_p, where $17\text{Å} < R_p < 51\text{Å}$, from order 0.01kT to 0.1kT per polymer segment at the protein surface, where k is the Boltzmann constant.

The aim of the work presented in this chapter is to support and confront the theoretical developments on the partitioning of proteins in two-phase aqueous polymer systems, which were presented in Chapters 3-6, through a comparison with more precise experiments. In doing so, we hoped to provide, in some cases, a verification of the theoretical predictions and, in other cases, some guidance for future developments. The experimental investigation reported in this chapter represents a significant departure from the many previous experimental investigations (Albertsson, 1985; Walter et al., 1985; Walter and Johansson, 1986; Carlson, 1988; Abbott et al., 1990; Walter et al., 1991) of protein paritioning in two-phase aqueous polymer systems in that we probe, using small angle neutron scattering (SANS) techniques, both the *structure* and the *thermodynamic properties* of aqueous polymer solution phases which contain proteins, rather than measuring only thermodynamic properties, such as the protein partitioning behavior. We also deal with a one-phase system, and in doing so, remove the ambiguity associated with the interpretation of protein partitioning behavior, where the experimental measurements reflect the *difference* between the interactions of proteins with each of *two* coexisting polymer solution phases.

Small angle scattering methods (x-rays, neutrons and light) interpret the interference patterns in the scattered radiation to yield information regarding the average correlations of the scattering centers (structure) within a sample (Guinier and Fournet, 1955; Cabane, 1987; Glatter and Kratky, 1982). For a given sample, the type of interference pattern produced, and thus the length scales of the average correlations measured by each scattering method, depends upon two factors: (1) the wavelength of the radiation source, λ, and (2) the scattering angle, θ. Reflecting these facts, the magnitude of the scattering vector (or the momentum transferred) is defined as (Guinier and Fournet, 1955; Cabane, 1987; Glatter and Kratky, 1982),

$$q = \frac{4\pi}{\lambda}\sin\theta \qquad (7.1)$$

For a given q, the scattering is primarily produced by structure in the solution on length scales of $2\pi/q$. Accordingly, to probe the polymer-protein solution structure in the range of length scales from approximately 20Å (typical sizes of proteins and polymers) to 500Å (many times the sizes of proteins and polymers), a q-range from about $0.4Å^{-1}$ to $0.01Å^{-1}$ is required. Light scattering, performed with typical wavelengths, λ, of around 5 500Å only provides access to the smaller q-range around $10^{-3}Å$, and is, therefore, not suitable for the present studies (Pecora, 1985). In contrast, both neutrons and x-rays used in scattering experiments have much smaller wavelengths (Guinier and Fournet, 1955, Cabane, 1987; Glatter and Kratky, 1982). For example, a typical radiation wavelength from a cold neutron source is 5Å, and thus provides ready access to a q-range of $0.02Å^{-1}$ to $0.3Å^{-1}$ with variations in the scattering angle, θ ($0.5° < \theta < 7°$). In addition, the scattering of neutrons is very sensitive to the isotopic substitution of hydrogen by deuterium, and, therefore, neutron scattering experiments conducted in D_2O exploit the difference in the number densities of deuterium atoms in, for example, hydrogenated macromolecules and the surrounding deuterium-rich solvent medium (D_2O) (Cabane, 1987).

While the above discussion has focussed on considerations related to deriving structural information from small angle scattering, it is also relevant to point out that in the limit of $q \to 0$, where very large length scales of the solution are probed, information on the thermodynamic state of the solution can also be obtained (Guinier and Fournet, 1955; Cabane, 1987; Glatter and Kratky, 1982). Provided that $q \ll 2\pi/d$, where d is the characteristic dimension of the macromolecules in solution, the scattering is no longer sensitive to the shapes of the molecules, but rather to the local fluctuations in the concentrations of the molecules within a volume, V, which is macroscopically small, but much larger than the macromolecular length scale (specifically, it must be large enough such that there are sufficient molecules within V for thermodynamic concepts to be relevant). The magnitude of the concentration fluctuations is related, through fluctuation

theory, to the isothermal osmotic compressibility of the solution (Guinier and Fournet, 1955; Cabane, 1987; Glatter and Kratky, 1982). Accordingly, by examining the scattered intensity of neutrons in the limit $q \ll 2\pi/d$, the thermodynamic properties (for example, the isothermal osmotic compressibility) of aqueous protein-polymer solutions can be measured, and consequently the important connection between the structure of the solutions and their thermodynamic properties (as explored theoretically in Chapters 3, 4 and 6 (Abbott et al., 1991a and b)) can be probed and investigated further.

The remainder of this chapter is organized as follows. In Section 7.2, experimental considerations associated with SANS from aqueous PEO solutions, aqueous bovine serum albumin (BSA) solutions, and their aqueous mixtures are discussed. Note that BSA was chosen as a model hydrophilic protein since it has been the subject of prior SANS investigations (Bendedouch and Chen, 1983; Nossal et al., 1986; Chen and Bendedouch, 1986), and its partitioning behavior in two-phase aqueous polymer systems containing PEO-rich phases has also been examined (Albertsson et al., 1987). In Sections 7.3 and 7.4, the measurement and interpretation of SANS from (i) aqueous PEO solutions, and (ii) aqueous BSA solutions are presented. In particular, Section 7.3 examines the proposal advanced in Chapter 3, that the underlying influence (on protein partitioning) of changes in PEO molecular weight in the two-phase aqueous PEO-dextran system is a transition in the structure of the PEO-rich solution phase (as discussed above) (Abbott et al., 1991a). Following the experimental confirmation of the existence of this transition, and using polymer solution models appropriate for describing the polymer solution structure determined in Section 7.3, a more quantitative interpretation is presented for the intensity of neutrons scattered at small angles from polymer solutions containing identifiable polymer coils. In particular, the connection between the thermodynamic and structural characteristics of the PEO solution is investigated. These studies highlight the fact that while certain polymer-polymer intermolecular potentials can successfully describe the thermodynamic properties of the PEO solution, they predict the average correlation functions (structure), as measured by SANS intensities, less adequately.

In Section 7.4, measurements presented for the neutron intensities scattered

from BSA solutions (without PEO) serve two central purposes. First, the measurements confirm that the solutions are sufficiently dilute so that protein-protein interactions are not a dominating factor in determining the intensity of scattered neutrons. Second, the measurements enable the determination of the contrast factor of BSA in D_2O, which is a prerequisite for the interpretation of SANS from solutions containing mixtures of BSA and PEO.

In Section 7.5, SANS measurements from mixtures of PEO and BSA in aqueous solution are presented. Interpretation of the scattering results provide the first independent experimental verification that, while the net interaction between BSA and PEO is repulsive, the strength of this repulsive interaction is less than that corresponding to excluded-volume interactions. This is consistent with our previous statistical-thermodynamic models (Abbott et al., 1991a and b) (and those of others (Baskir et al., 1987 and 1989; Forciniti and Hall, 1990)) which suggest that a weak attractive interaction exists between the PEO coils and certain protein molecules, mediated by water, although the net interaction is repulsive. A quantitative comparison is made between the strength of the attraction required to predict the SANS measurements from solutions containing BSA and PEO and that required to predict the partitioning behavior of BSA in two-phase aqueous PEO-dextran systems. Finally, Section 7.6 presents our concluding remarks.

7.2 Materials and Experimental Methods

7.2.A Materials

Molecular weight standard grade PEO was purchased from Polysciences Inc. (Warrington PA) having molecular weights of (in Da) 1 450 ($M_w/M_n=1.10$), 4 250 ($M_w/M_n=1.10$), 8 650 ($M_w/M_n=1.10$), 23 000 ($M_w/M_n=1.13$) and from Toyo Soda (Japan) 45 000 ($M_w/M_n=1.07$), 85 000 ($M_w/M_n=1.06$), 160 000 ($M_w/M_n=1.07$), 270 000 ($M_w/M_n=1.09$) and 860 000 ($M_w/M_n=1.17$), where M_w and M_n are the weight-average and number-average molecular weights, respectively. The polydispersivity

indices (M_w/M_n) were reported by the manufacturers. BSA was purchased from Sigma Chemical (St Louis, MO), catalogue #A-7030. The D_2O was purchased from Aldrich Chemical (Milwaukee, WI) and had a nominal purity of 99.8%. All other chemicals used were of analytical reagent grade.

7.2.B Sample Preparation and Measurements

For the SANS measurements of the PEO solutions reported in Section 7.3A, the solvent was pure D_2O (as detailed below, this contrasts to the experiments reported in Sections 7.3B, 7.4 and 7.5, where 0.5M sodium acetate was present in the samples). The PEO-D_2O solutions were prepared 10 hours before measurement and stirred with small magnetic stir bars to ensure complete dissolution of PEO. The solutions were prepared by weighing the desired mass of polymer into a known volume of D_2O. All experimental measurements were performed at 25°C in a thermostated cell holder and at ambient pressure.

For the SANS measurements of aqueous PEO solutions, aqueous BSA solutions, as well as aqueous BSA-PEO solutions, reported in Sections 7.3B, 7.4 and 5, respectively, all solutions were prepared with 0.5M sodium acetate at pH 5.6 (the isoelectric pH of BSA is approximately 4.9) (Squire et al., 1968). The salt was present to buffer the solution pH and screen the electrostatic interactions between the charged BSA molecules. The inclusion of 0.5M anhydrous sodium acetate had a negligible contribution to the incoherent scattering of the solution due to the hydrogens on the acetate ion (Cabane, 1987). As noted above, 0.5M sodium acetate was included in all the samples connected with the investigation of PEO-BSA interactions to ensure that any salt effects, for example, on the solvent quality for PEO (Ataman and Boucher, 1982; Florin et al., 1984), are uniformly present throughout the SANS measurements.

The SANS experiments were conducted at the Brookhaven National Laboratory's High Flux Beam Reactor (HFBR) using the Department of Biology low angle spectrometer (Schneider and Schoenborn, 1984). Before being scattered by the sample,

the neutron beam was conditioned by passing it through a Be filter, a monochrometer, and 3 collimators to produce an average neutron wavelength of 4.9Å. The neutron flux was typically $3.5x10^6$ neutrons/cm^2s. The liquid samples were housed in flat cylindrical cells made of quartz and with a path length of 2mm. The two-dimensional detector for the scattered neutrons contained 128 x 128 detector elements (pixels) and was 50cm x 50cm in size. The experimental quantity measured was the recorded number of neutron collisions with each detector pixel. The raw neutron scattering measurements were corrected for (i) background scattering, (ii) empty cell scattering, (iii) sample transmission, and (iv) variations in the efficiency of the detector elements (according to the method of Chen and Bendedouch (1986) which is discussed in Appendix 7.A).

7.3 Neutron Scattering from Aqueous PEO Solutions

7.3.A Measurement of the Polymer Solution Structure

In Section 7.1, the importance of the predicted transition in the structure of the top PEO-rich phase (from singly dispersed polymer coils to an entangled polymer web) of the two-phase aqueous PEO-dextran system was outlined. In view of the important consequences of this prediction (Abbott et al., 1991a and b), the first objective of the neutron scattering investigation was to experimentally test the existence of such a transition over the range of PEO concentrations and molecular weights typically encountered in two-phase aqueous PEO-dextran systems. A summary of this experimental investigation can be found in Chapter 3.

In general, the scattering of neutrons from macromolecules dispersed in a low molecular weight solvent (such as D_2O) reflects both spatial correlations between scattering sites within the same macromolecule (intramolecular correlations), as well as those correlations between scattering sites which belong to different macromolecules (intermolecular correlations) (Guinier and Fournet, 1955; Cabane, 1987; Glatter and Kratky, 1982). In the limit of vanishing concentration, the macromolecules are uncorrelated in their positions and only the intramolecular correlations between the

scattering sites will contribute to the measured intensity of scattered neutrons. For isotropic solutions, the scattering in the limit of very small angles (defined more precisely below) is independent of the precise shape of the macromolecule, being determined solely by its effective radius of gyration (Guinier and Fournet, 1955; Cabane, 1987; Glatter and Kratky, 1982). The term "effective radius of gyration" is used here to denote a radius which reflects the distribution of scattering sites within the macromolecule, rather than the distribution of mass. The result for the intensity of neutrons, I(q), scattered at very small angles is the well known Guinier limit (Guinier and Fournet, 1955)

$$\frac{I(x)}{I(0)} = 1 - \frac{x}{3} + O(x^2) \qquad \textbf{(7.2)}$$

where $x = q^2R^2_g$, with R_g the effective radius of gyration of the macromolecule. When the shape of a macromolecule is unknown, Eq.(7.2), which is a simple expansion of the intensity at small x (truncated at order x^2), will be accurate only for the small scattering angles satisfying the constraint $x \ll 1$. For flexible chain molecules (denoted as component 2), a slightly different form of the mathematical expansion in Eq.(7.2), which remains valid up to higher scattering angles ($x \sim 1$) has been suggested, namely (Cabane, 1987),

$$\frac{I_2(0)}{I_2(x)} = 1 + \frac{x}{3} \qquad \textbf{(7.3)}$$

Equation (7.3) constitutes a useful form for the interpretation of neutron scattering from dilute polymer solutions.

In contrast to the dilute solution limit considered above, for polymer solutions of sufficiently high molecular weight and concentration, the polymer coils overlap extensively and entangle to form a flexible mesh or net structure (de Gennes, 1988). Within the entangled mesh of polymer coils, the separate identities of the individual polymer coils are lost and the scattering of neutrons reflects both intramolecular and intermolecular correlations between polymer segments in the solution

(de Gennes, 1988). At short length scales which satisfy $r < \xi$, where ξ is the correlation length of the polymer web, or equivalently for scattering angles which satisfy $q > 1/\xi$, the correlations measured are those which occur between the polymer segments belonging to the same polymer chain (intramolecular correlations). Accordingly, for $q > 1/\xi$, the scattered intensity of neutrons will resemble the scattering measured for a single polymer chain. At larger length scales $r > \xi$, or equivalently $q < 1/\xi$, the interactions between polymer segments that dominate the correlations in the solution are those which occur between polymer segments belonging to different polymer chains, or at least, are distant along the contour length of the same chain (that is, both intramolecular and intermolecular correlations affect the scattering). The influence of the interactions between polymer segments on their correlations in an isotropic solution can be characterized by the radial distribution function, g(r), defined as (de Gennes, 1988)

$$g(r) = \frac{1}{c}[\langle c(0)c(r)\rangle - c^2] \tag{7.4}$$

Phyically, the radial distribution function in Eq.(7.4) can be thought of as the local concentration of polymer segments at a distance, r, from a reference polymer segment, relative to the average concentration of polymer segments, c, in the solution. For the range $r > \xi$, the radial distribution function of the polymer segments, g(r), has the Ornstein-Zernike form (de Gennes, 1988; Daoud et al., 1975; Edwards, 1966)

$$g(r) \sim \frac{c\,\xi}{r} e^{-\frac{r}{\xi}} \tag{7.5}$$

which leads to the following scattering law (by a Fourier transform)

$$I_2(q) = \frac{I_2(0)}{1 + \xi^2 q^2} \tag{7.6}$$

valid for $q < 1/\xi$. Comparing Eq.(7.3), valid for singly dispersed polymer coils, with Eq.(7.6), valid for entangled polymer coils, it is evident that the scattered intensity of

neutrons from polymer solutions, in general, can be interpreted using the unifying expression (Wiltzius et al., 1983; Schaefer, 1984)

$$\frac{I_2(0)}{I_2(q)} = (1 + \xi^2 q^2) \qquad (7.7)$$

where the correlation length, ξ, may be interpreted as $R_g/3^{1/2}$ in the limit of vanishing polymer concentration (provided, $q < 3^{1/2}/R_g$), or as proportional to the polymer mesh or "blob" size (de Gennes, 1988), ξ_b, for entangled polymer solutions (provided $q < 1/0.35\xi_b$). More precisely, $\xi = 0.35\xi_b$ for an entangled polymer solution (Cabane and Duplessix, 1987). For PEO molecules in the range 1 500 Da to 860 000 Da, the former limit, $q < 3^{1/2}/R_g$, corresponds to the range of scattering vectors $q < 0.1$ Å^{-1} and $q < 0.002$ Å^{-1}, respectively. The constraint, $q < 0.1$ Å^{-1}, was satisfied in our SANS measurements, and therefore, the presence of "dilute" polymer solutions with the low molecular weight polymers was detected. In contrast, the constraint, $q < 0.002$ Å^{-1}, was not satisfied, and, therefore, we could not detect the presence of single polymer coils for the high polymer molecular weights. However, at the polymer concentrations necessary to perform the SANS measurements, the high molecular weight PEO coils were entangled in solution, and thus the relevant constraint, $q < 1/0.35\xi_b$, was readily satisfied (note that the polymer blob size is always smaller than the polymer radius of gyration) in our measurements. Following the determination of the polymer solution correlation lengths from the SANS measurements, the range of q-values used was checked to ensure that the constraints outlined above were satisfied.

Before reporting the correlation lengths determined for the aqueous PEO solutions, the qualitative features of typical scattering intensity profiles will be discussed. For example, Figure 7.1 presents the intensity of neutrons scattered from an aqueous solution of PEO having a molecular weight of 21 000 Da as a function of the scattering vector, q, for four PEO solutions which differ in their PEO concentrations. In the low-q region ($q < 0.04$ Å^{-1}), the decrease in the intensity with increasing polymer concentration reflects the contribution of the steric (repulsive) interactions between polymer coils to the

structure of the solution. The fact that polymer-polymer interactions influence the observed scattering to this extent suggests that the polymer concentrations (0.025, 0.083, 0.124 and 0.204, as volume fractions) are in the vicinity of the cross-over concentration, c^*, for PEO 21 000 Da (Cabane, 1987). Note that c^* is a characteristic polymer concentration which reflects a region of polymer solution behavior where the extensive entanglement of polymer coils occurs with either increasing polymer concentration or molecular weight. For PEO 21 000 Da, c^* is in the vicinity of 0.05 (volume fraction). In the high-q region ($q > 0.14 Å^{-1}$), where correlations between polymer segments over shorter length scales determine the scattered intensity (specifically, correlations within PEO coils), the magnitudes of the scattered neutron intensities rank in the opposite order with increasing polymer concentration. This follows from the fact that in the large-q limit, the nature of the correlations within each polymer coil are relatively insensitive to polymer concentration, and each polymer coil acts as an independent scatterer. Consequently, the scattered intensity is simply proportional to the polymer concentration. For the higher molecular weight polymers (not shown in Figure 7.1), the intersections of the scattered intensity curves with increasing concentration (which are shown in Figure 7.1 for PEO 21,000 Da) were either not observed, within the range of scattering vectors accessible, or were observed at very low q values. This observation reflects the fact that for the large polymer coils, over the accessible q-range, only length scales smaller than the polymer coil size were probed, and therefore the measured intensity ranked in order of increasing polymer concentration.

Experimental measurements of the intensity of scattered neutrons as a function of q, analogous to those reported in Figure 7.1, were performed for the range of PEO molecular weights and volume fractions shown in Table 3.1. For all PEO solutions investigated, the scattered intensity was interpreted using Eq.(7.7) to yield a correlation length. For example, a plot of the data presented in Figure 7.1, in terms of the reciprocal intensity, $I_2^{-1}(q)$, as a function of q^2, as shown in Figure 7.2, yields the ordinate intercept as $I_2^{-1}(0)$, and the slope as $I_2^{-1}(0)\xi^2$. Accordingly, the correlation length, ξ, can be determined from the square root of the ratio of the slope and the ordinate intercept. Over the q^2-range of $0.001 Å^{-2}$ to $0.03 Å^{-2}$, the plots presented in

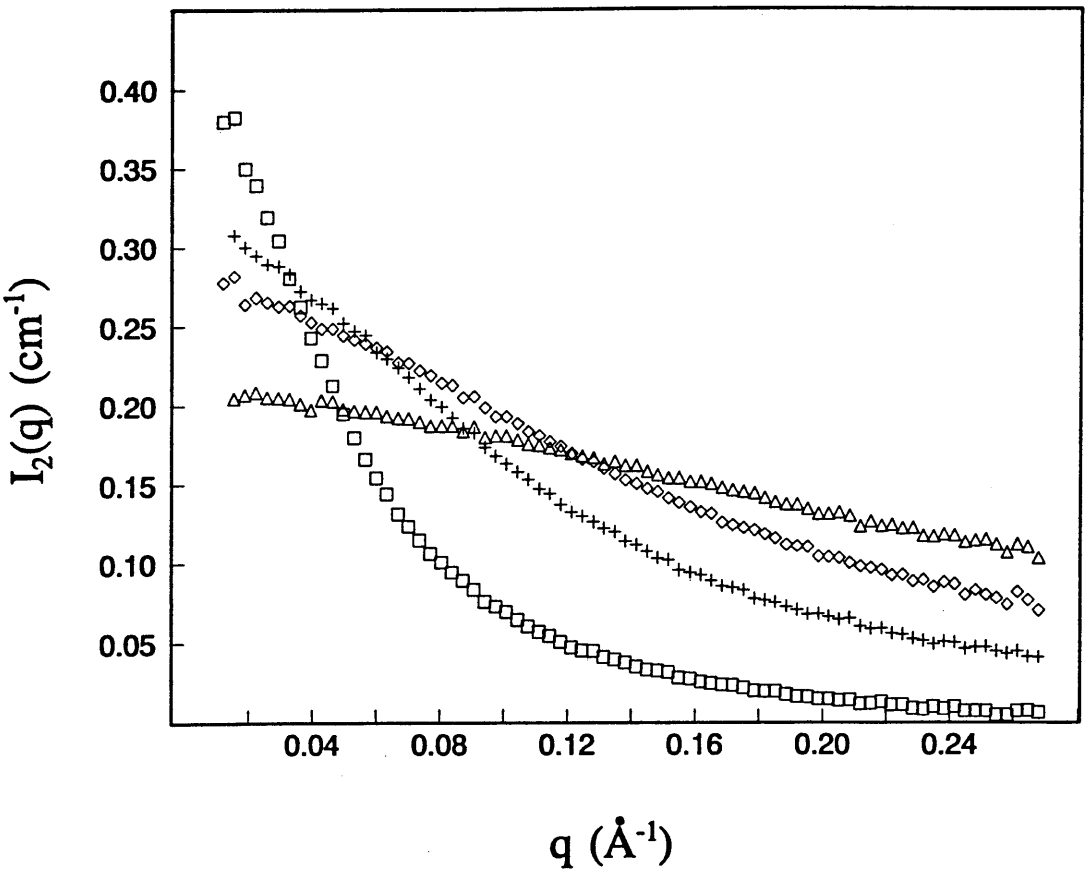

Figure 7.1. Measured neutron scattering intensity, $I_2(q)$, as a function of the magnitude of the scattering vector, q, for solutions of PEO 21 000 Da in D_20. Polymer volume fractions: (□) 0.025, (+) 0.083, (◇) 0.124, (△) 0.204.

Figure 7.2 are essentially linear in accordance with the form suggested by Eq.(7.7). This procedure of determining, ξ, was repeated for all the other polymer molecular weights and polymer volume fractions, and a summary of the measured correlation lengths is presented in Table 3.1. In Figure 3.5, the logarithm of the correlation lengths so determined is reported as a function of the logarithm of the PEO volume fractions for a range of polymer molecular weights between 1 500 Da and 860 000 Da (data taken from Table 3.1). Several regimes corresponding to different solution behavior can be identified from an inspection of Figure 3.5. For the higher molecular weight polymers ($M_2 \gg 10\ 000$ Da), the ξ values are observed to collapse onto a universal curve (solid line) over the range of polymer volume fractions reported in Table 3.1. For these polymers, the magnitude of ξ is independent of polymer molecular weight, being solely a function of the polymer volume fraction. This observation is consistent with the existence of an entangled polymer mesh within which the identities of the individual polymer coils are lost (de Gennes, 1988). For polymers in good solvents, and when probing length scales sufficiently large that excluded-volume interactions can swell the polymer coils locally, a simple scaling argument suggests that (de Gennes, 1988)

$$\xi \sim a\phi^{-3/4} \tag{7.8}$$

where ϕ is the volume fraction of polymer in solution, and a is proportional to the size of a statistical polymer segment. In Figure 3.5, a full line having a slope of -3/4 has been passed through the experimental data points for the high molecular weight data. A close agreement between the slope of the data points and the theoretical prediction in Eq.(7.8) is apparent up to volume fractions of at least 0.10 ($\log\phi = -1$, as indicated by the vertical arrow).

In contrast to the universal behavior (molecular weight independence) observed for the high molecular weight polymers, the ξ values determined from the PEO samples having molecular weights of 1 500 Da, 4 000 Da and 9 000 Da were sensitive to the molecular weight of the polymer. The deduced ξ values were observed to increase with an increase in polymer molecular weight. This suggests that the structure of these

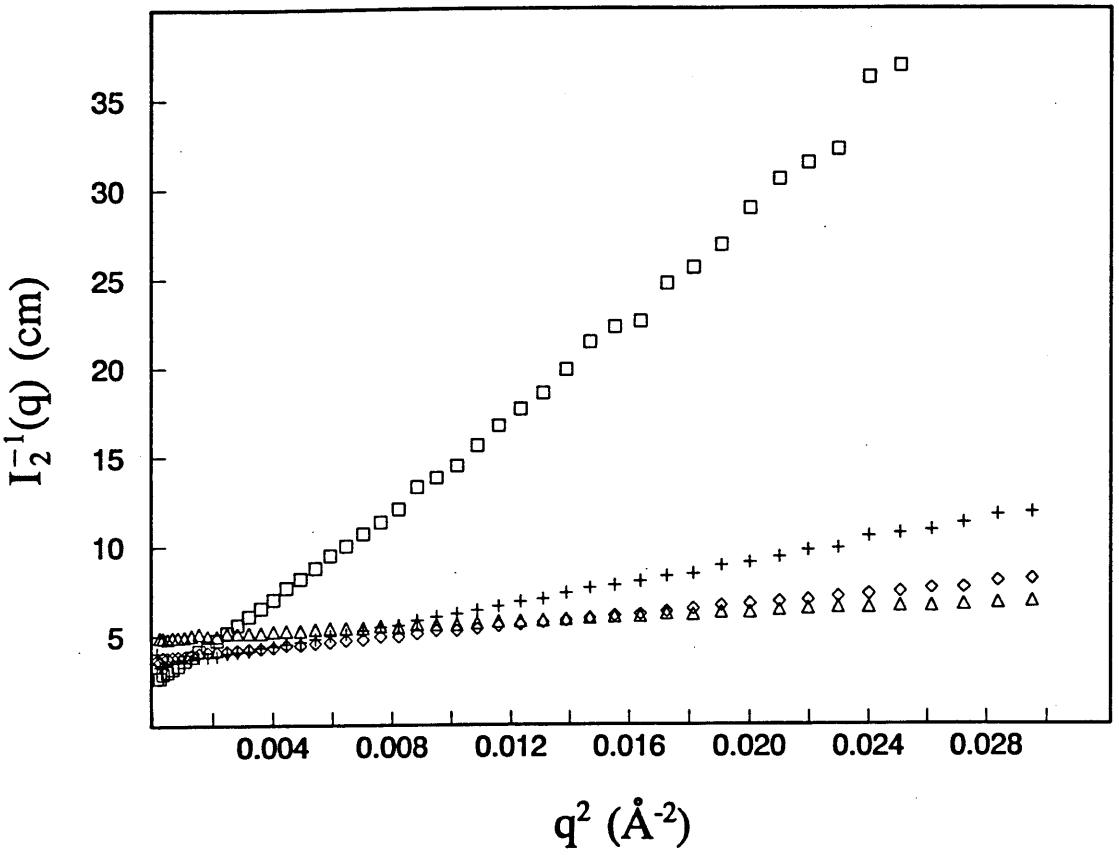

Figure 7.2. Reciprocal of the measured neutron scattering intensity, $I_2^{-1}(q)$, as a function of q^2, where q is the magnitude of the scattering vector, for solutions of PEO 21 000 Da in D_20. Polymer volume fractions: (□) 0.025, (+) 0.083, (◇) 0.124, (△) 0.204.

solutions is sensitive to the sizes of the polymer coils, and is therefore indicative of a polymer solution which contains identifiable polymer coils (Wiltzius et al., 1983; Schaefer, 1984). With decreasing polymer concentration, the ξ values for the low molecular weight polymers (1 500 Da, 4 000 Da and 9 000 Da) appear to be increasing towards a limiting value (dependent on the polymer molecular weight), which in the limit of vanishing polymer concentration should become equal to $R_g/3^{1/2}$ (according to Eq.(7.3)). In Figure 3.5, on the ordinate axis, the correlation lengths evaluated according to $\xi=R_g/3^{1/2}$ are indicated by the horizontal arrows for PEO 1 500 Da, 4 000 Da and 9 000 Da, where R_g was determined from independent theoretical predictions (Abbott et al., 1991b). The calculated ξ values (indicated by the arrows) appear to be in keeping with an extrapolation of the measured values of ξ to vanishing polymer concentration. Clearly, additional measurements are required at lower polymer concentrations to make a more precise comparison and reach a more definitive conclusion. At a fixed volume fraction of low molecular weight PEO, for example, $\log\phi=-1$, the value of ξ was observed to increase with molecular weight, but was always bounded by the ξ value of the solutions containing entangled high molecular weight PEO. The presence of the upper bound is consistent with the fact that with increasing molecular weight, the polymer coils entangle into a mesh. Within the entangled polymer mesh, the indentities of the individual polymer coils are lost and, therefore, the correlation length is observed to become independent of polymer molecular weight (de Gennes, 1988). Finally, a more tentative observation can be made at high polymer concentrations where the correlation length values are small. In Figure 3.5, it appears that in the limit of high polymer concentrations (approximately greater than a volume fraction of 0.1 or $\log\phi=-1$, which is indicated by the vertical arrow), the correlation lengths display a universal behavior similar to that observed for the very high molecular weight polymer meshes, but with a higher value of the slope relating $\log\xi$ to $\log\phi$. The observed higher slope is consistent with the notion that at sufficiently small $\log\xi$ (or alternatively sufficiently large $\log\phi$), excluded-volume interactions between the polymer segments do not swell the local chain configuration significantly (de Gennes, 1988; Schaefer, 1984). For this situation, a scaling argument similar to that used to obtain Eq.(7.8), but without excluded-volume

effects, leads to (de Gennes, 1988; Schaefer, 1984)

$$\xi \sim a\phi^{-1} \tag{7.9}$$

The dashed line having a -1 slope which is plotted in Figure 3.5 appears consistent with the experimental deduction of ξ in the high-concentration region, although more experimental measurements are required to reach a definitive conclusion.

The central conclusion resulting from the experimental determination of the correlation lengths of aqueous PEO solutions is the confirmation of the occurrence of a transition in the polymer solution structure, from one containing identifiable polymer coils to one containing an entangled polymer network. In particular, beyond a PEO volume fraction of about 0.1 (see the vertical arrow in Figure 3.5), which is close to the concentration of PEO typically encountered in the PEO-rich phase of a two-phase aqueous PEO-dextran system, the onset of the molecular weight dependence of the correlation length occurs in the vicinity of a PEO molecular weight of about 10 000 Da. This is consistent with the previously reported (Abbott et al., 1991a) hypothesis of a transition in the PEO-rich phase structure on the basis of experimentally observed protein partitioning (a thermodynamic property). As previously stated (Abbott et al., 1991a), the transition in the solution structure is a gradual one, and in practice, much of the protein partitioning occurs in the crossover region (with reference to Figure 3.5, the crossover for a particular molecular weight of PEO can be defined as the range of polymer concentrations where the correlation length of the polymer solution is a function of both PEO molecular weight and volume fraction). This conclusion is not only relevant to past (Abbott et al., 1991a and b) and future theoretical developments, but also impacted on our interpretation of the neutron scattering from polymer solutions containing proteins. That is, for the 5.9% w/w PEO solution of molecular weight 8 650 Da (with BSA) that we investigate in detail below, we have adopted an analysis which describes the interactions between identifiable polymer coils and protein molecules (rather than an entangled polymer net interacting with protein molecules).

7.3.B Neutron Scattering from Solutions of Identifiable PEO Coils

While in the previous section we reported polymer solution correlation lengths deduced from SANS measurements (in order to identify the polymer solution regime), here we seek to provide an analysis of the scattering of neutrons from PEO solutions containing identifiable polymer coils which can be generalized to solutions containing mixtures of protein and PEO. In particular, to develop a tractable description of the scattered intensity from aqueous solutions containing mixtures of BSA and PEO, it was first necessary to separate the contributions of intramolecular and intermolecular correlations to the scattered intensity from PEO solutions (see Section 7.5). For rigid particles in solution, where the intermolecular interactions do not perturb the shape of the particle, this separation is, in principle, straightforward. However, here, we are dealing with a flexible and deformable PEO coils with (fluctuating) configurations which reflect the coupling of both intramolecular and intermolecular interactions. In such a situation, in order to facilitate the separation of intramolecular correlations and intermolecular correlations, an approximation is required. Specifically, we adopt the approach of Benoit and Benmouna (1984), in which the intramolecular and intermolecular interactions are predicted from the average configurations of the polymer coils in solution. This approach (Benoit and Benmouna, 1984), which is further discussed below, has been successful in describing the scattering from polymer solutions over a wide range of polymer concentrations. Here, we also find that the scattered intensity measured from aqueous PEO solutions is successfully predicted using the theory of Benoit and Benmouna (1984). With this approximation in mind, for an ensemble of identical particles, the scattered intensity of neutrons can be expressed as (Guinier and Fournet, 1955; Cabane, 1987; Glatter and Kratky, 1982)

$$I_i(q) = \frac{N_i}{V}(\Delta\rho_i)^2 \, (V_i^o)^2 \, \langle P_i^2(q) \rangle \left[1 + \left[\frac{\langle P_i(q) \rangle^2}{\langle P_i^2(q) \rangle} \right] (S_i(q) - 1) \right] \qquad \textbf{(7.10)}$$

where N_i/V is the number density of macromolecules in solution, $\Delta\rho_i$ is the contrast

factor (number of scattering sites per unit volume) between the macromolecule and solvent, V_i^o is the molecular volume of the macromolecule, $P_i(q)$ is the form factor which reflects the intramolecular correlations between scattering sites within an individual macromolecule, $S_i(q)$ is the structure factor which reflects the contribution to the scattered intensity due to intermolecular correlations between scattering sites residing on different macromolecules, and the brackets, $<..>$, denote an averaging over all orientations of the macromolecule.

Here we make use of Eq.(7.10) for the scattering of neutrons from a solution of 5.9% w/w PEO having a molecular weight of 8 650 Da, since it is in this polymer solution that we have examined the excess scattering of neutrons in the presence of BSA. If we assume that the polymer coils are, on average, spherically symmetric, Eq.(7.10) can be simplified by noting that $<P_i(q)>^2$ and $<P_i^2(q)>$ are equal, and the intensity of the neutrons scattered from the PEO solutions can be interpreted using the following expression (Guinier and Fournet, 1955; Cabane, 1987; Glatter and Kratky, 1982)

$$I_2(q) = \frac{N_2}{V} \Delta\rho_2^2 \, (V_2^o)^2 \, \langle P_2^2(q) \rangle \, S_2(q) \qquad \textbf{(7.11)}$$

Note that when applying Eq.(7.11) to the case of PEO, the general subscript i is replaced by 2. To describe the intensity of neutrons scattered from aqueous PEO solutions we require the evaluation of $P_2(q)$ and $S_2(q)$ (all other quantities in Eq.(7.11) are available (Cabane, 1987)). First, we consider the form factor, $P_2(q)$, for flexible polymer chains. For a flexible polymer chain at θ-solvent conditions, where the polymer chain statistics are Gaussian, the form factor is given by the well-known result first derived by Debye (Debye and Bueche, 1949; Debye et al., 1957), namely,

$$P_2^2(x) = \frac{2}{x^2}\left(e^{-x} - 1 + x\right) \qquad \textbf{(7.12)}$$

where, as before, $x = q^2 R_g^2$. For polymers in good solvents, repulsive excluded-volume

interactions between polymer segments within the same coil will cause chains of sufficient length to swell in size, and, therefore, the chain statistics are no longer strictly Gaussian (Tsunashima and Kurata, 1986; Croxton, 1988; Boothroyd, 1988; Bishop and Saltiel, 1991). Accordingly, for swollen polymers one can expect some deviation from Eq.(7.12). However, in the low-q region, specifically for $x < 10$, the deviation has been determined to be small (Tsunashima and Kurata, 1986). At higher q some deviation from Eq.(7.12) can be expected, although, in view of other approximations (see Section 7.4), this does not appear to limit our conclusions.

Turning now to the structure factor, we report two approaches for the evaluation of $S_2(q)$ for the PEO solution. Pursuing these two approaches turned out to be quite illuminating, since a comparison of their predictions provided us with some useful insights on the relationship between the thermodynamic and structural properties of the PEO solution. In addition, this comparision also shed light on the interpretation of the neutron scattering measurements from solutions containing PEO and BSA.

First, we present an interpretation of the scattering data from the PEO solution based on the formulation of Benoit and Benmouna (1984), who generalized the classic Zimm model (1948) for the small angle scattering from dilute polymer solutions, to that from solutions of arbitrary polymer concentration. Using the so-called "single-contact approximation" between different chains to describe the interactions between polymer coils, in solutions of low polymer concentration, Zimm derived the result (Zimm, 1948)

$$S_2(q) = \frac{1}{1 + \nu\rho_2 N^2 \langle P_2^2(q) \rangle} \qquad \textbf{(7.13)}$$

where N is the number of polymer segments within a polymer coil, and ν is the binary cluster integral (de Gennes, 1988) characterizing the strength of the interaction between two polymer segments, and ρ_2 is the number density of polymer coils ($\rho 2 = N_2/V$). Although Eq.(7.13) was derived for the case of low polymer concentration and using the single-contact approximation (Zimm, 1948), at higher concentrations and with multiple

contacts occurring between polymer chains, the mathematical structure of Eq.(7.13) has been shown to be retained (Benoit and Benmouna, 1984). However, in the generalized form of Eq.(7.13), the parameter ν, which characterizes the strength of the interactions between two polymer segments, becomes an effective parameter which includes the contributions of multiple contacts between polymer chains, and also depends on the polymer concentration. If, in addition, the average configuration of the polymer coil is assumed to be concentration dependent, in which case the form factor, $P_2(q)$, is also a function of polymer concentration, Eq.(7.13) can be generalized for an arbitrary polymer concentration as follows (Benoit and Benmouna, 1984)

$$S_2(q) = \frac{1}{1 + \nu(c)\rho_2 N^2 \langle P_2^2(c,q)\rangle} \qquad \textbf{(7.14)}$$

In view of the generalized definition of ν(c) and the difficulty associated with its *a priori* estimation (Ullman et al., 1986), we have determined its value by fitting Eq.(7.14) to the neutron scattering intensity measured from a solution of 5.9 %w/w PEO having a molecular weight of 8 650 Da. For the theoretical prediction of $I_2(q)$ we have utilized Eqs.(7.12) and (7.14) in Eq.(7.11), along with the parameter values (Abbott et al., 1991b; Cabane, 1987), ρ_2=4.931x10^{-6} Å^{-3}, $\Delta\rho_2$=5.710x10^{-6} Å^{-2}, N=197 and R_g=36.5Å. In Figure 7.3, we show that a close agreement between the theoretically predicted $I_2(q)$ values and the experimental values is obtained for ν(c=5.9% w/w)=28Å^3. This deduced value of ν(c) appears consistent with the independent estimation (Venneman et al., 1987) of ν(c)=16Å^3 in the limit of vanishing PEO concentration in aqueous PEO solutions. At a higher polymer concentration, due to an increase in the number of multiple contacts between polymer coils, the value of ν(c) is expected to increase (Ullman et al., 1986). It is also relevant to note that the presence of 0.5M sodium acetate can also influence the ν(c) value that we determined. In general, the addition of salts will influence the effective solvent quality for PEO, and thus may also affect ν(c). Furthermore, the same change in solvent quality can be expected, in general, to influence the average configuration of the PEO coils, as described by R_g. However, using the

value of R_g=36.5Å for PEO with a molecular weight of 8 650 Da (determined in pure water and at a vanishing PEO concentration) (Abbott et al., 1991b), the measured intensity appears well predicted. This suggests that, in fact, the addition of 0.5M sodium acetate did not greatly influence the average configuration adopted by the PEO molecules.

The second approach to evaluate the polymer solution structure factor, $S_2(q)$, was motivated, in part, by the successful theoretical development, reported (Abbott et al., 1991b) in Chapter 6, leading to the prediction of the vapor pressure of aqueous PEO solutions (for $c<c^*$), that is, in the dilute solution regime. In this approach (Abbott et al., 1991b), the polymer-polymer interaction was captured in terms of an effective hard-sphere potential, and an equation of state (Ashcroft and Lekner, 1966; Hansen and McDonald, 1976) for the resulting effective hard-sphere system was used to predict thermodynamic properties of the solution, such as, the vapor pressure. Although a hard-sphere potential was used to describe the interactions between the PEO coils, the soft and penetrable nature of the coils was incorporated into the evaluation of their effective hard-sphere sizes (Abbott et al., 1991b). In a similar spirit, we have evaluated $S_2(q)$ using a hard-sphere description (Ashcroft and Lekner, 1966) of the PEO solution phase and the previously (Abbott et al., 1991b) developed effective hard-sphere potentials. In so doing we hoped to shed light on the following important questions. First, is the osmotic compressibility of the polymer solution, calculated thermodynamically using the hard-sphere sizes determined from vapor pressure measurements, consistent with the osmotic compressibility deduced from the intensity of scattered neutrons in the limit $q\rightarrow 0$? Second, is an effective hard-sphere potential, deduced from neutron scattering measurements, for the description of polymer-polymer interactions, a function of the polymer concentration? Finally, can the successful description of the thermodynamic properties of PEO solutions in terms of hard-sphere potentials be extended to the description of the structure of the PEO solution, as reflected in the SANS measurements?

Using an effective hard-sphere potential to characterize the interactions between polymer coils, the structure factor of the polymer solution, $S_2(q)$, was calculated

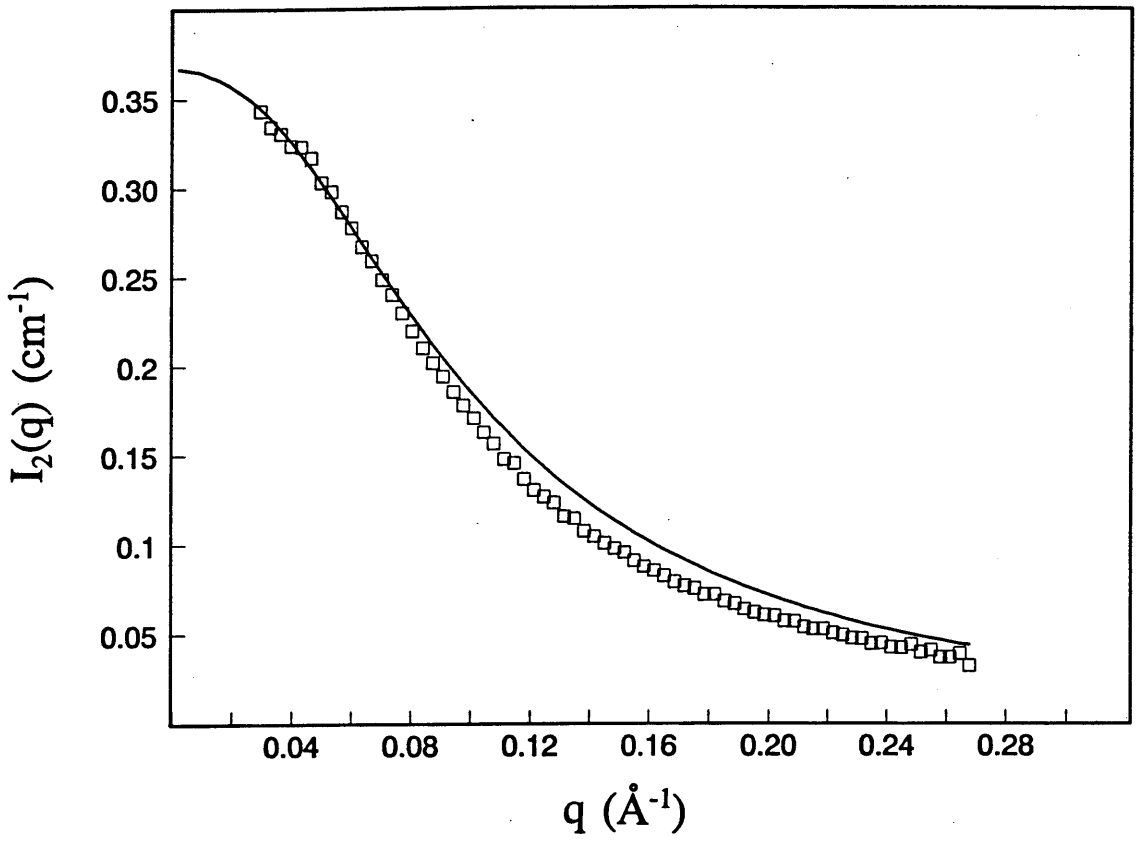

Figure 7.3. Neutron scattering intensity, $I_2(q)$, as a function of the magnitude of the scattering vector, q, for 5.9% PEO 8 650 Da in D_2O: (□) experimental measurement, (—) theoretical prediction using the theory of Benoit and Benmouna (1984).

from the direct correlation function, $C_2(q)$ (Hansen and McDonald, 1976), using the well known Ornstein-Zernicke equation (Ornstein and Zernike, 1914)

$$S_2(q) = \frac{1}{1 - \rho_2 C_2(q)} \tag{7.15}$$

The direct correlation function for a system of hard-spheres has been previously evaluated (Ashcroft and Lekner, 1966) using the theory of Percus and Yevick (1958), and a given by

$$C_2(q) = -4\pi D_2^3 \int_0^1 ds\, s^2 \frac{\sin(sqD_2)}{sqD_2}(\alpha + \beta s + \gamma s^3) \tag{7.16}$$

where

$$\alpha = \frac{(1 + 2\eta_2)^2}{(1 - \eta_2)^4} \tag{7.17}$$

$$\beta = -\frac{6\eta_2 (1 + \eta_2/2)^2}{(1 - \eta_2)^4} \tag{7.18}$$

$$\gamma = \frac{\eta_2 (1 + 2\eta_2)^2}{2(1 - \eta_2)^4} \tag{7.19}$$

The parameter, η_2, is the effective hard-sphere volume fraction of the polymer coils in the solution, and is given by

$$\eta_2 = \frac{\pi}{6}\rho_2 D_2^3 \tag{7.20}$$

where D_2 is the effective hard-sphere diameter of the polymer coils. It is important to

note that in Eqs.(7.16) to (7.20) the effective hard-sphere diameter of the polymer coil, D_2, (which captures the effect of polymer-polymer interactions) is different from $2R_g$, (where R_g describes the distribution of scattering sites in an individual polymer coil). Recall that R_g was used in Eq.(7.13) to evaluate the polymer form factor, $P_2(q)$. As previously reported (Abbott et al., 1991b), we have evaluated R_g and D_2 for PEO in water using the theories of Flory (1986), and Flory and Krigbaum (1950), respectively, and the predicted values of both R_g and D_2 were found to be in good agreement with independent experimental measurements (Abbott et al., 1991b). For PEO having a molecular weight of 8 650 Da in water, and using a Flory-Huggins interaction parameter (Flory, 1986; Huggins, 1941) of χ=0.45, the radius of gyration, R_g, and effective hard-sphere radius, $D_2/2$, were predicted to be 36.5 Å and 22.4 Å, respectively. In Figure 7.4, the predicted intensity of scattered neutrons, $I_2(q)$ vs q, obtained using Eqs.(7.11), (7.12) and (7.15) to (7.20), (full line) is compared to the experimentally measured intensity for the solution of 5.9% w/w PEO having a molecular weight of 8 650 Da (data points). The *multiplicative* contributions of the form factor (dashed line) and the structure factor (dotted line) to the total intensity are also shown in Figure 7.4.

Inspection of Figure 7.4 leads to several interesting observations. First, in the limit $q \to 0$, where the scattering reflects primarily the structure factor, $S_2(q)$, and thus the large-scale fluctuations in the system (Cabane, 1987), the magnitude of the predicted scattering intensity (full line) appears to agree with an extrapolation of the experimental measurements (data points). Note that the experimental measurements were limited to $q > 0.02 Å^{-1}$ by the beam-stop in the spectrometer. Through fluctuation theory (Cabane, 1987; McQuarrie, 1976; Knoll and Hermans, 1983), in the limit $q \to 0$, the structure factor can be related to the fluctuations in the number density of PEO coils in an imaginary volume of solution that is large compared to the size of the PEO coils, and yet is small compared to macroscopic scales. That is,

$$S_2(q \to 0) = \frac{\langle (N_2/V)^2 \rangle - \langle N_2/V \rangle^2}{\langle N_2/V \rangle^2} = \frac{K_T}{K_T^o} \qquad \textbf{(7.21)}$$

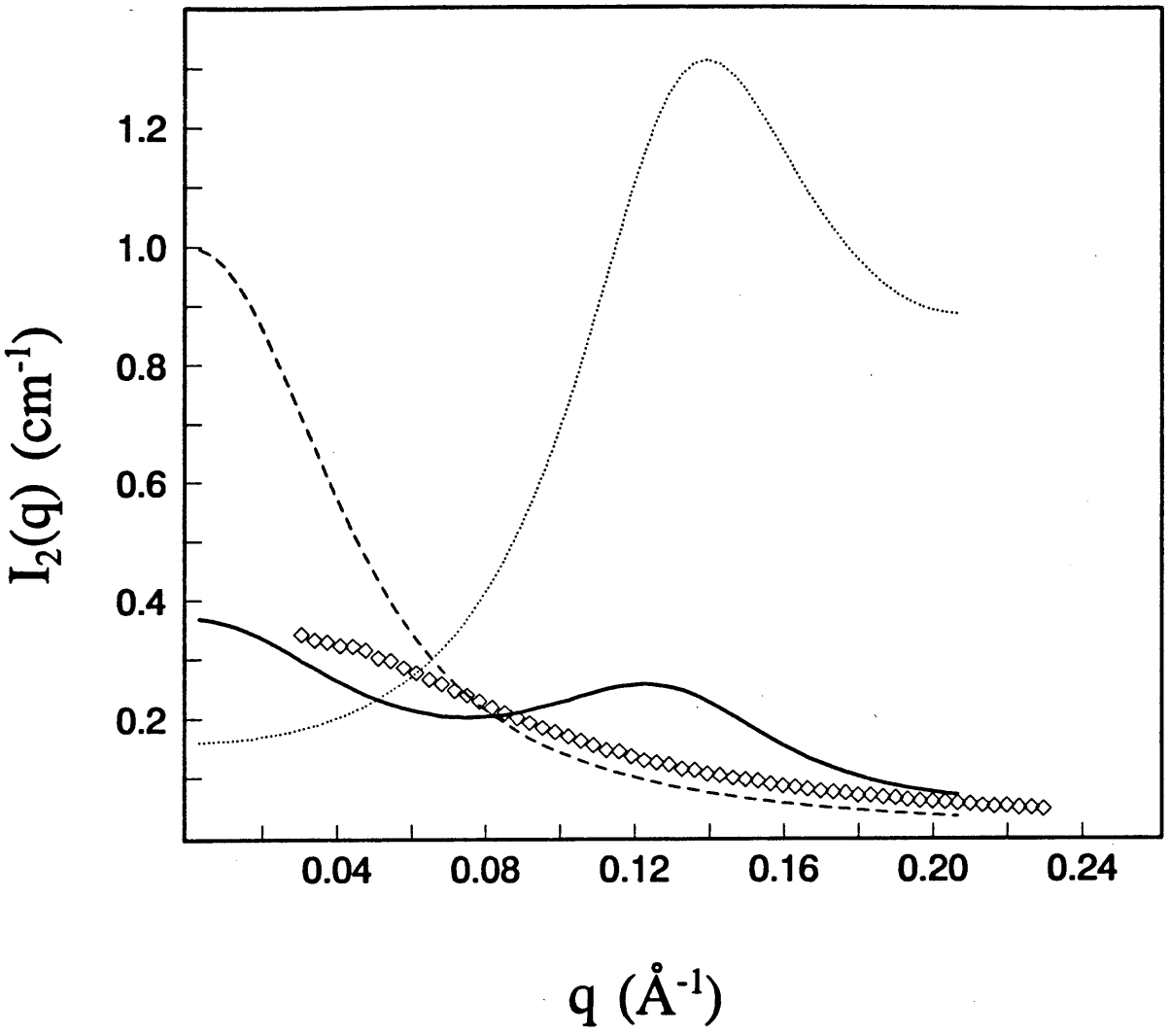

Figure 7.4. Neutron scattering intensity, $I_2(q)$, as a function of the magnitude of the scattering vector, q, for 5.9% PEO 8 650 Da in D_2O: (◇) experimental measurement, (—) theoretical prediction using a hard sphere structure factor, $S_2(q)$, and Debye form factor, $P_2(q)$. Multiplicative contributions to the theoretically predicted scattering: (- -) form factor $P_2(q)$, (···) structure factor, $P_2(q)$.

where $<(N_2/V)^2>$ and $<N_2/V>^2$ are the mean-square and squared-mean fluctuations in the number densities of PEO coils, K_T is the isothermal osmotic compressibility of the PEO solution, and K_T° is the isothermal osmotic compressibility of an ideal solution (Cabane, 1987; McQuarrie, 1976). In other words, the scattering in this limit is essentially a measure of the thermodynamic state of the system (Vennemann et al., 1987). Therefore, the agreement between the measured and predicted intensity in the limit $q \to 0$ is consistent with the previously demonstrated ability of the effective hard-sphere model to predict thermodynamic properties, such as the vapor pressure, of aqueous PEO solutions (Abbott et al., 1991b). This observation also supports our earlier assertion, that the addition of 0.5M sodium acetate does not greatly perturb the thermodynamic state of the aqueous PEO solution. It is also relevant to note that also in the limit $q \to \infty$, where $S_2(q) \to 1$, the form factor of the PEO coils, $P_2(q)$, predicts the correct magnitude of the measured intensity of scattered neutrons. This observation supports our description of the PEO molecules as Gaussian coils.

In contrast to the close agreement between the predicted and measured neutron scattering intensities in both the low- and the high-q regions of Figure 7.4, at intermediate q values a significant oscillation is observed in the predicted neutron scattering intensity which is absent in the experimentally measured $I_2(q)$. This suggests that the prediction of the structural properties of the solution using an effective hard-sphere model is less successful than the prediction of thermodynamic properties. In essence, the solution structure predicted by the effective hard-sphere model is greater than that observed experimentally for the PEO solution. Presumably, this arises from the fact that the actual interactions between the PEO coils are somewhat softer and longer-ranged than those accounted for by representing the polymer coils as effective hard spheres.

The observation that an intermolecular pair potential can predict quite accurately the thermodynamic properties of a solution, yet not adequately describe its structure, as reflected in the neutron scattering measurements, can be illustrated by a comparison of the properties of two simple model potentials. For simplicity and for the sake of illustration, we consider an isotropic fluid which is sufficiently dilute that only

pairwise interactions between molecules need to be considered in calculating its properties. In such a fluid, the deviation of thermodynamic properties from their ideal-solution values are described by the second virial coefficient, B_2, evaluated as (McQuarrie, 1976)

$$B_2 = \frac{1}{2}\int_0^\infty (1 - e^{\frac{-\phi(r)}{kT}})4\pi r^2 dr \tag{7.22}$$

where ϕ(r) is the (spherically symmetric) potential of mean force. The structure of the fluid is described by the radial distribution function, g(r), which can be expressed as an expansion in the concentration, ρ, namely (McQuarrie, 1976)

$$g(r,\rho) = g_o(r) + g_1(r)\rho + ... \tag{7.23}$$

where, for sufficiently dilute solutions ($\rho \ll 1$), g(r) is determined by a simple Boltzmann-factor term (McQuarrie, 1976)

$$g_o(r) = \exp\left[\frac{-\phi(r)}{kT}\right] \tag{7.24}$$

For two simple model potentials we have evaluated B_2 and g_o(r). The first model is

$$\frac{\phi(r)}{kT} = \begin{cases} \infty & r \leq \sigma \\ 0 & r > \sigma \end{cases} \tag{7.25}$$

where σ is a hard-sphere diameter. The second model potential, which is a continuous function of r, is

$$\frac{\phi(r)}{kT} = \frac{\alpha}{r^3} \tag{7.26}$$

For the parameter values σ=1, and α=0.0139, these two model potentials lead to

identical second virial coefficients, that is,

$$B_2 = \frac{4\pi}{6} \tag{7.27}$$

and, therefore, *identical thermodynamic properties* in dilute solution. On the other hand, the dilute solution radial distribution function, $g_o(r)$, presented for each model potential in Figure 7.5, shows a pronounced difference between the two cases. In other words, although the predicted thermodynamic properties of the solution are identical, the predicted structure of the fluid is markedly different.

The previous discussion and observations are consistent with the general comments of Vennemann and coworkers (1987) and others (Guinier and Fournet, 1955; Cabane, 1987; Glatter and Kratky, 1982) who point out that the thermodynamic state of a system, defined by the system temperature, pressure and composition, directly determines the scattering of a solution in the limit $q \to 0$. In contrast, at higher values of q, the scattering reflects less of the interparticle interferences, that is, $S(q \to \infty) = 1$, and is dominated by the configurations of the individual species (intramolecular correlations, as captured in P(q)). Therefore, in the region of higher q, the connection of the scattering to the thermodynamic properties of the system is more tenuous. Specifically, this connection depends on the extent to which the configurations of the PEO coils are coupled to their intermolecular interactions, and thus to the concentration of PEO in solution (Vennemann et al., 1987). If this coupling is significant, it may manifest itself not only in the form factor, $P_2(c,q)$, but also in the structure factor, $S_2(q)$, of the polymer solution. That is, in the context of the effective hard-sphere description of the aqueous PEO solution, the hard-sphere radius used to capture the polymer-polymer interactions may be a function of the concentration of polymer in solution. In view of the developments described in Chapter 6 (Abbott et al., 1991b), it is important to note that the Flory-Krigbaum theory (1950) evaluates the effective hard-sphere potential for the interaction of two *isolated* polymer coils, and, therefore, cannot capture any concentration dependence of the effective hard-sphere radii. To assess the extent to which the PEO concentration influences the effective hard-sphere potential that describes

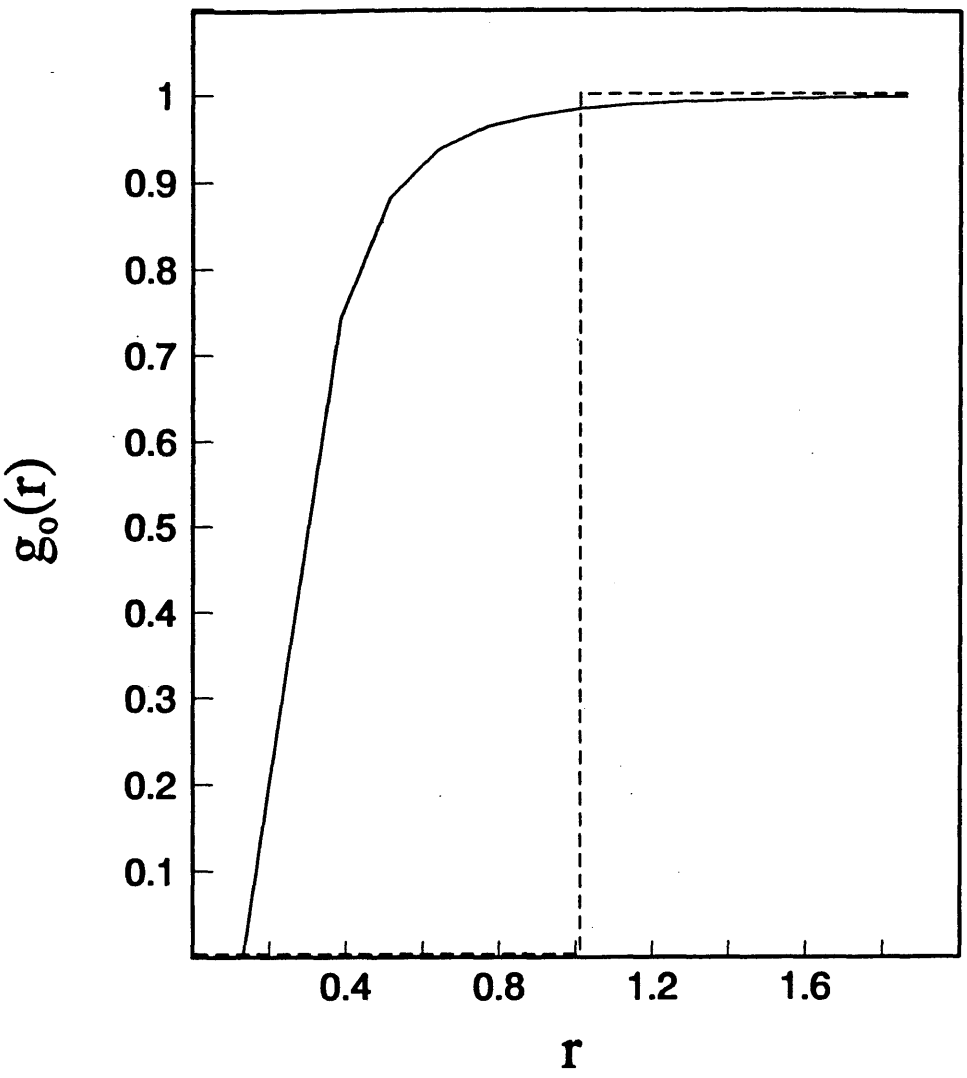

Figure 7.5. Dilute solution radial distribution functions, $g_o(r)$, as a function of the distance between the centers of mass, r, for the two intermolecular potentials, Eqs.(7.25) and (7.26), which predict the identical dilute solution thermodynamic properties: (- -) Eq.(7.25), (——) Eq.(7.26).

the polymer-polymer interactions, we have interpreted the measured intensity of scattered neutrons in the limit $q \to 0$ to obtain an effective hard-sphere diameter of the polymers as a function of polymer molecular weight and volume fraction. The result is presented in Figure 7.6, where the effective hard-sphere diameters, D_2, of PEO in solutions having molecular weights of 1450 Da (●), 4250 Da (■) and 8650 Da (▲) are reported over a range of polymer volume fractions between 0.05 and 0.25. It is evident that with increasing polymer concentration the effective hard-sphere diameter of the polymer coils decreases slightly. Although the decrease is small, less than 3Å, the predicted intensity of scattered neutrons was very sensitive to the effective hard-sphere diameter of the polymer coils and the precision of the hard-sphere diameters determinations is remarkably good; the uncertainty is typically less than 0.5Å. Furthermore, it is evident that the effective hard-sphere diameter of a 8650 Da PEO coil is more sensitive to changes in the polymer concentration than that of a 4 250 Da PEO or a 1 450 Da PEO. This observation is consistent with either a more compact chain configuration at higher polymer concentrations, as is observed in entangled polymer solutions (Daoud et al., 1975; Farnoux et al., 1975), or an increasing penetrability of the polymer coils to one another at higher concentrations.

7.4 Neutron Scattering from Aqueous BSA Solutions

Measurement of the neutron intensities scattered from aqueous bovine serum albumin (BSA) solutions (without PEO) served two central purposes. First, we confirmed that the protein solutions were sufficiently dilute so that protein-protein interactions had little effect (if at all) on the intensity of scattered neutrons. Second, the contrast factor, $\Delta\rho_p$, for BSA in D_2O was determined. Both of these considerations are a prerequisite for the interpretation of neutron scattering from aqueous solutions containing PEO and BSA.

The intensity of neutrons scattered from aqueous BSA solutions was measured and interpreted using Eq.(7.10), where the subscript i is now p to denote protein, N_p/V is the number density of proteins in solution, $\Delta\rho_p$ is the contrast factor

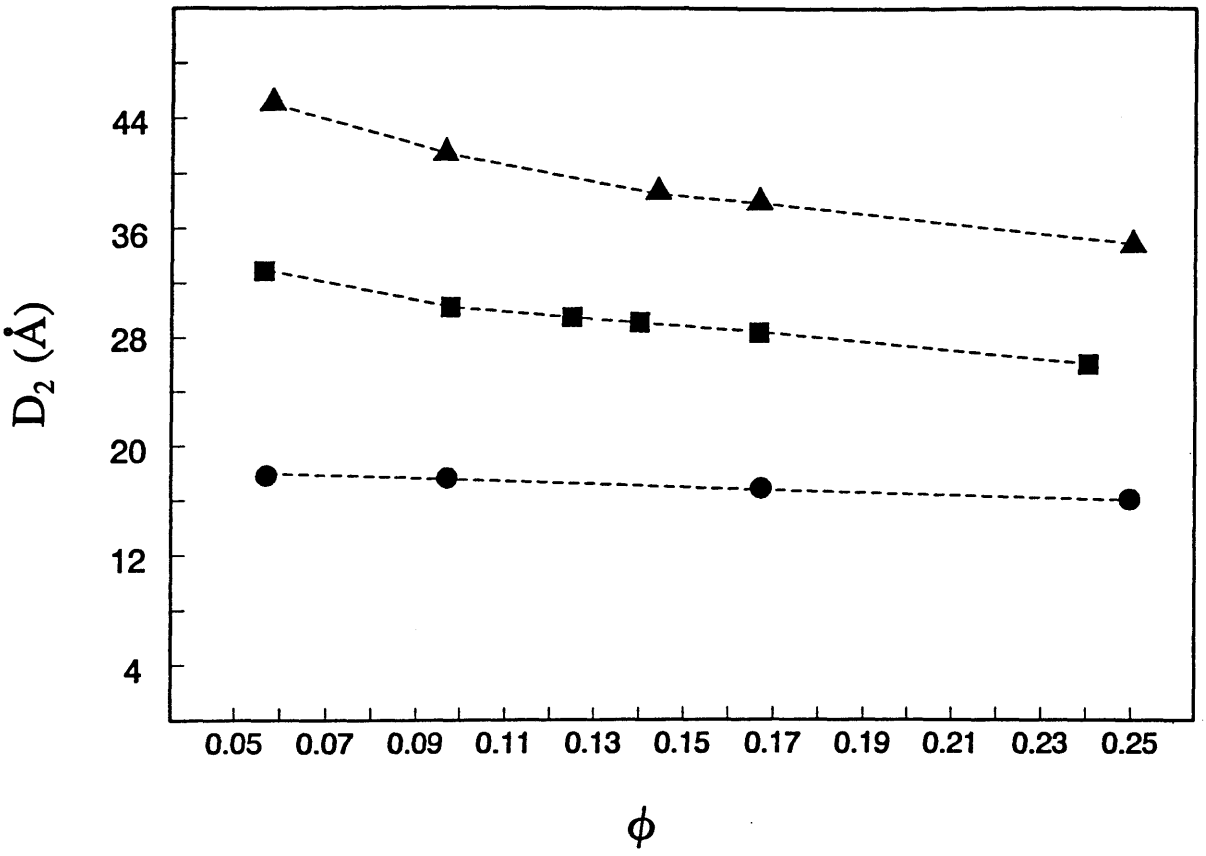

Figure 7.6. Predicted effective hard-sphere diameter, D_2, as a function of PEO volume fraction, ϕ, for PEO in D_2O. D_2 was determined from the intensity of neutrons scattered in the limit of zero angle using a hard-sphere structure factor. Polymer molecular weights in Da: (▲) 9 000, (■) 4 000, (●) 1 500.

between the solvent and BSA, V_p^o is the molecular volume of BSA, $P_p(q)$ is the form factor of the BSA molecules, and $S_p(q)$ is the structure factor reflecting the interactions between the BSA molecules. To simplify the interpretation of the BSA scattering, we have investigated solutions of BSA (in 0.5M sodium acetate) which are sufficiently dilute for the protein molecules to be uncorrelated in their positions. Accordingly, $S_p(q)=1$, and the scattered intensity of neutrons will reflect solely the intramolecular correlations between scattering sites within individual BSA molecule. Under the condition of $S_p(q)=1$, Eq.(7.10) simplifies to

$$I_p(q) = \frac{N_p}{V} \Delta\rho_p^2 \, (V_p^o)^2 \, \langle P_p^2(q) \rangle \tag{7.28}$$

The shape of a BSA molecule is ellipsoidal (Bendedouch and Chen, 1983; Nossal et al., 1986; Chen and Bendedouch, 1986), and therefore the simple form factor for a sphere does not adequately describe the intensity of neutrons scattered from BSA solutions. It is noteworthy that the previous neutron scattering investigations have represented the BSA molecules as prolate ellipsoids having dimensions 70x20x20 $Å^3$. The form factor of a prolate ellipsoid with dimensions, ta,a,a, where t is a numerical constant which is greater than unity and a is the minor axis, can be evaluated according to (Bendedouch and Chen, 1983; Nossal et al., 1986; Chen and Dendedouch, 1986)

$$\langle P_p^2(q) \rangle = \int_0^{\pi/2} P_l^2(q,\beta) \cos\beta \, d\beta \tag{7.29}$$

where

$$P_l^2(q,\beta) = P_{sp}^2(qa(\cos^2\beta + t^2\sin^2\beta)) \tag{7.30}$$

and

$$P_{sp}(qa) = 3\frac{(\sin(qa) - qa\cos(qa))}{(qa)^3} \tag{7.31}$$

In Eq.(7.31), $P_{sp}(qa)$ is the form factor for a spherical molecule of radius *a*.

In Figure 7.7, the measured intensity of neutrons scattered from a 9.9 g/l BSA solution is compared to the theoretical prediction using Eqs.(7.28) to (7.31), where we have assumed that the solution is sufficiently dilute so that the structure factor, $S_p(q)$, is unity, and the constrast factor, $\Delta\rho_p$, was treated as a fitting parameter. The assumption that $S_p(q)=1$ is supported by measurements of Bendedouch and Chen (1983). For the calculation of the intensity of scattered neutrons, $I_p(q)$, reported in Figure 7.7, we have used $V_p=117\ 300$ Å^3 (Bendedouch and Chen, 1983), and the number density of BSA molecules was calculated from the BSA concentration (9.9 g/l) as $N_p/V=9.02083\text{x}10^{-8}$ Å^{-3} using a BSA molecular weight of 66 700 Da (Squire et al., 1968). The best fit of the theoretical prediction and the experimental intensity was obtained with $\Delta\rho_p=2.1\text{x}10^{-6}$ Å^{-2}, which is comparable to the value of $2.5\text{x}10^{-6}$ Å^{-2} obtained by Bendedouch and Chen (1983). The good agreement between the measured and calculated neutron scattering intensities supports the view of the protein as being ellipsoidal, as well as the assumption of $S_p(q)=1$. The intensity of scattered neutrons was also calculated for spherical molecules with a volume equivalent to that of the BSA molecule (not shown), and a significant deviation of the theoretical prediction from the experimental data was evident.

7.5 Neutron Scattering from Aqueous Mixtures of PEO and BSA

Equation (7.10) can be generalized to describe the case of small angle neutron scattering from a binary macromolecular mixture (PEO and BSA) in solution (Tong et al., 1990). The general expression, simplified for the case where the protein is sufficiently dilute such that $S_p(q)=1$ (Section 7.4 and below), is

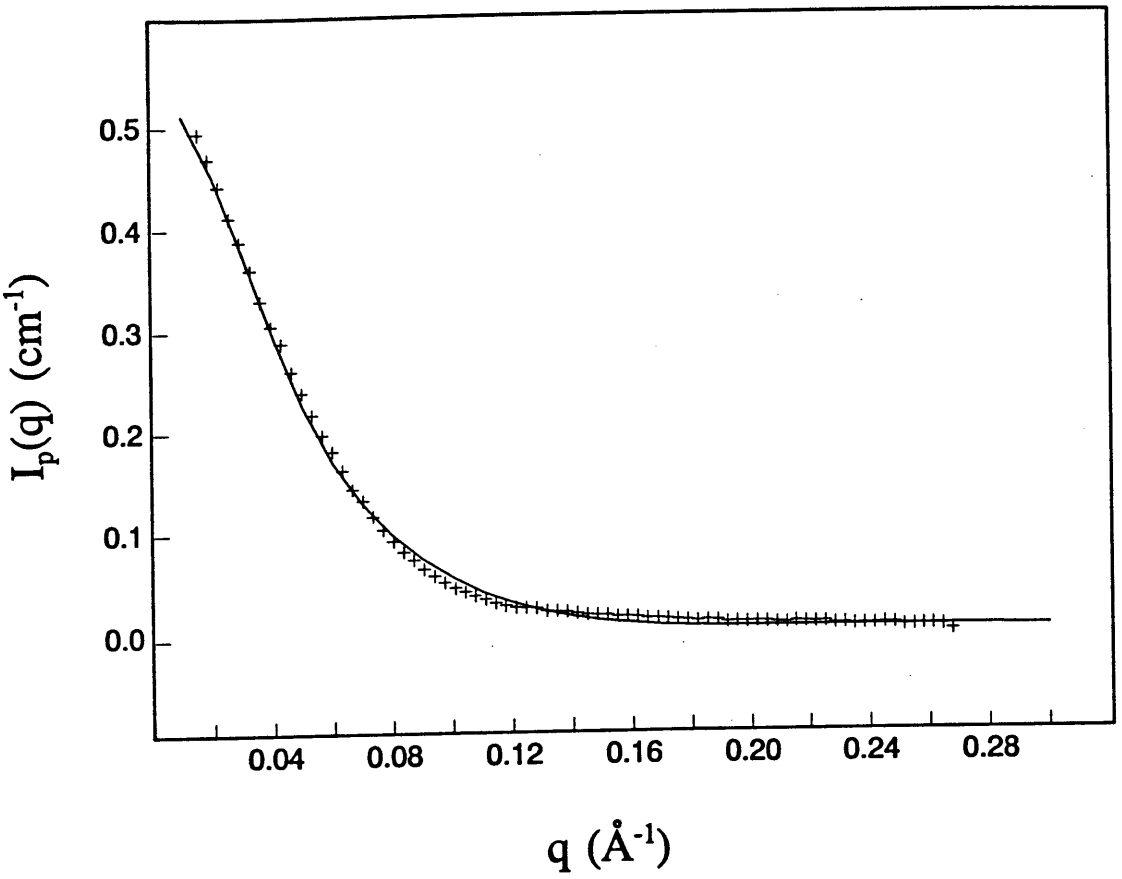

Figure 7.7. Neutron scattering intensity, $I_p(q)$, as a function of the magnitude of the scattering vector, q, for a solution of 9.9 g/l BSA in D_2O: (+) experimental measurement , (—) theoretical prediction using an ellipsoidal form factor and assuming a unity structure factor.

$$I(q) = \frac{N_p}{V} \Delta\rho_p^2 (V_p^o)^2 \langle P_p^2(q) \rangle + 2 \left[\frac{N_p N_2}{V^2} \right]^{1/2} \Delta\rho_p \Delta\rho_2 V_p^o V_2^o \langle P_p(q) \rangle \langle P_2(q) \rangle S_{p2}(q)$$
$$+ \frac{N_2}{V} \Delta\rho_2^2 (V_2^o)^2 \langle P_2^2(q) \rangle S_2(q) \qquad \textbf{(7.32)}$$

where $S_{p2}(q)$ is the partial structure factor which is of central interest to us since it contains the contribution of the interactions between the protein and polymer molecules to the correlations within the solution that are reflected in the scattered intensity. Accordingly, it is useful to define the excess scattering of the mixture, $I^{ex}(q)$, by subtracting from the total intensity, I(q), the intensity of neutrons scattered from aqueous solutions of protein and polymer, separately. Subtracting the first and third terms from Eq.(7.32) yields

$$I^{ex}(q) = 2 \left[\frac{N_p N_2}{V^2} \right]^{1/2} \Delta\rho_p \Delta\rho_2 \langle P_p(q) \rangle \langle P_2(q) \rangle S_{p2}(q) \qquad \textbf{(7.33)}$$

It is important to qualify the conditions under which the subtraction leading to Eq.(7.33) is valid. Specifically, subtraction of the single-component scattering from the mixture is only valid under the conditions for which the form factors, $P_p(q)$ and $P_2(q)$, and the structure factors, $S_p(q)$ and $S_2(q)$, are the same in the mixture and the single-component solutions. Experimentally this can be verified by measuring the excess scattered intensity of neutrons as a function of protein concentration. According to Eq.(7.33), if the subtraction is valid, the excess intensity, $I^{ex}(q)$, will be linearly proportional to the protein concentration ($S_{2p}(q)$ scales as $\rho_p^{1/2}$, see Eq.(7.37)). This has been verified to be true for aqueous solutions of PEO and BSA up to 5 g/l BSA, at least,

using light scattering measurements (Knoll and Hermans, 1983). Furthermore, and as reported in Section 7.4, the interpretation of the scattering of neutrons from a 9.9 g/l BSA solution (without polymer) was consistent with the interactions between BSA molecules making a negligible contribution to the overall scattered intensity of neutrons.

The measured excess scattered intensity from a solution containing 9.9 g/l BSA and 5.9% w/w PEO having a molecular weight of 8 650 Da is reported in Figure 7.8 (data points). The excess scattering was measured to be negative over the entire range of q values ($0.02Å^{-1}$ to $0.28Å^{-1}$). Qualitatively, the negative excess scattering reveals that the *net* interaction between polymer coils and protein molecules in solution is repulsive (Cabane, 1987). In the limit $q \to 0$, an equation analogous to Eq.(7.21) can be derived which relates the excess scattered intensity to the concentration fluctuations in solution. Specifically (Knoll and Hermans, 1983),

$$I^{ex}(q \to 0) = K \left\langle \frac{\delta N_p \delta N_2}{V^2} \right\rangle \qquad \textbf{(7.34)}$$

where $\delta N_i/V$ is the instantaneous fluctuation in the number density of molecules of type i (i=2 or p) in solution, and K is a positive constant. When a net repulsion exists between the two species, on average, the two species will tend to reside apart from one another, and as is seen in Figure 7.8, the right-hand side of Eq.(7.34) will be negative. Alternatively, for a net attraction between the molecules in solution the excess scattered intensity will be positive (Knoll and Hermans, 1983).

In Figure 7.8, as the magnitude of the scattering vector increases, the excess scattering approaches zero asymptotically. This is because the scattering in the high-q region is dominated by intraparticle correlations which are essentially the same in both the mixture and the single-component solutions (Guinier and Fournet, 1955; Cabane, 1987; Glatter and Kratky, 1982).

In Chapters 4 and 6, on the basis of theoretically predicted protein partitioning behavior as a function of PEO molecular weight, it was concluded that although a net repulsive interaction exists between the protein and the PEO molecules in

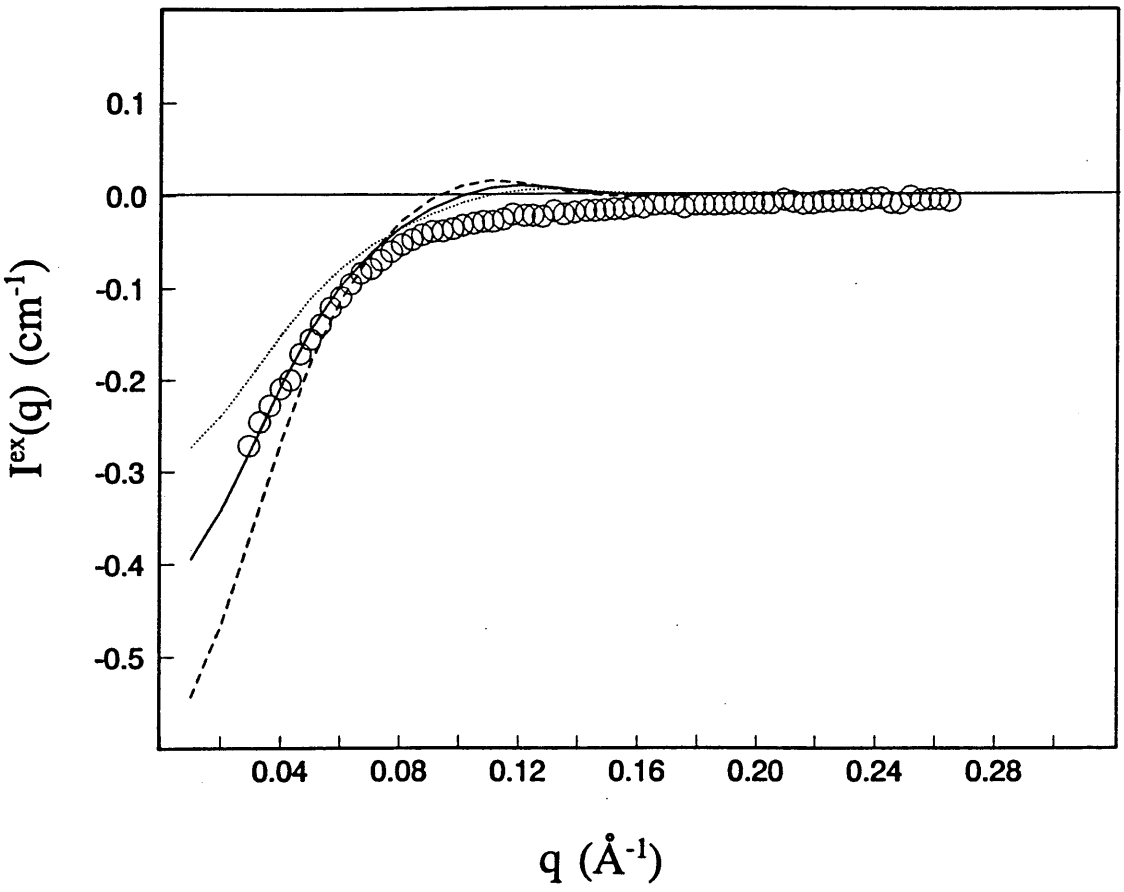

Figure 7.8. Excess neutrons scattering intensity, $I^{ex}(q)$, as a function of q, the magnitude of the scattering vector, for a solution of 9.9 g/l BSA and 5.9% w/w PEO 8 650 Da in D_2O: (O) experimental measurement, theoretical prediction using a hard-sphere mixture structure factor and 3 different protein sizes; (- -) 34Å, (——) 29Å, (···) 24Å.

solution, this repulsion is less than that expected based only on steric considerations (Abbott et al., 1991a and b). Such a situation is suggestive of an attractive interaction between PEO coils and proteins. In order to determine the possible roles of repulsive steric and attractive interactions on the structure of the solution containing proteins and polymers, a quantitative interpretation of the excess scattered intensity was developed. The challenge in predicting the excess scattered intensity, $I^{ex}(q)$, is in evaluating the partial structure factor $S_{p2}(q)$ (see Eq.(7.33)), since all other quantities required to predict $I^{ex}(q)$ can be evaluated from the scattering measurements reported in Sections 7.3 and 7.4. The partial structure factor, $S_{p2}(q)$, can be calculated using the Ornstein-Zernike equation (Ornstein and Zernike, 1914) for a two-component system from the direct correlation functions, $C_{ij}(q)$, as (Ornstein and Zernike, 1914; Lebowitz, 1964)

$$S_i(q) = \left[1 - \rho_i C_{ii}(q) - \frac{\rho_i \rho_j C_{ij}^2(q)}{1 - \rho_j C_{jj}(q)}\right]^{-1} \tag{7.35}$$

and

$$S_{ij}(q) = \frac{\rho_i^{1/2}\rho_j^{1/2} C_{ij}(q)}{[1 - \rho_i C_{ii}(q)][1 - \rho_j C_{jj}(q)] - \rho_i \rho_j C_{ij}^2(q)} \tag{7.36}$$

Eqs.(7.35) and (7.36) can be simplified since in Section 7.4 it was demonstrated that the protein concentration is sufficiently low such that $S_p(q)=1$. Furthermore, in the limit of vanishing protein concentration, the influence of the protein presence on the structure of the polymer solution will vanish, and, therefore, $S_2(q)$ will be independent of protein concentration. Substituting j=p for the protein and i=2 for the polymer into Eqs.(7.35) and (7.36), and taking the limit of vanishing protein concentration, $\rho_p \to 0$, yields

$$S_2(q) = \frac{1}{1 - \rho_2 C_2(q)} \tag{7.37}$$

$$S_{p2}(q) = \frac{\rho_p^{1/2}\rho_2^{1/2}C_{p2}(q)}{1 - \rho_2 C_2(q)} \qquad (7.38)$$

Note that Eq.(7.37) is identical to Eq.(7.15). As mentioned above, this reflects the fact that the correlations between PEO coils in solution are not affected by the very low BSA concentrations. To evaluate the direct correlation functions, $C_2(q)$ and $C_{p2}(q)$, in Eqs.(7.37) and (7.38) several approaches were explored (see below), each of which contained different approximations. Despite this, they all lead to the common conclusion suggesting the presence of attractive interactions between the protein molecules and the polymer coils (in addition to the steric repulsions).

In the first approach, the structure factors, $S_{p2}(q)$ and $S_2(q)$, were predicted from the direct correlation functions for a hard-sphere mixture, $C_{p2}(q)$ and $C_2(q)$ which have been erived previously by Lebowitz (1964) using the Percus-Yevick equation (1958) generalized for a multicomponent system (Ashcroft and Langreth, 1967 and 1968). The inputs which are required to evaluate the direct correlation functions are the effective hard-sphere potentials of the polymer and protein molecules. For PEO having a molecular weight of 8 650 Da, the effective hard sphere radius is 22.4Å (Abbott et al., 1991b). This is consistent with the hard-sphere potential used to predict the thermodynamic properties of aqueous PEO solutions in Chapter 6 (Abbott et al., 1991b), and was also the potential used to predict the small angle neutron scattering from PEO solutions in Section 7.3. The effective hard-sphere protein radius was initially treated as a fitting parameter, and subsequently compared with that evaluated using the Monte-Carlo method described in Chapter 6 (Abbott et al., 1991b). Note that the effective hard-sphere radius of the BSA molecule, when interacting with PEO, does not, in general, equal to the physical protein radius since the effective BSA hard-sphere radius includes the deformable nature of the PEO coil (Abbott et al., 1991b). In Figure 7.8 the experimental excess scattering (data points) are compared to the excess scattering predicted using the hard-sphere mixture structure factor (solid line) for three different effective hard-sphere protein sizes of 34Å, 29Å and 24Å. The best agreement between

the experimental data points and the theoretical prediction is when a BSA radius of 29Å is used. This value is significantly smaller than 37Å, the value obtained for the effective hard-sphere radius of BSA assuming only steric interactions between BSA and the PEO molecules (see Chapter 6) using the Monte-Carlo method (Abbott et al., 1991b). This observation is suggestive of an attractive interaction between the protein and the polymer molecules (in addition to the steric repulsion) (Guinier and Fournet, 1955; Cabane, 1987; Glatter and Kratky, 1982). The influence of an attractive interaction between PEO and BSA would be to decrease the effective hard-sphere radius of a BSA molecule. Despite the weak attraction, the net interaction between the protein and the polymer molecules (which includes the contribution of steric interactions) remains repulsive, and thus the excess scattering intensity is negative.

In the second approach, the direct correlation function $C_{p2}(q)$ was again calculated from the Percus-Yevick equation for hard-sphere mixtures (Lebowitz, 1964), but, in contrast to the first approach, the polymer structure factor, $S_2(q)$ (or alternatively $C_2(q)$), was evaluated using the previously described approach developed by Benoit and Benmouna (1984). This alternative description of the polymer solution was explored here because in Section 7.3 it was shown that it leads to a better description of the polymer structure factor than does the hard-sphere structure factor (particularly for intermediate q values). The effective hard-sphere polymer and protein radii were used for the evaluation of $C_{p2}(q)$ were unchanged. The result of this evaluation (not shown) was almost identical to the theoretical predictions presented in Figure 7.8. This suggests that the excess scattering intensity, $I^{ex}(q)$, is not very sensitive to the form of the PEO-PEO structure factor and, accordingly, that the correlations in the PEO coil positions (due to PEO-PEO coil interactions) do not have a dominating effect on the PEO-BSA correlations.

In the third approach, the excess scattering was predicted by explicitly introducing an attractive interaction between the protein and the polymer molecules, in addition to their steric repulsion. These two features, a repulsive core and an attractive part are captured in the sticky hard-sphere potential model introduced by Baxter (1968), which has been successfully applied to the description of microemulsions (Robertus et

al., 1989 and 1990) and other colloidal systems (de Kruif et al., 1989). The model interaction potential for the case of a binary mixture has the following form

$$\frac{\phi_{nm}(r)}{kT} = \begin{cases} \infty & 2r < S_{nm} \\ \log 12\tau_{nm}\dfrac{(D_n + D_m - S_{nm})}{D_n + D_m} & S_{nm} < r < D_n + D_m \\ 0 & 2r > D_n + D_m \end{cases} \quad (7.39)$$

where $S_{nm} \rightarrow D_n + D_m$, τ_{nm} is the stickiness parameter (Baxter, 1968) (which characterizes the strength of the attractive interaction between the polymer coils and the protein molecules, and where $\tau = \infty$ corresponds to the hard-sphere limit, namely, no stickiness), and D_n and D_m are the hard-sphere diameters. For the case of a hard-sphere mixture with attractions between unlike species only, an analytic equation can be derived (Barboy, 1975) for $C_{p2}(q)$ using the Percus-Yevick approximation (Percus and Yevick, 1958). The inputs to the evaluation of the sticky hard-sphere structure factor are the effective hard-sphere diameters of the proteins (D_p) and polymers (D_2), and the stickiness parameter, τ_{p2}. As discussed above, the effective hard-sphere diameters which characterize the PEO-PEO coil interaction and the PEO-BSA steric interaction have been determined previously to be 44.8Å and 74Å, respectively (Abbott et al., 1991b). In Figure 7.9, the excess scattering intensity measured experimentally (data points) is compared to the predicted intensity using the sticky hard-sphere structure factor for various values of the stickiness parameter, τ_{p2}. An inspection of Figure 7.9 shows that in the absence of any attraction between the protein and the polymer molecules ($\tau_{p2} = \infty$), the excess scattering is smaller than that observed experimentally in the low-q region. Furthermore, accompanying an increase in the strength of the attraction (a decrease in τ_{p2}), the predicted excess scattering intensity approaches that observed experimentally. A stickiness parameter of approximately $\tau_{p2} = 1.5$ was determined to produce the closest fit of the predicted excess scattering intensity to the experimental data. Finally, it is

relevant to discuss the "hump" that is present in the predicted excess scattering at $q \simeq 0.1 Å^{-1}$. In view of the earlier discussion of a similar "hump" in the predicted scattering of a PEO solution (see Figure 7.4), the most likely explanation lies in our characterization of the protein-polymer interaction using an effective hard-sphere model. In reality, the true interaction potential will be "softer" and longer-ranged than the effective hard-sphere potential and the effect of this "softness" will be reduce the strength of the correlations within the solution, that is, to damp the oscillations in the structure factor. However, it is important to note that these considerations do not affect our conclusions in the lower-q region and higher-q regions, where good agreement is observed between the experimental and theoretically predicted intensity.

To make a quantitative comparison between the strength of the attraction required to describe the neutron scattering data ($\tau_{p2}=1.5$, in the notation of the sticky hard-sphere model (Baxter,1968)) and the strength of the attraction required in Chapter 6 to account for the influence of PEO molecular weight on the protein partition coefficient (ε, in the notation of Chapters 4 and 6 (Abbott et al., 1991a and b)), the second virial coefficient reflection protein-polymer interactions (McQuarrie, 1976) was calculated for both models. For the sticky hard-sphere model (Baxter, 1968), the second virial coefficient describing the protein-polymer interactions, B_{p2}, is related to the stickiness parameter and the hard-sphere diameters by (de Kruif et al., 1989)

$$B_{p2} = \frac{\pi}{6}\left[\frac{D_p + D_2}{2}\right]^3\left[4 - \frac{1}{\tau_{p2}}\right] \qquad \textbf{(7.40)}$$

Substituting the sticky hard-sphere parameter values that describe the measured excess scattered intensity (determined above), that is, $\tau_{p2}=1.5$, $D_2=44.8Å$ and $D_p=74Å$, the crossed second virial coefficient was evaluated from Eq.(7.40) to be $4.66 \times 10^5 Å^3$. Using the Monte-Carlo approach described in Chapter 6, the same value of the crossed second virial coefficient is obtained with an attractive interaction energy of $\varepsilon=0.05kT$ (per polymer segment interacting with the protein surface). The strength of the attractive

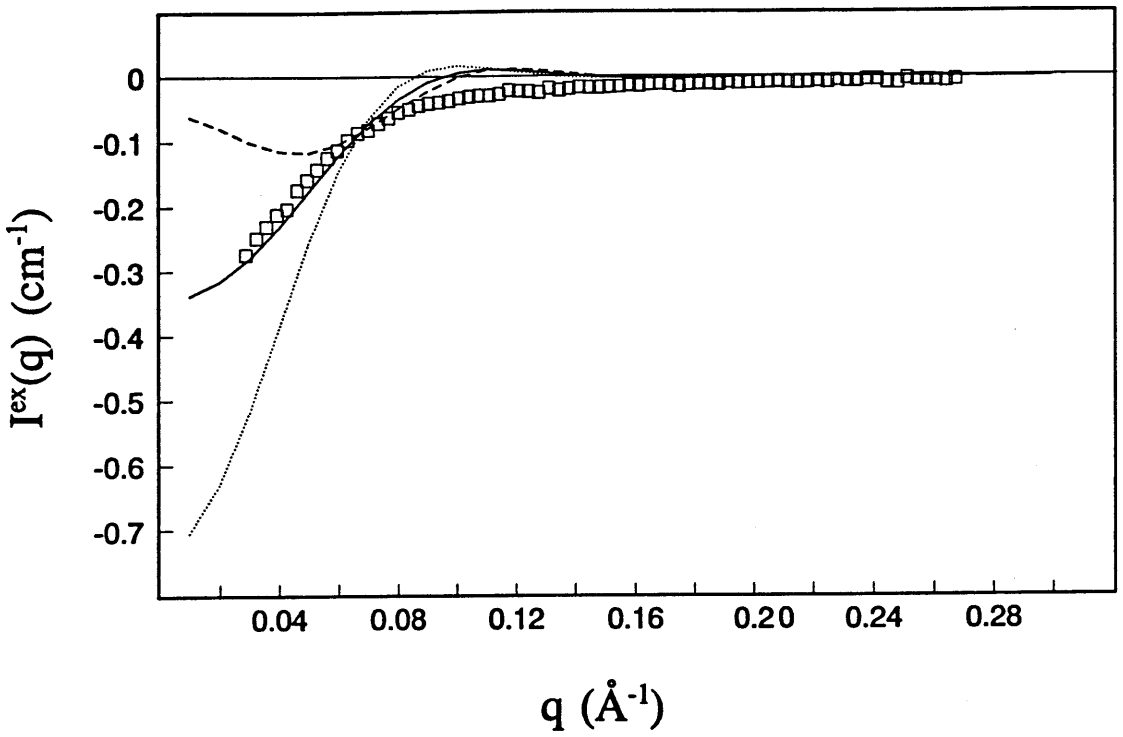

Figure 7.9. Excess neutron scattering intensity, $I^{ex}(q)$, as a function of q, the magnitude of the scattering vector, for a solution of 9.9 g/l BSA and 5.9% w/w PEO 8 650 Da in D_2O: (□) experimental measurement: theoretical prediction using a sticky hard-sphere mixture structure factor and 3 different stickiness parameters; τ_{p2} (- -) 0.3, (——) 1.5, (···) ∞.

interaction energy, ε=0.05kT, predicted here from the measured intensity of neutrons scattered from an aqueous BSA-PEO solution, is consistent with previous values (0.01-0.10kT) obtained on the basis of our earlier thermodynamic models for protein-polymer interactions (Abbott et al., 1991a and b), which predicted the partitioning behavior of proteins, such as BSA, in two-phase aqueous polymer systems containing PEO.

7.6 Concluding Remarks

Experimental measurements of the intensity of neutrons scattered from solutions of PEO in D_2O over a wide range of PEO concentrations and molecular weights were reported. Using these measurements, the correlations lengths of the PEO solutions were determined, and a transition in the nature of the polymer solution phase was observed. That is, with an increase in PEO molecular weight, the PEO-D_2O system undergoes a transition from a polymer solution containing individually dispersed polymer coils to one containing an entangled network of polymers. Significantly, the PEO solution conditions at which the transition is observed correspond closely to those encountered in the PEO-rich phase of a two-phase aqueous PEO-dextran system utilized in protein partitioning experiments. In the spirit of the microscopic models of polymer solutions containing proteins proposed in earlier chapters of this thesis (see also Abbott et al., 1991a and b), these experimental observations support our proposal that the underlying cause of a number of trends observed in protein partitioning measurements is the transition in the polymer solution structure (Abbott et al., 1991a). This recognition is fundamental for the development of physically based models of protein partitioning in two-phase aqueous polymer systems.

In addition to determining the correlation lengths of the PEO solutions using SANS measurements at intermediate q values, in the limit $q \to 0$, the thermodynamic state, as reflected in the osmotic compressibility, of the solutions was determined. The osmotic compressibility of PEO solutions containing identifiable polymer coils was well described using an effective hard-sphere potential to describe the interactions between

polymer coils. In the vicinity of the crossover in polymer solution regimes, a weak concentration dependence of the polymer-polymer effective hard-sphere potential was found. In view of the rather subtle effects which can influence the predicted protein partitioning behavior, it is important to consider the impact of the concentration-dependent effective hard-sphere potential on the predicted protein partitioning behavior. The effect of the concentration-dependent hard-sphere potential is to decrease the molecular weight dependence of the hard-sphere diameter (at constant polymer volume fraction). This arises because the higher molecular weight polymers are closer to the crossover, and therefore, de-swell or interpenetrate each other more than the low molecular weight polymers. Qualitatively, the effect of the reduction in the polymer-polymer effective hard-sphere potential (due to concentration effects) is to decrease the protein chemical potential at the higher molecular weights (Abbott et al., 1991a). This observation does not influence our previous suggestion that steric interactions alone appear not to account for certain protein partitioning behaviors in two-phase aqueous polymer systems (although it could influence, for example, the precise strength of the attractive interaction between the proteins and PEO required to account for the observed protein partitioning behavior) (Abbott et al., 1991a and b).

Neutron scattering measurements for solutions containing a mixture of PEO and BSA determined that the net interaction between the BSA and PEO molecules is repulsive. Despite this net repulsive interaction, quantitative modelling of the solution structure and the excess scattering from the solutions suggests that the repulsive interaction is significantly less than that expected on the basis of steric interactions only. Accordingly, the existence of an attractive interaction between the protein and the polymer molecules is proposed on the basis of the predicted structure of the solution, as reflected in the SANS intensity measurements. This is consistent with our previous statistical-thermodynamic models for the interactions of proteins and polymers which also suggested the presence of a weak attraction, in addition to the steric repulsion (Abbott et al., 1991a and b). Quantitatively, both statistical-thermodynamic models and structural models for PEO solutions containing BSA predict that an attractive interaction of approximately 0.05kT (per polymer segment at the protein surface) exists between PEO

and BSA.

In view of the increasing evidence, both structural and thermodynamic, which suggests the presence of a weak attractive interaction between the protein and polymer molecules, it is relevant to address the previous investigations (Knoll and Hermans, 1983), notably light scattering measurements, which were interpreted to suggest that the interactions between between BSA and PEO arise purely from excluded-volume interactions. Considering the rather small influence of the attraction on the BSA-PEO second virial coefficient (around 20% of the steric contribution), it appears conceivable that, due to the difficult extrapolations required by light scattering measurements (Knoll and Hermans, 1983), such a small effect may have been beyond the resolution of the experiments. Indeed, the neutron scattering measurements corroborate the view that the dominant contribution to the protein-polymer second virial coefficient is that due to steric interactions. While clearly additional experiments with PEO over a range of molecular weights, concentrations, and with a variety of proteins are required to solidify the propositions of this chapter, the consistency between the microscopic models, statistical-thermodynamic theories, protein partitioning and neutron scattering measurements is satisfying, and a unified description of interactions between certain types of proteins and polymers appears to be developing.

7.7 Literature Cited

Abbott, N.L.; Blankschtein, D.; Hatton, T.A. *Bioseparation*, **1990**, 1, 191.

Abbott, N.L.; Blankschtein, D.; Hatton, T.A. *Macromolecules* **1991**, 24, 4334.

Abbott, N.L.; Blankschtein, D.; Hatton, T.A. *Macromolecules* **1991**, submitted.

Albertsson, P.A. *Partition of Cell Particles and Macromolecules*; Wiley, New York, **1985**.

Albertsson, P.-A.; Cajarville, A.; Brooks, D.E.; Tjerneld, F. *Biochim. Biophys. Acta* **1987**, 926, 87.

Ashcroft, N.W.; Lekner, J., *Phys. Rev.*, **1966**, 145, 83.

Ashcroft, N.W.; Langreth, D.C., *Phys. Rev.*, **1967**, 156, 685.

Ashcroft, N.W.; Langreth, D.C., *Phys. Rev.*, **1968**, 166, 934.

Ataman, M.; Boucher, E.A., *J. Polymer Sci., Poly. Phys. Ed.*, **1982**, 20, 1585.

Barboy, B., *Chemical Physics*, **1975**, 11, 357.

Baskir, J.N.; Hatton, T.A.; Suter, U.W. *Macromolecules* **1987**, 20, 1300.

Baskir, J.N.; Hatton, T.A.; Suter, U.W. *J. Phys. Chem.* **1989**, 93, 2111.

Baxter, R.J., *J. Chem. Phys.*, **1968**, 49, 2770.

Bendedouch, D.; Chen, S.-H., *J. Phys. Chem.*, **1983**, 87, 1473.

Benoit, H.; Benmouna, M., *Polymer*, **1984**, 25, 1059.

Bishop, M.; Saltiel, C.J., *J. Chem. Phys.*, **1991**, 94, 6920.

Boothroyd, A.T., *Polymer*, **1988**, 29, 1555.

Cabane, B. in *Surfactant Science Series*, Volume 22, Ed., R. Zana **1987**.

Cabane, B.; Duplessix, R. *J. Physique* **1987**, 48, 651.

Carlson, A., *Separation Science and Technology*, **1988**, 23, 785.

Chen, S.-H.; Bendedouch, D., *Methods in Enzymology*, **1986**, 130, 79.

Croxton, C.A., *Polymer Communications*, **1988**, 29, 232.

Daoud, M.; Cotton, J.P.; Farnoux, B.; Jannink, G.; Sarma, G.; Benoit, H.; Duplessix, R.; Picot, C.; de Gennes, P.G., *Macromolecules*, **1975**, 8, 804.

Debye, P.; Bueche, A.M., *J. Appl. Phys.*, **1949**, 20, 518.

Debye, P.; Henderson, H.R.; Brumberger, H.; *J. Appl. Phys.*, **1957**, 28, 679.

de Gennes, P.-G. *Scaling Concepts in Polymer Physics*; Cornell University Press, Ithaca, **1988.**

de Kruif, C.G.; Rouw, P.W.; Briels, W.J.; Duits, M.H.G.; Vrij, A.; May, R.P., *Langmuir*, **1989**, 5, 422.

Edwards, S.F., *Proc. Phys. Soc. London*, **1966**, 88, 265.

Farnoux, B.; Daoud, M.; Decker, D.; Jannink, G,; Ober, R., *J. Physique*, **1975**, 36, L-35.

Flory, P.J. *Principles of Polymer Chemistry*; Cornell University Press, Ithaca and London, **1986.**

Flory, P.J.; Krigbaum, W.R., *J. Chem. Phys.*, **1950**, 18, 1086.

Florin, E.; Kjellander, R.; Eriksson, J.C., *J. Chem. Soc., Faraday Trans. 1*, **1984**, 80, 2889.

Forciniti, D.; Hall, C.K.; *A.C.S Symposium Series,* **1990**, 419, 53.

Glatter, O.; Kratky, O., *Small Angle X-Ray Scattering*, Academic Press, London, **1982**.

Guinier, A.; Fournet, G., *Small Angle Scattering of X-Rays*; Wiley, New York, **1955**.

Hansen, J.-P.; McDonald, I.R., *Theory of Simple Liquids*, Academic Press, London, **1976**.

Huggins, M.L. *J. Phys. Chem.* **1941**, 9, 440.

Hustedt, H.; Kroner, K.H.; Stach, W.; Kula, M.-R. *Biotechnol. Bioeng.* **1978**, 20, 1989.

Knoll, D.; Hermans, J.; *J. Biological Chem.*, **1983**, 258, 5710.

Lebowitz, J.L., *Phys. Rev.*, **1964**, 133, A895.

McQuarrie, D.A., *Statistical Mechanics*, Harper and Row, New York, **1976**.

Nossal, R.; Glinka, C.J.; Chen, S.-H., *Biopolymers*, **1986**, 25, 1157.

Ornstein, L.S.; Zernike, F., *Proc. K. Ned. Akad. Wet.*, **1914**, 17, 793.

Pecora, R., *Dynamic Light Scattering*, Plenum, New York, **1985**.

Percus, J.K.; Yevick, G.J., *Phys. Rev.*, **1958**, 110, 1.

Robertus, C.; Philipse, W.H.; Joosten, J.G.H.; Levine, Y.K., *J. Chem. Phys.*, **1989**, 90, 4482.

Robertus, C.; Joosten, J.G.H.; Levine, Y.K. *J. Chem. Phys.*, **1990**, 93, 7293.

Schaefer, D., *Polymer*, **1984**, 25, 387.

Schneider, D.K.; Schoenborn, B.P., *Neutrons in Biology*, Plenum, New York, B.P. Schoenborn, Ed., **1984**, 119.

Squire, P.G.; Moser, P.; O'Konsky, C.T., *Biochemistry*, **1968**, 7, 4261.

Tong, P.; Witten, T.A.; Huang, J.S.; Fetters, L.J., *J. Phys. France*, **1990**, 51, 2813.

Tsunashima, Y.; Kurata, M., *J. Chem. Phys.*, **1986**, 84, 6432.

Ullman, R.; Benoit, H.; King, J.S., *Macromolecules*, **1986**, 19, 183.

Vennemann, N.; Lechner, M.D.; Oberthur, R.C., *Polymer*, **1987**, 28, 1939.

Walter, H.; Brooks, D.E.; Fisher, D., Eds, *Partitioning in Aqueous Two-Phase systems*; Academic Press, New York, **1985**.

Walter, H.; Johansson, G. *Analytical Biochemistry*, **1986**, 155, 215.

Walter, H.; Johansson, G.; Brooks, D.E., *Analytical Biochemistry*, **1991**, (in press).

Wiltzius, P.; Haller, H.R.; Cannell, D.S.; Schaefer, D.W., *Phys. Rev. Lett.*, **1983**, 51, 1183.

Zimm, B.H., *J. Chem. Phys.*, **1948**, 16, 1093.

Appendix 7.A

Prior to interpretation, the raw neutron scattering data, that is, the recorded number of neutron collisions per detector pixel, were corrected for (i) sample transmission, (ii) empty cell scattering, (iii) background scattering, and (iv) variations in the efficiency of the detector elements. The method used, which is detailed below, is similar to that outlined previously by Chen and Bendedouch (1986).

The sample transmission, T_s, is defined as

$$T_s = \frac{I_s - I_b}{I_o - I_b} \qquad \textbf{(7.A1)}$$

where I_o is the incident intensity, I_s is the total number of detector counts, and I_b is the background intentsity. The sample transmission is simply the fraction of incident neutrons that reach a detector element. This quantity is less than unity since some neutrons are scattered at sufficiently wide angles that they do not intersect a detector element. From knowledge of the transmission of the sample, T_s, and the total number of incident neutrons during the scattering experiment, M_s, (measured upstream of the scattering sample) the total number of neutrons incident on the detector is M_sT_s. Note that the latter quantity is not determined by the integration of the number of scattering counts over the entire detector, since a beam stop is inserted during the scattering experiment to prevent the direct irradiation of the detector elements with an intense

neutron beam. The beam stop is absent during the measurement of the transmission of the sample. The background scattering, I_b, and scattering of the empty cell, I_e, are subtracted to provide the net scattering of the sample, I_s^{net}

$$I_s^{net} = \frac{I_s - \frac{I_b M_s}{M_b}}{T_s M_s} - \frac{I_e - \frac{I_b M_e}{M_b}}{T_e M_e} \qquad \textbf{(7.A2)}$$

where M_e and M_b are the total number of incident neutrons, measured upstream of the sample holder, during the empty-cell and background scattering experiments, amd T_e is the transmission of an empty sample cell. The net scattering of the sample was futher corrected for variations in the detector efficiency through a comparison of the measured scattering of water with that which would be measured in the event of uniform detector pixel efficiency. The measured net scattering of water, I_w^{net}, is corrected for the thickness of the water sample, t_w, to calculate the differential cross section, $(d\Sigma/d\Omega)_w$, that is

$$\left[\frac{d\Sigma}{d\Omega}\right]_w = \frac{I_w^{net}}{t_w} \qquad \textbf{(7.A3)}$$

To calculate the differential cross section of water, outside the intense forward peak (those neutrons which do not hit any scattering bodies) the scattering of water is assumed isotropic. With the understanding that during the transmission test the total counts are dominated by the unscattered neutrons, the fraction of incident neutrons that are isotropically scattered corresponds to $1\text{-}T_w$. With the isotropic scattering of the neutrons over a solid angle of 4π, the correction factor applied to the sample scattering takes the form

$$\frac{1 - T_w}{4\pi T_w I_w^{net}} \qquad \textbf{(7.A4)}$$

Accordingly, the intensity of scattered neutrons from the sample, corrected for the detector efficiency, that is, the differential cross section of the sample, is evaluated as

$$\left[\frac{d\Sigma}{d\Omega}\right]_s = \frac{(1 - T_w)\, I_s^{net}}{4\pi T_w t_s I_w^{net}} \qquad \textbf{(7.A5)}$$

The differential cross section of the sample, $(d\Sigma/d\Omega)_s$, contains both coherent scattering (containing information about the structure) and incoherent scattering (which contains no information about the structure or position of the atoms) (Cabane, 1987). The coherent portion is estimated as (Cabane, 1987)

$$\left[\frac{d\Sigma}{d\Omega}\right]_{coh} = \left[\frac{d\Sigma}{d\Omega}\right]_s - \frac{N_H \sigma_{inc}^H}{4\pi} \qquad \textbf{(7.A6)}$$

where N_H is the number density of hydrogen atoms within the sample, and σ^H_{inc} is the scattering cross section of a hydrogen atom (79.90×10^{-24} cm^2). For the highest weight fraction of PEO in D_2O used in the investigation, the contribution of the PEO hydrogens to the incoherent scattering was approximately 0.08 cm^{-1}, and therefore, represents an important correction for these samples. The inclusion of 0.5M anhydrous sodium acetate buffer in some of the PEO solutions had negligible contribution to the calculated incoherent scattering intensity. The differential cross section, $(d\Sigma/d\Omega)_{coh}$, which is denoted as $I_i(q)$ (i=2,p), is a quantity which is independent of the spectrometer used to perform the measurements.

Appendix 7.B

Derivation of the direct correlation function between hard spheres in a hard sphere mixture.

$$-C_{12}(r) = a_1 \qquad r < \frac{1}{2}(\sigma_2 - \sigma_1) \tag{7.B1}$$

$$= a_1 + \frac{[bR^2 + 4d\lambda R^3 + dR^4]}{r} \qquad \frac{1}{2}(\sigma_2 - \sigma_1) < r < \frac{1}{2}(\sigma_2 + \sigma_1) \tag{7.B2}$$

where

$$R = r - \frac{1}{2}(\sigma_2 - \sigma_1) \tag{7.B3}$$

$$\lambda = \frac{1}{2}(\sigma_2 - \sigma_1) \tag{7.B4}$$

$$d = \frac{\left[\eta_1 a_1 + \alpha^3 \eta_2 a_2\right]}{\sigma_1^3} \tag{7.B5}$$

$$b = \frac{-3(1+\alpha)}{\sigma_2}\left[\frac{\eta_1 g_{11}}{\alpha^2} + \eta_2 g_{22}\right] g_{12} \tag{7.B6}$$

where the functions g_{11}, g_{12} and g_{22} are defined as

$$g_{11} = \frac{(1+\frac{1}{2}\eta)+\frac{3}{2}\eta_2(\alpha-1)}{(1-\eta)^2} \qquad \textbf{(7.B7)}$$

$$g_{22} = \frac{(1+\frac{1}{2}\eta+\frac{3}{2}\eta_1)\left[\frac{1}{\alpha}-1\right]}{(1-\eta)^2} \qquad \textbf{(7.B8)}$$

$$g_{12} = \frac{(1+\frac{1}{2}\eta)+\frac{3}{2}\frac{1-\alpha}{1+\alpha}(\eta_1-\eta_2)}{(1-\eta)^2} \qquad \textbf{(7.B9)}$$

The functions a_1 and a_2 are

$$a_1 = \frac{\partial}{\partial\eta_1}\left[\frac{(\eta_1+\alpha^3\eta_2)(1+\eta+\eta^2)-3\eta_1\eta_2(1-\alpha)^2[1+\eta_1+\alpha(1+\eta_2)]}{(1-\eta)^3}\right] \qquad \textbf{(7.B10)}$$

$$a_2 = \frac{\partial}{\alpha^3\partial\eta_2}\left[\frac{(\eta_1+\alpha^3\eta_2)(1+\eta+\eta^2)-3\eta_1\eta_2(1-\alpha)^2[1+\eta_1+\alpha(1+\eta_2)]}{(1-\eta)^3}\right] \qquad \textbf{(7.B11)}$$

In Fourier space the direct correlation function $c_{ij}(y)$ becomes (Ashcroft and Langreth, 1967)

$$
\begin{aligned}
-n_1^{1/2}n_2^{1/2}C_{12}(y) = 3(1-\alpha)^3\frac{\eta(1-x)^{1/2}x^{1/2}}{x+(1-x)\alpha^3}a_1\frac{siny_\lambda - y_\lambda cosy_\lambda}{y_\lambda^3} \\
+24\eta\frac{x^{1/2}(1-x)^{1/2}\alpha^3}{x+(1-x)\alpha^3}[\frac{siny_\lambda}{y_1^4}\{\beta_{12}[2y_1cosy_1+(y_1^2-2)siny_1] \\
+\frac{\gamma_{12}}{y_1}[(3y_1^2-6)cosy_1-(y_1^3-6)siny_1+6] \\
+\frac{\gamma_1}{y_1^2}[(4y_1^3-24y_1)cosy_1+(y_1^4-12y_1^2+24)siny_1]\} \\
+cos\frac{y_\lambda}{y_1^4}\{\beta_{12}[2y_1siny_1-(y_1^2-2)cosy_1-2]+ \\
\frac{\gamma_{12}}{y_1}[(3y_1^2-6)siny_1-(y_1^3-6y_1)cosy_1] \\
+\frac{\gamma_1}{y_1^2}[(4y_1^3-4y_1)siny_1-(y_1^4-12y_1^2+24)cosy_1+24]\} \\
+\frac{a_1}{y_1}\{cosy_\lambda(\frac{siny_1-y_1cosy_1}{y_1^2}+\frac{1-\alpha}{2\alpha}\frac{1-cosy_1}{y_1})+ \\
siny_\lambda(\frac{cosy_1+y_1siny_1-1}{y_1^2}+\frac{1-\alpha}{2\alpha}\frac{siny_1}{y_1})\}]
\end{aligned}
\tag{7.B12}
$$

where the parameters are defined as

$$y_\lambda = \frac{1}{2}y\,(1-\alpha) \tag{7.B13}$$

$$\beta_{12} = \sigma_1 b \tag{7.B14}$$

$$\gamma_{12} = 2\,\gamma_1 \left[\frac{1-\alpha}{\alpha}\right] \qquad \textbf{(7.B15)}$$

Appendix 7.C

A clear account of the use of the Percus-Yevick equation for the calculation of the direct correlation functions in multicomponent sticky hard sphere fluids can be found in ref. X. The general formalism is simplified for the binary fluid case where attractive interactions (stickiness) exist only between unlike species. In addition, in the limit of vanishing protein concentration, only the direct correlation function $C_{12}(q)$ will be influenced by the attraction and the polymer-polymer direct correlation function will not be perturbed from that corresponding to the absence of the attractive interaction. Therefore the results derived for $C_{11}(q)$ in Appendix 7.B are still valid and here we report the influence of the stickiness on $C_{12}(q)$ only.

From Eq.(6) of reference X the direct correlation function $C_{12}(q)$ can be evaluated in terms of so-called Wiener-Hopf transforms, $Q_{12}(q)$, of $C_{12}(q)$.

$$-C_{12}(q) = Q_{11}(q)Q_{12}^{*}(q) + Q_{21}(q)Q_{22}^{*}(q) \qquad \textbf{(7.C1)}$$

where

$$Q_{ij}(q) = \delta_{ij} + \frac{\pi}{6}(x_i x_j)^{1/2} e^{iqD_i/2}$$

$$X\left[-\frac{\lambda_{ij}}{4} D_j(D_i+D_j)^2 j_o\left(\frac{qD_j}{2}\right) + 6\frac{D_j^2}{q(1-\xi_3)} j_1\left(\frac{qD_j}{2}\right) + 3\frac{D_j^2 D_i}{(1-\xi_3)} j_o\left(\frac{qD_j}{2}\right) - 12\frac{D_j^2 b_i}{qD_i} j_1\left(\frac{qD_j}{2}\right) 3i\frac{D_i D_m^2}{(1-\xi_3)} j_1\left(\frac{qD_j}{2}\right)\right] \qquad \textbf{(7.C2)}$$

$$\lambda_{12} = 3\left[\frac{\frac{3(D_1 + D_2)\xi_2}{2(1-\xi_3)} + \frac{(D_1 + D_2)^2}{2D_1D_2}}{\frac{3(D_1+D_2)\xi_2}{2(1 - \xi_3)}+\tau_{12}}\right] \tag{7.C3}$$

$$\lambda_{11}=0 \text{ and } \lambda_{22}=0$$

$$\xi_i = \frac{\pi}{6}(x_1D_1^i + x_2D_2^i) \tag{7.C4}$$

$$b_i = -3D_i^2\frac{\xi_2}{2(1 - \xi_3)^2} + D_i\frac{X_i}{2(1 - \xi_3)} \tag{7.C5}$$

$$X_i = \frac{\pi}{6}(x_1\lambda_{i1}D_{i1}^2D_1 + x_2\lambda_{i2}D_{i2}^2D_1) \tag{7.C6}$$

$$D_{ij} = \frac{(D_i + D_j)}{2} \tag{7.C7}$$

and j_o and j_1 are the zero and first order spherical Bessel functions.

Chapter 8.

Proteins in Entangled Polymer Solutions. II. Protein Partitioning Across a Semipermeable Membrane

8.1 Introduction

In two-phase aqueous polymer systems containing high molecular weight polymers, the coexisting solution phases contain entangled webs of polymer, within which the identities of the individual polymer coils are lost. In such two-phase aqueous polymer systems, the partitioning of proteins is insensitive to the molecular weight of the polymers but is sensitive to their concentration. Accordingly, in Chapter 3, novel physical pictures describing the interactions of globular proteins and entangled polymer solutions were proposed. A variety of different scenarios were shown to exist depending on the relative sizes of the polymer solution net, ξ_b, and the protein dimensions, R_p, in addition to the strength of energetic interactions between the protein and the polymer, ε (per polymer segment at the protein surface). For these various physical scenarios, scaling-thermodynamic theories were developed in Chapter 5 to predict the form of protein chemical potential in entangled polymer solutions and the associated protein partitioning behavior. The aim of the experimental investigation reported in this chapter is to confront these theoretical predictions. In doing so, we hoped to distinguish between the possible physical scenarios which describe proteins in entangled polymer solutions (which were presented in Chapter 3).

While the partitioning of proteins between entangled polymer solution phases can be studied using two-phase aqueous polymer systems, several factors introduce ambiguity into the interpretation of the results. First, the partitioning behavior

of proteins in two-phase aqueous polymer systems reflects the *relative interactions* between the proteins and *two* coexisting polymer solution phases. Second, the independent control of the polymer concentration in only one of the two coexisting phases of a two-phase aqueous polymer system is not possible. Therefore, in order to overcome these limitations, we have explored an alternative experimental technique, which does not suffer these limitations. Here, we report the measurement of the partitioning of proteins between an entangled polymer solution phase and an aqueous polymer-free phase using a diffusion cell (see Figure 8.1 and Section 8.2.C). In contrast to the two-phase aqueous polymer systems, such an experimental set-up allows us to study the interactions of the proteins and a *single* entangled polymer solution phase. We focus our attention on the interactions of certain globular hydrophilic proteins and PEO since the partitioning of these species has been the subject of previous investigations in two-phase aqueous polymer systems containing PEO as one of the "phase-forming" polymers (Sasakawa and Walter, 1970 and 1972; Walter, et al., 1972; Zaslavsky et al., 1983; Albertsson et al., 1987; Johansson, 1985; Diamond and Hsu, 1989 and 1990).

The remainder of this chapter is organized as follows. In Section 8.2 we discuss experimental considerations, including the construction of a diffusion cell for the measurement of the partitioning behavior of proteins between an entangled polymer solution phase and an aqueous solution. We also discuss precautions taken in our experimental procedure to ensure that *equilibrium* partition coefficients were measured. In addition, Section 8.2 summarizes the experimental difficulties which prevented the measurement of the partition coefficients of relatively large protein molecules, for example, ovalbumin, chymotrypsinogen and bovine serum albumin. These proteins appeared to take a prohibitively long time to reach equilibrium. In Section 8.3, we present results of the experimentally measured partition coefficients of two relatively small hydrophilic proteins, cytochrome-c and ribonuclease-a, between an entangled PEO solution and an aqueous solution. Since, in two-phase aqueous polymer systems, the presence of different salt types can have a pronounced effect on the partitioning behavior of proteins which bear net charges, we have also examined the partitioning of cytochrome-c in the diffusion cell in the presence of two different salt types, NaCl and

Na_2SO_4, in order to assess the importance of salt effects in the diffusion cell measurements. In Section 8.4 we compare and contrast the experimentally measured and theoretically predicted protein partition coefficients. In doing so, we are able to assess the importance of different physical mechanisms in determining the protein partitioning behavior. In addition, we consider the partitioning of another protein, carbonic anhydrase, which has different physical properties as compared with cytochrome-c and ribonuclease (Cleland and Wang, 1991). The partially refolded form of carbonic anhydrase used in the experiments is more hydrophobic than cytochrome-c and ribonuclease-a. Accordingly, the partitioning of carbonic anhydrase, which appears to reflect a strong attractive interaction with PEO, contrasts with cytochrome-c and ribonuclease-a. Finally, in Section 8.5 we present our concluding remarks.

8.2 Materials and Experimental Considerations

A. Materials

Poly(ethylene oxide) (PEO) with a nominal molecular weight of 5 000 000 Da was obtained from Polysciences Inc., Warrington, PA (Lot No. 60004). The radius of gyration of the PEO coils is about 1 900Å (Abbott et al., 1991b), which is at least six times larger than the average pore size of the membrane used in the diffusion cell experiments (see below), thus rendering the membrane effectively impermeable to the polymer (Deen, 1989). Although reptation of the PEO chains through the pores is still possible, at these large polymer molecular weights this mechanism will result in very small polymer fluxes. Type V-A, Bovine Heart Cytochrome-c and Type I-AS, Bovine Pancreas Ribonuclease-a were purchased from Sigma Chemical Company, St Louis, MO. The hydrodynamic radii of these proteins are both approximately 20Å (see Table 8.3), and therefore, these proteins are sufficiently small to diffuse, relatively unhindered, through the membrane in the diffusion cell. Additional properties of the proteins can be found in Table 8.3. Track-etched polycarbonate membranes (which have a narrow distribution of pore-sizes) having a 300Å pore size (Lot No. 86B9B55) were obtained

from Nucleopore Corp., Pleasanton, CA. All other reagents were of analytical reagent grade, and all solutions were prepared using deionized water which had been conditioned using a Milli-Q ion exchange system (Waters, Milford, MA).

B. Sample Preparation

All solutions were prepared in 10 mM sodium phosphate buffer to control the pH at 7.0, 1.5mM sodium azide to prevent bacterial growth in the samples, and either 0.1M NaCl or 0.05M Na_2SO_4 to screen electrostatic interactions between the protein molecules. The solution pH of 7.0 was chosen since cytochrome-c and ribonuclease-a are not known to associate or undergo large conformational changes in the vicinity of this pH (Sasakawa and Walter, 1970 and 1972; Walter et al., 1972; Zaslavsky et al., 1983; Albertsson et al., 1987; Johansson, 1985; Diamond and Hsu, 1989). A stock solution of 2% w/w PEO having a molecular weight of 5 000 000 Da was dissolved in the buffered salt solution by gently stirring it for at least 24 hours at 25°C. The polymer solutions were heated briefly (less than 1 hour) to 45°C to speed up the dissolution process. No degradation of the polymer under these conditions is expected (PEO 1 200 000 Da has been reported to be stable for several days at 50°C and stable for several weeks at 20°C) (Cabane and Duplessix, 1987 and 1982). All protein solutions were prepared in the same buffer that was used to dissolve the PEO, and the protein solutions were prefiltered (Amicon Co., Danvers, MA) through a polycarbonate ultrafiltration membrane with a 150Å pore size. This latter precaution was to ensure that any undissolved protein (aggregates) was removed from the solution prior to the experiment, and thus all the protein within the diffusion cell could freely diffuse through the 300Å membrane and reach an equilibrium distribution between the two compartments of the cell.

C. Description of Diffusion Cell

A diagram of the diffusion cell used to measure the partition coefficients of the proteins between polymer networks and aqueous (polymer-free) solutions is presented in

Figure 8.1. The diffusion cell contains two compartments which are divided by a semipermeable membrane. The bottom compartment, having a volume of approximately 0.8ml, contained the polymer solution. Since the polymer solution was typically viscous, a magnetic stir bar was used to mix the solution in the lower compartment. The top compartment, having a volume of approximately 7ml, contained the aqueous protein solution and was maintained free of polymer by the membrane which, for all practical purposes, was impermeable to the polymer species. The protein molecules diffused freely across the membrane and were partitioned between the top and bottom compartments. The device was constructed by carefully separating 8ml plastic sample tubes (Olympic Plastics, Los Angeles, CA) into two sections. A small teflon coated magnetic stir bar was inserted into the lower section and then the two sections were reattached across a polycarbonate membrane with an expoxy resin (Devcon, Danvers, MA). Care was taken to ensure that only a minimal amount of glue was used, and that all the membrane area was available for the diffusion of permeable solutes between the two chambers. Two small holes were made in the lower section, and the polymer solution (initially free of protein) was injected through the soft plastic tubing into the lower chamber at the start of the experiment. The second hole permitted the escape of air during injection of the polymer solution into the lower section and care was taken to remove all air bubbles from the lower chamber before the section was resealed with a small dot of epoxy resin. The prefiltered protein solution (free of PEO) was poured into the top chamber of the cell at the beginning of the experiment. The bottom chamber of the cell was stirred gently during the experiment since the diffusion of the protein through the polymer network appeared to be the rate controlling factor during equilibration of the protein concentration between the two chambers of the cell. The cell was discarded after one experiment.

All protein concentrations were determined by measurement of the solution absorbance using a Perkin-Elmer Corp. Lambda 3B UV-VIS spectrophotometer. The concentrations and molecular weight distributions of PEO solutions were determined using a Hewlett-Packard HP-1090 high-pressure liquid chromatograph. The carrier solvent was an aqueous solution of 10mM sodium phosphate at pH 7.0, 1.5mM sodium

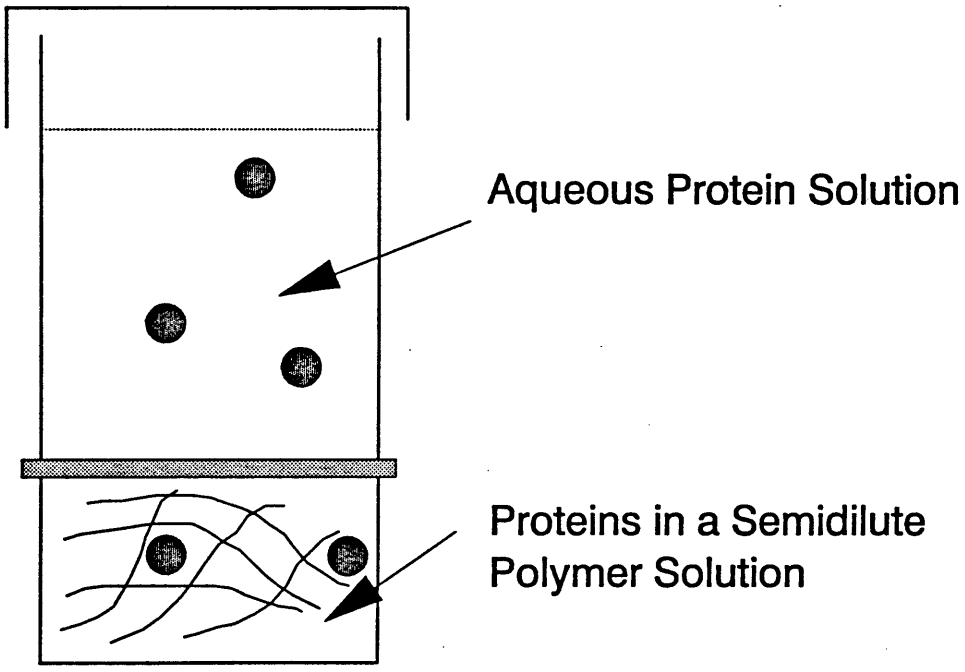

Figure 8.1 Schematic diagram of the diffusion cell constructed for the measurement of the protein partition coefficient between the top, polymer-free solution, and the bottom, entangled polymer solution phase. See Section 8.2 for details.

azide, and either 0.1M NaCl or 0.05M Na_2SO_4. The chromatograph was operated in a size exclusion mode using a Toya Soda TSK 3000PW, TSK 5000PW and guard column purchased from Varian Associates (Sunnyvale, CA). The presence of solutes in the eluent phase was detected with a Hewlett-Packard 1037A refractive index (RI) detector. The solute concentrations were calculated from the peak areas using the appropriate calibration standards.

D. Partitioning of Proteins into Entangled Polymer Solutions

Before the partitioning of proteins into a semidilute PEO solution was measured, a control experiment was performed to ensure that, in the presence of a PEO-free solution in the lower compartment, the protein was able to diffuse freely across the membrane and establish an equal concentration in the two compartments. This experiment also provided a lower bound on the time required to reach equilibrium during the partitioning experiments. Note that when PEO was present in the bottom chamber, the hindered diffusion of the protein molecules through the semidilute polymer network increased the time required to reach an equilibrium distribution of proteins between the two chambers. It is relevant to mention at this point, that a number of larger proteins, including ovalbumin, chymotrypsinogen and bovine serum albumin, could not be partitioned equally between the two compartments of the cell in a reasonable length of time even in the absence of PEO. Either the time taken to reach equilibrium was prohibitively long, or turbidity was detected in the protein solutions before equilibrium was reached thus suggesting the formation of protein aggregates. Only for the two relatively small proteins, cytochrome-c and ribonuclease-a, could the equilibrium be reliably and repeatedly obtained.

At the beginning of the partitioning experiment a buffered aqueous PEO solution (protein free) was injected into the bottom compartment of the cell, and a prefiltered and buffered aqueous protein solution (PEO free) was loaded into the top compartment of the cell. During the equilibration of the protein between the two compartments of the cell, the bottom compartment was stirred gently using a magnetic stir bar and the temperature

of the cell was thermostated at 15°C in a refrigerator. Multiple samples (typically 7) were prepared for each experiment, and these were sacrificed during the course of the experiment to monitor the approach of the system towards equilibrium. The time taken to reach equilibrium was typically greater than 3 days and less than one week (dependent on the polymer concentration). Upon reaching equilibrium, samples were aspirated with a syringe from the cell by piercing a hole in the wall of each compartment. The samples from each cell were analysed for both polymer and protein concentration.

The protein concentration in each compartment of the cell was measured by determining the absorbance of the solution. The ribonuclease concentration was determined by measuring the peak absorbance at a wavelength close to 280nm, and the concentration of cytochrome-c was determined by measuring the absorbance at wavelengths of 414nm and 549nm. Since the absorbance spectrum of cytochrome-c was found to be sensitive to the oxidation state of the heme-moiety, the cytochrome-c solutions were reduced with a molar excess of sodium ascorbate to ensure an accurate determination of protein concentration. All absorbance measurements were referenced to the absorbance of an identical solution without protein.

The polymer concentration was measured using size exclusion chromatography. The concentrations of polymer in the solutions of both compartments were found to change from the concentrations at the start of the experiment for several reasons: (i) the presence of the polymer in the bottom compartment of the cell produced an osmotic "pumping" of solvent towards the polymer rich-phase and a concomitant dilution of the polymer concentration within the lower compartment, and (ii) a small flux of polymer was observed to diffuse through the membrane into the top compartment, which contributed to the dilution of the polymer solution in the bottom compartment and also introduced very low concentrations of polymer into the top compartment (see below). It was considered very important to accurately monitor the concentration of polymer "introduced" into the (initially polymer-free) top compartment (by the polymer "leakage" through the membrane) to ensure that it was always *much less* than the polymer concentration in the bottom polymer-rich phase.

8.3 Experimental Results

The partition coefficient of the protein, K_p, is defined as the ratio of the protein concentrations in the top (PEO-free compartment) and bottom (PEO-rich) compartments, respectively. Figure 8.2 presents the partition coefficients measured as a function of the concentration of PEO in the bottom compartment, ϕ, for cytochrome-c in buffered salt solutions of concentrations 0.05M Na_2SO_4 (○) and 0.1M NaCl (△), and for ribonuclease (□) in a buffered solution of 0.05M Na_2SO_4. Figure 8.2 shows that as the concentration of PEO is increased, the partition coefficients of both proteins were observed to increase. The increase in the partition coefficients of the proteins reflects the tendency of the proteins to distribute away from the bottom PEO-rich solution phase at higher PEO concentrations. These measurements, which are suggestive of a physical exclusion of the protein by the volume occupied by the PEO, are compared to theoretical predictions in Section 8.4.

In Figure 8.2, in order to assess the influence of salt effects on the measured partition coefficients, the partitioning of cytochrome-c is presented in the presence of NaCl and Na_2SO_4. From an inspection of Figure 8.2, it can be seen that the influence of the different salt types is not large (see Section 8.4 and Table 8.2 for a statistical analysis of the experimental data). This observation contrasts with experimental measurements in two-phase aqueous PEO-dextran systems where the substitution of NaCl by Na_2SO_4 is found to have a profound effect on the observed protein partitioning (Walter et al., 1972). In order to reconcile this difference a few comments are in order. First, it is relevant to note that in two-phase aqueous PEO-dextran systems, the magnitude of the salt effect, traditionally characterized by a bulk electrical potential difference, $\Delta\psi$, between the two-phases, correlates linearly with the difference in concentration of PEO between the phases (Bamberger et al., 1984; Brooks et al., 1984). In two-phase aqueous PEO-dextran systems, this difference is typically 10% w/w PEO, and the corresponding $\Delta\psi$ is 1-2mV. In the diffusion cell experiments, we are dealing with PEO concentrations which are an order of magnitude less, typically 1% w/w, and thus the anticipated electrical effects are expected to be accordingly less

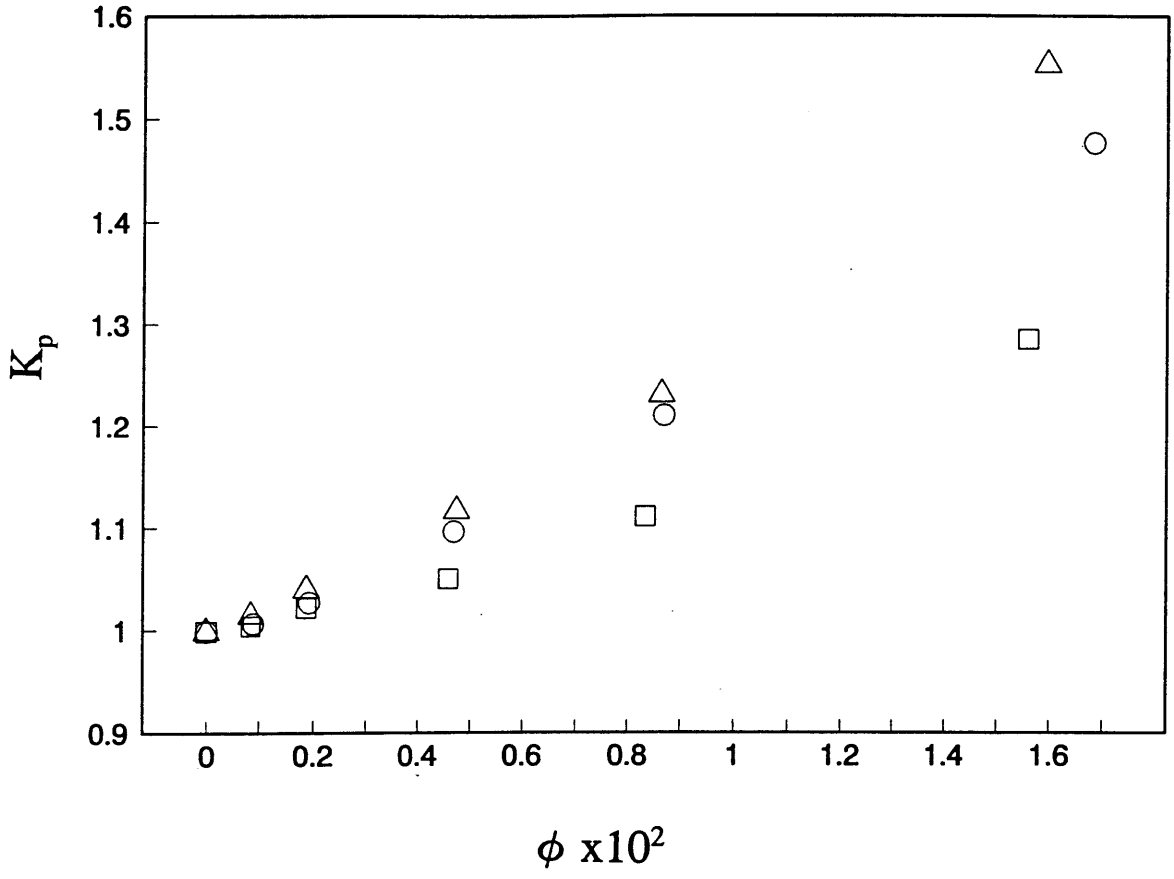

Figure 8.2 Measured protein partition coefficient, K_p, plotted as a function of PEO concentration in the bottom phase, ϕ; cytochrome-C in 0.05M sodium sulphate (△), cytochrome-c in 0.10M sodium chloride (○), and ribonuclease in 0.05M sodium sulphate (□). All solutions contained 10mM sodium phosphate pH 7.0 buffer and 1.5mM sodium azide.

pronounced. Indeed, we can make an estimate of the strength of $\Delta\psi$ from the partition coefficients measured for cytochrome-c in the presence of the two different salt types. The influence of the salt on the partition coefficient of the protein can be expressed as

$$lnK_p^{salt} = \frac{z_p e \Delta\psi}{kT} \qquad \textbf{(8.1)}$$

where z_p is the net charge of the protein, e is the elementary charge, k is the Boltzmann constant and T is temperature. At pH 7.0, the net charge of cytochrome-c is $z_p = +6$ (Theoreu and Akesson, 1941; Wu and Chen, 1987), and using the partition coefficient data in Figure 8.2 for cytochrome-c at $\phi = 1.6$, namely, $K_p^{NaCl} = 1.56$, $K_p^{Na2SO4} = 1.47$, the difference in the electrical potential, $\Delta\psi^{Na2SO4} - \Delta\psi^{NaCl}$, calculated using Eq.(8.1) is approximately 0.2mV. This value, which is an order of magnitude less than that typically encountered in two-phase aqueous PEO-dextran systems is consistent with the fact that we are dealing with concentrations of PEO which are concomitantly less also. While one could further investigate the influence of the salts by measuring the partition coefficient as a function of pH, as has been performed in two-phase aqueous polymer systems (Johansson, 1985), the interpretation of these measurements are complicated by conformational changes of the protein which, in general, accompany changes in the solution pH.

Table 8.1 presents the PEO concentrations measured in the top and bottom compartments of the diffusion cell after equilibration of cytochrome-c between the two compartments. An inspection of Table 8.1 shows that for the samples containing high initial PEO concentrations ($>0.85\%$ w/w in the lower compartment), small amounts of PEO are detected in the top (initially polymer-free) compartment after equilibration of the protein concentration. Although some polymer leaked through the membrane, the very low concentration of PEO in the top phase, as compared to that in the lower PEO-rich phase, demonstrates that the flux of PEO through the membrane is sufficiently slow, as compared to the flux of protein, to allow the measurement of an "effective" equilibrium partition coefficient of the protein between the bottom PEO-solution phase

PEO in Top Compartment (% w/w)	PEO in Bottom Compartment (% w/w)
0.00	0.00
0.00	0.08
0.00	0.19
0.00	0.46
0.024	0.85
0.047	1.65

Table 8.1 Concentrations of PEO measured in the top and bottom compartments of the diffusion cell after equilibration of cytochrome-c between compartments.

and the top polymer-free solution phase. The term "effective" equilibrium partition coefficient is used to emphasize the fact that the true equilibrium in the system would result in equal concentrations of both PEO and proteins in each compartment since, ultimately, all PEO molecules can reptate through the pores of the membrane, irrespective of their molecular weight. In our experiments, we exploit the fact that the polymer flux through the membrane is significantly slower than the protein flux (for the smaller proteins). Figure 8.3 presents the results of an HPLC analysis of the two samples reported in the bottom line of Table 8.1 (1.65%w/w and 0.047%w/w PEO, top and bottom phases, respectively). In Figure 8.3, the HPLC refractive index detector output (with a signal which is proportional to the concentration of polymer in the solution) is plotted as a function of the time following the sample injection. Interestingly, while the refractive index profile (full line) of the bottom PEO-rich phase contains only a single peak, that of the top phase (dashed line), which contains the PEO which has diffused through the membrane, has two large peaks. The presence of the two peaks in the RI profile is suggestive of a bimodal polymer molecular weight distribution. The second peak (as a function of increasing time) in the chromatogram, for the PEO solution sample from the top compartment, corresponds to a PEO fraction having a low molecular weight. This peak presumably arises due to the more rapid diffusion of the smaller PEO coils through the membrane pores (as compared to the higher molecular weight PEO molecules). Although the molecular weight distributions of the PEO are rather different in the two solution compartments, for our purposes, the polymer concentration in the top compartment is maintained sufficiently low such that it can be neglected when interpreting the protein partitioning results. However, it should be stressed, that if the polymer concentration in the top compartment was allowed to become comparable to that in the bottom compartment, the different molecular weight distributions could become a very important consideration when interpreting protein partitioning behavior.

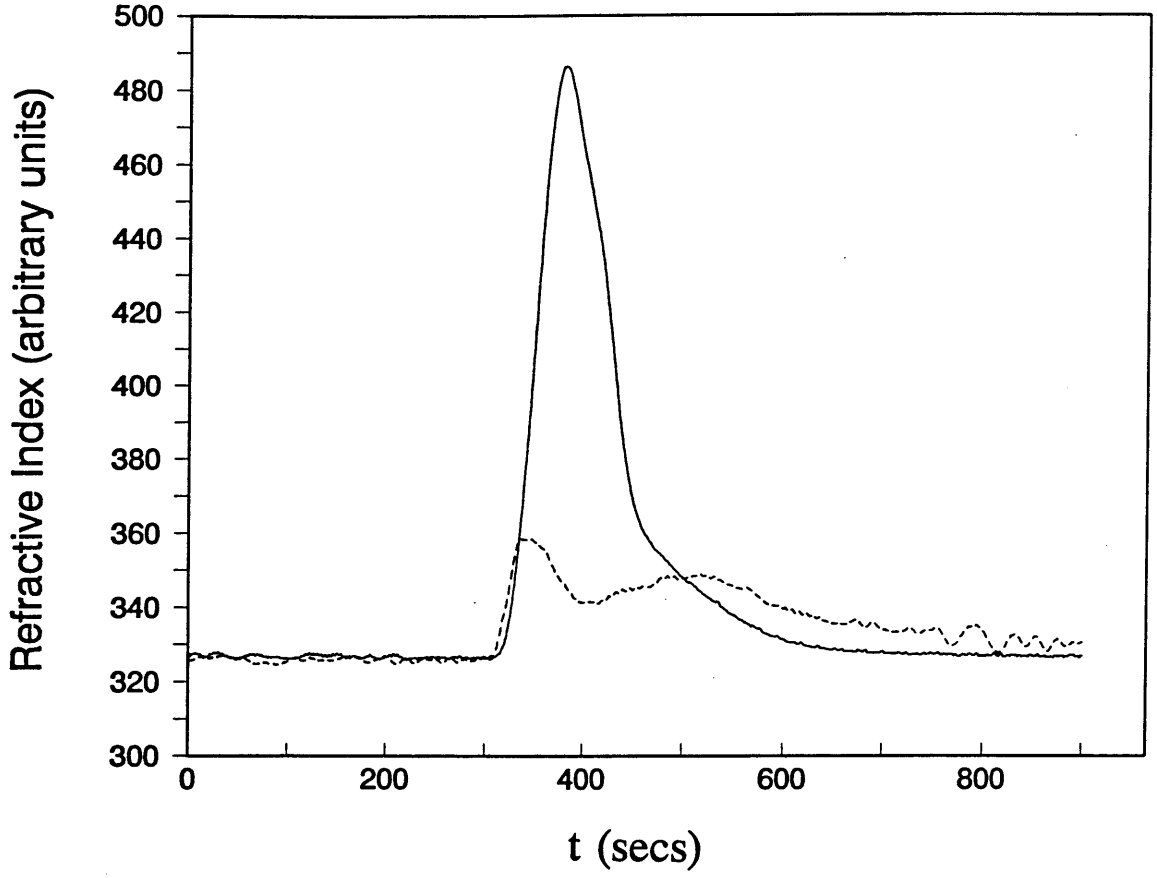

Figure 8.3 Refractive index (RI) of chromatograph eluent stream as a function of the time elapsed following the injection of samples, t, of top (broken line) and bottom (solid line) phases. Note that the RI unit of measurement for the bottom phase has been reduced by a factor of five for presentation purposes.

8.4 Discussion

We compare first the theoretical predictions for the protein partition coefficients reported in Chapter 4 to the experimental measurements presented in Figure 8.2. For the protein partition coefficient measurements presented in Figure 8.2, the exponents, α, and prefactors, β, which relate the logarithms of the measured protein partition coefficients to the PEO volume fractions have been evaluated according to the power-law

$$lnK_p = \beta\varphi^{\alpha} \tag{8.2}$$

The method of determination is presented in Figure 8.4. In this figure, the double logarithm of the protein partition coefficients are plotted as a function of the logarithm of the polymer volume fractions. The exponent, α, is determined from the slope of the plots, and the logarithm of the prefactor, $\ln\beta$, from the intercept of the plots. For the three sets of data in Figure 8.2, corresponding to cytochrome-c in buffered NaCl and Na_2SO_4 solutions and ribonuclease in Na_2SO_4 solutions, the exponents, α, and intercepts, $\ln\beta$, are presented in Table 8.2. It is interesting to note that the same exponent, $\alpha=1.22\pm0.06$, (within the statistical uncertainty) was determined for both cytochrome-c and ribonuclease in Na_2SO_4, and for cytochrome-c in the presence of the two different salts (NaCl and Na_2SO_4). In contrast, while the two intercepts determined for cytochrome-c were essentially the same, $\ln\beta=4.2\pm0.1$, the intercept for the ribonuclease data was significantly less, $\ln\beta=3.6\pm0.1$. We first interpret the values of the exponents, α, and then the prefactors, β.

Corresponding to the scenes depicted in Figures 3.7(a) and 3.7(b), in Chapter 5, the form of the protein partition coefficients were derived as

$$lnK_p = \phi\left[\frac{R_p}{a}\right]^{4/3}\left[1 - k_1\varepsilon\left[\frac{a}{R_p}\right]^{1/3}\right] \qquad R_p \ll \xi_b \tag{8.3}$$

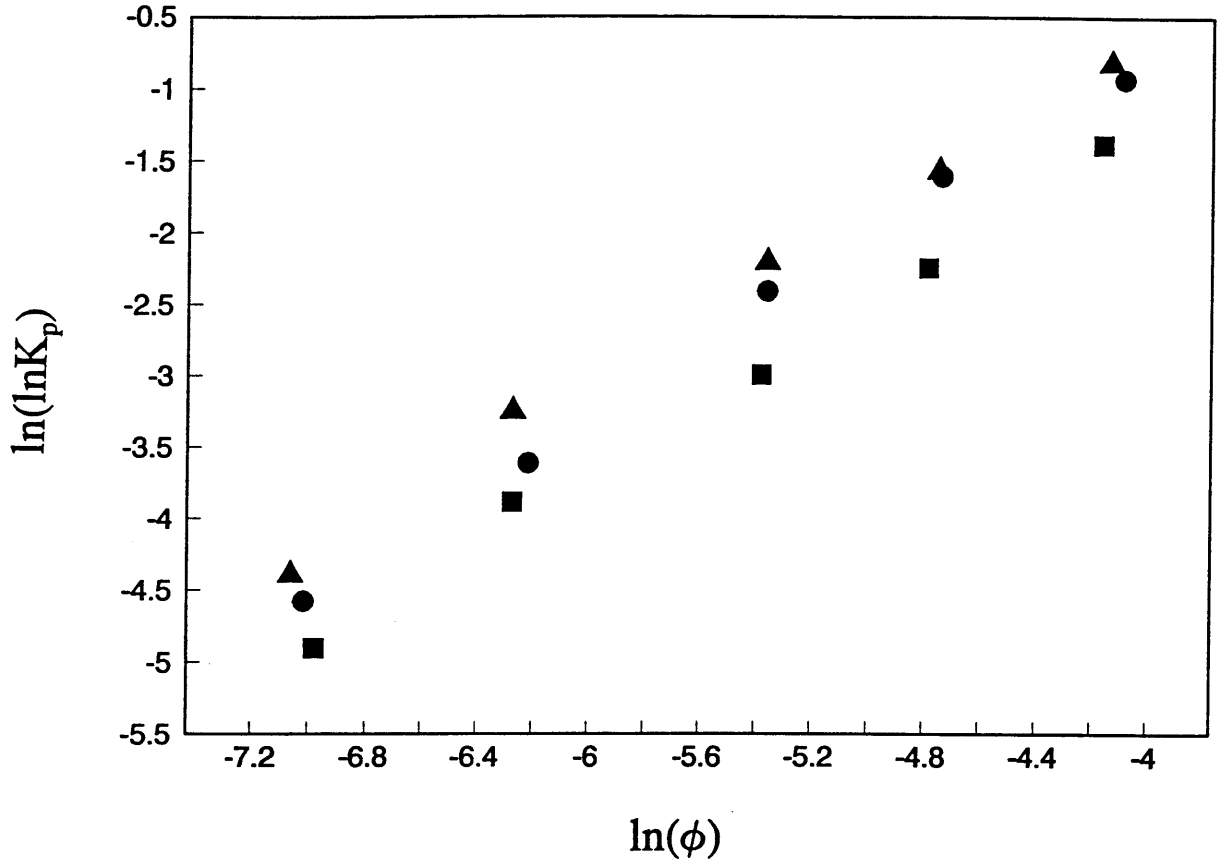

Figure 8.4 The double logarithm of the protein partition coefficient, ln(lnK_p), as a function of the logarithm of the volume fraction of PEO in the bottom compartment, ln(ϕ); cytochrome-C in 0.05M sodium sulphate (▲), cytochrome-c in 0.10M sodium chloride (●), and ribonuclease in 0.05M sodium sulphate (■). All solutions contained 10mM sodium phosphate (pH 7.0 buffer) and 1.5mM sodium azide.

Protein	Salt	Exponent	Prefactor
Cytochrome-c	0.10M NaCl	1.20±0.04	4.17±0.09
Cytochrome-c	0.05M Na_2SO_4	1.26±0.03	4.29±0.07
Ribonuclease-a	0.05M Na_2SO_4	1.22±0.04	3.64±0.10

Table 8.2 Exponents and prefactors obtained from a comparison of Eq.(34) to the experimental data in Figure 8.2.

and

$$lnK_p = \phi^{9/4}\left[\frac{R_p}{a}\right]^3\left[1 - k_2\varepsilon\frac{a}{R_p}\right] \qquad R_p \gg \xi_b \tag{8.4}$$

That is, Eqs.(8.3) and (8.4) predict the exponent α as 1 and 9/4, respectively. The experimentally determined value of 1.25 appears closer to the exponent predicted for Figure 3.7(a), where $R_p \ll \xi$. The effective spherical sizes (Stokes-Einstein radii, see Eq.(8.7) and Table 8.3) of cytochrome-c and ribonuclease are both approximately 20Å, and over the range of PEO concentrations, the accompanying variation in the polymer mesh size was from 80Å to 800Å. Clearly, this is consistent with the constraint of either $R_p \ll \xi$ or $R_p < \xi_b$. It is noteworthy that the presence of a weak attraction between the protein and polymer (see Eqs.(8.3) and (8.4)) does not influence the value of the exponent α (but, as shown below, it can, in principle, affect the value of the prefactor β). Finally, it is curious to note that while the experimentally determined exponent $\alpha = 1.22$, lies between the limits of $\alpha = 1$ and $\alpha = 9/4$, there is no indication of a crossover between these two exponents over the range of PEO concentrations investigated (which exceeded an order of magnitude variation).

While the values of the prefactors, β, determined from the two cytochrome-c experiments in Table 8.2 are the same ($\ln\beta = 4.2$), the value of β determined for ribonuclease ($\ln\beta = 3.6$) was significantly smaller. In accordance with the above discussion on the concentration dependence of the protein partition coefficient, in Figure 3.7(a), where $R_p \ll \xi_b$ and only steric interactions exist between the protein and polymer, the difference in the prefactors is given by (Eq.(8.3))

$$\ln\beta^{ribo} - \ln\beta^{cyto} = \frac{4}{3}\ln\left[\frac{R_p^{ribo}}{R_p^{cyto}}\right] \tag{8.5}$$

Using the experimental values for $\ln\beta_1$ and $\ln\beta_2$ from Table 8.2, the ratio of the protein sizes was predicted to be

Physical Property	Cytochrome-c[a]	Ribonuclease-a[b]
Molecular Weight (Da)	12 384	13 690
Diffusion Coefficient (cm^2/s)	$10.1x10^{-7}$	$10.7x10^{-7}$
Dimensions (Å)	15 x 17 x 17	19 x 14 x 11
Hydrodynamic Radius (Å)	21	20

[a](Dickerson et al., 1971; Cohn and Edsall, 1943), [b](Squire and Himmel, 1979)

Table 8.3 Physical properties of cytochrome-c and ribonuclease-a.

$$\frac{R_p^{cyto}}{R_p^{ribo}} = 1.8 \tag{8.6}$$

In Table 8.3, a comparison of some relevant physical properties of cytochrome-c and ribonuclease is presented. An inspection of Table 8.3 will show that, although the dimensions of the protein molecules (as determined from crystal structures) are somewhat different, the diffusion coefficients are essentially the same. From the diffusion coefficients reported in Table 8.3, and using the well-known Stokes-Einstein equation (Deen, 1989),

$$D = \frac{kT}{6\pi\eta R_h} \tag{8.7}$$

the effective hydrodynamic radius, R_h, has been evaluated (see Table 8.3). If R_h is assumed to be the relevant chracterization of the protein size for prediction of the partitioning, one would predict the ratio in Eq.(8.6) to be (using the diffusion coefficients from Table 8.3) approximately unity. In contrast, the experimental value of $R_p^{cyto}/R_p^{ribo}=1.8$ in Eq.(8.6) is significantly larger than unity. There may be several reasons for this: (1) the effective protein size determined from bulk diffusion coefficient measurements is not the correct characterization of the protein size for the prediction of the partitioning behavior, or (2) attractive interactions between the protein and polymers influence the value of the prefactor β.

The combined influence of repulsive steric and weak attractive interactions on the protein partition coefficient is described by Eq.(8.3). Since the influence of the attractions is only perturbative, the term in the brackets is very close to unity and can be written as

$$lnK_p = \phi\left[\frac{R_p}{a}\right]^{4/3} \exp\left[-k_1\varepsilon\left[\frac{b}{R_p}\right]^{1/3}\right] \tag{8.8}$$

This equation predicts the difference in β for cytochrome-c and ribonuclease-a to take the form

$$\ln\beta_{ribo} - \ln\beta_{cyto} = \frac{4}{3}\ln\left[\frac{R_{p,ribo}}{R_{p,cyto}}\right] - k_1\left[\varepsilon_{ribo}\left[\frac{a}{R_{p,ribo}}\right]^{1/3} - \varepsilon_{cyto}\left[\frac{a}{R_{p,cyto}}\right]^{1/3}\right] \quad \textbf{(8.9)}$$

The first term in Eq.(8.9) is the steric interaction term and the second term describes the influence of the attractive interactions. From Eq.(8.9) it can be seen that when $R_p^{cyto} \simeq R_p^{ribo}$ and $\varepsilon > 0$, the influence of the attraction on $\ln\beta_{ribo}$-β_{cyto} is

$$\ln\beta_{ribo} - \ln\beta_{cyto} = -k_1(\varepsilon_{ribo} - \varepsilon_{cyto})\left[\frac{a}{R_p}\right]^{1/3} \quad \textbf{(8.10)}$$

For a protein of size, R_p=20Å, and a=4Å, in order to account for the observed value of $\ln\beta_{ribo}$-β_{cyto}, the difference in the attractive interaction energies are estimated as $k_1(\varepsilon_{ribo}$-$\varepsilon_{cyto}) \simeq 1$. This difference in the attractive interactions appears to be very large and, in particular much larger than that required to account for the partitioning behavior of similar sized proteins in two-phase aqueous polymer systems (Abbott et al., 1991a, b, and c). Therefore, it appears that some other factor, for example, the protein shape, is contributing to the different partitioning behaviors of cytochrome-c and ribonuclease-a. Finally, it is relevant to note that these two proteins partition rather differently in two-phase aqueous polymer systems. Specifically, in a two-phase aqueous dextran-PEO system, at each protein isoelectric point, the partition coefficient of ribonuclease-a (K_p=0.8) is higher than cytochrome-c (K_p=0.5), indicating the preferred partitioning of ribonuclease towards the PEO-rich phase, as compared to cytochrome-c (Walter et al., 1972).

In Figure 8.5, we have reported the partitioning data of Cleland (1991) for the hydrophobic protein intermediate, carbonic anhydrase (data points) into a solution containing PEO of molecular weight 5x10^{6}Da. It is important to emphasize

that in Figure 8.5 the range of PEO concentrations is lower than those used in Figure 8.2, and it is not clear that the PEO concentration is sufficient for the polymers to be extensively entangled. Neverthe less, since the polymer coil size is much larger than the size of carbonic anhydrase (Cleland and Wang, 1991) (R_p=23Å), and a complexation of the protein and polymer appears to be taking place, a comparison with the partition coefficient measurements to those in Figure 8.2 is illuminating. In contrast to Figure 8.2, the partition coefficients of the protein are less than unity, indicating a preferential partitioning of the protein towards the PEO solution phase. Since $R_p \ll \xi_b$ (or R_g), this partitioning behavior is suggestive of Figure 3.7(c), where a complexation of the protein and polymer has occurred. The associated scaling prediction for the number of polymer segments within a single complex, N^*, is given by Eq.(5.25). Using the physical parameter values of R_p=23Å, a=4Å, g_2=0.1, and assuming that ε=1, N^* is predicted as $1400/k_2$, that is, a value of order 10^3. Associated with the conditions of strong binding, $K_1 \gg 1$, and the protein partition coefficient can be predicted from Eq.(5.32) as

$$K_p = \frac{[c_p]}{[N^*]_o + [c_p]} \tag{8.11}$$

where $[N^*]_o$, the total number of potential protein-binding domains, can be evaluated as

$$[N^*]_o = \frac{\varphi}{\nu_a N^*} \tag{8.12}$$

In Figure 8.5, along with the experimental measurements for the partition coefficeint of carbonic anhydrase reported by Cleland and Wang (1991), the protein partition coefficient predicted according to Eqs.(8.11) and (8.12) are reported as a function of the polymer concentration. The four curves correspond to different values for N^* in Eq.(8.12). In Figure 8.5, the predicted influence of an increase in N^* is to decrease the protein partition coefficient. This trend reflects the increasing number of polymer segments that are required to saturate each protein molecule. It is interesting to note that the order of magnitude of N^* which corresponds to the measured partition coefficients

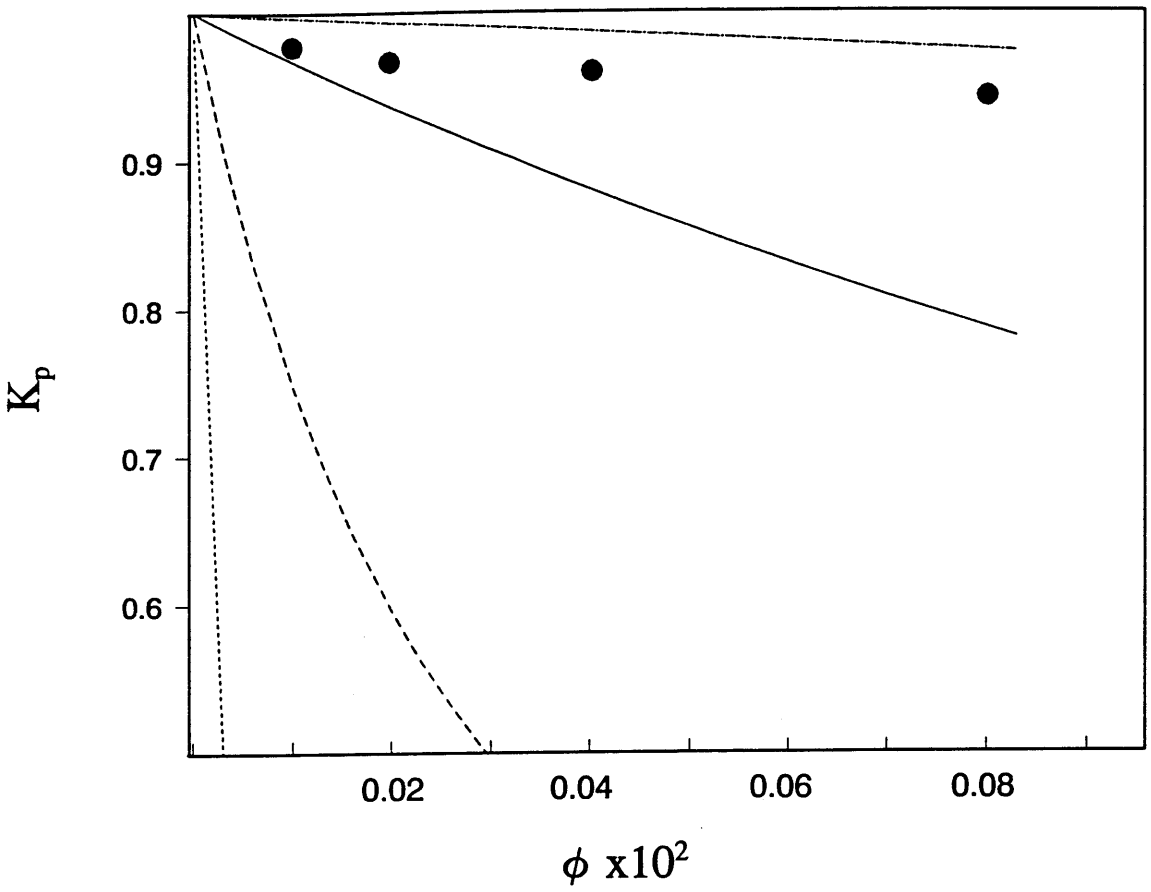

Figure 8.5 The partition coefficient of the carbonic anhydrase intermediate, $\ln K_p$, as a function of the volume fraction of PEO in the bottom compartment, ϕ. Experimental data (Cleland and Wang, 1991) (●); theoretical prediction according to Eq.(41), with differing numbers of PEO segments in each protein-polymer complex; 10 000 (- · - ·), 1 000 (——), 100 (- - -), 10 (···).

is approximately 3000. This value is indeed consistent with the scaling prediction of order 10^3. In conclusion, it appears that the partitioning data for carbonic anhydrase is consistent with the formation of a protein-polymer complex, as depicted in Figure 3.7(c), where roughly 10^3 polymer segments are associated with each protein molecule.

8.5 Conclusions

In order to eliminate the ambiguity associated with interpreting the partitioning of proteins in *two-phase* aqueous polymer systems, where the concentrations of the phase-forming polymers are coupled through the polymer solution equilibrium, the partitioning of proteins across a semipermeable membrane was measured. The much slower diffusion rate of poly(ethylene oxide) PEO through the membrane, as compared to the small protein species, allowed the equilibrium partition coefficients of the proteins to be measured. This situation was realized experimentally by partitioning the similarly-sized hydrophilic proteins, cytochrome-c and ribonuclease-a ($R_p \simeq 20$Å), across a semipermeable membrane which was impermeable to PEO (b=2Å) of molecular weight $5x10^6$ Da. Over the range of PEO concentrations 0.08% w/w to 1.7% w/w, corresponding to $80Å < \xi_b < 800Å$, the partition coefficients were interpreted using the form $\ln K_p = \beta\phi^{\alpha}$, where ϕ is the polymer volume fraction and K_p is the ratio of the protein concentration in the PEO-free and PEO-rich solution compartments. The experimental value of $\alpha = 1.22 \pm 0.06$ was found for both hydrophilic proteins. This exponent lies within the limits of $\alpha = 1$ ($R_p \ll \xi_b$) and $\alpha = 9/4$ ($R_p \gg \xi_b$) predicted for the physical exclusion of the proteins from the entangled PEO solution. In view of the similar sizes of the ribonuclease-a and cytochrome-c, the ratio of the prefactors, $\beta_{cyto}/\beta_{ribo} = 1.8 \pm 0.2$ could not be accounted for on the basis of protein size or realistic attractive interaction energies. Charge effects related to the Donnan equilibrium of ions were investigated by partitioning cytochrome-c in the presence of the two different salts, NaCl and Na_2SO_4 and were determined not to be a dominant contribution to the observed partitioning behavior.

The partitioning behavior of the partially refolded hydrophobic protein,

carbonic anhydrase, which partitions towards PEO with increasing polymer concentration, is contrasted to cytochrome-c and ribonuclease-a. A comparison of the partitioning behavior of the hydrophobic carbonic anhydrase intermediate species with scaling predictions for K_p, suggests that a protein-polymer complex forms, in which approximately 10^3 PEO segments are present per protein.

8.6 Literature Cited

Abbott, N.L.; Blankschtein, D.; Hatton, T.A. *Macromolecules* **1991a**, 24, 4334.

Abbott, N.L.; Blankschtein, D.; Hatton, T.A. *Macromolecules* **1991b**, submitted.

Abbott, N.L.; Blankschtein, D.; Hatton, T.A. *Macromolecules*, **1991c**, submitted.

Albertsson, P.-A.; Cajarville, A.; Brooks, D.E.; Tjerneld, F. *Biochim. Biophys. Acta*, **1987**, 926, 87.

Bamberger, S.; Seaman, G.V.F.; Brown, J.A.; Brooks, D.E., *J. Colloid Interface Sci.*, **1984**, 99, 187.

Brooks, D.E.; Sharp, K.; Bamberger, S.; Tamblyn, C.H.; Seaman, G.V.F.; Walter, H., *J. Colloid Interface Sci.*, **1984**, 102, 1.

Cabane, B.; Duplessix, R. *J. Physique* **1987**, 48, 651.(26)

Cabane, B.; Duplessix, R. *J. Phys.*, **1982**, 43, 1529.

Cleland, J.L.; Wang, D.I.C., PhD Thesis, Massachusetts Institute of Technology, 1991.

Cohn, E.J.; Edsall, J.T., *Proteins, Amino Acids and Dipolar Ions*, Reinhold, N.Y., **1943**.

Deen, W.M., *AIChE Journal*, **1989**, 33, 1409.

Diamond, A.D.; Hsu, J.T., *Biotechnol. Bioeng.*, **1989**, 34, 1000.

Diamond, A.D.; Hsu, J.T., *AIChE J.*, **1990**, 36, 1017.

Dickerson, R.E.; Takano, T.; Eisenberg, D.; Kallai, O.B.; Samson, L.; Cooper, A.; Margoliash, E., *J. Biol. Chem.*, **1971**, 246, 1511.

Johansson, G.; *J. Chromatography*, **1985**, 322, 425.

Sasakawa, S.; Walter, H., *Nature*, **1970**, 223, 329.

Sasakawa, S.; Walter, H., *Biochemistry*, **1972**, 11, 2760.

Squire, P.G.; Himmel, M.E., *Arch. Biochem. Biophys.*, **1979**, 196, 165.

Theoreu, H.; Akesson, A., *J. Am. Chem. Soc.*, **1941**, 63, 1812.

Walter, H.; Sasakawa, S.; Albertsson, P.A., *Biochemistry*, **1972**, 11, 3880.

Wu, C.F.; Chen, H.S., *J. Chem. Phys.*, **1987**, 87, 6199.

Zaslavsky, B.Y.; Mestechkina, N.M.; Rogozhin, S.V., *J. Chromatogr.*, **1983**, 260, 329.

Chapter 9.

Protein Partitioning in Two-Phase Aqueous Polymer Systems: The Coupling of Protein Concentration, Salt Type and Polymer Molecular Weight Effects.

9.1 Introduction

In Chapter 4, a general thermodynamic formulation was presented in order to relate the experimentally measureable protein partition coefficient, K_p, to the molecular-thermodynamic parameters of the system, namely,

$$lnK_p = \ln\left[\frac{c_{p,t}}{c_{p,b}}\right] = \ln\left[\frac{\gamma_{p,b}}{\gamma_{p,t}}\right] + \left[\frac{\mu^o_{p,b} - \mu^o_{p,t}}{kT}\right] + \left[\frac{z_p(\psi_b - \psi_t)}{kT}\right] \qquad \textbf{(9.1)}$$

where $\gamma_{p,i}$ is the activity coefficient of the protein in phase i, $\mu_{p,i}^{\circ}$ is the standard-state chemical potential of the protein in phase i, z_p is the net charge of the protein molecule (assumed to be independent of the polymer solution phase), and ψ_i is the electrical potential of phase i. From an inspection of Eq.(9.1) it is apparent that, in general, the prediction of the partition coefficient of a protein is a rather formidable task and requires the evaluation of the activity coefficients of the proteins, the standard state-chemical potentials of the proteins, the net protein charge, and the potential differences between the phases. However, as reported in Chapter 4, through the judicious choice of experimental conditions, it is possible to focus on *changes* in the protein partition coefficient which reflect only certain of these terms. For example, in the two phase aqueous polymer system containing poly(ethylene oxide) (PEO) and dextran,

accompanying a change in the PEO molecular weight, under the conditions of (1) vanishing protein concentration, (2) negligible PEO in the dextran-rich phase, and (3) constant weight fractions of polymers in each of the phases, Eq.(9.1) was suggested to simplify to

$$\Delta lnK_p = \ln\left[\frac{c_{p,t}}{c_{p,b}}\right] = \frac{\Delta\mu^o_{p,t}}{kT} \qquad \textbf{(9.2)}$$

where the symbol, Δ, denotes the changes in $\ln K_p$ and $\mu_{p,t}^{\circ}$ which accompany the change in the molecular weight of PEO in the two-phase system. In simplifying Eq.(9.1) to Eq.(9.2), certain terms have been neglected, and it is relevant to review the reasons (which are detailed in Chapter 4) for their elimination.

First, Eq.(9.2) was developed from Eq.(9.1) for the limit of vanishing protein concentration where it was assumed that protein-protein interactions become sufficiently infrequent such that they do not influence the observed partitioning behavior of the proteins. Curiously, the influence of protein-protein interactions on the partitioning behavior of proteins in two-phase aqueous polymer systems has not received systematic attention through experiments, particularly for the case where mixtures of different protein types are present (Walter et al., 1991). In general, the influence of protein-protein interactions on the protein partitioning behavior can be expected to be highly specific to the protein type. For example, a case where protein-protein associations have been observed to influence the partitioning of proteins between the two phases is a study of the tetramer-dimer dissociation of hemoglobin. In this instance, over the range of hemoglobin concentrations, 0.1 g/l to 0.7 g/l, a significant change in the protein partition coefficient was observed to accompany a change in the protein concentration (Middaugh, C.R.; Lawson, E.Q., 1980). In contrast, Albertsson (1986) reported the partitioning of human serum albumin (HSA) in the dextran-PEO two-phase system with 0.01M sodium phosphate buffer. In this system the partition coefficient of HSA was observed to be independent of the protein concentration up to 50 g/l, at least. On the basis of these experimental observations is appear necessary to examine the

potential role of protein-protein interactions on the protein partition coefficient before Eq.(9.2) can be reliably used for a particular system. As we show below, for the protein ovalbumin, over the range of protein concentrations between 0.2 g/l to 2 g/l, the protein partition coefficient was observed to be independent of the protein concentration. Thus, for the experimental system considered here, it appears justifiable to set the activity coefficients, $\gamma_{p,i}$, to unity in simplifying Eq.(9.1) to Eq.(9.2).

The second step in simplifying Eq.(9.1) to Eq.(9.2) was to assume that the standard state chemical potential of the protein in the bottom dextran-rich phase was invariant with changes in the PEO molecular weight. This assumption appears justified if the weight fractions of the polymers in the coexisting polymer solution phases are insensitive to the changes in the PEO molecular weight, and secondly, negligible PEO exists in the bottom dextran-rich phases. The conditions under which the above conditions are satisifed requires some clarification. While, in general, the phase equilibrium of two coexisting polymer solutions phases is a function of the molecular weights of the "phase forming polymers", the effect of the molecular weights of the polymers can be minimized with the judicious choice of experimental conditions. Specifically, for the PEO-dextran two-phase aqueous polymer system, the influence of PEO molecular weight on the phase compositions can be greatly reduced by taking two precautions. First, the dextran molecular weight in the two-phase system should be made as high as possible. Second, the concentrations of both the PEO and dextran should be chosen in order to place the two-phase system deep into the two-phase region of the equilibrium phase diagram. Under these carefully chosen experimental conditions, the compositions of the coexisting phases are observed experimentally to be quite insensitive to PEO molecular weights of 4 000 Da and greater (Albertsson, 1986; Abbott et al., 1991; Albertsson et al., 1987). While small changes in the polymer concentrations in the coexisting phases certainly occur, the results of this investigation, further support the assertion that changes in the polymer compositions are very small and are not the underlying cause of the observed protein partitioning behavior (at the conditions of these experiments). Therefore, while a recent paper is correct, in principle, in pointing out the well-known coupling of polymer molecular weight and phase compositions in these

systems, it is possible to find two-phase systems where the practical consequences of changes in polymer molecular weight and polymer concentration on the protein partition coefficient can be separated (Forciniti et al., 1991). Finally, it is relevant to point out that the same experimental conditions which provide PEO-dextran systems with phase compositions which are insensitive to the PEO molecular weight, also provide dextran-rich phases which contain only very small concentrations of PEO.

The third assumption made in arriving at Eq.(9.2) was based on the condition that the electrical potential between the two coexisting polymer solutions phases be independent of the PEO molecular weight. This assumption was based on intuitive reasoning which considered the interactions between the salts and the PEO to be short-ranged (in comparison to the polymer coil sizes). In other words, salt is assumed to interact with PEO at the length scale of the polymer segments rather than the polymer coil size, and is, therefore, a function of the polymer segment concentration (weight fraction of polymer) only. In view of the previous measurements of the compositions of the coexisting polymer solution phases, which found them to be essentially invariant over the range of PEO molecular weights for which the protein partition coefficients were measured (see the discussion above), it was concluded that in studying the *changes* in the protein partition coefficient, the salt effect would be eliminated. Although, no detailed prior experimental investigation appear to conclusively address this issues, the experimental observations which do exist, unfortunately, do not seem to reach a concensus. For example, Johansson investigated the influence of PEO molecular weight on the electrical potential difference (Johansson, 1978) for two PEO molecular weights, 6,000 Da and 35,000 Da. Using the partitioning behavior of the protein, bovine serum albumin, measured as a function of pH, the electrical potential was estimated for various compositions of the two-phase system. Johansson found that the electrical potential difference was a function only of the tieline length and was independent of the PEO molecular weight. While this observation supports our use of Eq.(9.2), other evidence exists which suggests a different conclusion. For example, Bamberger et al. (1985) determined the electrical potential difference between the coexisting polymer solution phases of several PEO-dextran systems, and then calculated the ratio of the electrical

potential difference and the tie-line length. These investigators observed that increasing the PEO molecular weight appeared to increase (slightly) the electrical potential difference, and decreasing the dextran molecular weight increased (slightly) the electrical potential difference.

In view of the importance of the above considerations in providing foundations for the development of a molecular-level understanding of protein partitioning in two-phase aqueous polymer systems, we considered it desirable to obtain experimental verifications for their validity. Accordingly, an experimental investigation was instigated with the main aim of answering two questions. First, are the protein partitioning measurements presented in Figure 2.4 (in Chapter 2) at sufficiently dilute protein concentrations such that protein-protein interactions make a negligible contribution to the protein partition coefficient? Although, several reports exist which have investigated the influence of protein concentration on the protein partition coefficient for different systems, it was considered important to perform the experiment over the range of PEO molecular weights investigated in Figure 2.4, since, in general, the molecular weight of the PEO (and other solution conditions) could also influence the strength of the protein-protein interactions. Accordingly, we have examined the influence of concentration on the partitioning of ovalbumin using the PEO molecular weights of 5 000 Da and 20 000 Da and over a range of protein concentrations from 0.2g/l to 2 g/l. The second question that we wanted to address was related to the possible coupling between the effects of the electrical potential difference and PEO molecular weight? That is, is the difference in the electrical potential, as characterized by ψ_t-ψ_b in Eq.(9.1), a function of the PEO molecular weight? If the electrical potential difference is dependent on the PEO molecular weight, it is also a function of the specific salt type, then the difference in the protein partition coefficient, $\Delta \ln K_p$, will also be a function of the salt type present in the system. Accordingly, we have measured the partition coefficient of ovalbumin as a function of PEO molecular weight in the presence of two different salts, and found that this quantity is, in fact, independent of the salt type.

9.2 Materials and Experimental Considerations

A. Materials

Molecular weight standard grade PEO was purchased from Polysciences Inc. (Warrington PA) with molecular weights of (in Da, according to manufacturers specifications) 5,000 ($M_w/M_n=1.05$), 9,000 ($M_w/M_n<1.10$), 11,000 ($M_w/M_n=1.10$), 15,000 ($M_w/M_n=1.2$), 20,000 ($M_w/M_n=1.07$), where M_w and M_n are the weight-average and number-average molecular weights, respectively. The polydispersivity indices (M_w/M_n) were reported by the manufacturers. Poly(ethylene) oxide of molecular weight 35,000 was purchased from Fluka (Switzerland). Dextran ($M_w=300,000$ Da) was also purchased from Polysciences Inc. Chicken egg albumin (ovalbumin) was purchased from Sigma Chemical (St Louis, MO). All other chemicals used were of analytical reagent grade.

B. Experimental Methods

All polymer solutions were prepared in aqueous buffered solutions containing 10 mM sodium phosphate to control the pH at 7.0, 1.5mM sodium azide to prevent bacterial growth in the samples, and either 0.1M NaCl or 0.05M Na_2SO_4. All polymer solutions were prepared by weight since the high viscosities of the solutions prevented the accurate measurement of the volumes of the solutions. First a stock solution of dextran was prepared in the aqueous buffer with a concentration of dextran equal to that desired in the two-phase system. The stock solution was then divided into 3g aliquots, into which the PEO was weighted. The resulting two-phase system was then thoroughly mixed. All two-phase systems were prepared in duplicate. Into one of the resulting two-phase systems, 60μl of protein solution was added, and to the other solution the same volume of buffered solution was added. The protein-free two-phase system served as the reference solutions in the spectrophotometer for the measurement of the protein concentrations. The resulting polymer solutions were thoroughly mixed, gently

centrifuged at 1000rpm (Centra 4, International Centrifuge) for 5 minutes, and then equilibrated for 12 to 18 hours in a temperature controlled water bath (Magni Whirl, Blue M). After equilibration, the samples were visually inspected, to ensure that the two coexisting polymer solution phases were clear and that no protein precipitate was present at the interface of the two phases. In order to determine the concentrations of proteins in each of the phases, using a syringe, samples of each of the two coexisting solution phases were collected. First, without disturbing the fragile liquid-liquid interface between the two phases, a sample of the top PEO-rich solution phase was carefully collected. Following the collection of the top-phase sample, the remainder of the top phase was sucked from the interfacial region using a pasteur pipette. The interfacial sample, which typically contained a mixture of the top and bottom phases, was then discarded. The remaining solution was the bottom phase, which was withdrawn from the testtube and then prepared for the measurement of protein concentration. Due to the high viscosities of the polymer solutions which were withdrawn from each of the phases, it was necessary to dilute the samples prior to measurement of the protein absorbance. If the samples were not diluted, streaks appeared in the polymer solutions as they were pipetted into the spectrophotometer cuvettes, which in turn scattered the light during the measurement of the protein absorbance. The absorbance of the ovalbumin was measured at 280nm using a Perkin-Elmer Corp. Lambda 3B UV-VIS spectrophotometer, an an identical polymer solution phase (protein-free) as a reference.

9.3 Results

In Figure 9.1, partition coefficient measurements for ovalbumin are presented as a function of the overall ovalbumin concentration in the two-phase system. The measurements are reported for two two-phase systems, one contained PEO with a molecular weight of 5 000 Da and the other containing PEO 20 000 Da. Both systems contained 0.05M Na_2SO_4. From Figure 9.1 it is apparent that over the range of protein concentrations, 0.2 g/l to 2 g/l, the same protein partition coefficient was measured for each PEO molecular weight. These observations supports our hypothesis that the protein

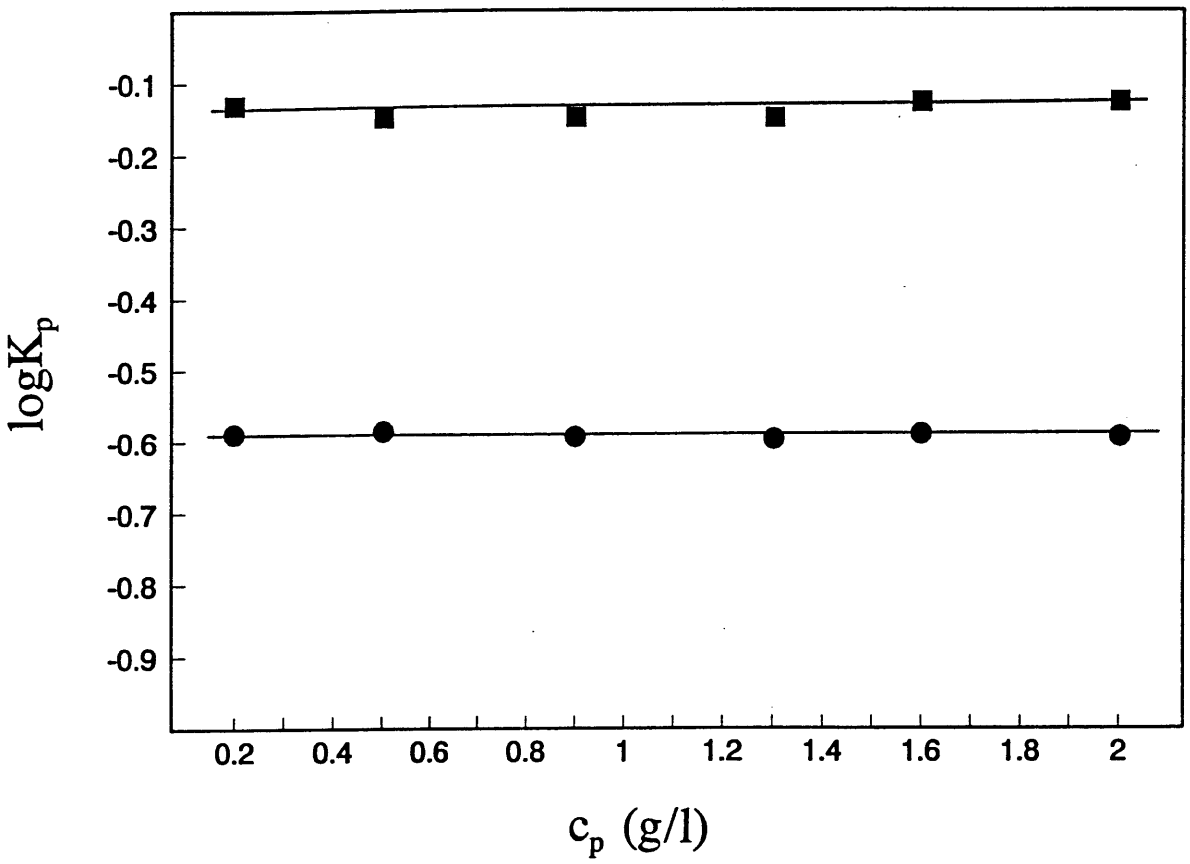

Figure 9.1 Logarithm of partition coefficient for ovalbumin, $\log K_p$, as a function of ovalbumin concentration, c_p, in the two-phase aqueous PEO-dextran system with either PEO 5,000 Da (■) or PEO 20,000 (●). Also present in the two-phase system was 10mM sodium phosphate buffer (pH 6.9) and 0.05M sodium sulphate.

concentrations were sufficiently low such that protein-protein interactions do not influence the protein partition coefficient.

In Figure 9.2, partition coefficient measurements for ovalbumin arepresented as a function of the molecular weight of the PEO. The two-phase systems contained either 0.05M Na_2SO_4 or 0.1M NaCl. While the partition coefficients of ovalbumin in the presence of Na_2SO_4 are higher than in the presence of NaCl, in each case, accompanying an increase in the molecular weight of the PEO is a decrease in the measured protein partition coefficients. A more careful inspection of Figure 9.2 reveals that the *change* in the protein partition coefficients accompanying a *change* in the PEO molecular weight is in fact independent of the salt type. This is also demonstrated in Figure 9.2, where the difference in the partition coefficients measured in the presence of the two salt types is plotted is plotted as a function of PEO molecular weight. From an inspection of Figure 9.2 it can be seen that this difference is insensitive to the PEO molecular weight. This supports the assumption leading to Eq.(9.2), that ψ_b-ψ_t is independent of PEO molecular weight.

9.4 Discussion and Conclusions

The results presented in Figure 9.1 clearly show that the protein partition coefficient of ovalbumin is independent of concentration over the range 0.2 g/l to 2 g/l. In view of the relatively low protein concentration (the average distance separating between protein molecules is 300Å to 1000Å, for the protein concentrations 0.2 g/l and 2 g/l, respectively), and the presence of salt (0.05M Na_2SO_4) to screen electrostatic interactions, it appears very reasonable that the protein partition coefficient is independent of protein-protein interactions. However, it appears somewhat remarkable that for the partitioning of human serum albumin (reported previously), the independence of the partition coefficient from the protein concentration is observed upto protein concentrations of 50 g/l. This is particularly suprising since small angle neutron scattering studies on aqueous solutions of bovine serum albumin, at similar concentrations and salinity, show evidence of protein-protein interactions (Bendedouch et al., 1983;

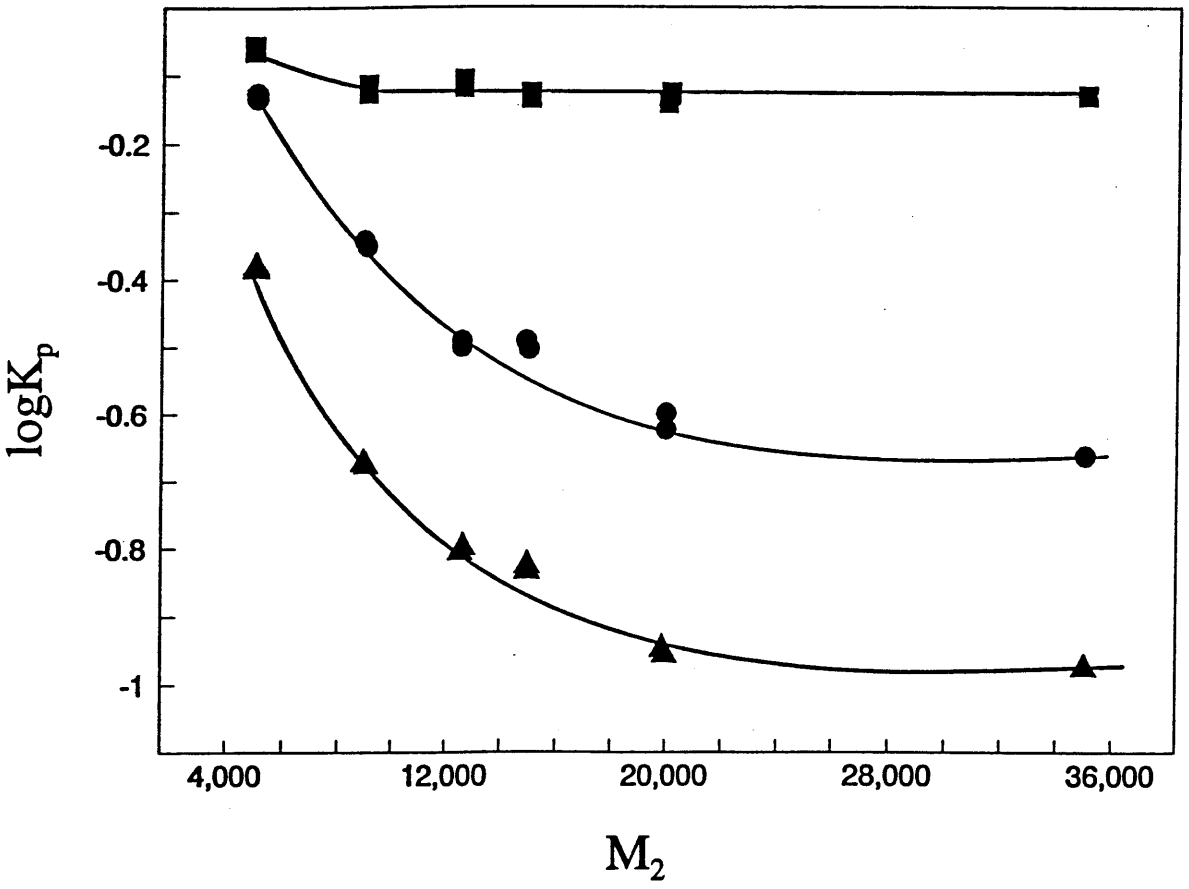

Figure 9.2 Logarithm of partition coefficient for ovalbumin, $\log K_p$, as a function of PEO molecular weight, M_2, in the two-phase aqueous PEO-dextran system with either 0.1M NaCl (▲) or 0.05M Na_2SO_4 (●). 10mM sodium phosphate buffer (pH 6.9) was present in all two-phase systems. Also shown is the change in the partition coefficients due to the different salt type at each polymer molecular weight (■) (for presentation purposes this plot has been translated to an arbitrary ordinate scale value.

Nossal et al., 1986; Chen et al., 1986). One possible explanation for the apparent insensitivity of K_p to the protein concentration may be that only the ratio of the protein activity coefficients (for protein in the top and bottom phases, respectively) enters theprediction of the protein partition coefficient, rather than their individual values (see Eq.(9.1)). Therefore, if the protein-protein interactions are similar in each of the phases, the contribution of the protein-protein interactions to the protein partition coefficient will tend to cancel each other, and thus the protein partition coefficient will be observed to be insensitive to the protein concentration.

While Figure 9.2 supports the hypothesis that changes in the protein partition coefficient are independent of the salt type (at least, for the phase system investigated here), it is interesting to consider this result in the light of a recent suggestion in the literature. Cabezas and coworkers (Cabezas et al., 1990) recently suggested that very low Na_2SO_4 concentrations can significantly alter the equilibrium of the coexisting polymer solution phases of the dextran-PEO system. If this was indeed true, then given that the influence of PEO molecular weight is coupled to the concentration of polymer solution in the system, it would appear unlikely that we would have observed the change in the protein partition coefficient, as shown in Figure 9.2, to be independent of the salt type. If the phase compositions had changed significantly, through the influence of the phase compositions on the electrical potential difference, one would not expect to find $\Delta \ln K_p$ independent of the salt type.

Finally, it is relevant to mention the recent work of Forciniti (Forciniti*et al.*, 1991) who have investigated the simultaneous effects of polymer molecular weight and pH, motivated by the possible coupling between charge related effects and polymer solution conditions. Over the range of conditions explored, they point out that they can not distinguish between the effects of polymer concentration and polymer molecular weight, due to their coupling. For example, at acidic pHs, the partition coefficient of lysozyme was observed to increase with PEO molecular weight from PEO 4 000 Da to PEO 10 000 Da and then decrease slightly from 10 000 Da to 20 000 Da. However, at alkaline pHs the partition coefficients decrease monotonically with increasing PEO molecular weight. These observations, and other involving chymotrypsinogen A,

albumin (type not defined) and catalase, suggests that the influence of the pH and polymer molecular weight are coupled through the influence of the polymer molecular weight on the phase concentrations and the dependence of the salt partitioning on the polymer concentrations. As the authors point out, the interpretation of the pH effects are also hampered by the influence of the pH on the conformational and aggregation states of the proteins. It is important to point out here that while the results of Forciniti et al. illustrate the richness of the protein partitioning problem, they conducted their experimental investigations over a range of conditions where the protein partitioning behavior reflects a variety of partitioning mechanisms. As such, until *all* the mechanisms of protein partitioning are understood, the interpretation of these measurements will be very difficult. Their approach in is contrast with our own, where we have carefully chosen experimental conditions with the objective of focussing on the individual parts of the protein partitioning problem. Indeed, this motivates our choice of two-phase systems that provide experimental conditions which permit use to focus our attention on understanding the protein stanard state chemical potential in the PEO-rich phase, as illustrated by Eq.(9.2).

9.5 Literature Cited

Abbott, N.L.; Blankschtein, D.; Hatton, T.A. *Macromolecules* **1991**, 24, 4334.

Albertsson, P.A. *Partition of Cell Particles and Macromolecules*; Wiley, New York, **1986**.

Albertsson, P.-A.; Cajarville, A.; Brooks, D.E.; Tjerneld, F. *Biochim. Biophys. Acta*, **1987**, 926, 87.

Bamberger, S.; Brooks, D.E.; Sharp, K.A.; van Alstine, J.M.; Webber, T.J., *Partitioning in Aqueous Two-Phase Systems*, Eds., H. Walter, D.E. Brooks, D. Fisher, Academic Press, New York, **1985**.

Bendedouch, D.; Chen, S.-H., *J. Phys. Chem.*, **1983**, 87, 1473.,

Chen, S.-H.; Bendedouch, D., *Methods in Enzymology*, **1986**, 130, 79.

Cabezas, H.; Kabiri-Badr, M.; Szlag, D.C., *Bioseparation*, **1990**, 1, 227

Forciniti, D.; Hall, C.K.; Kula, M.R., *Chemical Engineering Science*, **1991**, in press

Forciniti, D.; Hall, C.K.; Kula, M.R., *Biotech. Bioengineering*, **1991**, submitted.

Johansson, G., *J. Chromatogr.*, **1978**, 150, 63

Middaugh, C.R.; Lawson, E.Q., *Analytical Biochemistry*, **1980**, 105, 364.

Nossal, R.; Glinka, C.J.; Chen, S.-H., *Biopolymers*, **1986**, 25, 1157.,

Walter, H.; Johansson, G.; Brooks, D.E., *Analytical Biochemistry*, **1991**, in press

Chapter 10.

Conclusions: Facts, Philosophy and Future

10.1 Facts

The theoretical tools of polymer-scaling laws, statistical-thermodynamics, and liquid-state theory, as well as the complementary experimental techniques of equilibrium partitioning and small-angle neutron scattering have been used to illuminate certain facts regarding the partitioning of proteins in two-phase aqueous polymer systems. These facts are summarized below.

(1). In the two-phase aqueous poly(ethylene oxide) (PEO)-dextran system, with increasing PEO molecular weight, *scaling* predictions and the interpretation of *small angle neutron scattering* (SANS) measurements reveal a transition in the underlying structure of the PEO solution phase from individually dispersed PEO coils to an extensively entangled PEO mesh.

(2). In two-phase aqueous polymer systems, certain experimentally observed protein partitioning behaviors were found to correlate with the occurence of a transition (crossover) in the underlying structure of the PEO-rich phase (see (1) above). At the crossover, the correlation length of the PEO solution is similar to the size of the protein molecules, and therefore, the interactions of the proteins and polymers, as well as the associated protein partitioning behavior, are very sensitive to the presence of the crossover.

(3). The recognition of the crossover in the polymer solution regime etablishes a new physical basis for the formulation of molecular-level descriptions of protein partitioning in two-phase aqueous polymer systems. In solutions of identifiable polymer coils, the proteins interact with individual *polymer coils*. In contrast, in solutions of entangled polymer coils, within the mesh, the identities of the individual polymer coils are lost and the proteins interact with the *polymer mesh*. Novel molecular-level descriptions of globular proteins in two-phase aqueous polymer systems were proposed. The scenarios differed in (i) the polymer solution regime, (ii) the relative size of the protein and the polymer coil/mesh, (iii) the nature of the energetic interaction between the flexible polymer chains and the globular protein molecules.

(4). A statistical-thermodynamic framework was developed that related changes in the protein partition coefficient, under experimentally accessible conditions, to changes in the standard-state protein chemical potential in the PEO-rich phase of a two-phase aqueous PEO-dextran system. Specifically, under certain experimental conditions the additional influences of different salt types and protein concentration on the *change* in the protein partition coefficient associated with an increase in PEO molecular weight were eliminated.

(5). A scaling-thermodynamic treatment of proteins in polymer solutions of identifiable polymer coils was formulated in order to describe the qualitative influence of different molecular mechanisms on the partitioning behavior of proteins: At Θ-solvent conditions for the polymer, the excluded-volume interaction between the proteins and the polymer coils was unable to account for the influence of polymer molecular weight on the protein partition coefficient; at athermal-solvent conditions, where repulsive polymer-polymer interactions also influence the protein chemical potential, the predicted protein partition coefficient was shifted in a direction qualitatively consistent with experimental trends. For both athermal- and Θ-solvent conditions, the observed change in the protein partition coefficient was determined to be qualitatively consistent with the presence of a weak attraction between the polymer coils and the proteins. The presence of a strong attraction

between the polymer coils and the proteins, and the associated formation of an adsorbed polymer layer at the surface of the proteins, was shown to lead to a new partitioning behavior that has not yet been realized experimentally.

(6). A theoretical formulation to predict the thermodynamic properties of solutions containing globular protein molecules and identifiable polymers was developed using an equation of state/Monte-Carlo scheme. On the basis of the theoretical formulation it was concluded that (1) the deformability and penetrability of the polymer coils to the proteins is an essential feature of protein-polymer interactions, (2) direct steric interactions between hydrophilic proteins and PEO coils alone cannot account for the observed influence of PEO molecular weight on the protein partitioning behavior, (3) interactions between PEO coils, which are a function of PEO molecular weight, represent an important influence on the observed protein partitioning behavior observed to accompany a change in PEO molecular weight, (4) the presence of weak attractive interactions, of strength 0.01kT to 0.1kT, are consistent with the observed influence of PEO molecular weight on the experimentally observed protein partitioning behavior, (5) deviations of the protein shape from a spherical one can significantly influence the predicted protein partitioning behavior, and (6) evaluation of the standard-state protein chemical potential at constant solvent chemical potential, rather than at constant pressure, can lead to qualitatively incorrect predictions of the protein partitioning behavior.

(7). The measurement and interpretation of the intensity of *neutrons scattered at small angles (SANS)* from bovine serum albumin (BSA, R_p=35Å) in aqueous (D_2O) solutions containing singly dispersed PEO coils was found to be consistent with the existence of a weak attractive interaction (0.05kT) between BSA and PEO (in addition to repulsive steric interactions). The attractive interaction reduced the second virial coefficient for the BSA-PEO interaction to 80% of the value predicted for purely excluded-volume interactions.

(8). A scaling-thermodynamic formulation was developed to describe the

thermodynamic properties of proteins in solutions of entangled polymers. A variety of different partitioning behaviors were predicted depending on (i) the size of the protein molecules, (ii) the size of the polymer net, and (iii) the strength of energetic interactions between the proteins and the polymers.

(9). In order to eliminate the ambiguity associated with predicting and interpreting the partitioning of proteins in *two-phase* aqueous polymer systems, where the concentrations of the phase-forming polymers are coupled through the polymer solution equilibrium, the partitioning of proteins across a semipermeable membrane was considered. The application of the scaling-thermodynamic formulation (see (8) above) revealed important differences between the predicted protein partitioning behavior in systems with coexisting liquid phases and liquid phases separated by a mechanical membrane.

(10). The partitioning of proteins across a semipermeable membrane (between aqueous PEO-free phase and a PEO-rich phase) was achieved by exploiting the much slower diffusion rate of high molecular weight poly(ethylene oxide) PEO through the membrane, as compared to that of small protein species. This situation was realized experimentally by partitioning the similarly-sized hydrophilic proteins, cytochrome-c and ribonuclease-a ($R_p \simeq 20$Å), across a semipermeable membrane which was impermeable to PEO of molecular weight 5×10^6 Da. Over the range of PEO concentrations 0.08% w/w to 1.7% w/w, corresponding to $80\text{Å} < \xi_b < 800\text{Å}$, the partition coefficients were interpreted using the form $\ln K_p = \beta\phi^\alpha$, where ϕ is the polymer volume fraction and K_p is the ratio of the protein concentration in the PEO-free and PEO-rich solution compartments. The experimental value of $\alpha = 1.22 \pm 0.06$ was found for both hydrophilic proteins. This exponent lies within the limits of $\alpha = 1$ ($R_p \ll \xi_b$) and $\alpha = 9/4$ ($R_p \gg \xi_b$) predicted for the physical exclusion of the proteins from the entangled PEO solution. In view of the similar sizes of the ribonuclease-a and cytochrome-c, the ratio of the prefactors, $\beta_{cyto}/\beta_{ribo} = 1.8 \pm 0.2$ could not be accounted for on the basis of protein size or realistic attractive interaction energies. Charge effects related to the Donnan equilibrium of ions were investigated by partitioning cytochrome-c in the presence of the two different salts,

NaCl and Na_2SO_4, and were determined not to be a dominant contribution to the observed partitioning behavior.

(11). From a common molecular-level description, *structural* features and *thermodynamic* properties of aqueous polymer solutions containing globular proteins were predicted. Specifically, the interpretation of the excess scattering in SANS experiments (which directly reflects the average *structural* features) is consistent with the *statistical-thermodynamic* models of protein-polymer interactions and the associated protein partitioning behavior.

10.2 Philosophy

The philosophy behind this thesis was influenced by the French School of polymer physics, and the "scaling description" of polymer solution properties (de Gennes, 1988). Over several decades, this school of thought has prospered in the liquid-state physics community and their viewpoint has proven to be particularly useful in interpreting the small angle scattering of neutrons from fluids where the alternative mean-field theories are less successful. Scaling concepts have had particular success in describing universal physical features of well defined (model) polymer solutions (for example, see Cotton et al., 1972; Schaefer, 1984). However, our aim was rather different. Specifically, as engineers, we wanted to explore and develop the use of scaling concepts for more complicated and technologically relevant systems such as solutions of proteins and polymers. The physicist, the biologist and the protein chemist may question the applicability of such concepts to biological systems in which much of the interest arises from the differences in the chemical nature of the species. Therefore, having presented the results of this thesis, based on our experiences during its execution, it is relevant to consider the strengths and limitations of such a "scaling approach" to "real" complex fluids.

While proteins can possess a wide variety of physical properties, the collation of experimental protein partitioning measurements revealed that, for a certain group of

proteins at least, universal features are observed in their partitioning behaviors. This observation was an important signal, and suggested that a "coarse-grained" view of protein partitioning may indeed prove profitable. In contrast, however, one can imagine many other biological systems where the observed properties reflect local and chemically detailed interactions. For such systems, which will not display universality, it is evident that scaling is not applicable.

A major benefit derived from adopting the scaling approach to protein partitioning was in being provided with tools with which to understand the intricate relationship between transitions in the structure of the polymer solutions and the observed partitioning behaviors. Indeed, such transitions appear to have been overlooked by more computationally intensive and "quantitative" descriptions of protein partitioning. Due to the mathematical simplicity of the scaling approach, one does not have to commit to a single physical description of the system, but rather is encouraged to explore a variety of scenarios.

However, in the course of this thesis we also encountered limitations of the scaling approach which reflected its qualitative nature. Without a detailed knowledge of the prefactors appearing in the various scaling predictions, one cannot compare the contributions of additive terms, other than by orders of magnitude. While we could indentify the potentially important contributions of repulsive polymer-polymer and protein-polymer interactions and weak attractive protein-polymer interactions, we could not evaluate their relative magnitudes. However, the scaling approach highlighted the important contributions to be considered, and directed our attention to these considerations in subsequent and more precise theoretical developments (EOS/MC approach).

It is satisfying to mention that from the same physical basis, our theoretical developments were able to predict both thermodynamic properties and structural properties of the polymer solutions containing proteins. Independent conclusions, derived from the interpretation of protein partitioning and small angle neutron scattering, suggested that protein partitioning results from a delicate balance of repulsive steric interactions (polymer-polymer and protein-polymer) and weak attractive interactions

(protein-polymer).

In concluding, it is important to reiterate that the focus of this thesis has been on the influence of polymer solution properties on protein partitioning. For example, the influence of the detailed protein structure on partitioning has not been treated, and we have considered only the average properties of the protein molecules. Despite such approximations, certain protein partitioning behaviors *can* be rationalized using our unified description for the structural and thermodynamic properties of aqueous solutions of proteins and polymers. It is our hope that the philosophy which has been explored, and the physical mechanisms which have been identified, will provide, in part, the foundations for future developments.

10.3 Future

In tackling the protein partitioning problem, a variety of challenges were encountered. While some of these challenges were treated within the scope of this thesis, others were deferred for the future. Outlined below are some suggested directions for future research.

(1). A concensus which appears to have emerged from several theories of protein partitioning in two-phase aqueous polymer systems is the importance of attractions between proteins and polymers, in addition to excluded-volume interactions. At first, this seems a somewhat surprising conclusion since the partitioning of globular nonhemo-proteins appears to reflect nonspecific interactions between polymers and proteins, whereas attractions, arising, for example, from the interactions of the polymer with hydrophobic pockets on the proteins, would be expected to be specific to the protein type. Clearly, excluded-volume interactions are nonspecific and are determined solely by the geometry of the system, and one can wonder if the attractions necessary in the modelling approaches are introduced because the treatment of the excluded-volume interactions is inadequate. Nevertheless, one must also be aware of the distinctly different partitioning behaviors exhibited by other classes of proteins, such as hemo-

proteins. As the geometries are essentially identical for both hemo-proteins and nonhemo-proteins, this suggests that interactions other than those of the excluded-volume type may be of importance. If attractions are important, then theories can only adequately address the roles of the attractions in protein partitioning phenomena if the nature of the attractions is understood. In this thesis we have not speculated in detail on the origin of the attraction incorporated in the statistical-thermodynamic description, although we have discussed briefly the influence of the range of the attraction. In particular, when dealing with such small colloidal systems, where the role of van der Waals interactions may be important, the concept of a polymer interaction with the *surface* of the protein may not be appropriate. Indeed, the attraction may reflect the bulk properties of the proteins and not simply their surface properties, for example, if the attraction is of the van der Waals type. That is, the influence of the volumes and geometries of the interacting bodies on the interaction, as well as the possible long-range nature of the forces may be important. Such considerations may be important in proposing detailed statistical-thermodynamic descriptions of a variety of colloidal systems.

(2). It is further evident from this thesis that there is a clear need for alternative experimental studies to provide independent evidence for the existence of weak attractive interactions between this class of proteins and PEO. To this end, measurements using light scattering and (further) neutron scattering, analogous to those performed in this thesis and in the anionic surfactant-polymer systems, may be illuminating. To this end, reaction calorimetry may also prove a useful experimental technique to determine if there is an enthalpy change arising from interactions of proteins and polymers.

(3). Great mystery surrounds the potent effect that simple inorganic salts can have on the partition coefficient of proteins in these systems. Although one can correlate protein partition coefficients in terms of an effective interphase electrical potential difference, a more fundamental and complete answer to the origin of the salt effect must come from consideration of intermolecular and interionic forces which operate on a

length scale comparable to the protein size. Indeed, when compared to the molecular-level treatments for the interactions occurring between the phase-forming polymers and proteins, the treatment of salt effects using a macroscopic approach, as has occurred historically, is rather inconsistent. It must be recognized, however, that this approach has been adopted because the existing understanding of the influence of salts in nonionic systems is incomplete. Unlike the successful approximations available to treat salt effects between discrete charges in which, for example, water is regarded as a continuum, an understanding of salt effects in nonionic systems is likely to require a more explicit consideration of the unusual properties of water, including its structure. This represents a very challenging problem, particularly since the strength of the intermolecular forces involved is comparable to that between water molecules.

(4). Although the varied natures of the polymer solution phases have been recognized in the course of this thesis, and distinct physical pictures for the limits of low polymer molecular weight and high polymer molecular weight have been proposed, it is clear that much of the partitioning occurs in the crossover region between the regimes depicted. Thus, to develop a more complete quantitative description it will be necessary to describe the entire transition regime rather than the two extreme limits of dilute and semidilute polymer solutions addressed in this thesis.

Cumulative References

Abbott, N.L., Blankschtein, D., Hatton, T. A., presented at the *6th International Conference on Partitioning in Aqueous Two-Phase Systems*, Assmannshausen, West Germany, **1989**.

Abbott, N.L.; Blankschtein, D.; Hatton, T.A. *Bioseparation*, **1990**, 1, 191.

Abbott, N.L., Blankschtein, D., Hatton, T. A., *Macromolecules*, **1991**, 24, 4334.

Abbott, N.L.; Blankschtein, D.; Hatton, T.A. *Macromolecules*, **1991**, submitted.

Abbott, N.L.; Blankschtein, D.; Hatton, T.A. *Macromolecules*, **1991**, submitted.

Albertsson, P.-Å., *Nature*, **1958**, 4637, 709.

Albertsson, P.-Å.; Nyns, E. J., *Ark. Kemi*, **1961**, 17, 197.

Albertsson, P.-Å.; Sasakawa, S.; Walter, H., *Nature*, **1970**, 228, 1329.

Albertsson, P.-A., in *Partitioning in Aqueous Two Phase Systems*, Walter, H.; Brooks, D.E.; Fisher, D., Eds, Academic Press, N.Y., **1985b**.

Albertsson, P.A. *Partition of Cell Particles and Macromolecules*; Wiley, New York, **1986**.

Albertsson, P.-Å.; Cajarville, A.; Brooks, D.E.; Tjerneld, F., *Biochimica et Biophysica Acta*, **1987**, 926, 87.

Alexander, S., *J. Physique*, **1977**, 38, 977.

Ananthapadmanabhan, K.P.; Goddard, E.D., *J. Colloid Interface Sci.*, **1986**, 113, 294.

Ashcroft, N.W.; Lekner, J., *Phys. Rev.*, **1966**, 145, 83.

Ashcroft, N.W.; Langreth, D.C., *Phys. Rev.*, **1967**, 156, 685.

Ashcroft, N.W.; Langreth, D.C., *Phys. Rev.*, **1968**, 166, 934.

Ataman, M.; Boucher, E.A., *J. Polymer Sci., Poly. Phys. Ed.*, **1982**, 20, 1585.

Ataman, M., *Colloid Polymer Sci.*, **1987**, 265, 19.

Auvray, L.; Cotton, J.P., **1987**, 20, 202.

Axelsson, C.-G., *Biochimica et Biophysica Acta*, **1978**, 533, 34.

Bailey, F.E.; Kucera, J.L.; Imhof, L.G. *J. Polym. Sci.*, **1958**, 32, 517.

Bailey, F.E.; Koleske, J.V.; *Poly(ethyleneoxide)*, Academic Press, New York, **1976.**

Bamberger, S.; Seaman, G.V.F.; Sharp, K.A.; Brooks, D.E., *J. Colloid Interface Sci.*, **1984**, 99, 194.

Bamberger, S.; Brooks, D.E.; Sharp, K.A.; van Alstine, J.M.; Webber, T.J., *Partitioning in Aqueous Two-Phase Systems*, Eds., H. Walter, D.E. Brooks, D. Fisher, Academic Press, New York, **1985**.

Barboy, B., *Chemical Physics*, **1975**, 11, 357.

Barker, J.A.; Henderson, D., *J. Chem. Phys.*, **1967**, 47, 2856.

Baskir, J.N.; Hatton, T.A.; Suter, U.W., *Macromolecules*, **1987**, 20, 1300.

Baskir, J.N. *Ph.D. Thesis*, Massachusetts Institute of Technology, **1988**.

Baskir, J.N.; Hatton, T.A.; Suter, U.W. *Biotechnol. Bioeng.*, **1989**, 34, 541.

Baskir, J.N.; Hatton, T.A.; Suter, U.W., *J. Phys. Chem.*, **1989**a, 93, 969.

Baskir, J.N.; Hatton, T.A.; Suter, U.W., *J. Phys. Chem.*, **1989b**, 93, 2111.

Baxter, R.J., *J. Chem. Phys.*, **1968**, 49, 2770.

Beech, D.R.; Booth, C. *J. Poly. Sci.* A-2 **1969**, 7, 575.

Beijerinck, M. W., *Zentr. Bl-Bakt.*, **1896**, 2, 698.

Bendedouch, D.; Chen, S.-H., *J. Phys. Chem.*, **1983**, 87, 1473.,

Benoit, H.; Benmouna, M., *Polymer*, **1984**, 25, 1059.

Birkenmeier, G.; Kopperschlager, G.; Albertsson, P.A.; Johansson, G.; Tjerneld, F.; Akerlund, H.E.; Berner, S.; Wickstroem, H.; *J. Biotechnology*, **1987**, 5, 115.

Bishop, M.; Saltiel, C.J., *J. Chem. Phys.*, **1991**, 94, 6920.

Bockris, J.O'M.; Reddy, A.K.N., *Modern Electrochemistry 1*, Plenum Press, New York **1970**.

Booth, F., *J. Chem. Phys.*, **1951**, 19, 391.

Booth, F., *J. Chem. Phys.*, **1955**, 23, 453.

Boothroyd, A.T., *Polymer*, **1988**, 29, 1555.

Bouchaud, E.; Daoud, M., *J. Physique*, **1987**, 48, 1991.

Boucher, E.A.; Hines, P.M., *J. Poly. Sci.-Poly. Phys.*, **1976**, 14, 2241.

Boucher, E.A.; Hines, P.M., *J. Poly. Sci.-Poly. Phys.*, **1978**, 16, 501.

Boucher, E.A., *J. Chem. Soc., Faraday Trans. 1*, **1989**, 85, 2963.

Brooks, D.E.; Sharp, K.; Bamberger, S.; Tamblyn, C.H.; Seaman, G.V.F.; Walter, H.; *J. Colloid Interface Sci.*, **1984**, 102, 1.

Brooks. D.E.; Sharp, K.A.; Fisher, D. Chapter 2, *Partitioning in Aqueous Two-Phase Systems*, Eds Walter, H; Brooks, D.E.; Fisher, D. Academic Press, New York, **1985**.

Brönsted, J.N., *Z. Phys. Chem. Bodenstein-Festband*, **1931**, 155, 257.

Brönsted, J.N.; Warming, E., *Z. Phys. Chem. A.*, **1931**, 155, 343.

Brown, W.; Rymden, R., *Macromolecules*, **1986**, 19, 2942.

Cabane, B. *J. Phys. Chem.*, **1977**, 81, 1639.

Cabane, B.; Duplessix, R., *J. Physique*, **1982**, 43, 1529.

Cabane, B.; Duplessix, R., *J. Physique*, **1987**, 48, 651.

Cabane, B. in *Surfactant Science Series*, Volume 22, Ed., R. Zana, **1987**.

Cabezas, H.; Kabiri-Badr, M.; Szlag, D.C., *Bioseparation*, **1990**, 1, 227

Carlson, A., *Separation Science and Technology*, **1988**, 23, 785.

Carnahan, N.F.; Starling, K.E.; *J. Chem. Phys.*, **1969**, 51, 635.

Carnahan, N.F.; Starling, K.E.; *J. Chem. Phys.*, **1970**, 53, 600.

Casassa, E.F., *J. Polymer Sci.*, **1976**, 54, 53.

Chen, S.-H.; Bendedouch, D., *Methods in Enzymology*, **1986**, 130, 79.

Chevalier, Y.; Zemb, T. *Rep. Prog. Phys.*, **1990**, 53, 279.

Cleland, J.L., *PhD Thesis*, Massachusetts Institute of Technology, **1991**.

Cohen-Stuart, M.A.; Cosgrove, T.; Vincent, B., *Adv. Colloid Interface Sci.*, **1986**, 24, 143.

Cohn, E.J.; Edsall, J.T., *Proteins, Amino Acids and Dipolar Ions*, Reinhold, N.Y., **1943**.

Cohn, E.; Edsall, J., *Proteins, Amino Acids and Peptides as Ions and Dipolar Ions, ACS Monograph Series*, Reinhold Publishing Corporation, N.Y, **1943**.

Cordes, A.; Flossdorf, J.; Kula, M-R., *Biotechnol. Bioeng.*, **1987**, 30, 514.

Cotton, J.P.; Farnoux, B.; Jannink, G. *J. Chem. Phys.*, **1972**, 57, 290.

Creighton, T.E. *Proteins: Structures and Molecular Properties*, Freeman: New York, **1984**.

Croxton, C.A., *Polymer Communications*, **1988**, 29, 232.

Dahuron, L.; Cussler, E.L., *AIChE Journal*, **1988**, 34, 130.

Daoud, M.; Cotton, J.P.; Farnoux, B.; Jannink, G.; Sarma, G.; Benoit, H.; Duplessix, R.; Picot, C.; de Gennes, P.G., *Macromolecules*, **1975**, 8, 804.

Debye, P.; Bueche, A.M., *J. Appl. Phys.*, **1949**, 20, 518.

Debye, P.; Henderson, H.R.; Brumberger, H.; *J. Appl. Phys.*, **1957**, 28, 679.

Deen, W.M., *AIChE Journal*, **1989**, 33, 1409.

de Gennes, P.G., *J. Physique*, **1976**, 37, 1445.

de Gennes, P.G., *Comptus Rendus Acad. Sci.*, **1979**, 288, 359.

de Gennes, P.-G., *Scaling Concepts in Polymer Physics*, Cornell University Press, Ithaca, N.Y., **1979**.

de Gennes, P.G., *Macromolecules*, **1981**, 14, 1637.

de Gennes, P.G., *Adv. Colloid Interface Sci.*, **1987**, 27, 189.

de Hek, H.; Vrij, A. *J. Colloid Interface Sci.* **1981**, 84, 409.

Dekker, M.; Van'T Riet, K.; Weijers, S.R.; Baltussen, W.J.A.; Laane, C.; Bijsterbosch, B.H., *Chem. Eng. J.*, **1986**, 33, B27.

de Kruif, C.G.; Rouw, P.W.; Briels, W.J.; Duits, M.H.G.; Vrij, A.; May, R.P., *Langmuir*, **1989**, 5, 422.

Dey, D.; Hirtzel, C.S. *Colloid Polym. Sci.*, **1991**, 269, 28.

Diamond, A.D.; Hsu, J.T., *Biotechnol. Bioeng.*, **1989**, 34, 1000.

Diamond, A.D.; Hsu, J.T., *AIChE J.*, **1990**, 36, 1017.

Dickerson, R.E.; Takano, T.; Eisenberg, D.; Kallai, O.B.; Samson, L.; Cooper, A.; Margoliash, E., *J. Biol. Chem.*, **1971**, 246, 1511.

Dill. K.A.; Alonso, D.O.V. *Protein Structure and Protein Engineering*, **1988**, 39, 51.

Dobry, A.; Boyer-Kawenoki, F., *J. Poly. Sci.*, **1947**, 2, 90.

Douglas, J.F. *Macromolecules*, **1989**, 22, 3707.

Edmond, E.; Ogston, A.G., *Biochem. J.*, **1968**, 109, 569.

Edwards, S.F., *Proc. Phys. Soc. London*, **1966**, 88, 265.

Farnoux, B.; Daoud, M.; Decker, D.; Jannink, G.; Ober, R.; *J. Phys.* **1975**, 36, L-35.

Fauquex, P.F.; Hustedt, H.; Kula, M.R., *J. Chem. Tech. Biotechnol.*, **1985**, 35B, 51.

Flanagan, S.D.; Barondes, S.H., *J. Biological Chem.*, **1975**, 250, 1484.

Fleer, G.J.; Scheutjens, J.M.H.M.; Cohen-Stuart, M.A., *Colloids and Surfaces*, **1988**, 31, 1.

Florin, E.; Kjellander, R.; Eriksson, J.C., *J. Chem. Soc., Faraday Trans. 1*, **1984**, 80, 2889.

Flory P.J.; Krigbaum W.R. *J. Chem. Phys.* **1950**, 18, 1086.

Flory, P.J., *Statistical Mechanics of Chain Macromolecules*, Interscience Publishers, N.Y, **1968**.

Flory, P.J., *Disc. Faraday Soc.*, **1970**, 49, 7.

Flory, P.J. *Principles of Polymer Chemistry*; Cornell University Press, Ithaca and London, **1986**.

Forciniti, D.; Hall, C.K., *ACS Symp. Ser.*, **1990**, 419, 53.

Forciniti, D.; Hall, C.K.; Kula, M.R., *J. Biotechnology*, **1990**, 16, 279.

Forciniti, D.; Hall, C.K.; Kula, M.R., *Chem. Eng. Sci.*, **1991**, in press.

Forciniti, D.; Hall, C.K.; Kula, M.R., *Biotechnol. Bioeng.*, **1991**, in press.

Gekko, K.; Timasheff, S.N. *Biochem.* **1981**, 20, 4667.

Gelsema, W.J.; DeLigny, C.L., *Sep. Sci. and Technol.*, **1982**, 17, 375.

Gerson, D.F., *Biochim. Biophys. Acta*, **1980**, 602, 269.

Gerson, D.F.; Akit, J., *Biochim. Biophys. Acta*, **1980**, 602, 281.

Gerson, D.F.; Scheer, D., *Biochim. Biophys. Acta*, **1980**, 602, 506.

Glatter, O.; Kratky, O., *Small Angle X-Ray Scattering*, Academic Press, London, **1982**.

Goddard, E.D. *Colloids and Surfaces*, **1986**, 19, 255.

Goddard, E.D. *Colloids and Surfaces*, **1986**, 19, 301.

Goklen, K.E.; Hatton, T.A., *Biotech. Prog.*, **1985**, 1, 1985.

Goklen, K.E.; Hatton, T.A., *Sep. Sci. Tech.*, **1987**, 22.

Goldstein, R.E., *J. Chem. Phys.*, **1984**, 80, 5340.

Guinier, A.; Fournet, G., *Small Angle Scattering of X-Rays*; Wiley, New York, **1955**.

Guo, X.H.; Zhao, N.M.; Chen, S.H.; Teixeira, J.; *Biopolymers*, **1990**, 29, 335.

Hammes, G.; Roberts, P.B. *J. Am. Chem. Soc.* **1968**, 90, 7119.

Hansen, J.-P.; McDonald, I.R., *Theory of Simple Liquids*, Academic Press, London, **1976**.

Haynes, C.A.; Beynon, R.A.; King, R.S.; Blanch, H.W.; Prausnitz, J. *J. Phys. Chem.*, **1989**, 93, 5612.

Heller, W.; Pugh, T.L. *J. Chem. Phys.*, **1956**, 22, 1778.

Hermans, J. *J. Chem. Phys.*, **1982**, 77, 2193.

Hermans, J.J.; Hermans, J. *J. Polymer Sci.*, **1984**, 22, 279.

Hill, T.L., *J. Am. Chem. Soc.*, **1957**, 79, 4885.

Hill, T.L., *J. Chem. Phys.*, **1959**, 30, 93.

Huggins, M.L. *J. Phys. Chem.*, **1941**, 9, 440.

Huggins, M.L., *Annal. N.Y. Acad. Sci.*, **1942**, 43, 1.

Hughes P.; Lowe, C.R, *Enzyme Microb. Technol.*, **1988**, 10, 115.

Husted, H.; Kroner, H.K.; Stach, W.; Kula, M-R., *Biotechnol. Bioeng.*, **1978**, 20, 1989.

Hustedt, H.; Kroner, K.H.; Kula, M.R., *Proc. Eur. Congr. Biotechnol.*, **1984**, 1, 597.

Ingham, K.C.; *Arch. Biochem. Biophys.*, **1977**, 184, 59.

Ingham, K.C. *Arch. Biochem. Biophys.*, **1978**, 186, 106.

Israelachvili, J.N.; Mitchell, D.J.; Ninham B.W. *J. Chem. Soc. Faraday Trans. II*, **1976**, 72, 1525.

Israelachvili, J.N. *Intermolecular and Surface Forces with Applications to Colloidal and Biological Systems*, Academic Press: London, **1985**.

Jansen, J.W.; de Kruif, C.G.; Vrij, A. *J. Colloid Interface Sci.*, **1986**, 114, 471.

Jansen, J.W.; de Kruif, C.G.; Vrij, A. *J. Colloid Interface Sci.*, **1986**, 114, 481.

Jansen, J.W.; de Kruif, C.G.; Vrij, A. *J. Colloid Interface Sci.*, **1986**, 114, 492.

Jansons, K.M.; Phillips, C.G.; *J. Colloid Interface Sci.* **1990**, 137, 75.

Johansson, G., *Biochim. Biophys. Acta*, **1970**, 222, 387.

Johansson, G., *Biochim. Biophys. Acta*, **1970**, 222, 381.

Johansson, G., *Proceedings of the International Solvent Extraction Conference*, **1971**, 2, 928.

Johansson, G., *Molecular and Cellular Biochemistry*, **1974**, 4, 169.

Johansson, G., *Biochimica et Biophysica Acta.*, **1976**, 451, 517.

Johansson, G., *J. Chromatogr.*, **1978**, 150, 63.

Johansson, G., *J. Chromatogr.*, **1985**, 322, 425.

Johansson, G.; Andersson, M., *J. Chromatogr.*, **1984**, 291, 175.

Johansson, G.; Andersson, M., *J. Chromatogr.*, **1984**, 303, 39.

Johansson, G.; Andersson, M.; Akerlund, H.E., *J. Chromatogr.*, **1984**, 298, 483.

Johansson, G.; Hartman, A.; Albertsson, P-Å., *Eur. J. Biochem.*, **1973**, 33, 379.

Johansson, G.; Joelsson, M., *J. Chromatogr.*, **1987**, 393, 195.

Johansson, G.; Kopperschläger, G.; Albertsson, P-Å., *Eur. J. Biochem.*, **1983**, 131, 589.

Johansson, G.; Shanbhag, V.P., *J. Chrom.*, **1984**, 284, 63.

Jones, M.N. *J. Colloid and Interface Sci.*, **1967**, 23, 36.

Kang, C.H.; Sandler, S.I., *Macromolecules*, **1988**, 21, 3088.

Kang, C. H., Sandler, S. I., *Biotechnol. Bioeng.*, **1988**, 32, 1158.

Karlstrom, G., *J. Phys. Chem.*, **1985**, 89, 4962.

Kern, R.J.; Slocombe, R.J., *J. Poly. Sci.*, **1955**, 15, 183.

Kern, R.J., *J. Poly. Sci.*, **1956**, 21, 19.

King, R.S.; Blanch, H.W.; Prausnitz, J.M., *AIChE Journal*, **1988**, 34, 1585.

Kjellander, R., Florin, E., *J. Chem. Soc., Faraday Trans. I*, **1981**, 77, 2053.

Knoll, D.; Hermans, J.; *J. Biological Chem.*, **1983**, 258, 5710.

Koenig, J.L.; Angood, A.C. *J. Poly. Sci.*, A-2 **1970**, 8, 1787.

Kopperschläger, G.; Johansson, G., *Anal. Biochem.*, **1982**, 124, 117.

Kopperschläger, G.; Lorenz, G.; Usback, E., *J. Chromatogr.*, **1983**, 259, 97.

Kroner, K. H.; Hustedt, H.; Kula, M.R., *Biotech. Bioeng.*, **1982**, 24, 1015.

Kuboi, R.; Tanaka, H.; Komasawa, I., *Kagaku Kogaka Ranbunshu*, **1990**, 16, 1.

Kula, M.-R.; Kroner, K.H.; Hustedt, H.; Schutte, H., *Ann. N. Y. Acad. Sci.*, **1981**, 341.

Kula, M.-R.; Kroner, K.H.; Hustedt, H., *Advances in Biochem. Eng*, **1982**, 24, 73.

Kula, M.-R.; Kroner, K.H.; Hustedt, H., *Enzyme Engineering*, **1982**, 6, 69.

Lebowitz, J.L., *Phys. Rev.*, **1964**, 133, A895.

Lee, S.H.; Ruckenstein, E. *J. Colloid Interface Sci.*, **1988**, 125, 365.

Leser, M.E.; Wei, G.; Luisi, P.L.; Maestro, M., *Biochem. Biophys. Res. Commun.*, **1986**, 135, 629.

Lin, T.H.; Phillies, G.D.J., *J. Phys. Chem.*, **1982**, 86, 4073.

Lin, T.H.; Phillies, G.D.J., *J. Colloid Interface Sci.*, **1984**, 100, 82.

Lin, T.H.; Phillies, G.D.J., *Macromolecules.*, **1984**, 17, 1686.

Lin, M.Y.; Lindsay, H.M.; Weitz, D.A.; Ball, R.C.; Klein, R.; Meakin, P. *Nature*, **1989**, 339, 360.

Liu, K.-J.; Parsons, J.L. *Macromol.*, **1969**, 2, 529.

Liu, K.-J.; Anderson, J.E. *Macromol.*, **1970**, 3, 163.

Luisi, P.L.; Magid, L.J., *CRC Crit. Rev. Biochem.*, **1986**, 20, 409.

Luisi, P.L.; Giomini, M.; Pileni, M.P.; Robinson, B.H., *Biochim. Biophys. Acta*, **1988**, 947, 209.

McQuarrie, D.A., *Statistical Mechanics*, Harper-Row, New York, **1976**.

Marques, C.M.; Joanny, J.F., *J. Physique*, **1988**, 49, 1103.

Martinek, K.; Levashov, A.V.; Klyachko, N.; Khmelnitski, Y.L.; Berezin, I.V., *Eur. J. Biochem.*, **1986**, 155, 453.

Maxfield, J.; Shepherd, I.W. *Polymer*, **1975**, 16, 505.

Middaugh, C.R.; Lawson, E.Q, *Anal. Biochem.*, **1980**, 105, 364.

Modell, M.; Reid, R.C., *Thermodynamics and Its Applications*, Prentice-Hall, N.Y., **1983**.

Molyneux, P. *Water Soluble Synthetic Polymers; Properties and Behavior* 1, CRC Press, **1982.**

Momii, T.; Numasawa, N.; Kuwamamoto, K.; Nose, T. *Macromolecules*, **1991**, 24, 3964.

Nagarajan, R.; Kalpacki, B. *Microdomains in Polymer Solutions*, Editor P.Dubin, Plenum Press N.Y., **1982**.

Napper, D.H. *Polymeric Stabilization of Colloidal Dispersions*; Academic Press, London, **1983**.

Nossal, R.; Glinka, C.J.; Chen, S.-H., *Biopolymers*, **1986**, 25, 1157.

Ornstein, L.S.; Zernike, F., *Proc. K. Ned. Akad. Wet.*, **1914**, 17, 793.

Orofino, T.A.; Flory, P.J. *J. Chem. Phys.*, **1957**, 26, 1067.

Patel, P.D.; Russel, W.B. *J. Colloid Interface Sci.* **1989**, 131, 192.

Patel, P.D.; Russel, W.B. *J. Colloid Interface Sci.* **1989**, 131, 201.

Patrickios, C.; Abbott, N.L.; Foss, R.P., Hatton, T.A., *Biosep. Technol.* **1991**, in press.

Pecora, R., *Dynamic Light Scattering*, Plenum, New York, **1985**.

Percus, J.K.; Yevick, G.J., *Phys. Rev.*, **1958**, 110, 1.

Perrau, M.B.; Iliopoulos, I.; Audebert, R., *Polymer*, **1989**, 30, 2112.

Peters, T. *Adv. Protein Chem.*, **1985**, 37, 161.

Phillies, G.D.J.; Ullmann, G.S.; Ullmann, K.; Lin, T.H., *J. Chem. Phys.*, **1985**, 82, 5242.

Pincus, P.A.; Sandroff, C.J.; Witten, T.A., *J. Physique*, **1984**, 45, 725.

Puvvada, S.; Blankschtein, D., *J. Chem. Phys.*, **1990**, 92, 3710; and references cited therein.

Robertus, C.; Philipse, W.H.; Joosten, J.G.H.; Levine, Y.K., *J. Chem. Phys.*, **1989**, 90, 4482.

Robertus, C.; Joosten, J.G.H.; Levine, Y.K. *J. Chem. Phys.*, **1990**, 93, 7293.

Ruckenstein, E.; Chi, J.C. *J. Chem. Soc. Faraday Trans* II, **1975**, 71, 1690.

Ryden, J.; Albertsson. P.A., *J. Colloid Interf. Sci.*, **1971**, 37, 219.

Sanchez, I.C.; Balazs, A.C., *Macromolecules*, **1989**, 22, 2325.

Sasakawa, S.; Walter, H., *Nature*, **1970**, 223, 329.

Sasakawa, S.; Walter, H., *Biochemistry*, **1972**, 11, 2760.

Sasakawa, S.; Walter, H., *Biochemistry*, **1974**, 13, 29.

Schaefer, D., *Polymer*, **1984**, 25, 387.

Scheutjens, J.M.H.M.; Fleer, G.J., *J. Phys. Chem.*, **1979**, 83, 1619.

Scheutjens, J.M.H.M.; Fleer, G.J., *J. Phys. Chem.*, **1980**, 84, 178.

Schneider, D.K.; Schoenborn, B.P., *Neutrons in Biology*, Plenum, New York, B.P. Schoenborn, Ed., **1984**, 119.

Schurch, S.; Gerson, D.F.; McIver, D.J.L., *Biochim. Biophys. Acta*, **1981**, 640, 557.

Shanbhag, V.P.; Johansson, G., *Biochem. Biophys. Res. Communications*, **1974**, 61, 1141.

Shanbhag, V.P.; Axelsson C-G., *Eur. J. Biochem.*, **1975**, 60, 17.

Shanbhag, V.P.; Johansson, G., *Eur. J. Biochem.*, **1979**, 93, 363.

Shirahama, K. *Colloid & Polymer Sci.*, **1974**, 252, 978.

Shirahama, K.; Ide, N. *J. Colloid Interface Sci.*, **1976**, 54, 450.

Sjoberg, A.; Karlstrom, G., *Macromolecules*, **1989**, 22, 1325.

Squire, P.G.; Moser, P.; O'Konsky, C.T., *Biochemistry*, **1968**, 7, 4261.

Squire, P.G.; Himmel, M.E., *Arch. Biochem. Biophys.*, **1979**, 196, 165.

Suh, S-S.; Arnold, F.H., *Biotech. Bioeng.*, **1990**, 35, 682.

Sutherland, I.A.; Fisher, D., *Separations using Aqueous Two-Phase Systems*; Plenum, New York, **1989**.

Tadokoro, H.; Chatani, Y,; Yoshihara, T,; Tahara, S,; Murahashi, S. *Makrol. Chem.*, **1964**, 73, 109.

Tanford, C. *Physical Chemistry of Macromolecules*, Wiley, New York, **1961**.

Tanner, R.E.; Herpigny, B.; Chen, S.-H.; Rha, C.K. *J. Chem. Phys.*, **1982**, 76, 3866.

Theoreu, H.; Akesson, A., *J. Am. Chem. Soc.*, **1941**, 63, 1812.

Tjerneld, F., Berner, S.; Cajarville, A.; Johansson, G., *Enzyme Microb.Technol.*, **1986**, 8, 417.

Tokiwa, F.; Tsujii, K. *Bull. Chem. Soc. Japan*, **1973**, 46, 2684.

Tong, P.; Witten, T.A.; Huang, J.S.; Fetters, L.J., *J. Phys. France*, **1990**, 51, 2813.

Tsunashima, Y.; Kurata, M., *J. Chem. Phys.*, **1986**, 84, 6432.

Ullmann, G.S.; Ullmann, K.; Linder, R.M.; Phillies, G.D.J., *J. Phys. Chem.*, **1985**, 89, 692.

Ullman, R.; Benoit, H.; King, J.S., *Macromolecules*, **1986**, 19, 183.

Vennemann, N.; Lechner, M.D.; Oberthur, R.C., *Polymer*, **1987**, 28, 1939.

Vincent, B.; Luckham, P.F.; Waite, F.A. *J. Colloid Interface Sci.*, **1979**, 73, 508.

Vrij, A. *Pure & Appl. Chem.*, **1976**, 48, 471.

Wall, F.T.; Mandel, F., *J. Chem. Phys.*, **1975**, 63, 4592.

Walter, H.; Sasakawa, S.; Albertsson, P.Å. *Biochemistry*, **1972**, 11, 3880.

Walter, H.; Brooks, D.E.; Fisher, D., *Partitioning in Aqueous Two Phase Systems*, Academic Press, N.Y., **1985**.

Walter, H.; Johansson, G. *Analytical Biochemistry*, **1986**, 155, 215.

Walter, H.; Johansson, G.; Brooks, D.E., *Analytical Biochemistry*, **1991**, (in press).

Wilcoxen, J.P.; Martin, J.E.; Schaefer, D.W. *Phys. Rev. A*, **1989**, 39, 2675.

Wiltzius, P.; Haller, H.R.; Cannell, D.S.; Schaefer, D.W., *Phys. Rev. Lett.*, **1983**, 51, 1183.

Woodhead, J.L. *J. Physique Colloque C1*, **1986**, 47, C1-3.

Wu, C.F.; Chen, H.S., *J. Chem. Phys.*, **1987**, 87, 6199.

Zaslavsky, B. Yu; Miheeva, L.M.; Mestechkina, N.M.; Pogorelov, V.M.; Rogozhin, S.V., *Febs Letters*, **1978**, 94, 77.

Zaslavsky, B.Yu; Miheeva, L.M.; Rogozhin, S.V., *Biochimica et Biophysica Acta*, **1979**, 588, 89.

Zaslavsky, B.Yu; Miheeva, L.M.; Mestechkina, N.M.; Shchyukina, L.G.; Chlenov, M. A.; Kudrjashov, L.I.; Rogozhin, S.V., *J. Chromatography*, **1980**, 202, 63.

Zaslavsky, B.Yu; Miheeva, L.M.; Rogozhin, S.V., *J. Chromatography*, **1981**, 216, 103.

Zaslavsky, B.Yu; Mestechkina, N.M.; Miheeva, L.M.; Rogozhin, S.V., *J. Chromatography*, **1982**, 240, 21.

Zaslavsky, B.Yu; Mestechkina, N.M.; Rogozhin, S.V., *J. Chromatography*, **1983**, 260, 329.

Zaslavsky, B.Yu; Bagirov, T.O.; Borovskaya, A.A.; Gasanova, G.Z.; Gulaeva, N.D.; Levin, V.Yu; Masimov, A.A.; Mahmudov, A.V.; Mestechkina, N.M.; Niheeva, L.M. Osipov, N.N.; Rogozhin, S.V., *Colloid Polymer Sci.*. **1986**, 264, 1066.

Zaslavsky, B.Yu; Mahmudov, A.V.; Bagirov, T.O.; Borovskaya, A.A.; Gasanova, G. Z.; Gulaeva, N.D.; Levin, V.Yu; Mestechkina, N.M.; Miheeva, L.M.; Rodnikova, N. N., *Colloid Polymer Sci.*, **1987**, 265, 548.

Zaslavsky, B.Yu; Miheeva, L.M.; Aleschko-Ozhevskii, Y.Y.P.; Mahmudov, A.V.; Bagirov, T.O; Garaev, E.S., *J. Chrom.*, **1988**, 439, 267.

Zimm, B.H., *J. Chem. Phys.*, **1948**, 16, 1093.

Zimm, B.H.; Stockmayer, W.H.; Fixman, M. *J. Chem. Phys.*, **1953**, 21, 1716.